

Kinetic Isotope Effects in the Study of Organometallic Reaction Mechanisms

Mar Gómez-Gallego* and Miguel A. Sierra*

Departamento de Química Orgánica I, Facultad de Química, Universidad Complutense, 28040 Madrid, Spain

CONTENTS

1. Introduction	4857	3.7. KIEs in the Study of C–H Activation Mechanisms by Other Transition Metal Complexes	4896
2. Basis of KIEs	4858	4. KIEs in the Study of Si–H Activation Mechanisms	4900
2.1. Origin of Isotope Effects	4858	4.1. Si–H Activation	4900
2.2. Magnitude of the Observed KIEs	4859	4.2. Hydrosilylation of Ketones	4902
2.3. Secondary KIEs	4859	4.3. Hydrosilylation of C=C Bonds	4904
2.4. Equilibrium Isotope Effects	4860	5. Hydrogen Addition and Hydride Transfer	4904
2.5. Solvent Isotope Effects	4860	5.1. Hydrogen Addition Mediated by Ru Catalysts	4904
3. KIEs in the Study of C–H Bond-Activation Mechanisms	4860	5.2. Interaction of H–H Bonds with Other Transition Metal Centers	4911
3.1. General Considerations	4861	5.3. Hydrogen Addition to Dinitrogen Compounds	4912
3.2. KIEs in the Study of C–H Activation Mechanisms by Ir Complexes	4864	5.4. Hydride Transfer	4913
3.3. KIEs in the Study of C–H Activation Mechanisms by Pt Complexes	4868	6. β -Elimination/Migratory Insertion	4915
3.3.1. Protonolysis of Pt(II) Complexes	4868	7. KIEs in the Study of C–C Couplings Mediated by Transition Metal Complexes	4921
3.3.2. C–H Reductive Elimination from Pt(IV) Complexes	4871	7.1. Sequence Ad–Ox–Transmetalation	4921
3.3.3. C–H Activation by Cationic Pt(II) Complexes Having Diimine Ligands	4872	7.2. Heck Coupling	4923
3.3.4. C–H Activation by Dicationic Platinum(II) Diimine Complexes	4876	8. Cycloisomerizations: Dienes, Enynes, Eneamines	4932
3.3.5. C–H Activation by Pt(II) Complexes Bearing Phosphine Ligands	4877	9. KIEs in the Study of Transition Metal-Mediated Cycloadditions and Sigmatropic Shifts	4935
3.3.6. C–H Activation by Pt(0) Complexes	4878	9.1. [n + m]-Cycloadditions	4935
3.3.7. Reactions at Pt Complexes with Anionic Donor Ligands	4878	9.1.1. [2 + 1]-Cycloadditions	4935
3.3.8. Cyclometalations	4880	9.1.2. [2 + 2]-Cycloadditions	4938
3.3.9. C–H Activation by Pt(IV) Complexes	4882	9.1.3. [3 + 2]-Cycloadditions	4939
3.4. KIEs in the Study of C–H Activation Mechanisms by Rh Complexes	4883	9.1.4. [3 + 3]-Cycloadditions	4940
3.4.1. Hydrocarbon C–H Activation by Rh(II) Complexes	4883	9.2. [4 + 2 + 2]-Cycloadditions	4940
3.4.2. Hydrocarbon C–H Activation by Rh(III) Complexes	4885	9.3. [1,n]-Sigmatropic Shifts	4941
3.4.3. Hydrocarbon C–H Activation by Rh(I) complexes	4885	10. Reactions of Metal–Carbene Complexes	4941
3.5. KIEs in the Study of C–H Activation Mechanisms by Ru Complexes	4887	10.1. Fischer Carbene Complexes	4941
3.5.1. Hydroarylation of Olefins	4887	10.2. Vinylidene Complexes	4943
3.5.2. Hydroamination of Alkenes and Alkynes	4889	10.3. Non-Stabilized Metal Carbene Complexes, Metallocycles, Carbynes, and Nitrenes	4947
3.5.3. Other Ru-Catalyzed C–H insertions	4890	10.4. Bridging Carbene Complexes	4953
3.6. KIEs in the Study of C–H Activation Mechanisms by Zr and Ti Complexes	4891	11. Concluding Remarks	4955
		Author Information	4955
		Biographies	4955
		Acknowledgment	4956
		References	4956

1. INTRODUCTION

In the last 40 years, metal-mediated reactions have passed from being considered unconventional and in some way *peculiar*

Received: December 16, 2010

Published: May 05, 2011

processes, to priceless tools to achieve many different transformations, most of them impossible to be made by means of the standard organic methodologies.¹ In spite of these facts, the study of the mechanisms of organometallic reactions has been somewhat neglected, particularly when compared to the degree of development reached by mechanistic organic chemistry.² It could be claimed that transition metal reactions are not always easy to study. As the chemistry of the *metal* determines the course of the reaction, the standard approaches of physical organic chemistry are sometimes of little use in the study of the insights of the reactions. The elemental steps are fast and complex, and to probe the rate-determining step (rds) is not a simple task. Furthermore, the detection of a presumed intermediate in the reaction medium could mean no more than the interception of a kinetically inactive species outside the cycle.³ As a result, although many organometallic reactions have been studied, the details of many others are almost unknown.

Nevertheless, the last years have witnessed a growing interest for the understanding of the insights of organotransition metal chemistry. The high number of new transformations that can be achieved with transition metals and the importance of the industrial processes that are currently being developed by using different types of metal catalysts have drawn the interest of researchers in academy and industry to a better and deeper understanding of the way in which these processes work.

The classical tools of physical organic chemistry (i.e., crossover experiments, kinetic studies, and isotope labeling) have been applied in mechanistic organometallic chemistry.⁴ A quick glance into the literature reveals that H/D labeling and crossover experiments are possibly the most widely methods used in the studies aimed at establishing the insights of metal-mediated reaction courses. The availability of efficient synthetic procedures for deuterium labeling, together with more sensitive detection techniques, has made these tools fundamental in the study of cycloadditions; cyclotrimerizations; diene, enyne, and enedione cyclizations; and, of course, C–H bond-activation processes. However, other classical mechanistic tools based on kinetic measurements are more difficult to apply, as often the rates of the successive steps are too fast to be observed separately. Fortunately, because of the enormous progress in computational chemistry in the last few years, theoretical methods (density functional theory (DFT) calculations) are increasingly playing an important role in identifying possible elementary reactions. More restricted in their use than isotope labeling experiments, kinetic isotope effects are possibly the physical organic chemistry tools most benefited by DFT calculations. The kinetic isotope effect (KIE) experiments can be designed to support a computational reaction coordinate, and the comparison between theoretical and experimental KIE values provides essential information to consider or reject the calculated mechanistic pathway.

This article deals with the use of KIEs in the study of the mechanisms of organometallic reactions. Our aim is to focus on those examples in which the determination of KIEs has translated into significant mechanistic insights. For the sake of clarity, the review has been organized following the most significant metal-mediated transformations, rather than covering individual reactions. To maintain the thematic coherence of the review, the use of KIEs in the study of transition metal-mediated biological processes has been excluded.

2. BASIS OF KIES⁵

Although isotopic labeling, crossover experiments, and kinetic analysis are essential tools in the study of a reaction mechanism, they are of little use to interpret which bonds are broken, formed, or rehybridized during the rate determining step (rds) of the reaction. Kinetic isotope effects (KIEs) can make these interpretations. In

consequence, the measurement of the changes in the reaction rate when replacing an atom (generally H) with an isotope (generally D) provide very valuable information about the rds of the process. As the KIEs are expressed as a ratio of rate constants, the effect of the isotopic substitution must be relatively large to be measured, and for this reason, H/D KIEs are the most studied. Isotope effects with atoms other than deuterium are known (*heavy atom isotope effects*), but they are typically small, require accurate experimental techniques, and sometimes are difficult to quantify.

From a mechanistic point of view, the most solid conclusions are obtained from the magnitude of the $k_{\text{H}}/k_{\text{D}}$ ratios (that is, the variation of the $k_{\text{H}}/k_{\text{D}}$ ratio from unity). If $k_{\text{H}}/k_{\text{D}} = 1$, there is no isotope effect, and the conclusion of the experiment is that the bond where the isotopic substitution has occurred is not involved in the rds of the process. Values of $k_{\text{H}}/k_{\text{D}} > 1$ or $k_{\text{H}}/k_{\text{D}} < 1$ are called, respectively, *normal* or *inverse* KIEs. When the isotope replacement X–H/X–D has been made in a bond that is broken in the rds, values of $k_{\text{H}}/k_{\text{D}} \gg 1$ are expected (*primary isotope effect*). However, when the isotope replacement is made far from the reactive center or in bonds that only change their hybridization in the slow step of the reaction, we talk of *secondary isotope effects*, and the $k_{\text{H}}/k_{\text{D}}$ values are considerably lower than the primary KIEs, either *normal* ($k_{\text{H}}/k_{\text{D}} \approx 1.1–1.2$) or *inverse* ($k_{\text{H}}/k_{\text{D}} \approx 0.8–0.9$).

In other cases, the isotopic change affects the individual rate constants of equilibrium, modifying the K_{eq} values (*equilibrium isotope effect*). Finally, the rate changes observed when the isotopic substitution is made in the reaction solvent are referred to as *solvent isotope effects*.

2.1. Origin of Isotope Effects

The origin of all isotope effects relies on the difference in zero-point energies (ZpEs) between unlabeled (X–H) and labeled (X–D) bonds. For a bond-breaking event, the stretching vibration of the bond is defined as the reaction coordinate and is related to the bond force constant (k) and to the reduced mass (m_{r}) by eq 1. The reduced mass of a X–H bond (X = C, O, N) is considerably affected by the replacement of the light H by a heavier D, and in consequence, the stretching frequency of a X–D bond is lower than that of a X–H bond. Figure 1 represents a Morse potential for a C–H bond. As the ZpE is related to the stretching bond vibration (eq 2), the homolysis of a C–D bond requires higher activation energy (AE) than that of a C–H bond.

$$\nu = \frac{1}{2\pi} \sqrt{\frac{k}{m_{\text{r}}}} \text{ where } m_{\text{r}} = \frac{m_1 m_2}{m_1 + m_2} \quad (1)$$

$$e_n = \left(n + \frac{1}{2}\right) h\nu \text{ where } n = 0 \quad (2)$$

In the hypothetical case in which a C–H bond is completely broken at the transition state (TS), the stretching vibration in the reactant has totally disappeared and has been converted to a translational degree of freedom. That is, the force constant associated with the bond (k in eq 1) has disappeared in the TS. In this case, the difference in the C–H/C–D breaking activation energies is the difference between the zero-point energies of the starting bonds. This is the situation in which the maximum $k_{\text{H}}/k_{\text{D}}$ isotope effect would be expected, and its value has been estimated to be about 6.5–7 (measured at 298 K).^{5,6} Typically, experimental KIEs are far from this value, as the complete breaking of a C–H bond in the TS is rare. Generally, while the bond is partially broken, a new bond is being formed in the transition state,

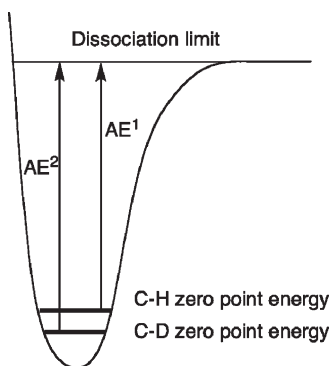


Figure 1

which attenuates the isotope effect. Equations 1 and 2 also explain why *heavy atom isotope effects* are very small, due to the small differences in ZpEs between labeled and unlabeled bonds when the isotopic replacement is made in other atoms different from H.

2.2. Magnitude of the Observed KIEs

The magnitude of a H/D KIE is related to the changes in the C–H/C–D vibration modes when passing from the reactants to the activated complex in the TS. The simplest way to study the reaction coordinate is to use conventional two-dimensional diagrams in which only the changes in vibrational modes along the reaction coordinate are considered. The reaction coordinate in Figure 2 is representative for a typical primary H/D KIE. As the C–H/C–D bond is being broken in the activated complex, the ZpEs of C–H and C–D bonds are not so different. In fact, they are much closer than in the reactants. In consequence, the C–H activation energy (AE^H) is smaller than the C–D activation energy (AE^D), leading to a faster reaction ($k_H/k_D > 1$). The magnitude of the kinetic isotope effect will be related to the differences in the zero-point energies in the reactants (ZpE^R) and in the transition state (ZpE^{TS}). All the vibrations for the bonds undergoing transformations when passing from the reagents to the transition state contribute to the observed KIE. In consequence, the experimental k_H/k_D values are affected not just by the geometry and the degree of bond breaking–bond making in the TS but also by the position of the transition state in the reaction coordinate, that is, they depend on the exothermic (early TS), endothermic (late TS), or thermoneutral (centered TS) nature of the process.

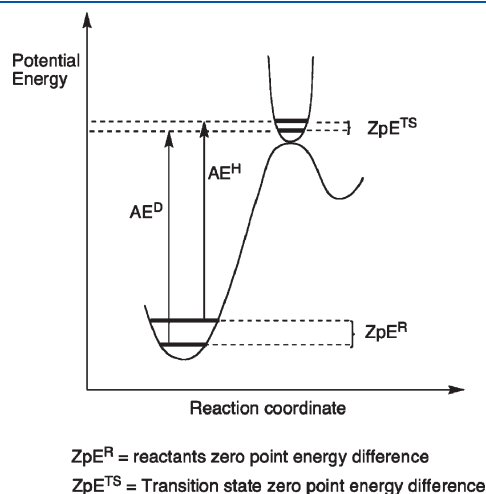


Figure 2

2.3. Secondary KIEs

Secondary kinetic isotope effects are observed when the isotopic substitution has been made in a bond that is not broken in the rds but experiences a *change* in the transition state. Typically, changes in hybridization (sp^3 to sp^2 , sp^2 to sp , and the reverse), or the involvement in hyperconjugation (i.e., with a carbocation placed next to the C–H/C–D bond), produce observable secondary KIEs. The magnitude of these isotope effects is much smaller than that of the primary KIEs.

Rehybridization processes are classical examples to discuss *normal* and *inverse* secondary KIEs. The change in hybridization from Csp^3 to Csp^2 mainly affects the out-of-plane bending vibration of a C–H bond that is much stiffer for the Csp^3 (1350 cm^{-1}) than for the Csp^2 (800 cm^{-1}). The replacement H/D in a Csp^3 to Csp^2 undergoing rehybridization provokes a remarkable difference between the ZpEs in the labeled and unlabeled bonds in the reactants. However, as depicted in Figure 3, the transition state is developing sp^2 character (looser bending vibrations than the reactants). As a result, the C–H/C–D rates are mainly determined by the difference of zero-point energies in the reactants, and the k_H/k_D observed is >1 . The estimated maximum theoretical value is 1.4 but typical experimental values for *normal* secondary KIEs are around 1.1–1.2.

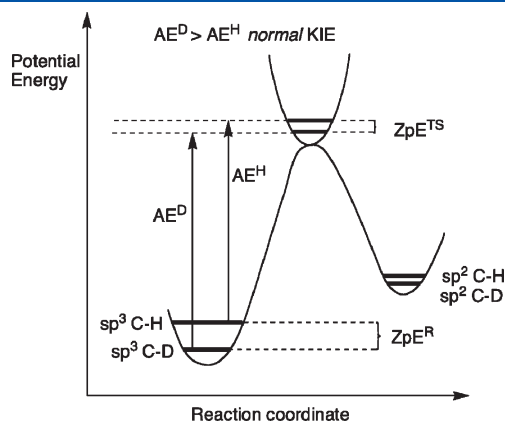


Figure 3. C–H/C–D bonds are not being broken during the process, but the carbon atoms experience an sp^3 to sp^2 hybridization change.

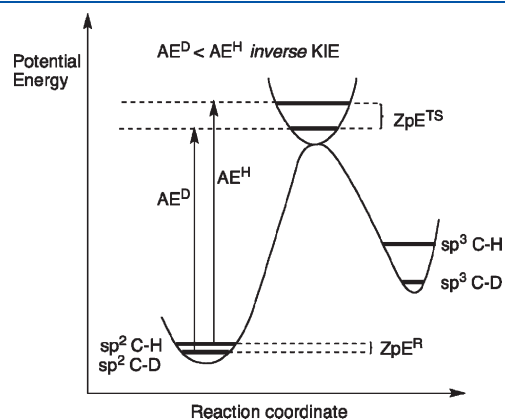


Figure 4. C–H/C–D bonds are not being broken during the process, but the carbon atoms experience an sp^2 to sp^3 hybridization change.

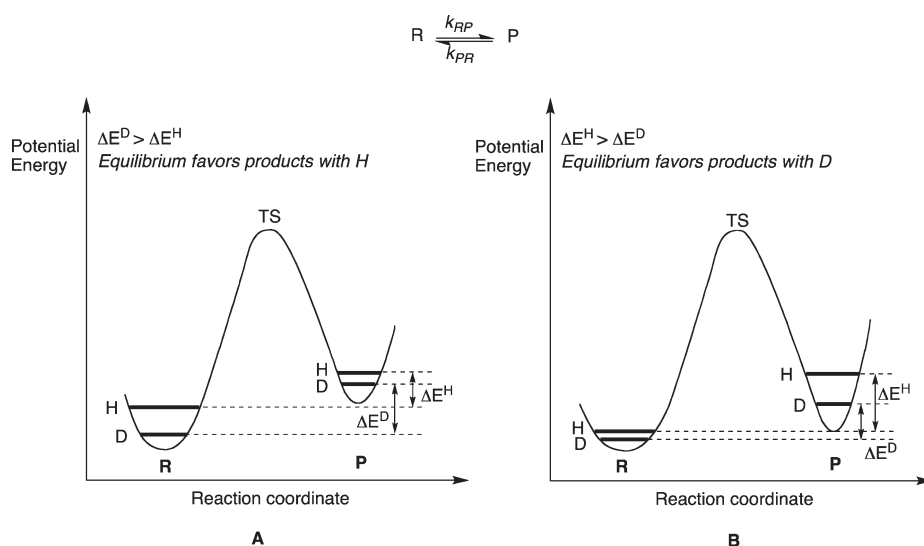


Figure 5

The reverse process is depicted in Figure 4. Now, the transition state is developing a sp^3 character, the C–H(D) out of plane bending vibration is larger (stiffer), and the differences in ZPEs for C–H/C–D bonds are larger in the TS than in the reactants. Hence, the reaction is faster with D than with H and k_H/k_D observed is <1 . Typical values for *inverse* KIEs are around 0.8–0.9.

Secondary KIEs are also observed when the C–H(D) bond is involved in hyperconjugation in the rds. Carbocations in S_N1 reactions or cations β of silicon can be stabilized by hyperconjugation with C–H(D) bonds placed next to the cationic center. This overlapping weakens the C–H(D) bond in the TS and produces a *normal* isotope effect.

2.4. Equilibrium Isotope Effects

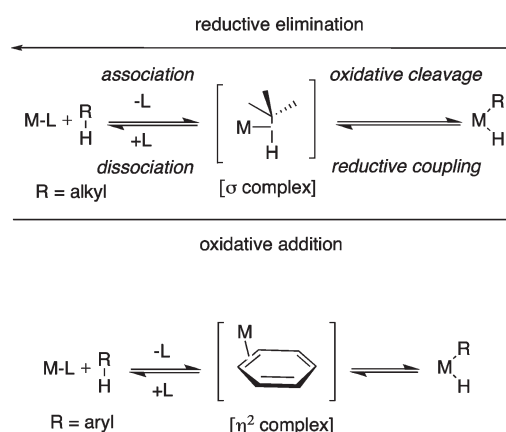
The replacement of a C–H bond by a C–D bond can also influence equilibria. The shifts in equilibrium upon isotopic substitution are called *equilibrium isotope effects* (EIEs) and would be originated by any of the previous mentioned changes in the vibration modes of C–H(D) bonds, that is, by breakage, rehybridization, or hyperconjugation. For the equilibrium involving compounds R and P in Figure 5, the EIE is the ratio of the forward and reverse KIEs (eq 3). Figure 5A shows a situation in which the ZPE difference is larger for the deuterated case, and the equilibrium lies further to the right for the nondeuterated compound. The opposite situation is represented in Figure 5B, with the equilibrium now lying further to the right for the deuterated compound. The determination of EIEs is very important in the study of KIEs in reactions in which equilibria precede the rate-determining step and has resulted in being particularly relevant in the analysis of C–H activation processes.

$$K_{eq} = \frac{k_H^{RP}/k_D^{RP}}{k_H^{PR}/k_D^{PR}} \quad (3)$$

2.5. Solvent Isotope Effects

The changes in reaction rate or the position of equilibrium when a deuterated solvent replaces a solvent are called *solvent isotope effects*. Their interpretation is not always obvious, as the observed

Scheme 1

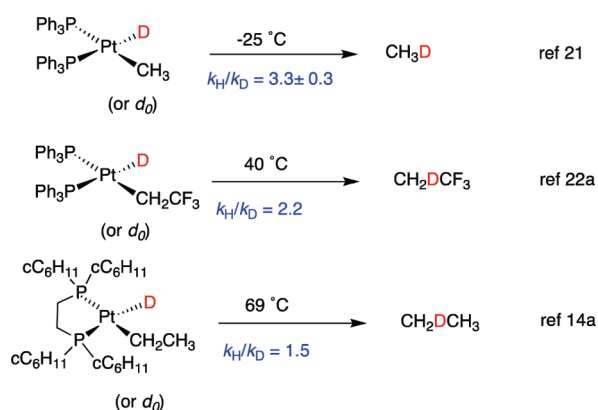


isotope effect can arise from different ways. Some solvents (i.e., protic solvents) can readily interchange with specific positions of the reactants (i.e., OH, NH, SH groups readily scramble their H atoms by D with D_2O) leading to in situ generated labeled compounds in the reaction medium. Reactions in which the reagents or products scramble positions with the solvent are good candidates to observe significant KIEs, in particular when the exchangeable position is involved in the rds. In other cases, the isotope effect arises from the differences in the solvation of the activated complex compared to the reactants, when normal or deuterated solvents are used.

3. KIES IN THE STUDY OF C–H BOND-ACTIVATION MECHANISMS

Since the early reports by Shilov and co-workers⁷ and Crabtree et al.,⁸ the understanding of the activation of C–H bonds in hydrocarbons by a transition metal complex has been a subject of great interest.⁹ Several general mechanisms for C–H activation by transition metal complexes have been identified, including (i) electrophilic activation, (ii) oxidative addition,

Scheme 2. Some Examples Of Normal KIEs in the Study of C–H Activation Mechanisms



(iii) σ -bond metathesis, (iv) 1,2-addition to metal–ligand multiple bonds, (v) H-atom abstraction by metal–oxo complexes, and (vi) metalloradical activation.^{9d} The subject also has been studied from a computational perspective.¹⁰

It is now well established that oxidative addition of C–H bonds to an unsaturated metal species M–L is a two-step reaction, depicted as a reversible process in Scheme 1. The first step is the association of the hydrocarbon at the metal. This requires a coordination site, and the departing ligand L may be displaced in an associative or a dissociative fashion, depending on the metal complex. The association generates a hydrocarbon–metal complex intermediate (σ -alkane or η^2 -arene complex, depending on the aliphatic or aromatic nature of the substrate). The second step is the oxidative cleavage of the C–H bond of the coordinated hydrocarbon. For the reverse process, the reductive elimination comprises two steps: reductive coupling, generating the intermediate metal complex, followed by hydrocarbon dissociation. This terminology proposed by Jones¹¹ and Parkin and co-workers¹² helps to distinguish the individual steps from the overall mechanistic connotations. The reaction steps are shown as equilibria, because in many cases the formation of alkyl or aryl hydride product is reversible. Overall the process can be regarded as an oxidative addition/reductive elimination sequence.

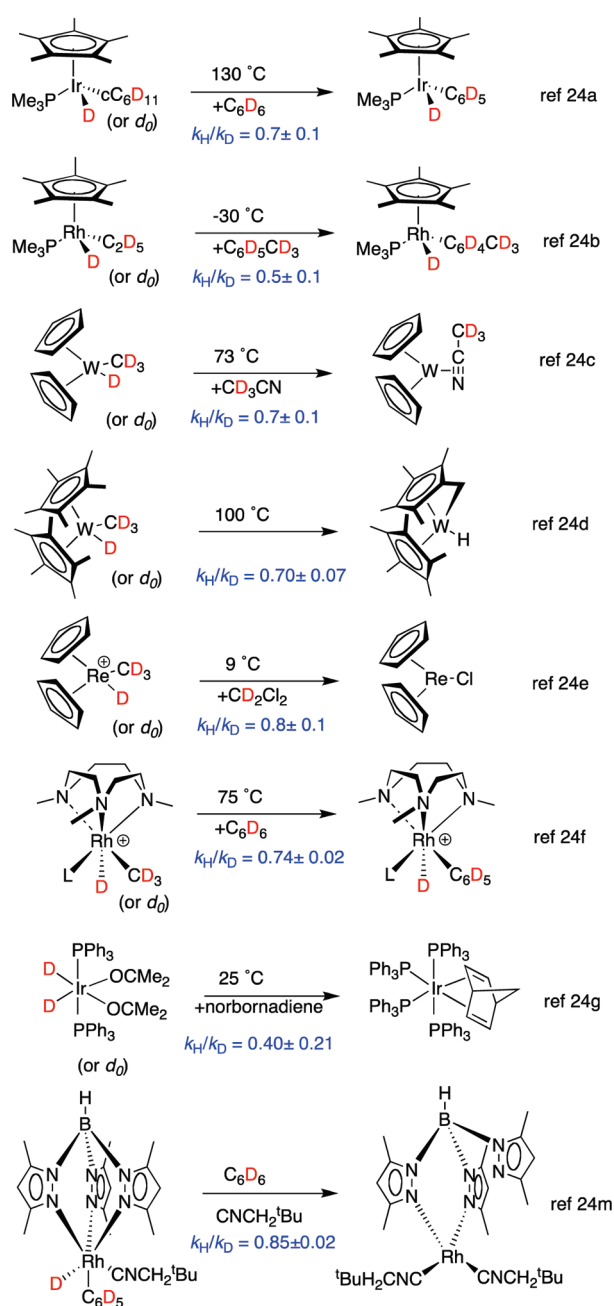
Although the structure of the σ -alkane complexes has not been experimentally determined, there is enough evidence for their existence.^{13,14} In the case of arene activation, there is also substantial evidence of arene η^2 -(C,C) intermediates.^{12,15} Additionally, less stable η^2 -(C,H)¹⁶ or even η^1 -(C)¹⁷ coordination modes have been considered.

3.1. General Considerations

As C–H activation chemistry involves the cleavage of C–H bonds, it is not surprising that measurements of H/D KIEs and interpretations of their physical meaning had been crucial to the mechanistic advances in the area. The in-depth study of the process has been the concern of many groups, in particular those of Bergman and co-workers,^{4a} Jones,¹¹ and Parkin and co-workers.^{12,13} Most of the mechanistic studies have been carried out on the reductive elimination sequence of alkyl/aryl hydride transition metal complexes (Scheme 1). The mechanistic studies on the reverse oxidative addition are less frequent.^{14g,19}

Early mechanistic studies²⁰ on C–H activation with *cis*-platinum complexes by Halpern and co-workers²¹ and others^{14a,22} showed appreciable KIEs (1.5–3.3) that were interpreted as *normal* primary isotopic effects. These results are in agreement with the general

Scheme 3. Some Representative Examples of Inverse KIEs in C–H Activation Studies



mechanism in Scheme 1 having a rate-determining step involving Pt–H(D) bond breaking (Scheme 2).²³ However, *inverse* primary KIEs²⁴ were observed in the studies of reductive eliminations of many other alkyl/aryl hydride transition metal complexes (Scheme 3), and hence, the search for the origin of these *inverse* KIEs has been the subject of mechanistic considerations. An experimental *inverse* isotope effect could be accommodated in these cases by a single-step mechanism, provided the transition state is sufficiently late (i.e., a very productlike transition state, eq 1 in Scheme 4).²⁵ However, it is much more reasonable to consider that the general two-step mechanism depicted in Scheme 1 is operative for all the C–H activation processes, and that the observed *inverse* KIEs arose from an *equilibrium* isotope effect in a (fast) preequilibrium

step prior to the formation of the product, rather than from an intrinsic *inverse* isotope effect in the reductive elimination transition state. The existence of a preequilibrium implies the formation of a reactive intermediate, which is an indirect evidence for the intermediacy of a σ -complex (or η^2 -complex) in the process (eq 2 in Scheme 4).

A deep kinetic analysis of the origin of the *inverse* KIEs has been reported by Jones¹¹ and Parkin and co-workers¹² and is out of the scope of the present review. However, one of the main conclusions of these studies is that a two-step mechanism in which three different rate constants (k_{rc} , k_{oc} , and k_d in Scheme 4) are contributing to the observed H/D isotope effect requires the measurement of at least two KIEs, which has proved experimentally difficult. For this reason, the conclusions obtained from C–H activation mechanistic studies that only rely on the determination of a single isotope effect must be taken with care.¹²

Another conclusion of Jones' and Parkin's studies is that the observation of *inverse* KIEs means a stepwise C–H activation process, necessarily involving an equilibrium step, which makes the H/D *equilibrium isotope effects* (EIEs) relevant in the mechanistic studies. In this regard, it is interesting to notice that some published mechanistic studies based on the analysis of EIEs give contradictory data. For example, a *normal* EIE ($K_H/K_D = 1.33$ at -93°C) was reported for the coordination of cyclohexane to $[\text{CpRe}(\text{CO})_2]$,^{14f} whereas coordination of cyclohexane to $[\text{Cp}^*\text{Rh}(\text{CO})]$ is characterized by a large *inverse* EIE ($K_H/K_D = 0.1$ at -100°C).^{9,14g,26}

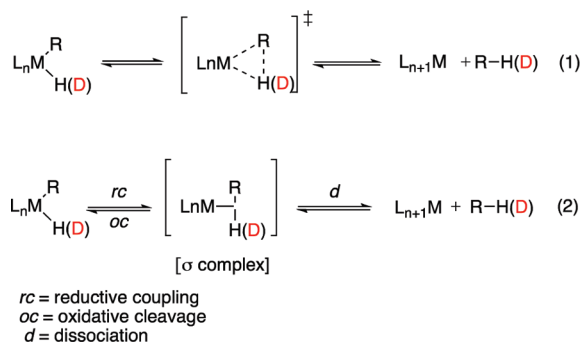
A classical example on the importance of EIEs in the analysis of KIEs in C–H activations is the elegant work by Jones and co-workers^{11,27} demonstrating that the EIE for the interconversion

of $[\text{TpMe}_2]\text{Rh}(\text{L})(\text{Me})\text{X}$ and $[\text{TpMe}_2]\text{Rh}(\text{L})(\sigma\text{-XMe})$ ($\text{L} = \text{CNCH}_2^t\text{Bu}$; $\text{X} = \text{H}, \text{D}$) is *inverse* ($K_H/K_D = 0.5$), even though the individual KIEs for oxidative cleavage ($k_H/k_D = 4.3$) and reductive coupling ($k_H/k_D = 2.1$) are *normal*. Another interesting study is the notable *inverse* KIE ($k_H/k_D = 0.47$) reported by Parkin and co-workers on the methane elimination from ansa-tungstenocene **1**,¹² which is consistent with the interconversion between **1** and the σ -complex **2** prior to rds elimination of methane. The *inverse* KIE for the overall reductive elimination of methane is a consequence of the *inverse* EIE for the formation of **2** and not the result of an *inverse* KIE for a single step (Scheme 5).

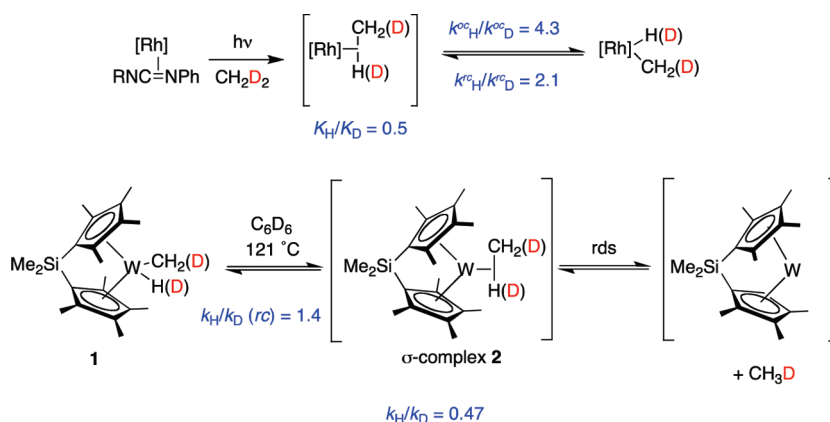
The analysis of EIEs has been also applied to the study of arene C–H activation processes. In a clever use of inter- versus intramolecular KIEs, Jones and co-workers^{15d,28} studied the activation of arene C–H bonds by the coordinatively unsaturated complex **3** (generated by photolysis of $\text{Cp}^*\text{Rh}(\text{PMe}_3)_2$). The absence of KIE ($k_H/k_D = 1.05 \pm 0.06$) in the reaction of **3** and a 1/1 mixture of $\text{C}_6\text{H}_6/\text{C}_6\text{D}_6$ indicated no C–H bond breaking in the step in which the complexation of the arene occurs, which is consistent with the formation of the η^2 -complex as intermediate (Scheme 6). This data combined with the KIE observed in the reaction of **4** and 1,3,5-trideutero benzene ($k_H/k_D = 1.4$) (the oxidative cleavage of the C–H bond of the η^2 -complexed arene) is in agreement with the breakage of a C–H bond through a nonlinear transition state and, hence, with the coordination of the arene occurring prior to the oxidative addition.^{15d}

In parallel, the same research group determined an EIE ($K_H/K_D = 0.37$) for the H/D exchange between the hydride and the other positions around the arene ring.^{15d,29} With the EIE and the KIE for the oxidative cleavage, it is possible to calculate the kinetic isotope effect for the reductive coupling ($0.37 \times 1.4 = 0.52$), which is in good concordance with the experimental value ($k_H/k_D = 0.51$) obtained for the reductive elimination (reductive coupling plus dissociation) of *m*-xylene and *m*-xylene- d_1 , respectively, from the complexes $\text{Cp}^*\text{Rh}(\text{PMe}_3)(3,5\text{-C}_6\text{H}_3\text{Me}_2)\text{H}$ and $\text{Cp}^*\text{Rh}(\text{PMe}_3)(3,5\text{-C}_6\text{H}_3\text{Me}_2)\text{D}$ in C_6D_6 (Scheme 7). This study is an example in which the observed *inverse* KIE results from the combination of an *inverse* opposing a small *normal* isotope effect. The differences between intra- and intermolecular KIEs reported by Jones in this study have been a referent for other authors as evidence in favor of the formation of η^2 -complexes as intermediates in the arene C–H activation (see below).

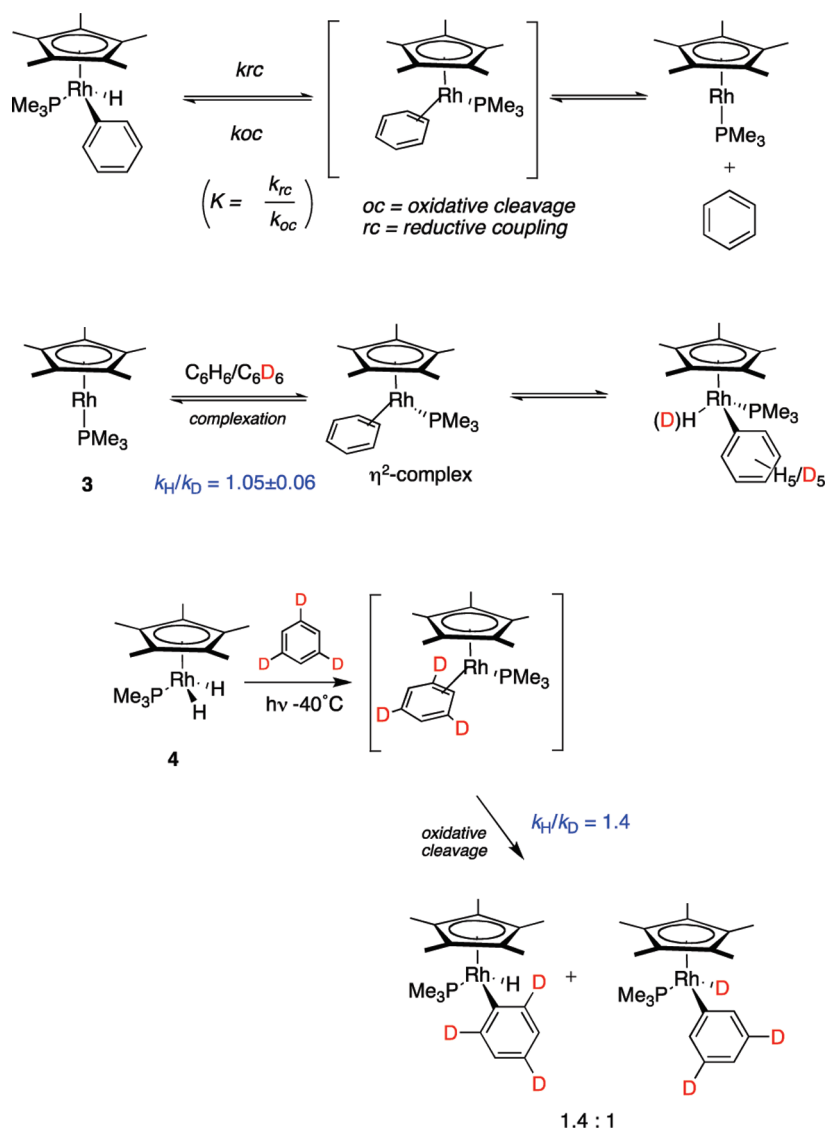
Scheme 4



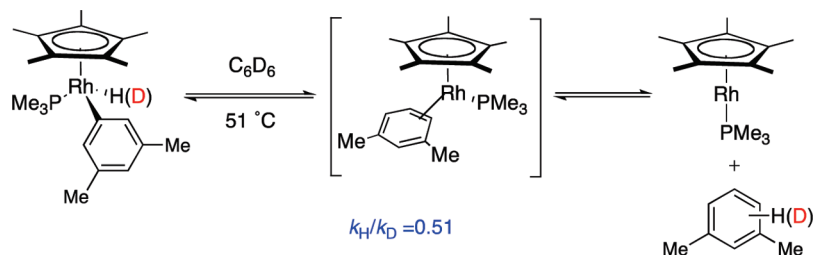
Scheme 5



Scheme 6



Scheme 7



The experimental difficulties in extracting KIEs for individual steps of a multistep process have turned the attention to the use of computational methods to complement the experimental isotope investigation. Conventional explanations of isotope effects rely on an assessment of zero-point energy (ZpE) differences between reactants and products (EIE) or between transition-state species (KIE) (see section 2). However, from the

results of many studies it became evident that a correct analysis of primary KIEs and EIEs in C–H activation processes cannot simply be achieved by considering only the ZpEs associated with the high-energy stretching frequencies.^{12,30} As the interpretations of EIEs based solely on ZpE differences are insufficient, a full statistical mechanical treatment of the isotopic equilibrium is required to complement the experimental information.

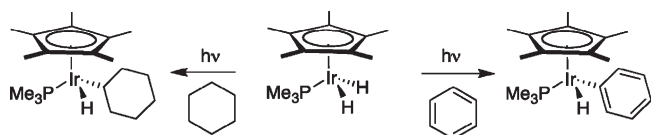
This theoretical-experimental approach has been used recently by Parkin and co-workers in their studies of the temperature dependence of isotope effects in C–H and H–H interactions with transition metal centers.^{12,18,31} Most reported KIEs arise from single-temperature measurements. However, in these studies it was found that, depending upon the temperature, both *normal* and *inverse* EIEs may be obtained for coordination of a C–H bond in the same system. This unusual behavior may be rationalized by considering the different molecular, translational, rotational, and vibrational partition functions whose ratios contribute to the EIEs.³¹

3.2. KIEs in the Study of C–H Activation Mechanisms by Ir Complexes

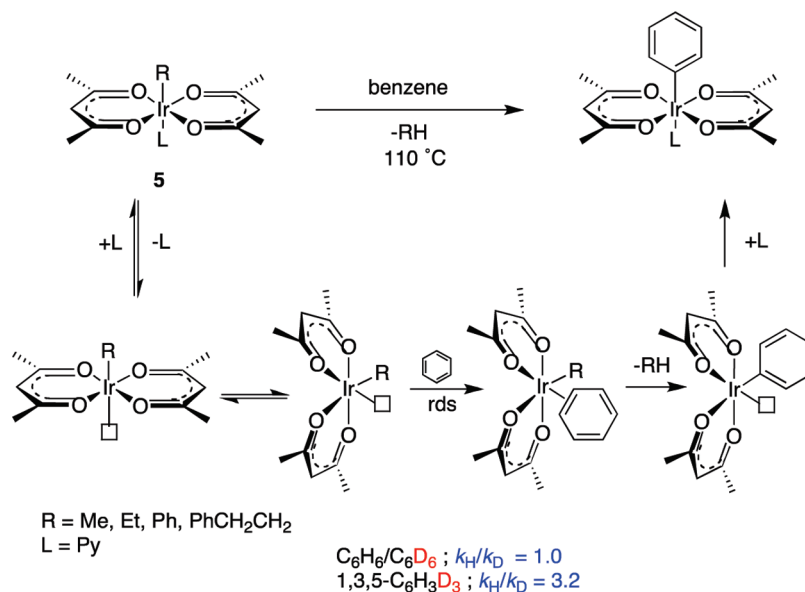
Since the pioneering studies by Janowicz and Bergman in 1982,³² reporting the oxidative addition of benzene and cyclohexane to a photochemically generated reactive Ir(I) species (Scheme 8), many other iridium complexes have been used in the mechanistic studies of hydrocarbon activation.

The procedure reported by Jones and Feher^{15d} comparing the deuterium KIE obtained with a mixture of C₆H₆ and C₆D₆ with that for 1,3,5-trideuterobenzene was also used by Periana and co-workers³³ to study the mechanism of CH activation with (acac-O, O)Ir(R)(L) complexes **5**. The experiments allow the distinction between a mechanism involving rate-determining benzene coordination or rate-determining CH cleavage (assuming negligible secondary isotope effects). In this case, the kinetic deuterium isotope effects obtained in the reaction of **5** with C₆H₆/C₆D₆ ($k_{\text{H}}/k_{\text{D}} = 1.0$) and with 1,3,5-C₆H₃D₃ ($k_{\text{H}}/k_{\text{D}} = 3.2$) were consistent with the CH activation proceeding through four key steps: (a) preequilibrium loss of pyridine that generates a *trans*-five-coordinate, square-pyramidal intermediate; (b) unimolecular isomerization of the *trans*-five-coor-

Scheme 8



Scheme 9

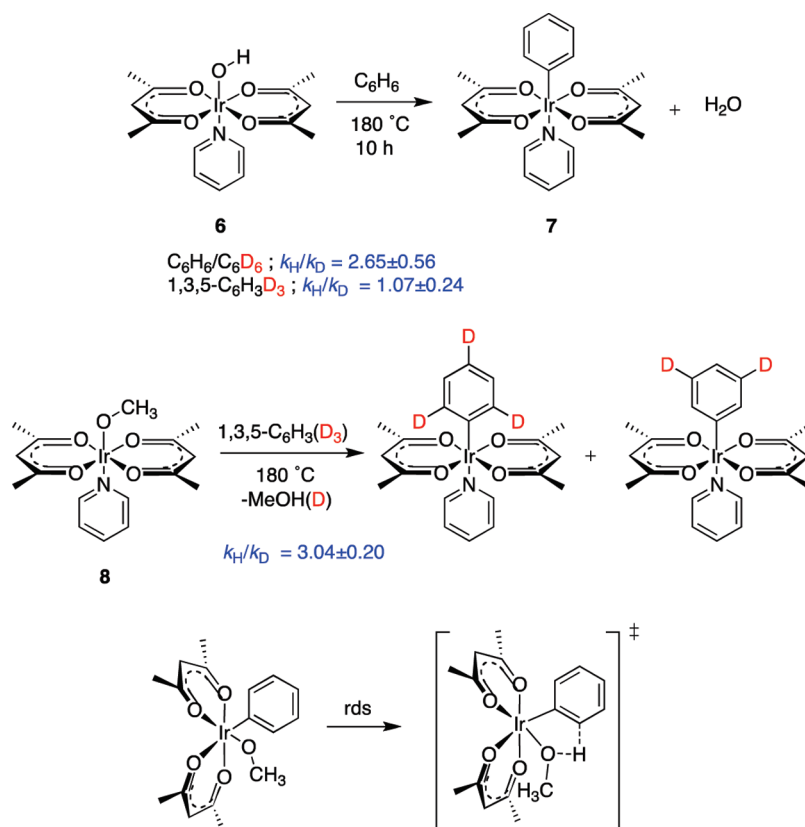


dinate to generate a *cis*-five-coordinated intermediate; (c) rate-determining coordination of this species to benzene to generate a discrete benzene complex; and (d) rapid C–H cleavage (Scheme 9).

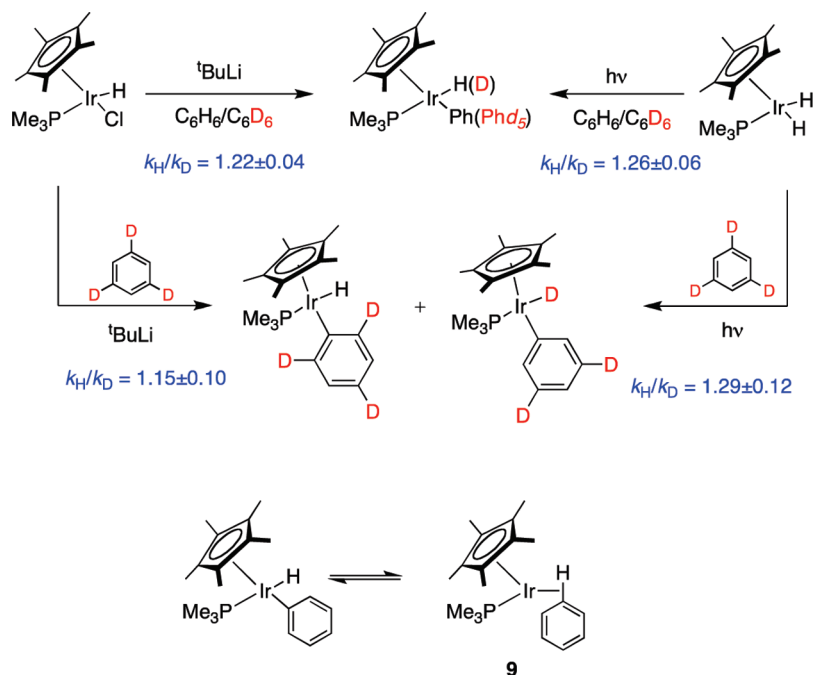
Subsequently, the same research group³⁴ used a similar methodology to study the reaction of stable hydroxo complex **6** with benzene to generate the corresponding phenyl complex **7** with cogeneration of water. An inverse dependence of the H/D exchange rate on added pyridine, the KIE values ($k_{\text{H}}/k_{\text{D}} = 2.65 \pm 0.56$ for CH activation with 1,3,5-trideuteriobenzene and $k_{\text{H}}/k_{\text{D}} = 1.07 \pm 0.24$ with C₆H₆/C₆D₆), and DFT calculations were consistent with the CH activation proceeding via rate-determining benzene coordination followed by fast CH cleavage through a σ -bond metathesis transition state. However, theoretical-experimental studies of C–H activation in the structurally referable Ir(acac)₂(OCH₃)(C₆H₆) suggested a change in the rds and an internal electrophilic substitution (IES) mechanism instead of a σ -bond metathesis. In the IES mechanism, the C–H activation in the transition state was proposed to occur by direct hydrogen transfer from benzene to the OMe group. The experimental KIE was determined to be $k_{\text{H}}/k_{\text{D}} = 3.04 \pm 0.20$ by reaction of **8** with neat 1,3,5-trideuterobenzene, and it was in good agreement with the computationally predicted value ($k_{\text{H}}/k_{\text{D}} = 3.2$) (Scheme 10).³⁵

Bergman's group reported the viability of σ -intermediates instead of the expected η^2 -complexes in arene C–H activation in iridium complexes. By comparing the inter- and intramolecular KIEs ($k_{\text{H}}/k_{\text{D}} = 1.20 \pm 0.02$) and ($k_{\text{H}}/k_{\text{D}} = 1.28 \pm 0.04$), respectively, for the oxidative addition of benzene to [Cp*Ir(η^3 -allyl)IrH]³⁶ with those previously observed by Jones for the precomplexation of benzene in the closely related [Cp*(PMe₃)Rh] system ($k_{\text{H}}/k_{\text{D}} = 1.05$ and $k_{\text{H}}/k_{\text{D}} = 1.4$, see above),^{15d} they concluded that the difference was not significant enough to postulate η^2 -coordination of benzene prior to the oxidative addition. An analogous experiment of benzene activation performed with [Cp*Ir(PMe₃)], generated by two different activation methods (Scheme 11), revealed almost identical inter- and intramolecular isotope effects within experimental error.³⁷ These results suggested the arene precomplexation in the iridium system through a C–H benzene σ -complex **9** instead of the generally proposed π -complex.

Scheme 10



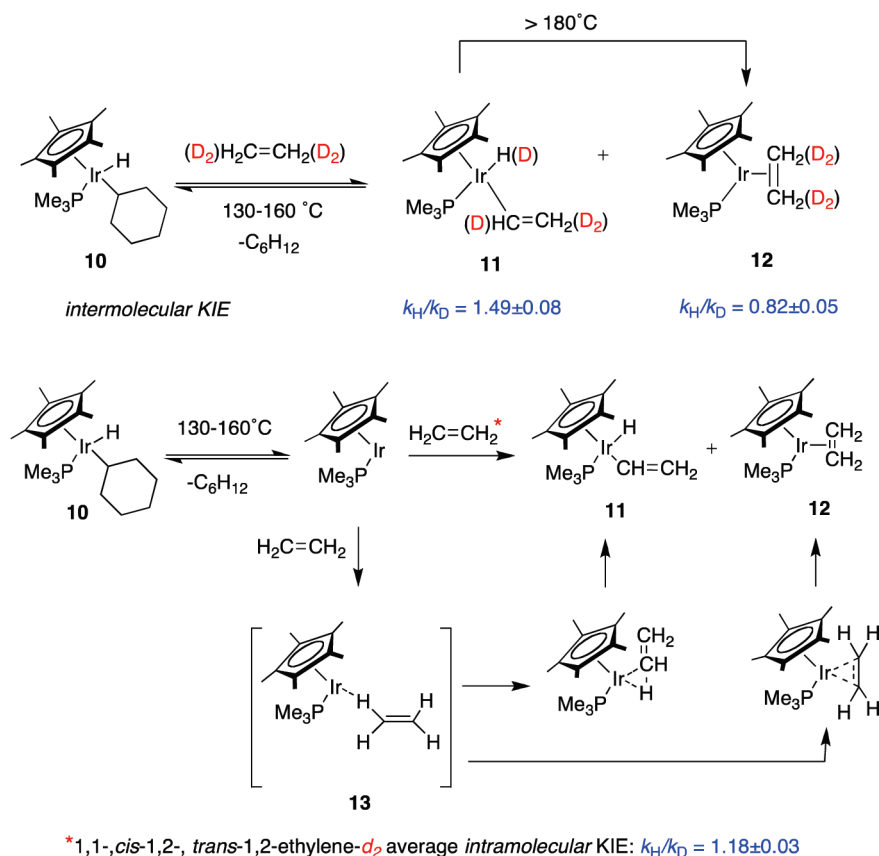
Scheme 11



Bergman and co-workers^{32,38} also used the analysis of inter- versus intramolecular KIEs to establish the nature of the intermediate complexes in the insertion of unactivated olefins into

C–H bonds. Thermolysis of the iridium cyclohexyl hydride **10** in the presence of ethylene yields a mixture of the C–H insertion product **11** and the π -ethylene complex **12**. This product can be

Scheme 12



obtained from thermolysis of **11**. The relative reaction rates of **10** with ethylene and ethylene- d_4 allowed the determination of an average KIE for the ethylene C–H insertion of $k_{\text{H}}/k_{\text{D}} = 1.49 \pm 0.08$, a primary isotope effect probably associated to an early transition state. In turn, the secondary KIE for the formation of π -complex **12** was $k_{\text{H}}/k_{\text{D}} = 0.82 \pm 0.05$. Similarly, intramolecular isotope effects were obtained by thermolysis of **10** in the presence of each of the isomers of ethylene- d_2 (ethylene-1,1- d_2 , *cis*-ethylene-1,2- d_2 , and *trans*-ethylene-1,2- d_2), leading to an average value of $k_{\text{H}}/k_{\text{D}} = 1.18 \pm 0.03$. The comparison of *inter*- and *intramolecular* KIEs for the ethylene C–H insertion cannot be accommodated by a π -alkene intermediate structurally referable to **12** but by an intermediate that, on the average, has access to all the hydrogen and deuterium atoms in each isomer of the C–H-coordinated ethylene on a time scale that is rapid with respect to further reaction of the intermediate. Rapidly equilibrating σ -complexes **13** in Scheme 12 account for this result. The involvement of these species has been also discussed on computational grounds.³⁹

The difference in KIEs has been used to distinguish between C–H and C–C bond-activation pathways in the reaction of Ir complexes **14** and substituted cyclopropanes **15**–**18**.⁴⁰ Although the reaction products in all cases are π -allyl complexes **19**–**20**, the mechanism of the process depends on the substitution on the cyclopropane ring. Thus, the large KIE ($k_{\text{H}}/k_{\text{D}} = 3.8 \pm 0.3$) observed in the reaction of **14** and cyclopropanes **15-*d*₀**/**15-*d*₆** indicated that the reaction might proceed by initial C–H bond activation, followed by extrusion of methane, to afford cyclopropyliridium complex **21** (Scheme 13). However, the modest $k_{\text{H}}/k_{\text{D}}$ of 1.22 ± 0.03 measured in the reaction between **14** and a 1:1 mixture

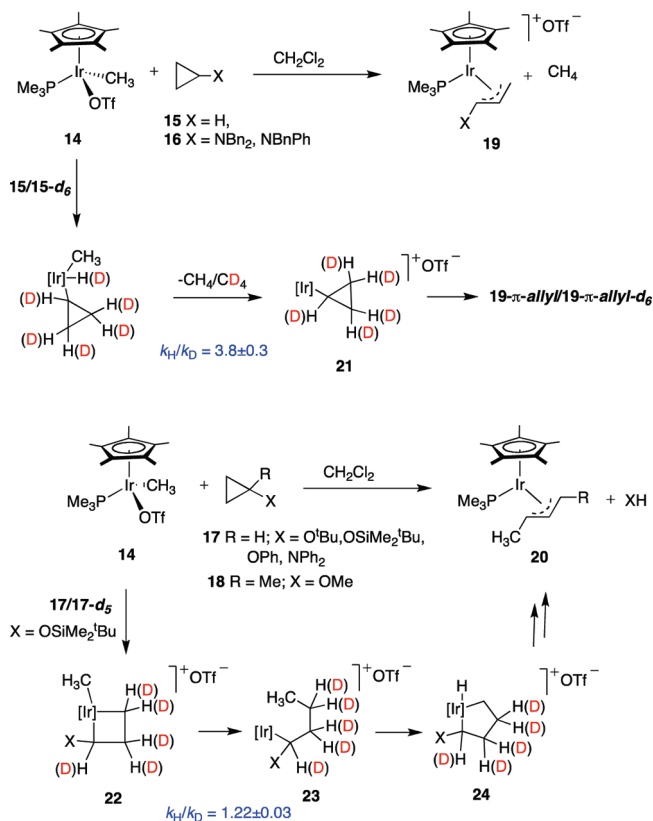
of siloxy ethers **17-*d*₀**/**17-*d*₅** argues against a C–H bond activation occurring during or before the rate-determining step. Therefore, the proposed most reasonable mechanistic alternative for the reaction of amino- and alkoxy-substituted cyclopropanes **17** and **18** and complex **14** involves initial C–C bond cleavage to yield metalacyclobutane **22** followed by C–C reductive elimination to afford the cationic complex **23**, and C–H bond activation of the terminal methyl to yield **24** (Scheme 13). Deuterium and ¹³C isotope labeling experiments supported this proposal, and several alternative evolution pathways for **24** to the final products were discussed.

Jones and co-workers⁴¹ reported the C–H activation of phenyl imines and 2-phenylpyridines by $[\text{Cp}^*\text{MCl}_2]_2$ (M = Ir, Rh). On the basis of the faster reaction rates with substrates having electron-donating substituents, the effect of polar solvents, and a large primary KIE ($k_{\text{H}}/k_{\text{D}} > 5$) observed in the reaction of $[\text{Cp}^*\text{IrCl}_2]_2$ and phenyl imine **25-*d*₀**/**25-*d*₅**, they proposed an electrophilic C–H activation mechanism in which cation $[\text{Cp}^*\text{M}(\text{OAc})]^+$ **26** is the species responsible for the electrophilic activation of the aromatic C–H bond. The KIEs observed indicate that C–H/C–D cleavage, not imine binding, must be the rate-determining step (Scheme 14).

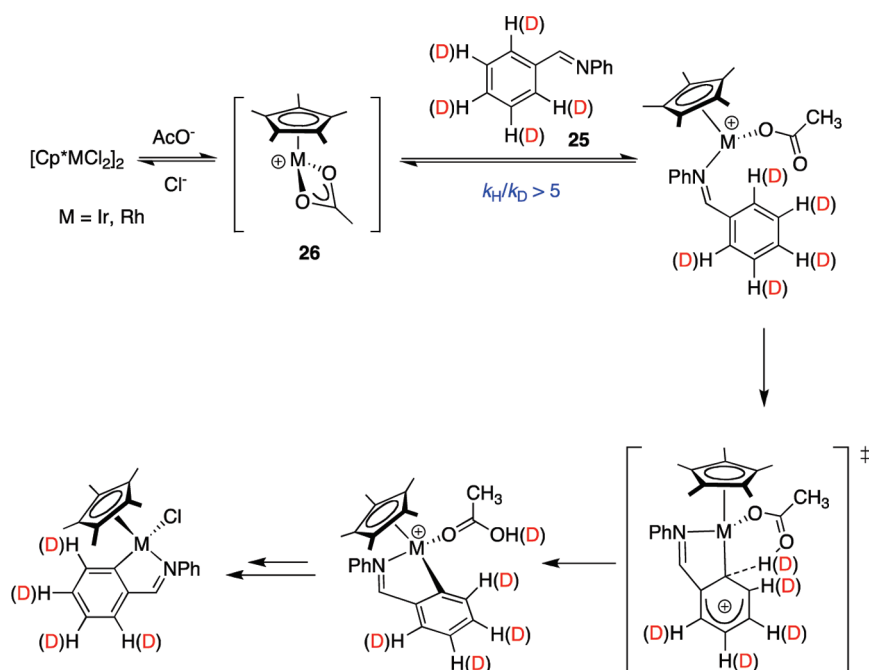
Crabtree⁴² and co-workers have reported a full study of double alkyne insertion into the Ir–H bond of *trans*-Ir(III) hydride **27** observing that different mechanisms operate depending on the alkyne structure. Deuterium labeling and crossover experiments for the reaction of **27** with electron-rich alkynes indicate that double insertion occurs stepwise, with each alkyne undergoing independent rearrangement to give a vinylidene intermediate and, finally, Ir(III) η^2 -butadienyl **28** (Scheme 15). Competition experiments with **27**

and phenylacetylenes **29** showed a kinetic isotope effect for the first alkyne to vinylidene rearrangement of $k_H/k_D = 1.5$, but no detectable KIE ($k_H/k_D = 1.0$) for the second. These results suggested that the C–H bond breaking required in this rearrangement was not the rds

Scheme 13



Scheme 14



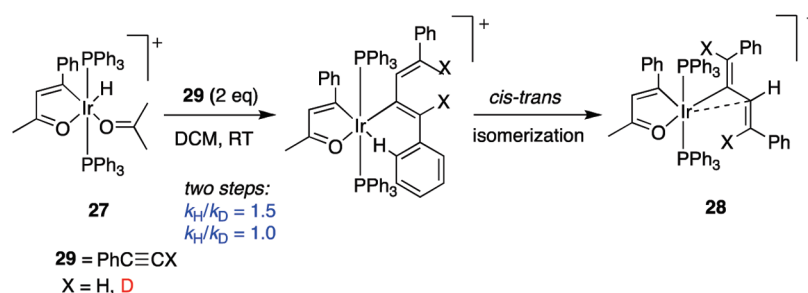
and supported a rate-determining slippage of an $\eta^2(\text{C}=\text{C})$ -alkyne intermediate to an $\eta^2(\text{C}=\text{H})$ -agostic species, in consonance with the known alkyne–vinylidene pathway.

The analysis of inter- ($k_H/k_D = 1.54 \pm 0.04$) and intramolecular ($k_H/k_D = 1.63 \pm 0.15$) KIEs was also used to study the benzene C–H insertion into dinuclear Ir complex **30**.⁴³ The values obtained (both close to 1.6) showed no significant difference between the two types of effects, in contrast with the previous studies by Jones.¹¹ Although the authors did not discard the involvement of a η^2 -arene complex in these processes, they postulated the intermediacy of coordinatively unsaturated dinuclear complex **31** rather than the analogous complex having benzene π -coordinated to one of the iridium centers (Scheme 16).

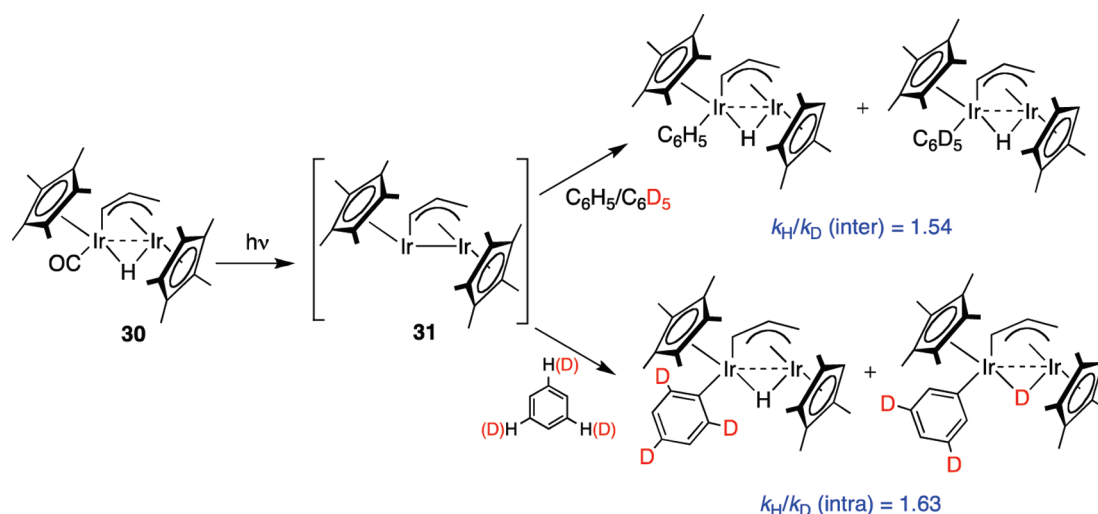
Nocera⁴⁴ and co-workers reported the first example of an *inverse* isotope effect involving C–H bonds measured in a bimetallic system. Arylation of Ir₂^{0,II}(tfepma)₃Cl₂ **32** (tfepma = bis[(bistrifluoroethoxy)phosphino]methylamine) with RMgBr (R = C₆H₅ and C₆D₅) is followed by C–H bond activation to furnish the bridging benzyne complex Ir₂^{II,II}(tfepma)₃(μ -C₆H₄)(C₆H₅)H **33** as the kinetic product. At ambient temperature, **33** undergoes redox isomerization to form Ir₂^{I,III}(tfepma)₃(μ -C₆H₄)(C₆H₅)H **34** (the thermodynamic product) in which the benzyne moiety is conserved and the Ir^{III} center is ligated by terminal hydride and phenyl groups. The isomerization of **33-d**₁₀ (obtained by reaction of **32** with C₆D₅MgBr) to **34-d**₁₀ yields a noticeable *inverse* isotope effect ($k_H/k_D = 0.44$), strongly indicating that the rate-determining step involves Ir–H(D)/C–H(D) bond-making/breaking events, with any subsequent rearrangement steps leading to the formation of **34** occurring quickly on the NMR time scale. The kinetic data collected, however, do not allow for the KIE to be assigned as an *inverse* equilibrium isotope effect or a true *inverse* kinetic isotope effect for a single step (Scheme 17).

Goldman and colleagues⁴⁵ have recently proposed an unusual mechanism to explain the oxidative addition of pincer-ligated iridium complex **35** to anisole. On the basis of a high KIE ($k_H/k_D = 4.3 \pm 0.03$) and DFT calculations, the authors discard a S_N2 mechanism and

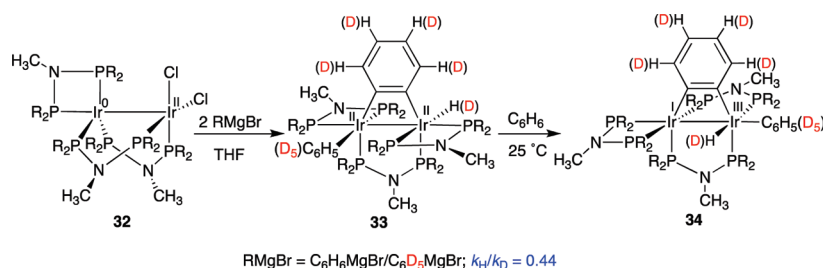
Scheme 15



Scheme 16



Scheme 17



instead propose a methoxy $\text{C}(\text{sp}^3)\text{—H}$ activation followed by α -aryloxy elimination and subsequent 1,2-migration of H from Ir to an intermediate carbene (Scheme 18). The proposal, however, cannot account for the results obtained in the reactions of **35** with ethyl aryl ethers.

3.3. KIEs in the Study of C—H Activation Mechanisms by Pt Complexes

Pt complexes are capable of activating aliphatic and aromatic C—H bonds. The strong Pt—H and Pt—C bonds that can be formed in a C—H activation reaction undoubtedly contribute to the success of these processes. C—H activation can occur at complexes that have cationic, neutral, and anionic metal centers with Pt in formal oxidation states 0, +2, and +4. Additionally, Pt complexes are capable of reacting by diverse mechanisms (Scheme 19), including oxidative

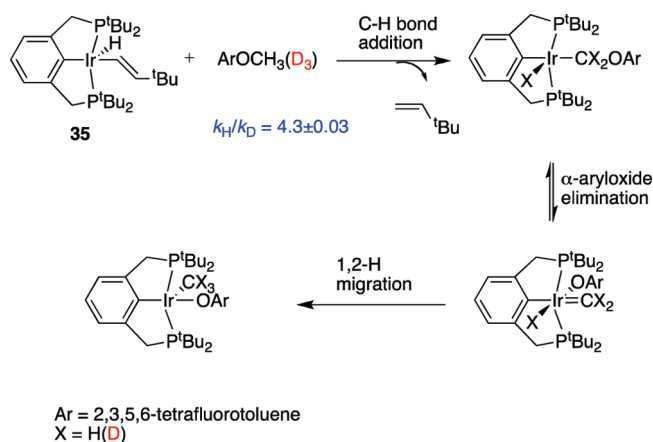
addition (a) involving a Pt(IV) octahedral, 18-electron species, and electrophilic substitution (b), the actual C—H activation mechanism being determined not only by the nature of the metal center but also by the reaction conditions (Scheme 19).^{9a–d,15a,46}

3.3.1. Protonolysis of Pt(II) Complexes. As the protonation of the Pt—C bond is the *microscopic reverse* of C—H bond activation by platinum complexes (see Scheme 19), the mechanism of protonolysis of Pt(II) complexes has received considerable attention. Early studies by Romeo and colleagues⁴⁷ discussed the intermediacy of aryl(hydrido)platinum(IV) species in the cleavage of *cis*-arylplatinum(II) complex **36** with HCl to give *cis*-[PtClAr(PEt₃)₂] **37** and ArCl. The large kinetic isotope effect ($k_H/k_D \approx 6$) observed with DCl in MeOD/D₂O for *cis*-[PtAr₂(PEt₃)₂] (Ar = *p*-MeO-Ph and *p*-Me-Ph) complexes **36** provided solid evidence for the

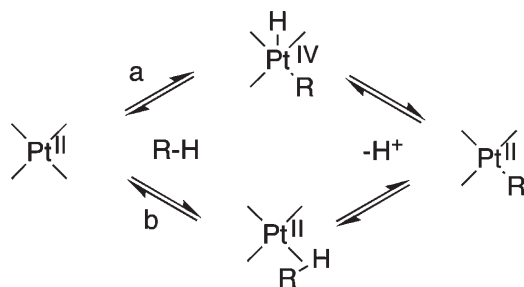
protonolysis as the rate-determining step. This argument, together with the fact that intermediates **38** were not directly detected, was considered against a stepwise prior oxidative addition on the central metal followed by reductive elimination (S_{Eox} mechanism). High KIEs ($k_{\text{H}}/k_{\text{D}} = 15\text{--}16$) in the reaction of tetramethyl platinum complexes with acids⁴⁸ or in the studies of protonolysis of the Pt–Me bond in *trans*-[Pt(PEt₃)₂(Ar)(Me)] ($k_{\text{H}}/k_{\text{D}} = 7$)⁴⁹ have been claimed also as strong evidence for a concerted attack at the metal–carbon bond (S_{E2} protonolysis mechanism) for platinum involving substantial proton transfer in the transition state (Scheme 20).

A study from Bercaw's group⁵⁰ provided a detailed understanding of the mechanism of protonation of several alkylplatinum(II)

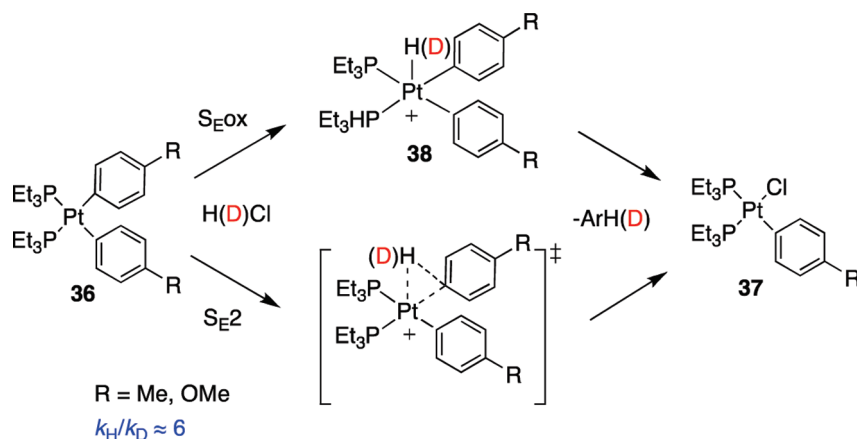
Scheme 18



Scheme 19



Scheme 20



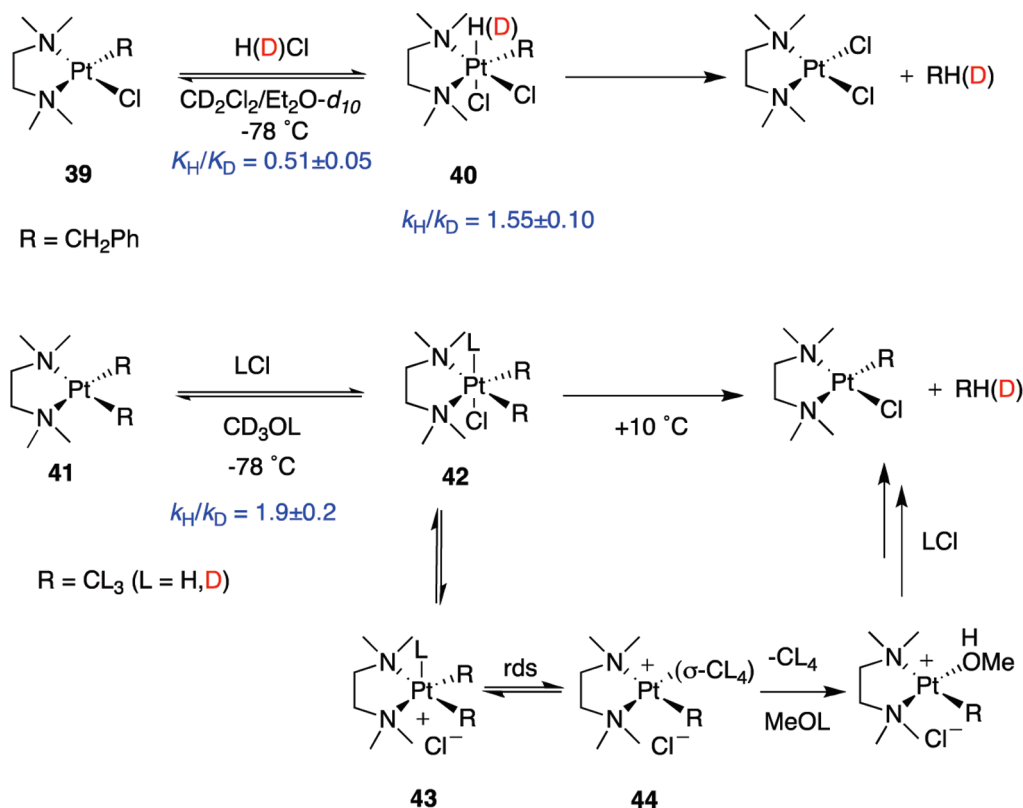
complexes. Protonation of (tmeda)Pt(R)(Cl) (R = Me, CH₂Ph) complexes **39** (tmeda = *N,N,N',N'*-tetramethylethylenediamine) with HCl in CD₂Cl₂ at $-78\text{ }^{\circ}\text{C}$ led to reversible formation of observable Pt(IV) hydrides **40**, which eliminated methane or toluene upon warming (Scheme 21). A mechanistic study of complex **39** indicated that the HCl addition was reversible ($K_{\text{H}}/K_{\text{D}} = 0.51 \pm 0.05$ at $-28\text{ }^{\circ}\text{C}$) and the reductive elimination was clearly associative ($\Delta S^{\ddagger} = -77 \pm 29\text{ J K}^{-1}\text{ mol}^{-1}$), exhibiting a $k_{\text{H}}/k_{\text{D}} = 1.55 \pm 0.10$ for the overall toluene elimination ($k_{\text{H}}/k_{\text{D}} = 3.1 \pm 0.6$ calculated only for the elimination step). The observed KIE values pointed to the C–H elimination as the rds of the process.

Protonation of (tmeda)Pt(Me)₂ complexes **41** with HCl in CD₃OD/CD₂Cl₂ also generated Pt(IV) hydrides. The H/D exchange kinetics into the Pt–Me groups revealed a $k_{\text{H}}/k_{\text{D}} = 1.9 \pm 0.2$ ($-47\text{ }^{\circ}\text{C}$) and the overall reductive elimination showed $k_{\text{H}}/k_{\text{D}} = 0.29 \pm 0.05$ ($-27\text{ }^{\circ}\text{C}$), with both processes being inversely dependent on the rate on [Cl[−]]. The experimental data are in agreement with reversible protonation of **41** to give the observed Pt(IV) hydridoalkyl species **42** that, after dissociation, generates the cationic pentacoordinate intermediate **43**. This species reversibly undergoes reductive coupling to give the σ -methane intermediate **44**, crucial to H/D exchange and the *inverse* isotope effect. The KIE value implies that C–H reductive coupling, rather than R–H elimination, is the rds of the process (Scheme 21).

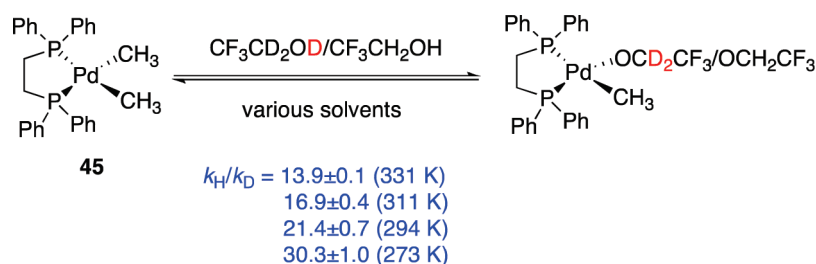
The same research group⁵¹ reported large KIEs ($k_{\text{H}}/k_{\text{D}} \approx 20$) for the protonolysis of several dimethylpalladium(II) complexes **45** with trifluoroacetyl (TFA) at room temperature, in sharp contrast with the *inverse* or *normal* KIEs reported for the corresponding Pt(II) analogues (see above) (Scheme 22). Exceptionally, a $k_{\text{H}}/k_{\text{D}} = 17.5 \pm 0.3$ ($21\text{ }^{\circ}\text{C}$) was determined for the TFA protonolysis of platinum complex (COD)Pt^{II}(CH₃)₂ (COD = 1,5-cyclooctadiene) structurally comparable to **45**.⁵¹ KIE values clearly >10 at room temperature suggested a significant contribution of quantum mechanical tunneling in the proton transfer reactions,⁶ which was confirmed from a study on the temperature dependence of the KIE in both types of complexes. The abnormally large KIEs and the observed tunneling effect observed for **45** and (COD)Pt^{II}(CH₃)₂ suggested a similar mechanism, although the authors could not decide between the direct protonation or oxidative addition pathways.

Protonation of *trans*-(PEt₃)₂Pt(Me)Cl **46** with HCl forms the Pt(IV) phosphine complex (PEt₃)₂PtCl₂(Me)(H) **47** that loses

Scheme 21



Scheme 22



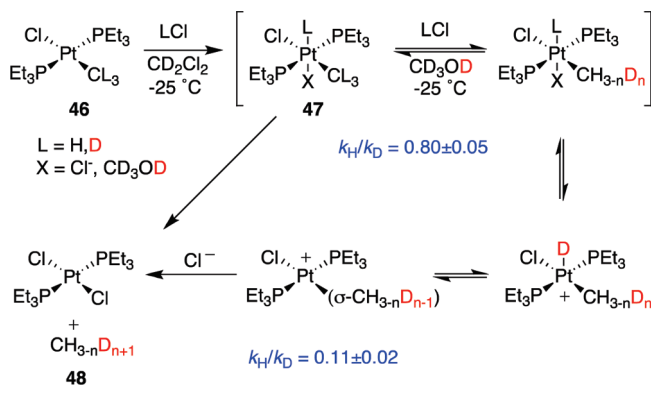
methane upon warming to form **48**.^{50a,b} Both the rate of H/D exchange and the rate of protonolysis/methane elimination were first-order dependent on $[\text{Cl}^-]$ with KIE values of $k_{\text{H}}/k_{\text{D}} = 0.80 \pm 0.05$ (-27°C) for H/D exchange and $k_{\text{H}}/k_{\text{D}} = 0.11 \pm 0.02$ (-12°C) for methane loss, respectively. To accommodate the findings, the authors proposed an initial solvent- or chloride-assisted protonation to generate the six-coordinate Pt(IV) hydride. Dissociation of the solvent or chloride provides a five-coordinate species, which after reductive coupling gives the σ -methane species responsible for the H/D exchange. This exchange is reversible in the absence of chloride. Excess chloride facilitates the rate-limiting methane elimination to form **48**, which is in agreement with the *inverse* KIEs observed (Scheme 23).

Romeo and D'Amico⁵² studied in detail the kinetic and NMR features of the protonolysis reactions on Pt(II) alkyl complexes of the types *cis*-[PtMe₂L₂], [PtMe₂(L–L)], *cis*-[PtMeClL₂], and [PtMeCl(L–L)] (L = PEt₃, P(Pr)₃, PCy₃, P(4-MePh)₃, L–L = dpmm, dppe, dppp, dppb) in MeOH and compared them with those of the corresponding *trans*-[PtMeClL₂] species. The deuterium

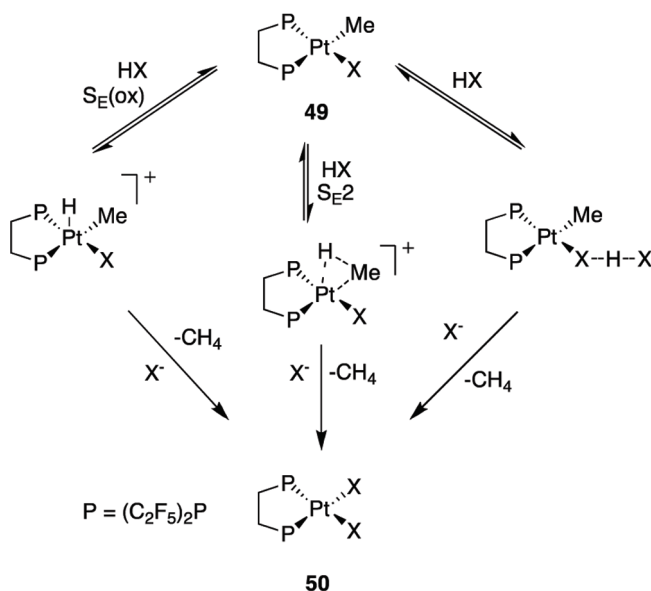
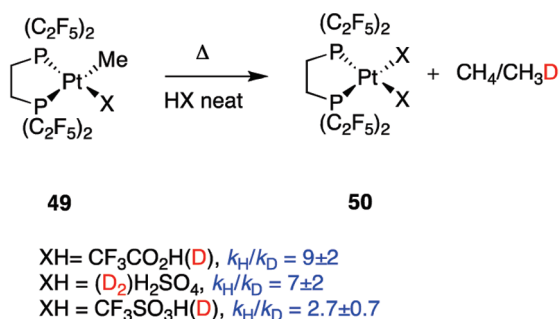
KIEs for the protonolysis of the Pt–methyl bond in the complexes were relevant. Thus, *cis*-[PtMe₂L₂] (and *cis*-[PtMeClL₂]) complexes showed *normal* KIE values ranging from 1.36 to 4.74, whereas *trans*-[PtMeClL₂] showed *inverse* KIEs in the range 0.38–0.69. On the basis of these and other experimental results, the authors propose a rate-determining proton transfer to the substrate (either to the Pt–C σ -bond or to the metal) for protonolyses on *cis*-[PtMe₂L₂] and *cis*-[PtMeClL₂]. In contrast, for the *trans*-[PtMeClL₂] species, *inverse* KIE values are more in agreement with a multistep oxidative–addition–reductive–elimination (S_{Eox}) mechanism involving the intermediacy of Pt(IV) species.

Protonolysis of (dfepe)Pt(Me)X complexes **49** (dfepe = (C₂F₅)₂PCH₂CH₂P(C₂F₅)₂; X = O₂CCF₃, OSO₂H, OSO₂CF₃, OSO₂F) in their respective neat acid solutions cleanly yield (dfepe)–Pt(X)₂ products **50** with rates dependent on relative acid strengths.⁵³ High $k_{\text{H}}/k_{\text{D}}$ values for the formation of **50** were obtained from competitive protonolysis studies (CF₃CO₂H, 9 ± 2 (20°C); H₂SO₄, 7 ± 2 (100°C); CF₃SO₃H, 2.7 ± 0.7

Scheme 23

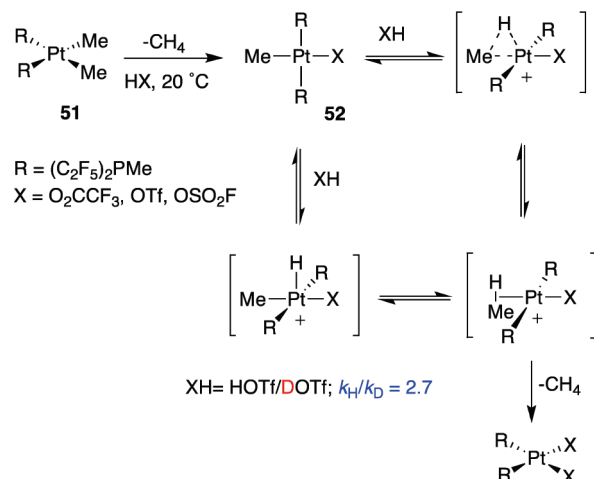


Scheme 24



(100 °C)). However, these values were taken with care as data obtained from $\text{CF}_3\text{CO}_2\text{H}$ in separate kinetic runs in protio and deuterio acids gave a lower $k_{\text{H}}/k_{\text{D}}$ value of 3.6 ± 0.4 . High KIEs have previously been cited as strong evidence for a concerted $\text{S}_{\text{E}}2$ protonolysis mechanism for platinum involving substantial proton transfer in the transition state.^{47a,48} However, the kinetic data and the negative entropy of activation found for $(\text{dfepe})\text{Pt}(\text{Me})(\text{OTf})$

Scheme 25



protonolysis are also consistent with either $\text{S}_{\text{E}}2$, $\text{S}_{\text{E}}\text{ox}$, or $\text{H}-\text{X}$ preassociation with coordinated X , because each of these pathways are associative in nature (Scheme 24).

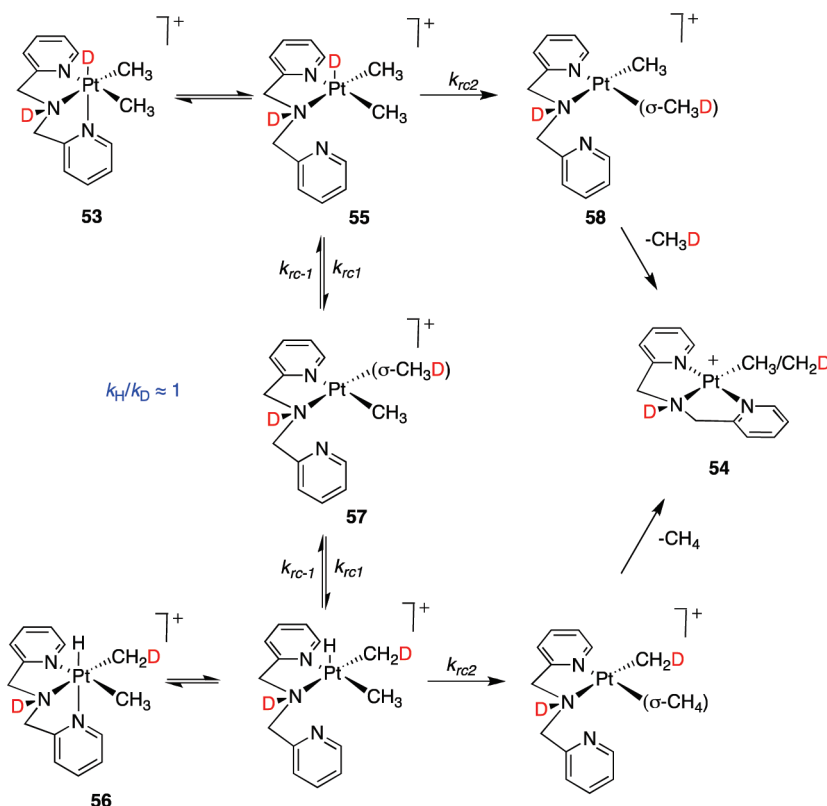
The reactivity of chelated Pt complexes **49** in Scheme 24 was compared with that of *cis*-($\text{PMe}(\text{C}_2\text{F}_5)_2$)₂ PtMe_2 **51** and *trans*-($\text{PMe}(\text{C}_2\text{F}_5)_2$)₂ $\text{Pt}(\text{Me})(\text{X})$ **52** (Scheme 25).⁵⁴ Dissolving **51** in neat trifluoroacetic, triflic, or fluorosulfonic acid at ambient temperature cleanly produces the corresponding *trans* complexes **52** that revealed a kinetic protolytic stability that is dependent on the nature of the *trans*- X ligand. Thermolysis of **52** in HOTf/DOTf resulted in deuteration of the methyl ligand prior to methane loss, indicating the reversible protonation to form a methane adduct intermediate with a $k_{\text{H}}/k_{\text{D}} = 2.7$, identical to the value observed for the *cis*-chelated Pt complex **49** ($\text{X} = \text{OTf}$).

The kinetics of methane reductive elimination from the stable *cis*-methyl(hydrido)-platinum(IV) complex $[\text{Pt}(\text{H})(\text{CH}_3)_2(\text{BPMA})]^+$ **53** (BPMA = bis(pyridylmethyl)amine) to form **54** were studied (*cis*, referring to the position of the hydride relative to the amine nitrogen).⁵⁵ Analysis of the H/D scrambling products in TfOD/acetone- d_3 (Scheme 26) demonstrated that D-scrambling occurred selectively into the Me *trans* to amine ($\text{Pt}-\text{CH}_2\text{D}$ but not $\text{Pt}-\text{CHD}_2$ was seen), and the rate of H/D scrambling was ca. 1.6 times faster than the methane elimination, with $k_{\text{H}}/k_{\text{D}} \approx 1$. These observations are rationalized in Scheme 26, where two H/D reductive coupling pathways are available from the five-coordinate platinum complex **55** as a steady-state intermediate. One is reversible ($k_{\text{rc1}}, k_{\text{rc-1}}$) and leads to scrambling (complex **56**) but not methane loss. The other is irreversible (k_{rc2}), somewhat slower, and leads to methane loss. The greater *trans*-influenced amine ligand weakens the *trans*-Pt-C bond, facilitating the C-H reductive coupling of the *trans*-methyl relative to the *cis*-methyl, causing $k_{\text{rc1}} > k_{\text{rc2}}$. However, the *trans*- σ -methane complex **57** has the wrong geometry to readily form the Pt(II) product, while the *cis*- σ -methane isomer **58** has the correct geometry. The pyridine is conveniently located for an intramolecular associative displacement of methane by a nucleophilic attack at Pt.

3.3.2. C-H Reductive Elimination from Pt(IV) Complexes.

The only thoroughly studied alkyl-H reductive eliminations from neutral Pt(IV) complexes without dissociable "X" ligands appear to be those of *fac*-(dppe)PtMe₃H and *fac*-(dppbz)PtMe₃H **59**.⁵⁶ Methane elimination occurs from both complexes at ambient temperature (Scheme 27). The kinetic parameters were essentially identical for both: $k_{\text{H}}/k_{\text{D}} = 2.2$ for *fac*-(dppe)PtMe₃-H(D) and

Scheme 26

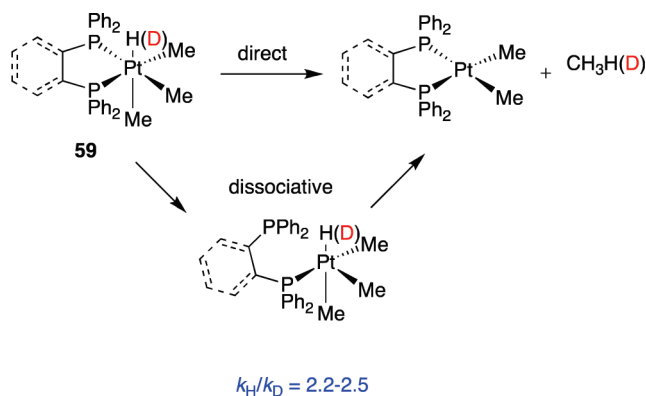


$k_H/k_D = 2.5$ for *fac*-(dppbz)PtMe₃H(D). Thermolysis of the monodeuterides in C₆D₆ yielded CH₃D as the only methane isotopomer. C–C reductive elimination proceeded dramatically faster from (dppe)PtMe₄ than from (dppbz)PtMe₄, which led to the conclusion that C–C elimination was a dissociative process, despite the presence of chelating phosphine ligands. The similarities of the kinetic parameters for elimination from the two hydridoalkyl complexes, with very different chelate rigidity, strongly suggest that a chelate opening cannot be operative here and that a direct elimination occurs. The isotope effects cannot be used to distinguish the mechanisms but do suggest that C–H reductive coupling, rather than alkane dissociation, is rate-limiting. The dissociative versus nondissociative nature of these elimination reactions has, in part, been confirmed by recent DFT-B3LYP computational studies on different stereoisomers of *cis*-(PH₃)₂PtCl₂(H)(CH₃) and *cis*-(PMe₃)₂PtCl₂(H)(CH₃) model systems.⁵⁶

3.3.3. C–H Activation by Cationic Pt(II) Complexes Having Diimine Ligands. The chemistry of Pt complexes having neutral N₂- and N₃-donor ligands relevant to C–H activation is extensive, as nitrogen-based ligands stabilize higher oxidation state complexes to a greater extent than phosphine ligands do. *Aquo* cationic Pt(II) diimine complexes **60** are capable of activating aromatic, benzylic, and aliphatic C–H bonds according to Scheme 28. Most mechanistic studies have been conducted in trifluoroethanol (TFE), a poorly coordinating solvent easily displaced by the hydrocarbon. The *aquo* and TFE complexes coexist in TFE solution.

The C–H activation is typically a multistep process, and the general picture is depicted in Scheme 29 for complex **61**. The first two steps are displacement of the coordinated solvent by

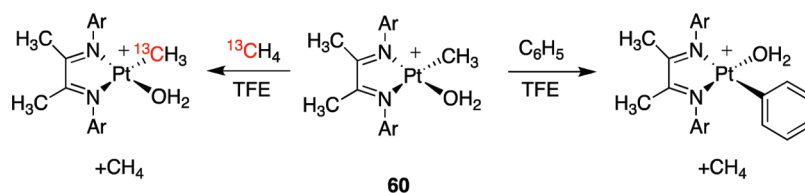
Scheme 27



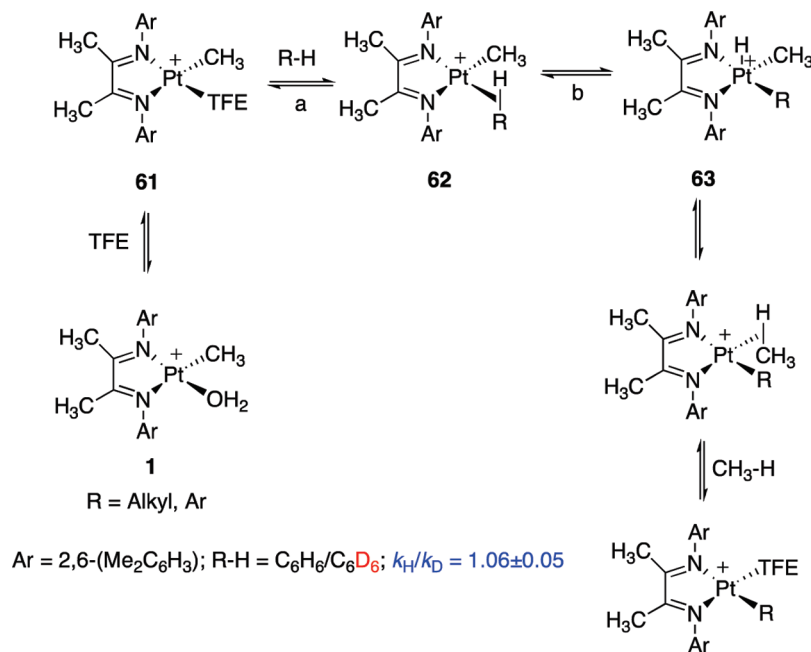
substrate (a), leading to an intermediate σ - or η^2 -complex **62**, followed by oxidative cleavage of the coordinated C–H bond (b), to generate a Pt(IV) alkyl hydride **63** that goes on to reductively eliminate methane. In principle, either path a or path b in Scheme 29 might be the rate-determining step, and in fact, the reversibility of the reaction and the identity of the rds are often at issue. As described below, the Bercaw/Labinger and Tilsted groups, who found a direct influence of the presence of relatively bulky *N*-aryl groups on the rds of the reaction, have carried out most of the mechanistic studies in solution.

Thus, the small KIE ($k_H/k_D = 1.06 \pm 0.05$ at 25 °C) observed by Bercaw and co-workers^{16b} in C₆H₆ versus C₆D₆ during the activation reaction of complexes **61** (Ar = 2,6-(Me₂C₆H₃)) is consistent

Scheme 28



Scheme 29



with a rate-limiting benzene coordination step rather than C–H bond cleavage (Scheme 29). Gerdes and Chen⁵⁷ carried out a similar study in the gas phase. The KIE observed was ~ 1 ($k_{\text{H}}/k_{\text{D}} = 1.18 \pm 0.06$), which was considered as evidence in favor of rate-determining benzene coordination, but suggesting that the solvent assistance by TFE at the transition state proposed previously was not operative. This assessment has been a subject of strong debate as it is extrapolating conclusions obtained in gas chromatograph (GC) gas-phase experiments to reactions in solution.⁵⁸

Zhong, Labinger, and Bercaw⁵⁹ also conducted a thorough investigation of the ligand electronic and steric effects in benzene activation at a series of cationic Pt(II) complexes **64**–**66** in TFE. Although the same rate law was obeyed in all cases, distinctly different reactivity patterns were recognized depending on the nature of the Ar groups (Figure 6). When the diimine *N*-aryl groups were sterically undemanding (complexes **64**, having substituents in the 3,4,5-positions), the kinetics exhibited a significant KIE in the range 1.6–2.2, in reactions of C₆H₆ / C₆D₆. This was accompanied by H/D scrambling from C₆D₆ into the methane product or the PtMe group of unconsumed reactant. On the other hand, when the *N*-aryl groups were 2,6-dimethyl-substituted (complexes **65**), the KIEs were near unity ($k_{\text{H}}/k_{\text{D}} \approx 1.1$) and significant scrambling of D from C₆D₆ occurred into the produced methane and the Pt–methyl group of unreacted Pt complex. Finally, when the methyl groups at the

diimine backbone in compounds **64** were replaced by H atoms (complexes **66**), KIEs as great as 3.6–5.9 and even less scrambling between C₆D₆ and reacting Pt–methyl were observed.

These results are consistent with rate-limiting C–H oxidative cleavage of a coordinated benzene C–H bond (step b in Scheme 29) as rate-limiting in complexes **64** and **66**, whereas the substitution of benzene for TFE (step a in Scheme 29) is the rds for the sterically demanding complexes **65**. The change in rate-limiting step also provides a rationale for the differences in the extent of isotope label exchange between C₆D₆ and Pt–Me in the products as well as in unreacted starting complexes. Also, KIEs consistent with the C–H activation step as rate-determining ($k_{\text{H}}/k_{\text{D}} = 4.1 \pm 0.5$) were reported⁶⁰ in the activation of substituted arenes with cationic (diimine)Pd(Me)(H₂O)⁺ complexes with substitution patterns related to **64**. In these cases, the reaction did not produce the corresponding phenyl complexes; however, they were invoked as intermediates that decomposed by disproportionation or ligand redistribution to give biaryls.

Tilset and colleagues⁶¹ have used KIEs combined with spin-saturation transfer (SST) and qualitative ¹H NMR EXSY spectroscopy to study arene C–H activation reactions. Protonation of complex **67** yields phenyl/ π -benzene Pt(II) complex **68** in noncoordinating solvents and hydridodiphenyl Pt(IV) species in coordinating solvents. The SST and EXSY spectra demonstrate that the phenyl and π -benzene ligand protons in the Pt(II)

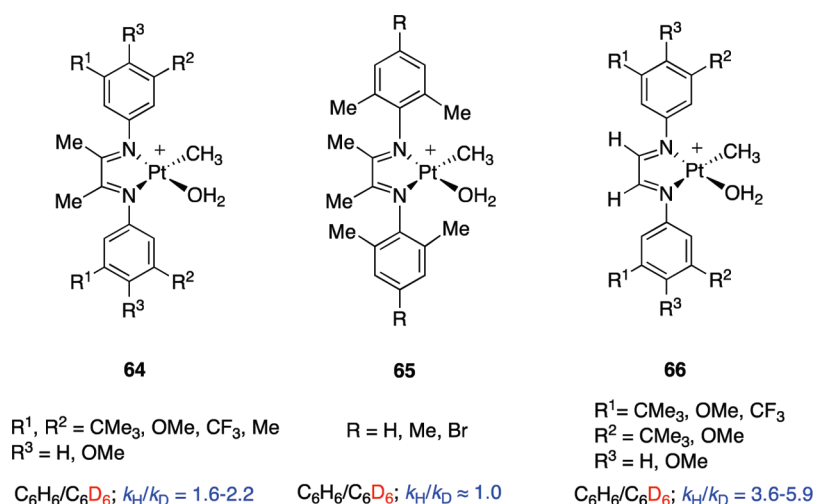
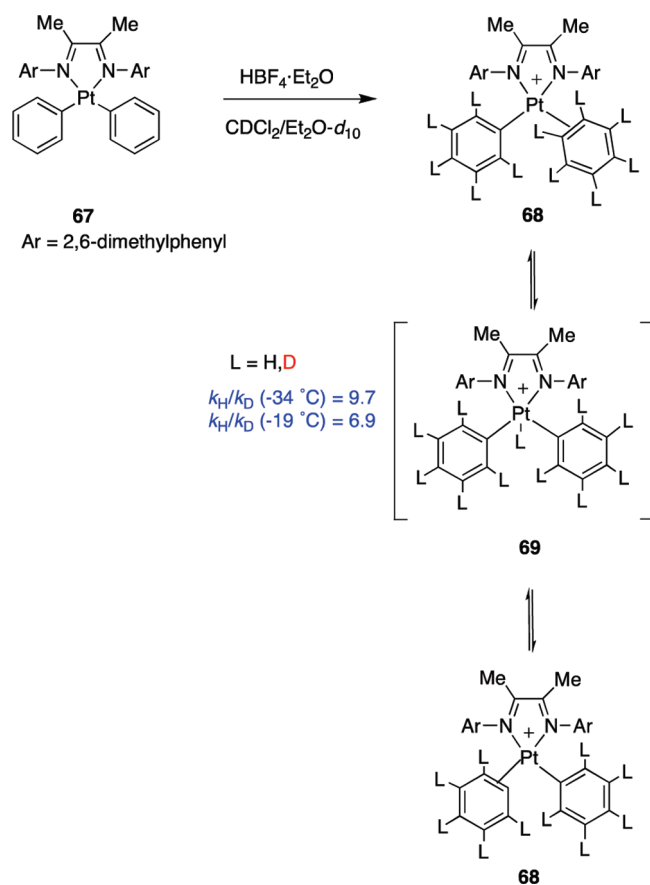


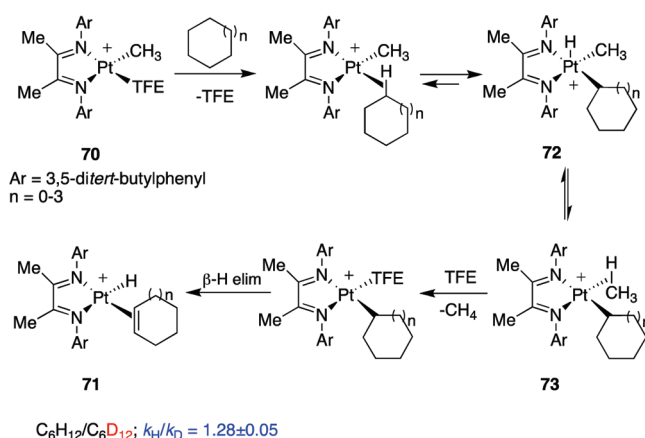
Figure 6

Scheme 30



species **68** undergo dynamic exchange processes that most likely involve facile C–H bond cleavage reactions that access Pt(IV) hydridodiphenyl intermediates **69**. A large, strongly temperature-dependent H/D kinetic isotope effect ($k_{\text{H}}/k_{\text{D}} = 9.7$ at -34°C ; $k_{\text{H}}/k_{\text{D}} = 6.9$ at -19°C) was measured for the dynamic behavior of **68-d₀** versus **68-d₁₀**, consistent with the proposed π -benzene C–H bond cleavage (Scheme 30).

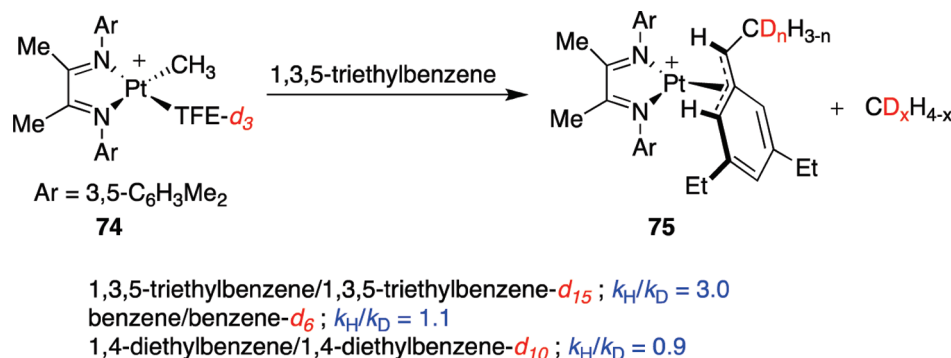
Scheme 31



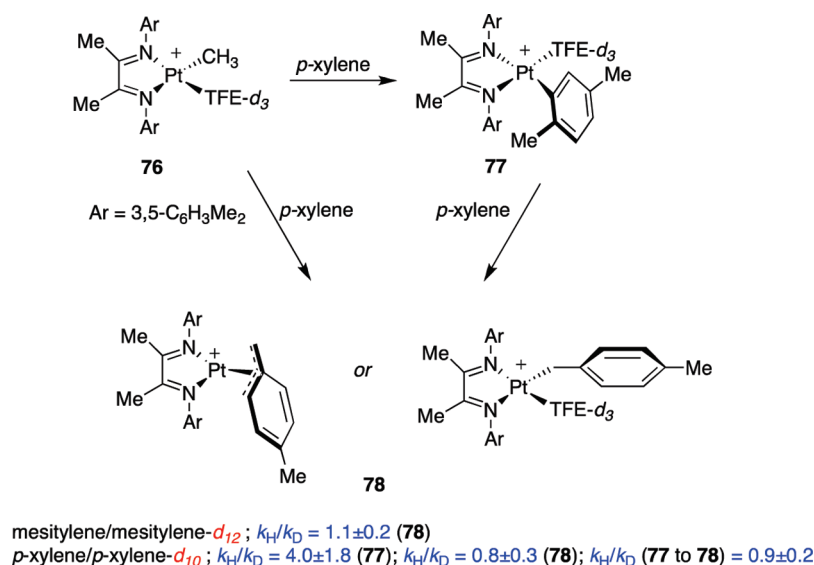
The rates of C–H bond activation for various linear and cyclic alkanes by cationic complex **70** (Ar = 3,5-di-*tert*-butylphenyl) were studied.⁶² The reaction affords the corresponding alkene–hydride cation $[(N\text{--}N)\text{Pt}(\text{H})(\text{alkene})]^+$ **71** (Scheme 31). The small KIE ($k_{\text{H}}/k_{\text{D}} = 1.28 \pm 0.05$) for cyclohexane, together with statistical isotopic scrambling in the methane released, suggested a mechanism in which C–H bond coordination is rate-determining and is followed by (i) fast oxidative cleavage of the coordinated C–H bond to give a Pt(IV) alkyl–methyl–hydride intermediate **72**, (ii) reductive coupling to generate a methane σ -complex **73**, (iii) dissociation of methane, and (iv) β -H elimination to form the observed product. The small KIE is similar to values measured for iridium- and rhodium-based C–H activation systems where C–H coordination is rate-determining ($k_{\text{H}}/k_{\text{D}} = 1.1\text{--}1.4$).^{14b,24b}

A change in the rds from coordination to oxidative addition of the ethyl C–H bond has been reported by Bercaw and co-workers⁶³ in the reaction of diimine Pt(II) methyl cations **74** with bulky 1,3,5-triethylbenzene. The KIE value ($k_{\text{H}}/k_{\text{D}} = 3.0$) was compared with benzene and 1,4-diethylbenzene KIEs ($k_{\text{H}}/k_{\text{D}} = 0.9\text{--}1.1$), suggesting that the initial activation occurs at aryl C–H bonds with subsequent conversion to the η^3 -benzyl product **75** via intramolecular isomerization (Scheme 32).

Scheme 32



Scheme 33

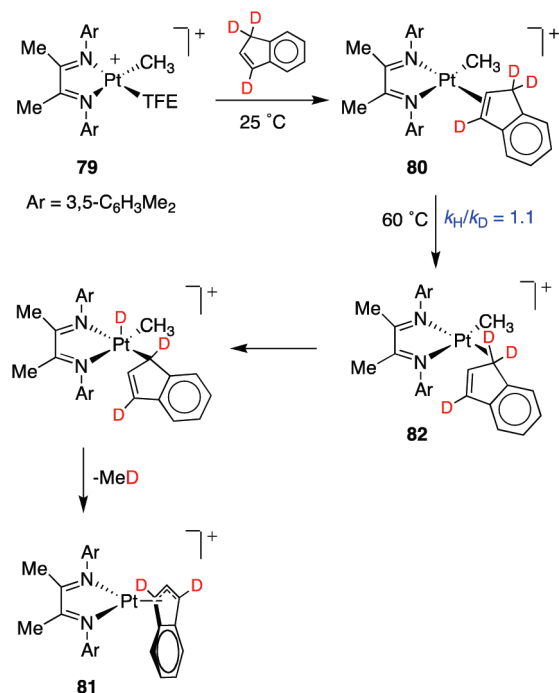


The selectivity of aryl versus benzylic C–H bond activation with cationic Pt(II) complexes was studied in the reaction of the anhydrous cationic Pt(II) complex **76** with substituted benzenes.⁶⁴ Although previous observations on reactions of methylbenzenes with Pt(II) complexes supported an apparent strong preference for aromatic activation (which could be overridden by steric crowding),⁵⁹ the conclusions of the study were somewhat surprising. Whereas C–H activation at mesitylene occurred exclusively at the benzylic position ($k_{\text{H}}/k_{\text{D}} = 1.1 \pm 0.2$), *p*-xylene reacted with **76** to give products of both aromatic (Pt–(2,5-Me₂C₆H₃), **77**) and benzylic (Pt–(CH₂C₆H₄Me), **78**) activation. However, the initial product distribution was not stable. *p*-Xylene aromatic activation was preferred ($k_{\text{H}}/k_{\text{D}} = 4.0 \pm 1.8$) over benzylic activation ($k_{\text{H}}/k_{\text{D}} = 0.8 \pm 0.3$), but the product of benzylic activation **78** is thermodynamically preferred (Scheme 33). This conversion displayed first-order dependence on *p*-xylene concentration ($k_{\text{H}}/k_{\text{D}} = 0.9 \pm 0.2$), indicating a reaction of **77** with *p*-xylene rather than an intramolecular isomerization process. The difference in KIEs for sp² and sp³ C–H bond activation was unexpected, and the thermodynamic preference for benzylic C–H activation appears to result from the additional contribution of the η^3 -bonding that might stabilize **78** relative to **77**.^{16b}

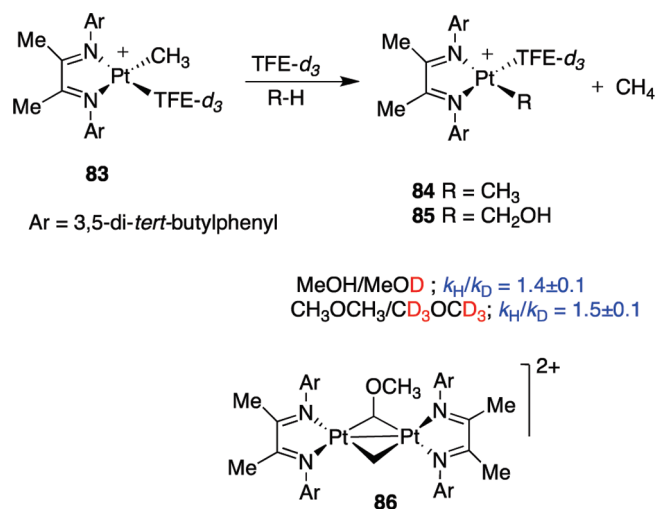
Indene and substituted indoles displace the TFE ligand from platinum cationic diimine complexes **79** to form stable π -coordination complexes **80** that, upon heating, underwent the C–H activation complexes **81**. The first-order kinetics, the small positive value for ΔS^\ddagger (10 eu), and the small KIE ($k_{\text{H}}/k_{\text{D}} = 1.1$ at 60 °C) determined for the conversion of indene- d_3 to deuterated indenyl complex **81** are suggestive of an intramolecular **80**-to-**81** process *not* involving rate-determining C–H oxidative addition. A mechanistic scenario that is in accord with these features involves rate-determining rearrangement of π -complex **80** to C–H σ -complex **82**, followed by more rapid C–H oxidative cleavage and reductive elimination of methane (Scheme 34).⁶⁵

Cationic Pt(II) complexes **83** have been used as a model to investigate the relative rates and mechanism of C–H activation for methane, methanol, and dimethyl ether (DME).⁶⁶ Whereas the activation products from methane and methanol **84** and **85** could be characterized, the reaction with DME yielded the methoxymethylene-bridged dimer **86**. The C–H activation relative rates show that the platinum center is relatively unselective: $k_{\text{methane}}/k_{\text{methanol}} = 1/1.3$, 330 K and $k_{\text{methane}}/k_{\text{dimethyl ether}} = 1/2$, 313 K. The low selectivities in this model suggest that C–H coordination is probably rate-determining. The small KIEs (methanol $k_{\text{H}}/k_{\text{D}} = 1.4 \pm 0.1$, dimethyl ether $k_{\text{H}}/k_{\text{D}} = 1.5 \pm 0.1$) are consistent with this

Scheme 34



Scheme 35

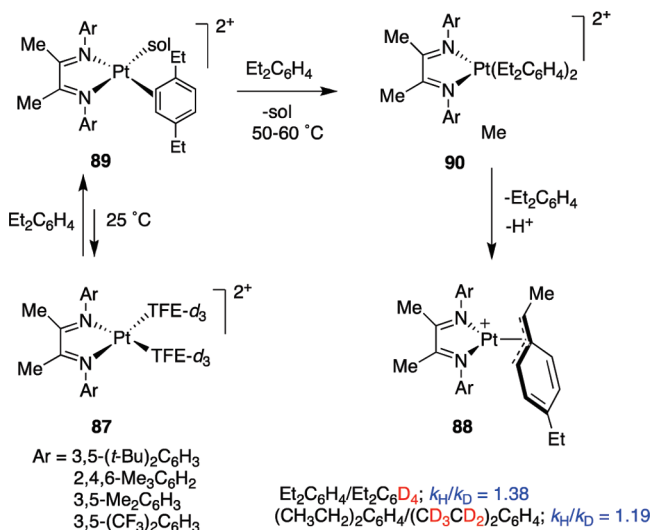


assumption, and displacement of TFE by a C–H bond appears to be the rate-determining step for all three substrates (Scheme 35).

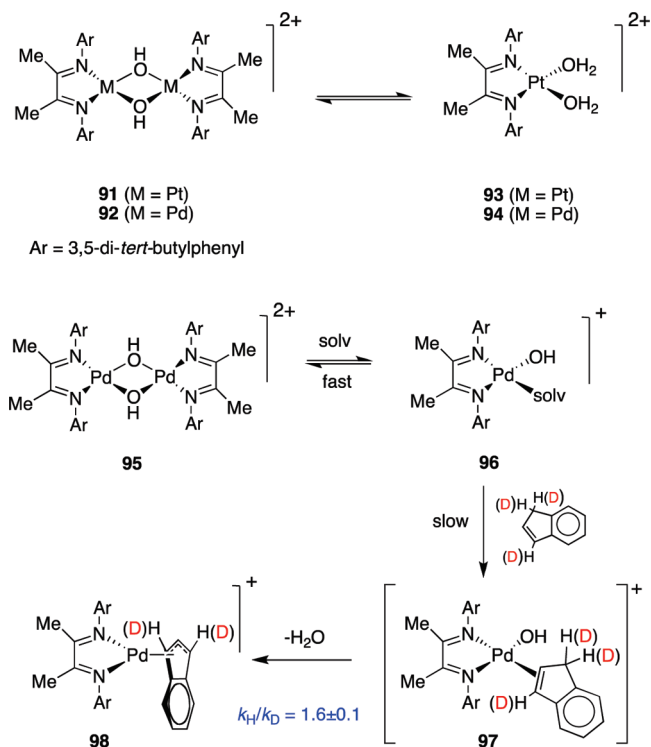
3.3.4. C–H Activation by Dicationic Platinum(II) Diimine Complexes.

Platinum dications **87** can activate C–H bonds to afford organoplatinum complexes that are stable to acids.⁶⁷ However, these dicationic platinum complexes exhibit major differences of reactivity and mechanism as compared to those of the corresponding methylplatinum monocations (**83** in Scheme 35). Thus, although platinum dications **87** can activate 1,4-diethylbenzene to form η^3 -benzyl complexes **88**, the reaction is slower than in the case of **83** and also requires higher temperature (Scheme 36). The kinetic studies revealed that only small KIEs were found using 1,4-diethylbenzene-(aryl)-*d*₄ ($k_H/k_D = 1.38$) or 1,4-diethylbenzene-*d*₁₀

Scheme 36

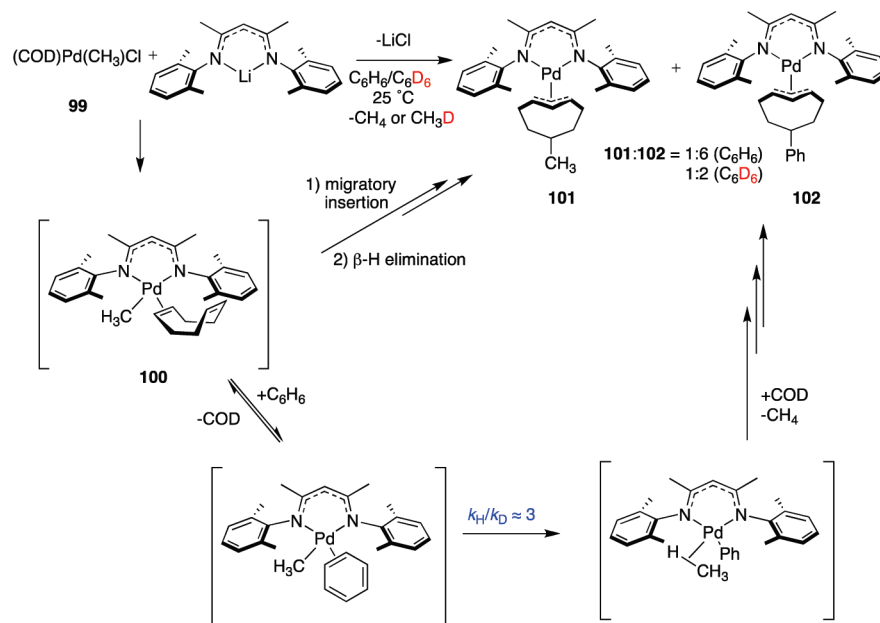


Scheme 37

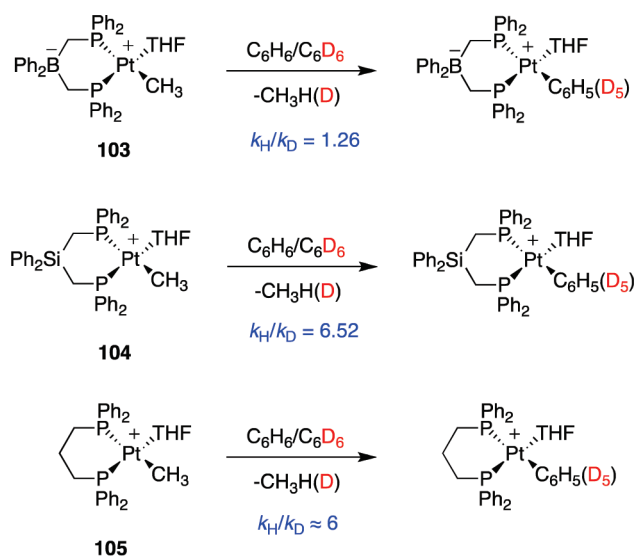


($k_H/k_D = 1.19$). These findings support the substitution of trifluoroethanol by 1,4-diethylbenzene in **87** to form a π -arene **89** before a second arene molecule undergoes C–H activation as the rate-determining step. Formation of the bis(arene) intermediate **90** might involve coordination of a second π -bond or a benzylic C–H bond generating a σ -complex. The low KIE values could be consistent with either reaction pathway. Labeling experiments indicate that the benzylic position is the site of initial C–H bond activation by **89**, whereas it was an aryl position for the cationic complexes **83**. The reasons for this difference are not clear.

Scheme 38



Scheme 39



Bercaw's group⁶⁸ has recently reported that the air- and water-tolerant dimeric hydroxy-bridged dimers $[(\text{diimine})\text{M}(\text{OH})_2]^{2+}$ ($\text{M} = \text{Pt}$ (**91**), Pd (**92**)) can effect activation of a variety of C–H bonds. The process was suggested to involve initial acid-mediated conversion of dimeric $[(\text{diimine})\text{M}(\text{OH})_2]^{2+}$ dimers into the active monomeric species $[(\text{diimine})\text{M}(\text{OH}_2)_2]^{2+}$ **93** and **94**. However, mechanistic studies carried out with the Pd complex **92** and indene revealed that there are many differences between both processes. The Pd dimeric complex reacts faster in acid than its Pt counterpart, the activation of C–H bonds is not inhibited by water, and the kinetic experiments suggested a direct pathway for C–H activation with Pd dimeric complex **92** that does not involve monomeric dicationic species **94** as intermediate. The experimental

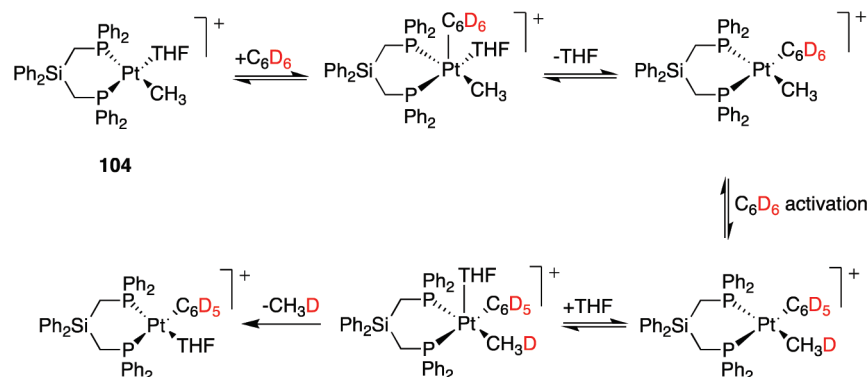
findings are consistent with the mechanism shown in Scheme 37, consisting of an equilibrium involving the fast, solvent-assisted separation of **95** into two monocationic monomers **96**, followed by rate-determining displacement of coordinated solvent by indene to form **97** and finally by fast C–H activation to yield the indenyl complex **98**. The kinetic isotope effect ($k_{\text{H}}/k_{\text{D}} = 1.6 \pm 0.1$) for the conversion of 1,1,3-trideuteroindene into the deuterated indenyl complex **98** is slightly larger than expected for rate-determining π -coordination of indene ($k_{\text{H}}/k_{\text{D}} = 1$) but significantly lower than would be expected for rate-determining C–H activation ($k_{\text{H}}/k_{\text{D}} = 3.5\text{--}6$). As the measured KIE reflects both steps, the value indicates that neither coordination of the substrate nor C–H activation is fully the rds and that there is an important solvent-assisted component in the rate law.

Monomethylpalladium(II) complex **99** in the presence of an anionic β -diketiminate ligand can undergo both benzene C–H activation and migratory insertion of olefin (the former faster than the latter), at room temperature.⁶⁹ The reaction is proposed to take place via the formation of a (monomethyl)palladium(II) β -diketiminate **100** with COD as the fourth ligand, followed by competitive benzene C–H activation and migratory insertion of olefin (Scheme 38). On the basis of the **101**/**102** products ratio in $\text{C}_6\text{H}_6/\text{C}_6\text{D}_6$, the KIE for benzene C–H activation was estimated as $k_{\text{H}}/k_{\text{D}} \approx 3$, which suggests that C–H bond breaking is the rate-determining step in the formation of **102** (Scheme 38).

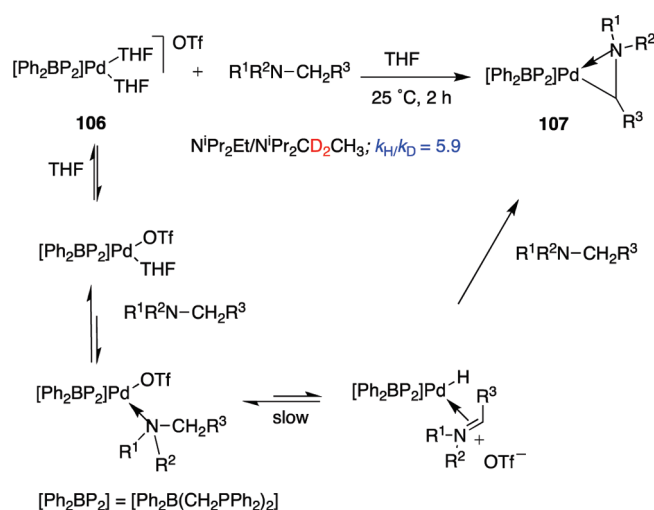
3.3.5. C–H Activation by Pt(II) Complexes Bearing Phosphine Ligands. Benzene C–H activation processes have been studied in neutral (formally zwitterionic) and cationic Pt complexes derived from bidentate phosphine ligands **103–105** (Scheme 39),⁷⁰ and primary KIEs have helped to establish the different reaction mechanisms.

Examination of the kinetics of each C–H bond activation process at 55°C shows that neutral **103** reacts faster than both of the cations **104** and **105**. The magnitude of the primary KIE measured for the neutral versus the cationic systems also differs

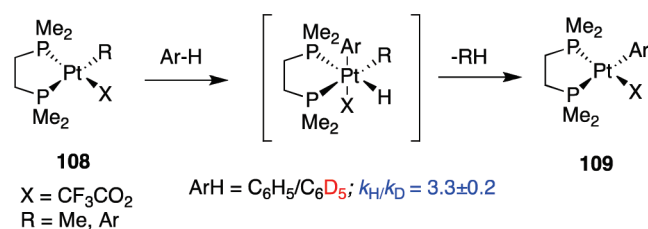
Scheme 40



Scheme 41



Scheme 42



markedly ($k_{\text{H}}/k_{\text{D}}$ **103** = 1.26; **104** = 6.52; **105** \approx 6). Mechanistically, the cationic complexes **104** and **105** were suggested to activate benzene by associative, reversible displacement of tetrahydrofuran (THF) by benzene followed by a rate-limiting C–H oxidative addition that resulted in large KIEs (Scheme 40). However, the electron density at Pt in the neutral **103** is appreciably higher than that in the two cationic species. The predominant pathway was proposed to be THF displacement by a π -bonded phenyl and intramolecular C–H activation of the phenyl group before benzene coordination and C–H activation.

Palladium complex $[(\text{Ph}_2\text{BPd}_2)\text{Pd}(\text{THF})_2][\text{OTf}]$ **106** (where $[\text{Ph}_2\text{BPd}_2] = [\text{Ph}_2\text{B}(\text{CH}_2\text{PPh}_2)_2]^+$) reacts with trialkylamines to

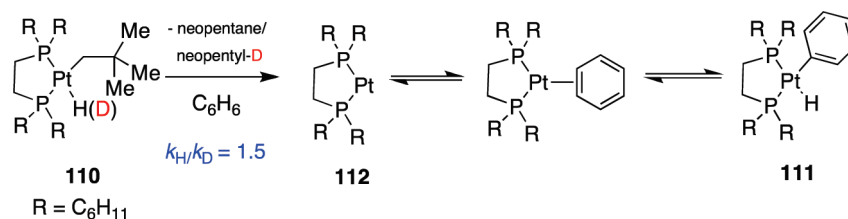
activate a C–H bond adjacent to the amine *N*-atom, thereby producing iminium adduct complexes **107**.⁷¹ The relative rate of the reaction between **106** and $\text{N}^i\text{Pr}_2\text{Et}$ or $\text{N}^i\text{Pr}_2\text{CD}_2\text{Me}$ was examined in THF. A dramatic attenuation in rate was observed for the deuterated amine substrate providing a $k_{\text{H}}/k_{\text{D}} = 5.9$. The kinetics of the amine-activation process was explored, and β -hydride elimination appeared to be the rate-limiting step (Scheme 41).

Roddick and co-workers⁷² reported the activation of aromatic C–H bonds with a series of $(\text{dmpe})\text{Pt}(\text{R})(\text{X})$ ($\text{X} = \text{O}_2\text{CCF}_3$, OTf; $\text{R} = \text{Me}$, aryl) complexes **108**. Thermolysis of $(\text{dmpe})\text{Pt}(\text{Me})(\text{O}_2\text{CCF}_3)$ in benzene at 125 °C results in methane loss and the formation of $(\text{dmpe})\text{Pt}(\text{Ph})(\text{O}_2\text{CCF}_3)$ **109** as the major product (>90%) (Scheme 42). Kinetic studies in C_6H_6 and C_6D_6 indicate that the disappearance of $(\text{dmpe})\text{Pt}(\text{Me})(\text{O}_2\text{CCF}_3)$ is first-order, with an overall KIE = 3.3 ± 0.2 . The authors reject a mechanism involving homolysis of Pt–R bonds and anion dissociation as prerequisite for C–H bond activation. However, although a preequilibrium involving phosphine dissociation cannot be excluded,⁷³ the high observed KIE for aryl C–H activation suggests a direct oxidative addition for this particular Pt(II) system.

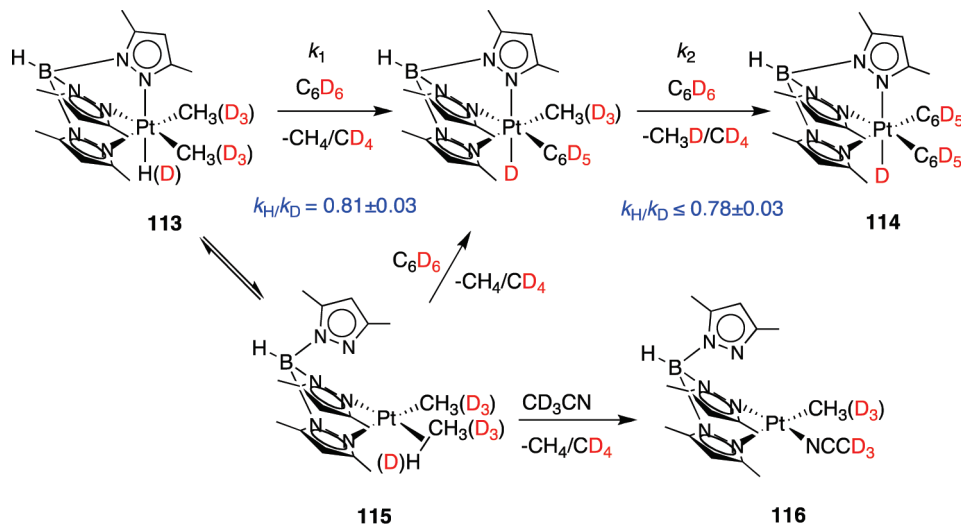
3.3.6. C–H Activation by Pt(0) Complexes. The Pt(0) intermediates that result from the alkane eliminations are capable of oxidatively adding to hydrocarbon C–H bonds. When $(\text{dcpe})\text{Pt}(\text{CH}_2\text{CMe}_3)(\text{H})$ **110** (dcpe = bis(dicyclohexylphosphino)ethane) is heated in benzene solution, neopentane is reductively eliminated. Oxidative addition of a C–H bond of benzene produces *cis*-[bis(dicyclohexylphosphino)ethane]hydrido-phenylplatinum(II) **111**. The $(\text{dcpe})\text{Pt}(0)$ intermediate **112** is not stable but can be trapped with diphenylacetylene or added dcpe (Scheme 43).^{14a} Reductive elimination of neopentane was inferred to be the rate-limiting step for the overall reaction on the basis of observed first-order kinetics, indistinguishable rates for C_6H_6 and C_6D_6 activation, and a $k_{\text{H}}/k_{\text{D}} = 1.5$ for reductive elimination. It is likely that η^2 -benzene complex formation precedes benzene activation, although this was not rigorously proven.

3.3.7. Reactions at Pt Complexes with Anionic Donor Ligands. The Shilov mechanism⁴⁶ (Scheme 19) requires the oxidation of Pt(II) alkyl to Pt(IV) alkyl complexes. Experimental evidence has suggested that the cationic Pt complexes, based on neutral diimine and other *N*-*N* ligands, are not very susceptible to oxidation. The presumption that anionic ligands would give neutral Pt(II) alkyls that should be more prone to oxidation has inspired efforts to explore the C–H activation chemistry of Pt complexes

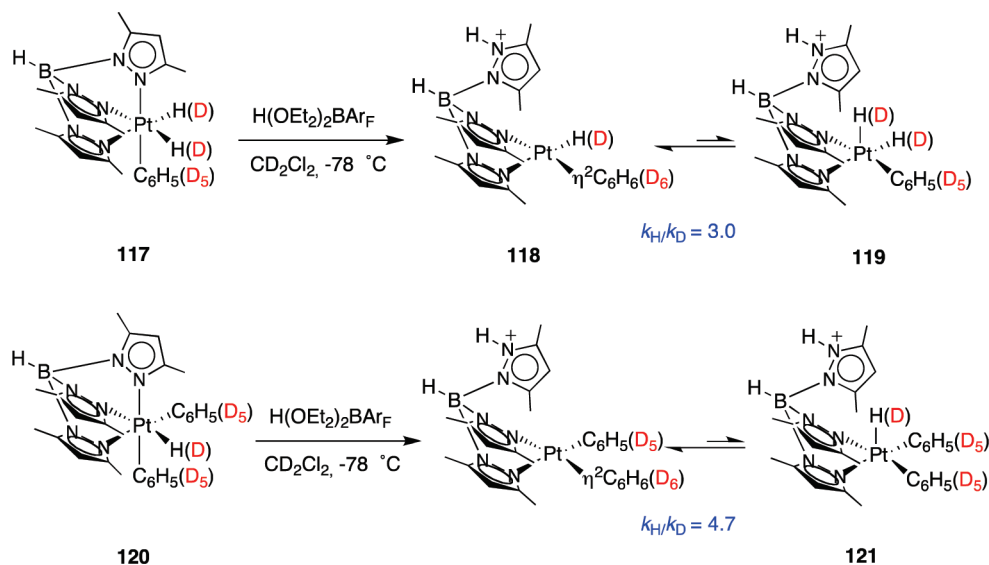
Scheme 43



Scheme 44



Scheme 45

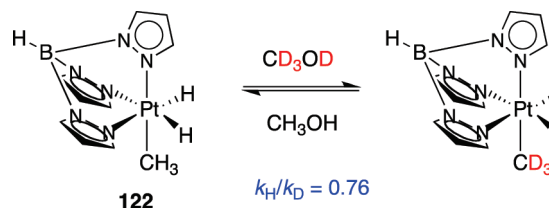


with a number of anionic ligands, mostly *N* donors. This led to the development of chemistry based on the anionic hydridotris-(pyrazolyl)borate (Tp) and diketiminate ligand systems.

Thermolysis of $\text{Tp}^{\text{Me}_2}\text{PtMe}_2\text{H}$ ($\text{Tp}^{\text{Me}_2}\text{PtMe}_2\text{H}$) **113** in C_6D_6 at 110°C resulted in two successive methane elimination/benzene

addition reactions to yield isotopically labeled methane and $\kappa^3\text{-Tp}^{\text{Me}_2}\text{Pt}(\text{IV})(\text{C}_6\text{D}_5)_2\text{D}$ **114** (Scheme 44).²⁴ⁱ On the basis of kinetic analysis, the authors proposed two successive unimolecular reactions and a Pt(II) σ -methane complex **115** suggested as a common intermediate in both the scrambling and reductive

Scheme 46



elimination processes. *Inverse* KIEs were observed for both steps ($k_{\text{H}}/k_{\text{D}} = 0.81 \pm 0.03$ for k_1 and $k_{\text{H}}/k_{\text{D}} \leq 0.78 \pm 0.03$ for k_2), and the activation parameters were in agreement with two dissociative steps. The kinetic results are consistent with rate-determining decoordination of a pyrazole ring and reductive C–H coupling to produce the coordinatively unsaturated intermediate **115** that leads to the products by oxidative addition (hydrocarbon solvents) or methane substitution (acetonitrile- d_3 , **116**).

Protonation of $\text{Tp}^*\text{Pt}(\text{Ar})(\text{H})(\text{R})$ platinum(IV) complexes **117** with $\text{H}(\text{OEt}_2)_2\text{BAR}_{\text{F}}$ (BAR_{F} = tetrakis-(3,5-trifluoromethylphenyl)borate] in CD_2Cl_2 at -78°C induced reductive C–H coupling to yield the chiral, cationic square-planar $\text{Pt}(\text{II})$ η^2 -benzene complexes **118** (Scheme 45).^{16a,74} These η^2 -arene platinum(II) adducts exhibit dynamic ^1H NMR spectra that can be attributed to equilibration of **118** with a five-coordinate platinum aryl hydride intermediate **119** via arene C–H oxidative addition, with the equilibrium favoring the platinum(II) η^2 -arene structure. Adduct **120**, lacking an adjacent hydride ligand, leads to a hydridodiphenyl intermediate **121**. The primary KIEs for intramolecular C–H(D) bond activation in the phenyl deuterated benzene hydride adduct **117** and the complex **120** were $k_{\text{H}}/k_{\text{D}} = 3.0$ at 259 K and $k_{\text{H}}/k_{\text{D}} = 4.7$ at 241 K, respectively, consistent with significant cleavage of a C–H(D) bond to reach the transition state.

Complex TpPtMeH_2 **122** is stable toward reductive elimination of methane at 55°C , but deuterium incorporation from methanol- d_4 occurs rapidly into the hydride positions and subsequently, more slowly, into the methyl position (Scheme 46). The reaction is a rare example of a hydridoalkylmetal complex that undergoes isotopic scrambling without concomitant liberation of either alkane or dihydrogen.⁷⁵ The scrambling into the methyl position has been attributed to reversible formation of a $\sigma\text{-CH}_4\text{-Pt}(\text{II})$ complex, whose existence is strongly indicated by the observed *inverse* kinetic isotope effect ($k_{\text{H}}/k_{\text{D}} = 0.76$) in the H/D exchange reaction.

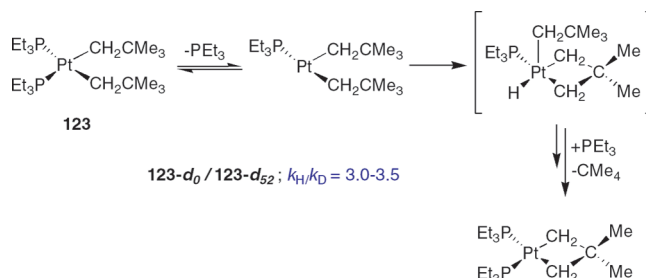
Scheme 47



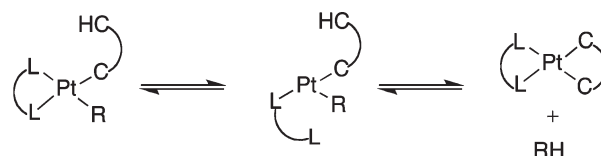
3.3.8. Cyclometalations. This special case of Pt-mediated homogeneous C–H bond activations in which C–H bond cleavage on a saturated hydrocarbon ligand is accompanied by metal–carbon bond formation has received considerable interest. Reaction sequences generally involve the formal oxidative–addition of a C–H bond to the metal center followed by reductive–elimination of another fragment (Scheme 47).

Particularly well-characterized examples are bis(phosphine)-platinum dialkyl complexes **123** (Scheme 48). The mechanism of

Scheme 48



Scheme 49



this process involves creation of a vacant coordination site on Pt by dissociation of phosphine, oxidative addition of a Me C–H bond to $\text{Pt}(\text{II})$, and reductive elimination of the alkane fragment from the resulting adduct. Although the significant KIE alone ($k_{\text{H}}/k_{\text{D}} = 3.0\text{--}3.5$) is not sufficient to distinguish between oxidative addition and reductive elimination as the overall rds, studies of isotopic scrambling and Arrhenius parameters support the reductive elimination as the slow step of the process.⁷⁶

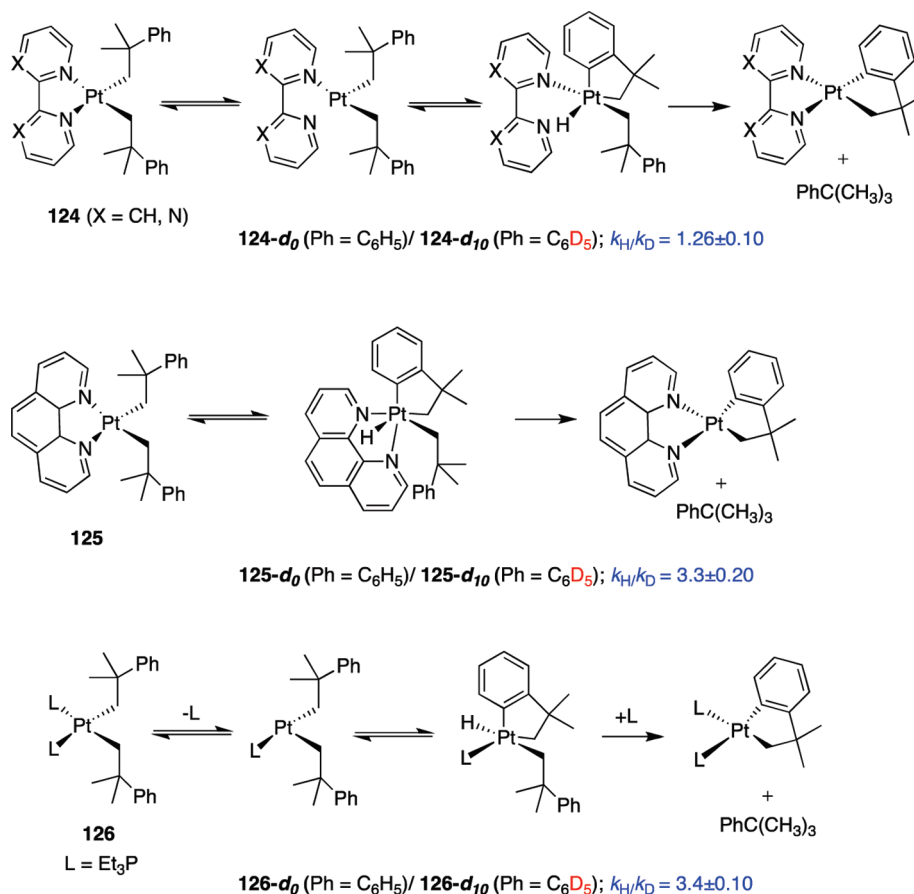
Griffiths and Young provided an interesting example of ligand-dependent C–H activation⁷³ in the thermolytic rearrangement of dineophylplatinum(II) complexes $\text{Pt}(\text{CH}_2\text{CMe}_2\text{Ph})_2\text{L}_2$ with bidentate, *N*-donor ligands ($\text{L}_2 = 2,2'$ -bipyridyl, $2,2'$ -bipyrimidyl, 1,10-phenanthroline, 4,7-diphenyl-1,10-phenanthroline, and 3,4,7,8-tetramethyl-1,10-phenanthroline) and with *P*-donor ligands ($\text{L} = \text{PEt}_3$, PPh_3). The overall process depicted in Scheme 49 involves preliminary, reversible $\text{Pt}\text{--}\text{L}$ cleavage, to form a tricoordinate intermediate that, after aromatic δ -hydrogen transfer, generates a 3,3-dimethylplatinaindan L_2 complex.

The mechanism of the reaction is dependent on the nature of the bidentate ligand. For the flexible *N*-donors, $2,2'$ -bipyridyl or $2,2'$ -bipyrimidyl **124**, the kinetic data and the small kinetic isotope $k_{\text{H}}/k_{\text{D}} = 1.26 \pm 0.10$ found on the bipyridyl system are consistent with a rate-limiting $\text{Pt}\text{--}\text{N}$ scission. However, the rigid phenanthrolines **125** exhibit a stronger KIE ($k_{\text{H}}/k_{\text{D}} = 3.3 \pm 0.20$) more in agreement with a hydrogen transfer–reductive C–H elimination contributing substantially to rate control (Scheme 50).

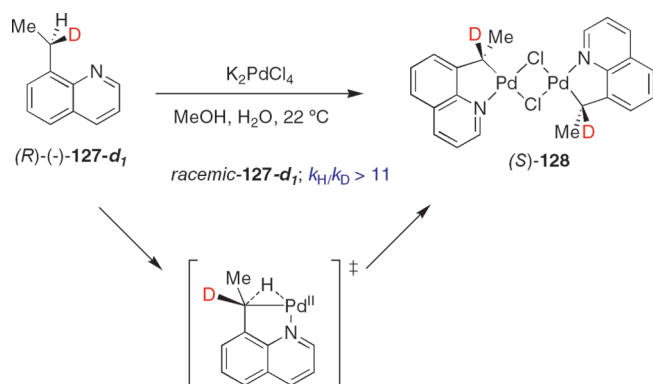
Complexes with monodentate phosphine ligands **126** are the most labile. Detailed studies of $\text{cis-Pt}(\text{CH}_2\text{CMe}_2\text{Ph})_2(\text{PEt}_3)_2$ reveal that cyclometalation rate shows a strong inverse dependence on phosphine concentration and a substantial deuterium isotope effect ($k_{\text{H}}/k_{\text{D}} = 3.4 \pm 0.10$), which would not be expected if preliminary ligand loss were rate-determining. The proposed mechanism involves the preliminary phosphine dissociation and reductive C–H elimination, making the most energetic contribution to rate control (Scheme 50).

Cyclometalation of (*R*)-(-)-8-(*R*-deuterioethyl) quinoline, (*R*)-**127-d**₁, by palladium(II) salts results in formation of the palladium–carbon bond in **128** with net retention of

Scheme 50



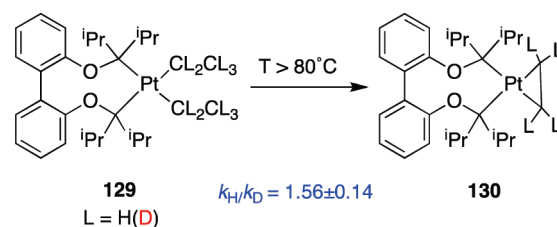
Scheme 51



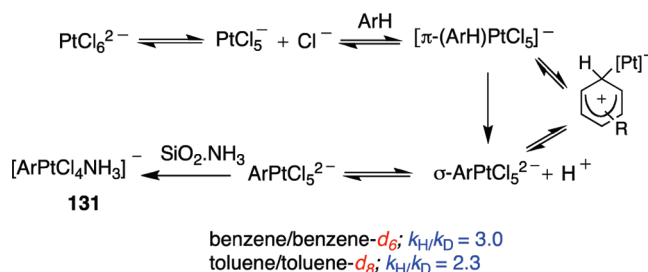
configuration at carbon (Scheme 51). The high KIE observed for *racemic-127- d_1* ($k_{\text{H}}/k_{\text{D}} > 11$) and the absence of isotopic scrambling were used as evidence for a front side interaction of the H with the electrophilic metal.⁷⁷

The thermal decomposition of Biphen(OP^iPr)PtEt₂ **129** was investigated in the temperature range of 353–383 K.⁷⁸ The clean and quantitative formation of the adduct **130** was observed. The reaction kinetics were measured for **129** having perdeuterated ethyl groups yielding a significant but small KIE ($k_{\text{H}}/k_{\text{D}} = 1.56 \pm 0.14$), which was almost temperature-independent. These data,

Scheme 52



Scheme 53

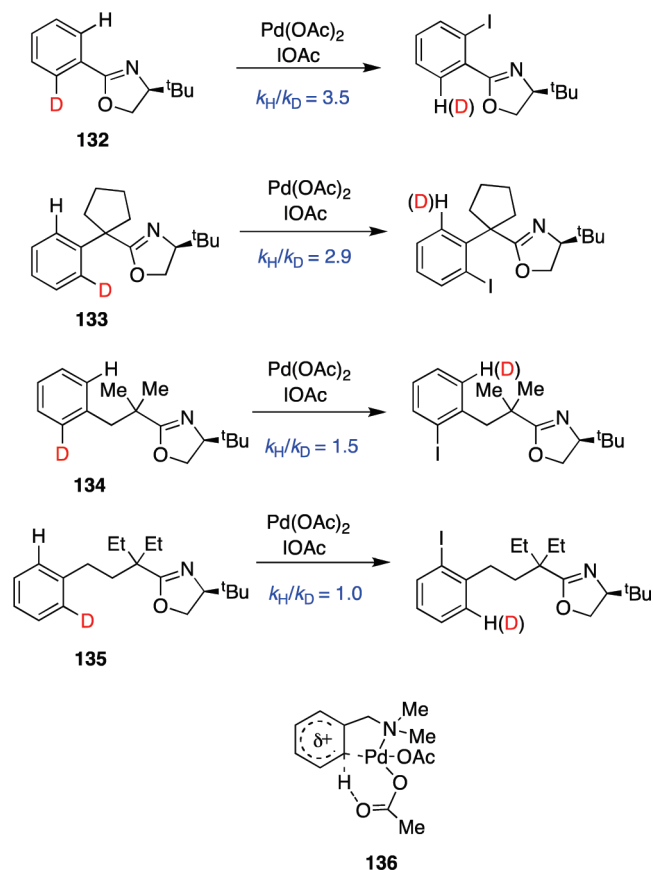


together with first-order kinetic and dissociative activation parameters ($\Delta H^\ddagger = 173.8 \pm 16.2 \text{ kJ/mol}$ and $\Delta S^\ddagger = 104.7 \pm 44.1 \text{ J/(mol K)}$)

prompted the authors to suggest a process involving dissociation of ethene and formation of a Pt(0) intermediate as the key steps of the reaction (Scheme 52).

3.3.9. C–H Activation by Pt(IV) Complexes. Pt(II) systems have been most frequently studied for C–H activation, yet it has been shown that Pt(IV) species are also capable of activating aromatic C–H bonds, affording Pt(IV) aryl complexes like (aryl)–PtCl₅^{2–} or (aryl)PtCl₄(H₂O)[–].⁷⁹ The study of the reaction of H₂PtCl₆ with monosubstituted benzenes revealed the formation of only *meta*- and *para*-isomers of PtCl₄(Ar)(NH₃)[–]NH₄⁺ complexes **131**, with a

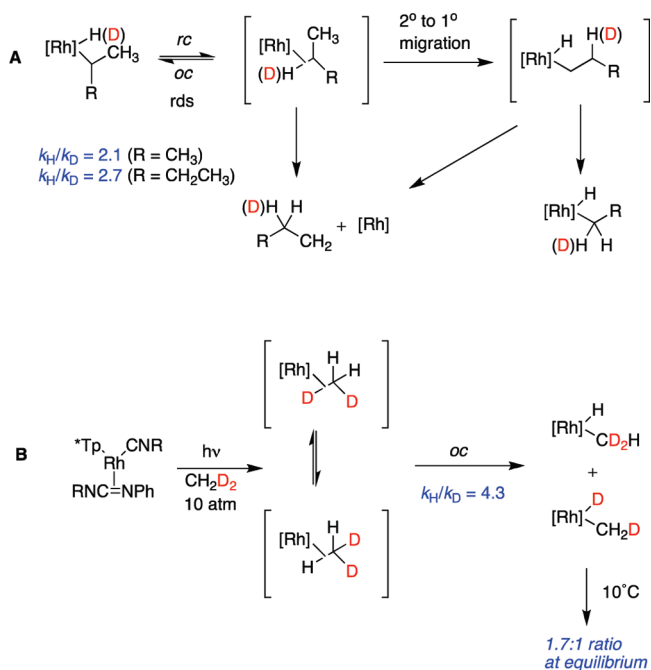
Scheme 54



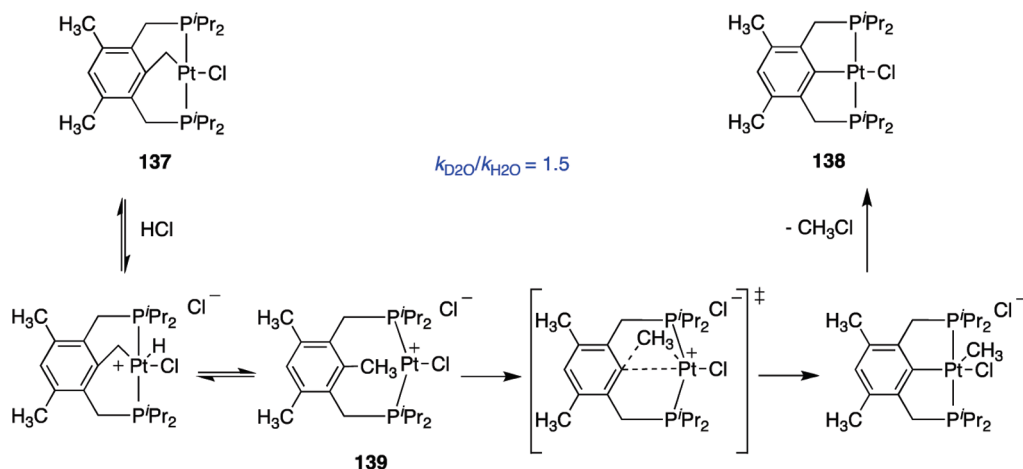
kinetic preference for the *para*-isomer (Scheme 53). The proposed mechanism involved Cl[–] dissociation followed by coordination of the arene to give a Pt(IV) π -arene complex, which possibly evolves into a Wheland-type complex. Deprotonation leads to the σ -aryl complex. The observed *meta/para* isomerization may proceed via a Wheland-type intermediate or via the π -complex. The relatively small KIEs ($k_{\text{H}}/k_{\text{D}} = 3$ in benzene-*d*₆ and $k_{\text{H}}/k_{\text{D}} = 2.3$ in toluene-*d*₈) led to the suggestion that the rate-limiting step is the formation of the Wheland complex rather than the subsequent deprotonation.^{79a}

A Pd(IV) intermediate has been arguably proposed during iodination of aryl C–H bonds located four, five, or six bonds away from the directing group, using palladium acetate as the catalyst and IOAc as the oxidant.⁸⁰ The mechanism of remote C–H bond activation was investigated by systematic kinetic isotope studies on the *ortho*-iodination of substrates **132**–**135** (Scheme 54). The value of the intramolecular isotope effect gradually decreases from $k_{\text{H}}/k_{\text{D}} = 3.5$ to 1.0 when the C–H

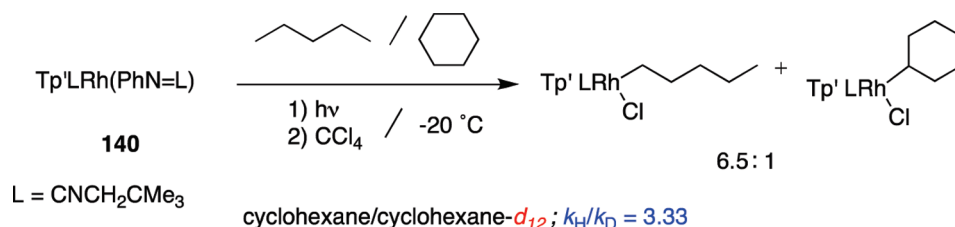
Scheme 56



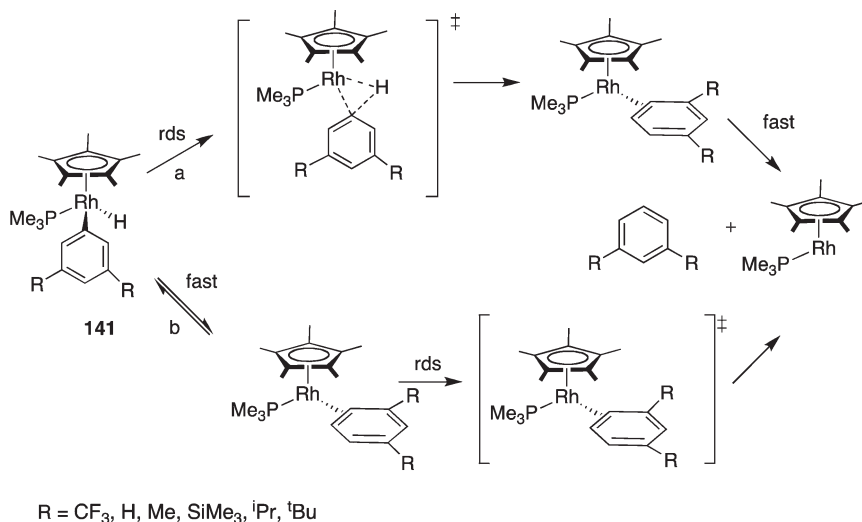
Scheme 55



Scheme 57



Scheme 58



bonds are further away from oxazoline groups. The experimental results suggest that an electrophilic pathway (via the Wheland intermediate **136**), in which the initial palladation is slower than the C–H bond cleavage, can be operative in the palladium-catalyzed functionalization of remote aryl C–H bonds.

Treatment of benzylic Pt(II) complex **137** with an excess of HCl results in selective C–C bond activation at room temperature to afford **138** and MeCl (Scheme 55).⁸¹ Formally, the transformation from **137** to **138** involves transferring of a methylene group to HCl by activation of a strong C–C single bond. An isotope effect of 1.5 was observed at 130 °C when the reaction of **137** and HCl was compared in dioxane/D₂O versus dioxane/H₂O solutions. It is likely that C–C bond activation becomes more competitive with C–H bond cleavage upon deuterium incorporation in the ArCH₃ group. The transformation of **137** to **138** is postulated to take place through protonation and reductive elimination to **139**, the common intermediate for C–H and C–C bond-activation pathways. This latter process can occur directly by a concerted oxidative addition process (as in Scheme 55), although the formation of an arenium intermediate was not discarded.

3.4. KIEs in the Study of C–H Activation Mechanisms by Rh Complexes

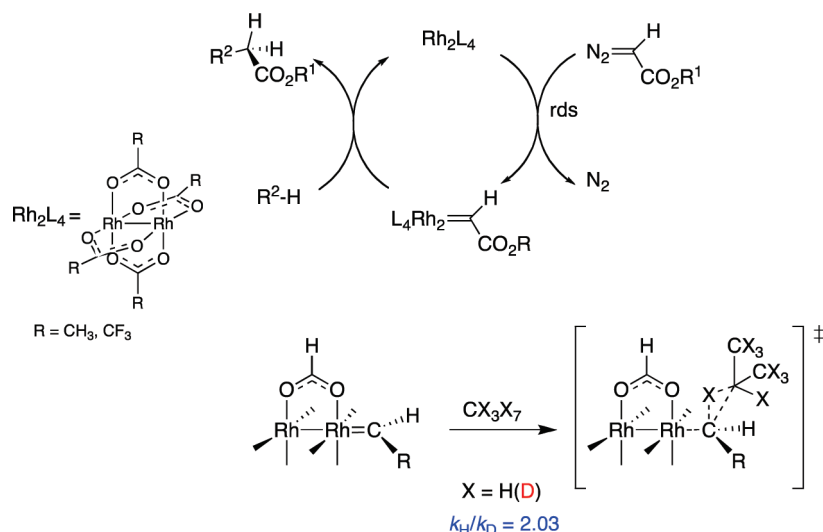
3.4.1. Hydrocarbon C–H Activation by Rh(II) Complexes. Jones and co-workers²⁷ studied the selective activation in compounds having primary and secondary C–H bonds by Rh complexes in the reductive elimination of Tp'Rh(L)(R)H complexes (R = methyl, ethyl, propyl, butyl, pentyl, hexyl;

L = CNCH₂C(CH₃)₃; Tp' = tris-(3,5-dimethylpyrazolyl)borate). The study showed that selective activation of primary C–H bonds was kinetically preferred exclusively over secondary C–H bonds. Additionally, secondary alkyl hydride complexes were observed to rearrange intramolecularly to give the more stable linear *n*-alkyl hydride isomers. Thus, isopropyl hydride complex Tp'Rh(L)(CHMe₂)H was found to rearrange to the *n*-propyl hydride complex Tp'Rh(L)(CH₂CH₂CH₃)H in an intramolecular reaction.

The reaction served as an excellent ground to obtain indirect evidence for the involvement of alkane σ -complexes. The KIEs for the reductive couplings (rc) in Scheme 56A were found to be $k_H/k_D \approx 2$, whereas the KIE for the reverse oxidative cleavage (oc, the unimolecular conversion of the σ -alkane complex into an alkyl hydride complex) was determined to be $k_H/k_D = 4.3$ (Scheme 56B). These two values led to an equilibrium isotope effect (k_{rc}/k_{oc}) of 0.49, an *inverse* value resulting from the combination of two *normal* KIEs. The calculated EIE was in quite good agreement with the experimental value ($1/1.7 = 0.59$), obtained from the equilibration of the alkyl hydride complexes over time at 10 °C (Scheme 56B).

Bergman, Harris, and co-workers⁸² also observed the preference for primary/versus secondary C–H activation in the process of activation of hydrocarbons with $\eta^3\text{-Tp}'\text{Rh}(\text{CO})_2$. This process was faster for linear alkanes than for cyclic alkanes. A *normal* KIE ($k_D/k_H \approx 2.3$) was observed in this case. The competitive activation of C–H bonds of linear, cyclic, and branched hydrocarbons using the coordinatively unsaturated 16-electron [Tp'RhL] reactive fragment has been recently

Scheme 59



reported ($\text{Tp}' = \text{tris-(3,5-dimethylpyrazolyl)borate}$; $\text{L} = \text{CNCH}_2\text{CMe}_3$) (Scheme 57).⁸³ Activation of the hydrocarbons leads to the formation of $\text{Tp}'\text{Rh}-(\text{L})(\text{R})(\text{H})$ alkyl complexes, which were converted to the stable chlorides immediately following the activation of the bonds via photolysis of complex **140** in the solvent mixture. The experiments described provide relative rates for the coordination of primary and secondary C–H bonds. Direct comparison of the product ratios from the separate activation experiments of pentane/cyclohexane and pentane/cyclohexane- d_{12} yields KIE of $k_{\text{H}}/k_{\text{D}} = 3.33$ for the overall process of oxidative addition (alkane coordination plus oxidative cleavage), but whether this reflects coordination or C–H cleavage (or a composite of both) could not be determined. A recent computational-experimental study by Hartwig and co-workers has provided detailed mechanistic insights for the selective functionalization of primary over secondary sp^3 C–H bonds in alkanes by borane reagents catalyzed by $\text{Cp}^*\text{Rh}(\text{H})_2(\text{Bpin})_2$ (pin = pinacolate).⁸⁴

The influence of electronic effects on the rate of reductive elimination of arene and the η^2 -complex stability was studied for a series of disubstituted aryl hydride complexes of the type **141** (Scheme 58).⁸⁵ In this study, activation parameters and KIEs gave contradictory information. A dramatic change in the activation entropies from $+16.4 \text{ cal mol}^{-1} \text{ K}^{-1}$ (dissociative) to $-19 \text{ cal mol}^{-1} \text{ K}^{-1}$ (associative) for the complexes where $\text{R} = \text{CH}(\text{CH}_3)_2$ and $\text{C}(\text{CH}_3)_3$ suggested that a change in the rate-determining step might have occurred. The negative activation entropies would be consistent with rate-determining formation of the η^2 -arene complex followed by rapid loss of coordinated arene on the basis of the associative three-centered transition state in Scheme 58, path a. However, the absence of KIE in the irradiation of **141** in the presence of 1,3-di-*tert*-butylbenzene led to the conclusion that arene precoordination is still the rate-determining step in all of these C–H bond-activation processes (Scheme 58, path b). Correlated with the large enthalpy change, the dramatic change in the activation entropies could suggest that a looser transition state is achieved for electron-poor arenes as compared to the electron-rich arenes.

Although the nitrogen extrusion is the rate-limiting step of the catalytic cycle on the C–H insertion reaction of ethyl diazoacetate and dirhodium tetracarboxylate, several studies have focused

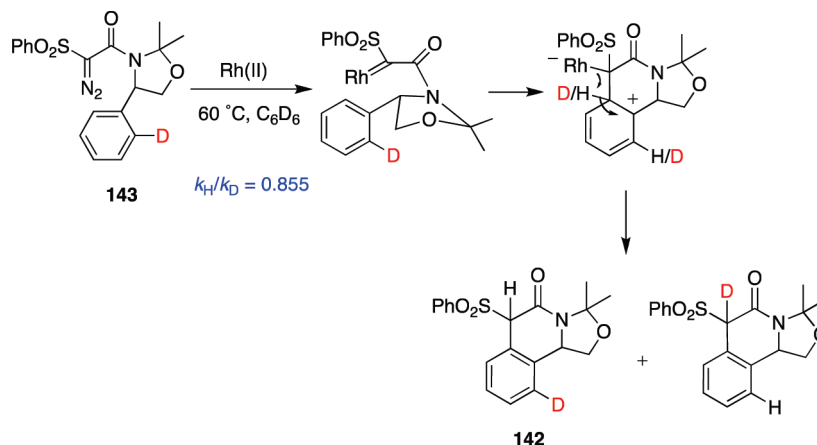
on the C–H insertion step. Thus, qualitative structure/reactivity correlations indicated a reactivity order of primary, secondary < tertiary C–H bond and the enhanced reactivity of a C–H bond adjacent to a heteroatom. There was also retention of the configuration of the carbon at which the C–H activation occurs, and H/D KIEs of the C–H bond activation were shown to depend on the nature of the carboxylate ligands in the rhodium catalyst. Thus, Noels and co-workers⁸⁶ reported KIE values of $k_{\text{H}}/k_{\text{D}} = 2.45$ and $k_{\text{H}}/k_{\text{D}} = 1.55$ for the reaction of ethyl diazoacetate with a cyclohexane/cyclohexane- d_{12} pair under the catalysis of $\text{Rh}_2(\text{OAc})_4$ and $\text{Rh}_2(\text{OCOCF}_3)_4$, whereas Wang and Adams⁸⁷ reported only noticeable KIEs ($k_{\text{H}}/k_{\text{D}} = 2.0$) in their studies of the intramolecular C–H activation of 1-methyl-1-(diazoacetyl)cyclohexane derivatives with $\text{Rh}_2(\text{Cap})$ (Cap = caprolactam). These values are supported by DFT studies⁸⁸ and are consistent with the C–H activation/C–C formation proceeding in a single step through a three-centered hydride transferlike transition state with small activation energy (Scheme 59).

A formal aromatic C–H insertion of rhodium(II) carbenoids was recently reported in the synthesis of isoquinolinones **142** (Scheme 60).⁸⁹ The intramolecular secondary KIE ($k_{\text{H}}/k_{\text{D}} = 0.855$) observed for the reaction of labeled diazo compound **143** ruled out a direct C–H activation pathway, such as an aliphatic C–H insertion, and was more consistent with sp^2 - to sp^3 -hybridization change during the rate-determining step. The proposed mechanism was an electrophilic aromatic substitution, in which the addition of a rhodium carbenoid to the sp^2 -center of the aromatic ring to form a σ -complex adduct was the slow step of the reaction.

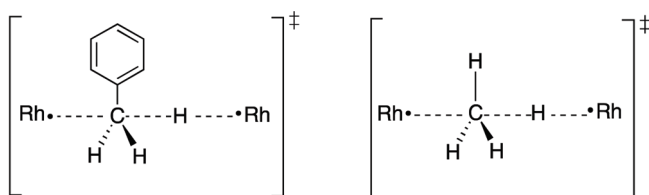
(Tetramesitylporphyrinato)rhodium(II) complexes can activate methane and toluene.⁹⁰ The reaction with toluene takes place exclusively at the benzylic C–H bond. Large deuterium isotope effects for reaction with methane ($k_{\text{H}}/k_{\text{D}}$ (298 K) = 8.6; $k_{\text{H}}/k_{\text{D}}$ (353 K) = 5.1 ± 0.5) and with toluene, ($k_{\text{H}}/k_{\text{D}}$ = 6.5 ± 0.5 , 353 K) (without any evidence for aromatic C–H bond activation) clearly implicate in both cases a four-centered linear $\text{Rh} \cdots \text{C} \cdots \text{H} \cdots \text{Rh}$ transition state (Scheme 61).

An analogous four-centered transition state was proposed for the reactions of a *m*-xylyl diether tethered diporphyrin $\text{Rh}(\text{II})$ bimetallo radical with H_2 , and with the methyl C–H bonds for a

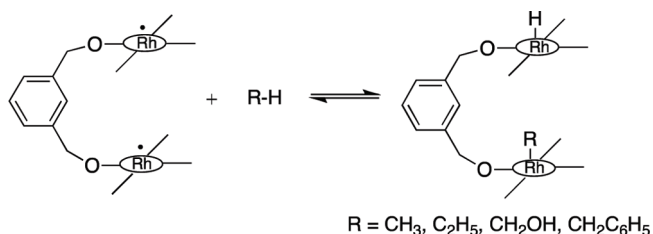
Scheme 60



Scheme 61



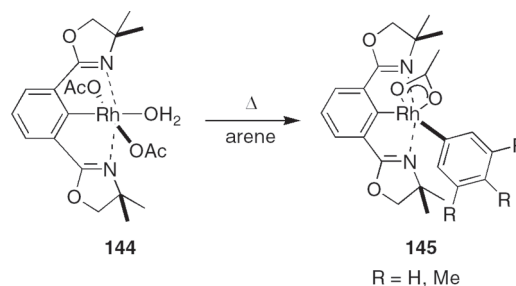
Scheme 62



CH₄/CD₄; $k_{\text{H}}/k_{\text{D}} = 10.8 \pm 1.0$
 CH₃OH/CD₃OD; $k_{\text{H}}/k_{\text{D}} = 9.7 \pm 0.8$
 toluene- d_0 /toluene- d_8 ; $k_{\text{H}}/k_{\text{D}} = 5.0 \pm 0.7$

series of substrates CH₃R (R = H, CH₃, OH, C₆H₅) (Scheme 62).⁹¹ The bimetallo-radical ($\cdot\text{Rh}(m\text{-xylyl})\text{Rh}\cdot$) reacts to form products that reflect total regioselectivity for alkyl C–H groups, in preference to O–H and C–C bonds and with complete exclusion of aromatic C–H bond reactions. The products formed are uniquely consistent with the intramolecular use of two Rh(II) \cdot centers in the alkyl C–H bond reactions of methane, ethane, methanol, and toluene. The large KIEs observed for each of the reactions studied (296 K) ($k_{\text{H}}/k_{\text{D}}(\text{CH}_4) = 10.8 \pm 1.0$; $k_{\text{H}}/k_{\text{D}}(\text{CH}_3\text{OH}) = 9.7 \pm 0.8$; $k_{\text{H}}/k_{\text{D}}(\text{CH}_3\text{C}_6\text{H}_5) = 5.0 \pm 0.7$) are consistent with a $\text{Rh}\cdots\text{H}\cdots\text{X}\cdots\text{Rh}$ transition state. The range of $k_{\text{H}}/k_{\text{D}}$ values and the temperature dependence of the isotope effects are comparable to those previously observed for the (TMP)Rh(II) system.^{90a}

Scheme 63



toluene- d_0 /toluene- d_8 ; $k_{\text{H}}/k_{\text{D}} = 5.4$

3.4.2. Hydrocarbon C–H Activation by Rh(III) Complexes.

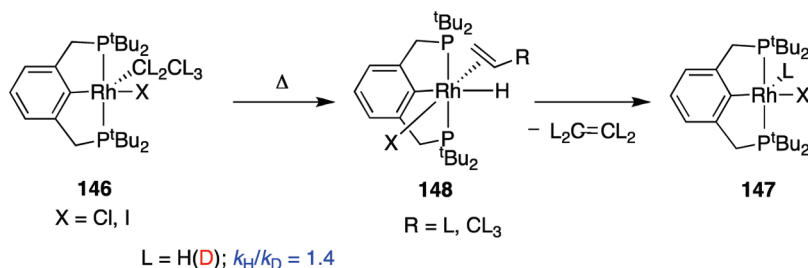
Thermolysis of the Rh(III) complex [$(dm\text{-Phebox-}dm)\text{-Rh}(\text{OAc})_2(\text{H}_2\text{O})$] [**144**; $dm\text{-Phebox-}dm$ = 2,6-bis(4,4-dimethyloxazolynyl) phenyl] in various arenes results in the formation of the corresponding aryl complexes **145** (Scheme 63).⁹² The large KIE ($k_{\text{H}}/k_{\text{D}} = 5.4$) obtained in toluene suggests that the C–H arene bond cleavage is the rds, where the acetate ligand acts as a proton acceptor. The relatively large and negative value of the activation entropy ($\Delta S^\ddagger = -24 \pm 5 \text{ cal mol}^{-1} \text{ K}^{-1}$) suggests a rigid transition state.

The unsaturated pentachlorophenol (PCP)-type complexes $\text{Rh}(\text{L})\{2,6-(\text{CH}_2\text{P}^t\text{Bu}_2)_2\text{C}_6\text{H}_3\}\text{X}$ (L = Et, ⁿPr; X = Cl, I) convert upon heating to the corresponding Rh(III)–hydride complexes $\text{Rh}(\text{H})\{2,6-(\text{CH}_2\text{P}^t\text{Bu}_2)_2\text{C}_6\text{H}_3\}\text{X}$ (X = Cl, I) **147** and ethylene or propylene, products indicative of a β -H elimination process (Scheme 64). The rate order was Et < ⁿPr, ⁱPr, and a $k_{\text{H}}/k_{\text{D}} = 1.4$ was observed for the PCP complex **146- d_0** /**146- d_5** .⁹³ Although the experimental KIE value is not high, it indicates that neither the ligand dissociation to create a free coordination site cis to the alkyl group nor the rearrangement of the complex are rate-determining. Rather, the rds is a later step such as the β -C–H cleavage or the dissociation of the olefin from the unobserved alkene–hydride species **148**. In support of this argument, the ¹³C labeling experiment shows that the β -H elimination is irreversible.

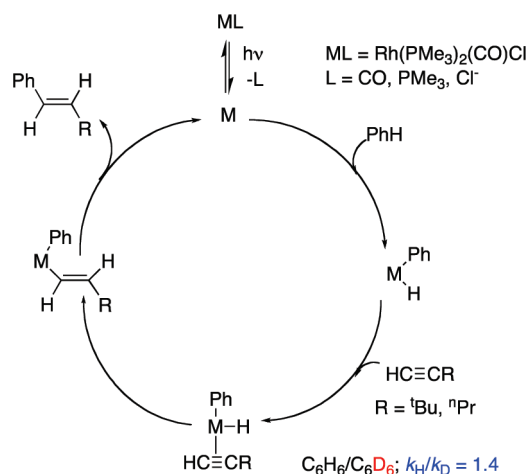
3.4.3. Hydrocarbon C–H Activation by Rh(I) complexes.

Rhodium–trimethylphosphine species have been found to catalyze the insertion of alkyne C–C triple bonds into phenyl–H and alkynyl–H bonds.⁹⁴ On the basis of the results of crossover

Scheme 64



Scheme 65



experiments, the determination of product stereochemistry (and high stereospecificity), and the isotope effects for the aryl C–H bond ($k_{\text{H}}/k_{\text{D}} = 1.4$), the authors proposed a mechanism involving a concerted addition across a triple bond; in particular, addition of the Rh–H bond of a hydridophenylrhodium species is suggested (Scheme 65).

Bercaw, Hazari, and Labinger⁹⁵ have already studied with neutral Rh complexes the activation of indene that they reported with cationic Pt and Pd complexes.⁶⁸ They found that, although the reactions with neutral $[(\text{COD})\text{Rh}(\mu_2\text{-OH})]_2$ **149** and cationic $[(\text{diimine})\text{M}(\mu_2\text{-OH})]_2^{2+}$ ($\text{M} = \text{Pd}, \text{Pt}$) complexes have the same stoichiometry, the detailed mechanisms are significantly different. Pd and Pt complexes require cleavage of the dimer before reaction with indene, and displacement of solvent by indene is rate-determining, whereas in the case of Rh complexes, reaction takes place directly from the dimeric species and the kinetic isotope effect ($k_{\text{H}}/k_{\text{D}} = 4.2 \pm 0.2$) is consistent with rate-determining C–H bond cleavage. The detailed mechanism of C–H bond cleavage is unclear, but as a consequence of the change in the rds, the overall reaction with indene is actually somewhat slower for Rh complexes than for Pd complexes (Scheme 66).

The C–H activation step governing the Rh(I)-catalyzed coupling of *N*-heterocycles and olefins has attracted wide attention (Scheme 67).⁹⁶ By combining kinetic, structural, and computational data, it is possible to draw a plausible general mechanism for the C–H activation of *N*-heterocycles by Rh(I)/PCy₃.⁹⁷ On the basis of these studies, a directed intramolecular hydrogen transfer pathway proceeding via Rh–H intermediates

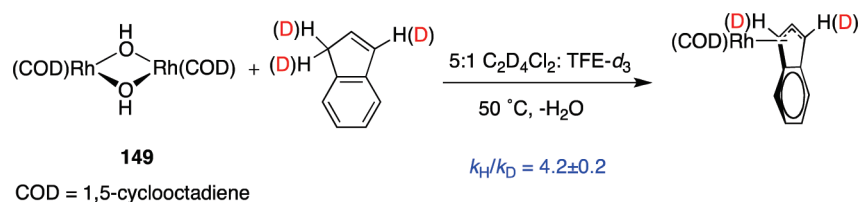
was implicated as the operative reaction mechanism. The observed deuterium KIE ($k_{\text{H}}/k_{\text{D}} = 1.8 \pm 0.1$) is consistent with cleavage of the C2–H bond during or prior to the rate-determining step. Similarities between the reactivity patterns of dihydroquinazolines and other *N*-heterocycles activated by $(\text{PCy}_3)_2\text{RhCl}$ suggest that this mechanism may be a common route to reactive M–NHC intermediates.

The mechanism of photochemical alkane dehydrogenation catalyzed by $\text{Rh}(\text{PMe}_3)_2(\text{CO})\text{Cl}$ **150** has been studied by Goldman and colleagues⁹⁸ with an emphasis on characterizing the initial C–H activation step and understanding the effect of added CO on selectivity (Scheme 68). The kinetic isotope effect for the dehydrogenation of cyclohexane-*d*₀/cyclohexane-*d*₁₂ was found to be dependent upon CO pressure, ranging from $k_{\text{H}}/k_{\text{D}} = 10$ in the absence of CO to $k_{\text{H}}/k_{\text{D}} = 0.42$ under high CO pressure. This *inverse* KIE strongly suggests that the adducts are alkyl hydrides-(deuterides) rather than solvated or σ -bound species and supports that the intermediate responsible for C–H activation is ground-state $[\text{Rh}(\text{PMe}_3)_2\text{Cl}]$. It is also concluded that inhibition of the reaction by CO operates primarily via addition of CO to the intermediate alkyl hydrides $(\text{R})(\text{H})\text{Rh}(\text{PMe}_3)_2\text{Cl}$. Addition of CO prior to C–H bond addition is apparently not a kinetically significant process, even under high CO pressure.

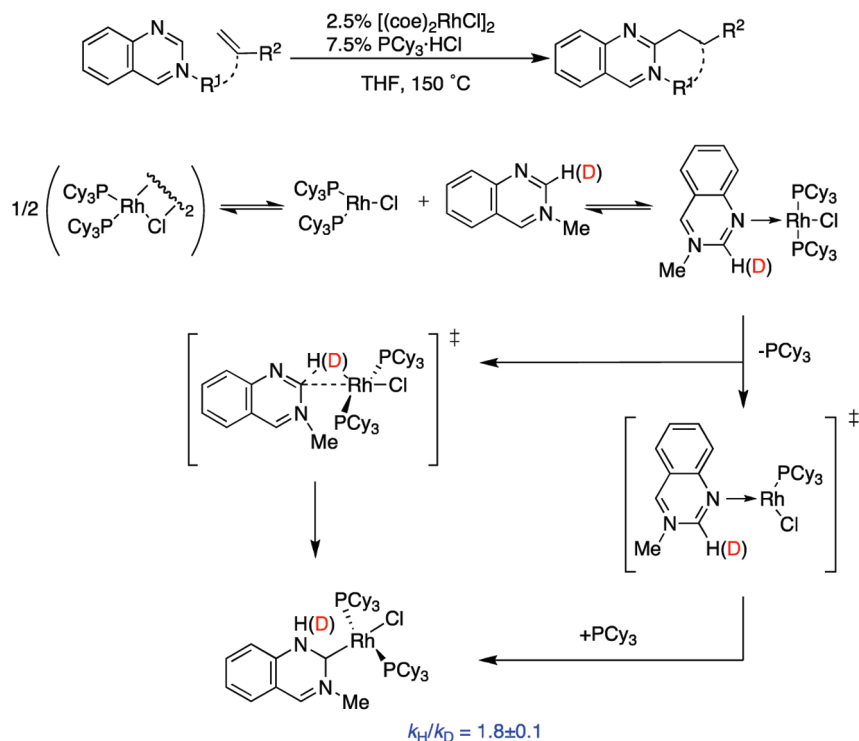
Several organorhodium(I) complexes of the general formula $(\text{PPh}_3)_2(\text{CO})\text{RhR}$ ($\text{R} = p\text{-tolyl}, o\text{-tolyl}, \text{Me}$) **151** were shown to insert aryl aldehydes into the aryl–rhodium(I) bond. Under anhydrous conditions, these reactions provided ketones in good yield (Scheme 69).⁹⁹ The stability of the arylrhodium(I) complexes allowed these reactions to be run also in mixtures of THF and water. Diarylmethanols were generated exclusively in this solvent system. Mechanistic studies support the formation of ketone and diarylmethanol by insertion of aldehyde into the rhodium–aryl bond and subsequent β -hydride elimination or hydrolysis to form diaryl ketone or diarylmethanol products. The absence of KIEs was used as a strong argument against an oxidative addition followed by reductive elimination from the ketone pathway. This work represents a rare example of directly observed insertion of aldehydes into a late transition metal carbon and oxygen bonds, particularly in unstrained systems.

Experimental and theoretical studies were undertaken to understand the mechanism of the $[\text{Rh}(\text{I})((\text{R})\text{-L})]\text{BF}_4$ ($\text{L} = \text{bidentate phosphine}$) catalyzed intramolecular hydroacylation of ketones to afford seven-membered lactones in large enantiomeric excess (Scheme 70).¹⁰⁰ KIEs ($k_{\text{H}}/k_{\text{D}} = 1.8$) and Hammett plot studies indicated that insertion of the ketone into the rhodium hydride is the rds, a proposal consistent with the calculated reaction barriers. This result represents a significant difference between the mechanism of ketone hydroacylation and

Scheme 66



Scheme 67



the related olefin hydroacylation for which it is well established that reductive elimination is rate-determining.¹⁰¹

3.5. KIEs in the Study of C–H Activation Mechanisms by Ru Complexes

3.5.1. Hydroarylation of Olefins. The direct addition of aromatic C–H bonds across olefin C=C bonds (i.e., olefin hydroarylation) provides an atom-economical method for the formation of C–C bonds with aromatic substrates and offers an advantageous alternative to the methods for C–C bond formation that require the incorporation of halide functionality into the aromatic substrate. The group of Gunnoe has thoroughly investigated the use of TpRu(II) [Tp = hydridotris-(pyrazolyl)borate] complexes as catalysts for the hydroarylation of olefins.¹⁰² TpRu(CO)(NCMe)R (R = Me or Ph) systems initiate stoichiometric C–H activation of aromatic substrates including benzene, furan, and thiophene. In particular, TpRu(CO)(NCMe)Ph **152** catalytically produces ethylbenzene from ethylene and benzene and is the most active catalyst for the hydrophenylation of ethylene. The process takes place through a metal-mediated C–H activation pathway. Mechanistic studies¹⁰³ of the C–H activation process are based on the

observation of similar primary intermolecular KIEs for the catalytic hydroarylation reaction of ethylene with **152** ($k_{\text{H}}/k_{\text{D}} = 2.1 \pm 0.1$) and for the stoichiometric benzene C–H activation by TpRu(CO)(NCMe)Me **153** ($k_{\text{H}}/k_{\text{D}} = 2.5 \pm 0.5$). The results are consistent with the pathway depicted in Scheme 71, with the benzene C–H activation being rate-determining.

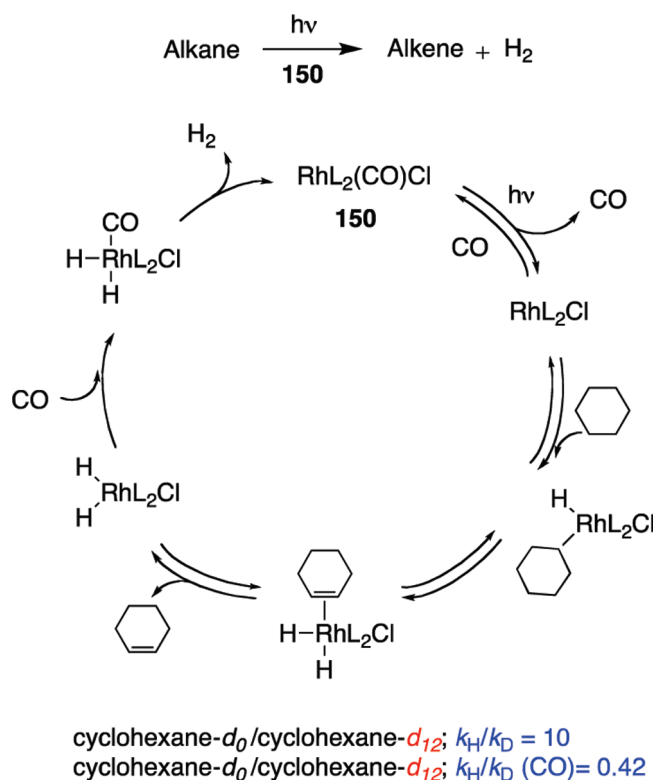
A further study¹⁰⁴ to determine the impact of metal electron density in TpRu(L)R systems **152** on olefin-insertion processes revealed that benzene C–H activation by TpRu(PMe₃)(NCMe)Me **154** showed an average $k_{\text{H}}/k_{\text{D}} = 2.7 \pm 0.1$, suggesting that benzene C–H(D) activation by TpRu–(L)(η^2 -benzene)R (L = CO or PMe₃) may have geometrically similar transition states (Scheme 72). The mechanism in Scheme 71 is also operative in these cases. TpRu(PMe₃)(NCMe)Ph initiates C–D activation of C₆D₆ at rates that are ~2–3 faster than TpRu(CO)(NCMe)Ph (depending on substrate concentration). However, the catalytic hydrophenylation of ethylene using TpRu(PMe₃)(NCMe)Ph is substantially less efficient than catalysis with TpRu(CO)(NCMe)Ph.

The cationic ruthenium complex $[(\text{PCy}_3)_2(\text{CO})(\text{CH}_3\text{CN})_2\text{-RuH}]^+ \text{BF}_4^-$, formed from Ru₃(CO)₁₂ with NH₄PF₆ or HBF₄·OEt₂ as additive, was found to be a very effective catalyst for the C–H bond-activation reaction of arylamines and terminal

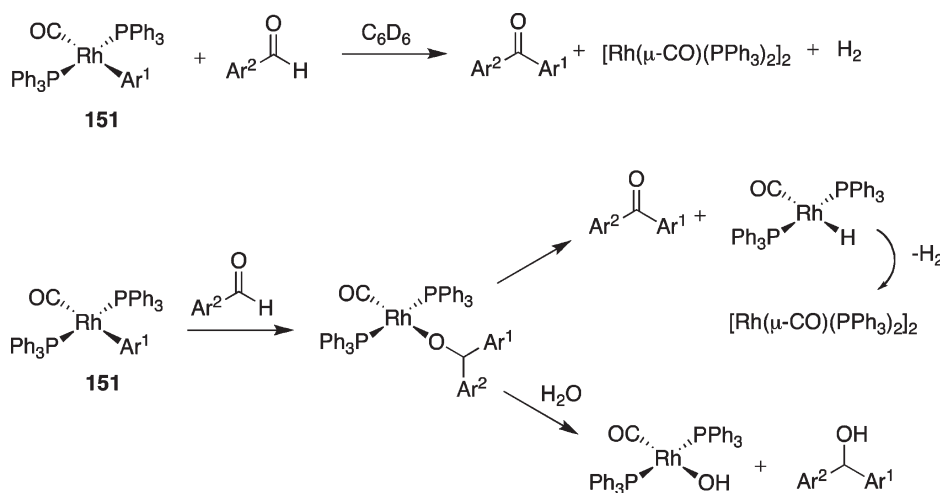
alkynes.¹⁰⁵ The mechanism of the catalytic reaction was examined by employing acyclic arylamines. First, a normal deuterium KIE ($k_{\text{H}}/k_{\text{D}} = 2.5 \pm 0.1$) was observed from the reaction of $\text{C}_6\text{H}_5\text{NH}_2$ and $\text{C}_6\text{D}_5\text{NH}_2$ with propyne (Scheme 73). In contrast, analogous reactions of $m\text{-(MeO)C}_6\text{H}_4\text{NHCH}_3$ and $m\text{-(MeO)C}_6\text{H}_4\text{NDCH}_3$ with propyne and $m\text{-(MeO)C}_6\text{H}_4\text{NHCH}_3$ with HCCPh and DCCPh at 95°C gave negligible isotope effects of $k_{\text{NH}}/k_{\text{ND}} = 1.1 \pm 0.1$ and $k_{\text{CH}}/k_{\text{CD}} = 1.05 \pm 0.1$, respectively. These results are consistent with a reversible alkyne C–H bond-activation step and with arene *ortho*-C–H bond activation as the rds for the catalytic reaction (Scheme 73).

Indoles can be prepared from *o*-tolyl isocyanides using $\text{Ru}(\text{dmpe})_2(\text{H})(\text{naphthyl})$ **155** ($\text{dmpe} = (\text{dimethylphosphino})$ -

Scheme 68



Scheme 69

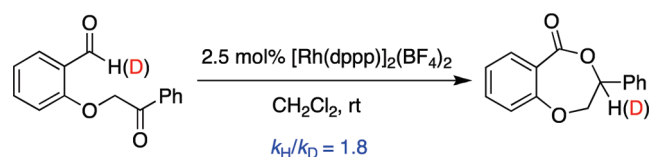


ethane) and $\text{Ru}(\text{dmpe})_2\text{H}_2$ as catalysts. Competitive KIE experiments¹⁰⁶ were done to differentiate the key product-determining steps of the cycle (Scheme 74). An intermolecular experiment using unlabeled and d_8 -labeled 4-*tert*-butyl-2,6-xylyl isocyanides indicate virtually no isotope effect ($k_{\text{H}}/k_{\text{D}} \approx 1.08$). However, when the metal was forced to compete intramolecularly for C–H and C–D bonds in **155**, a normal KIE ($k_{\text{H}}/k_{\text{D}} \approx 2.6$) was obtained. These results are consistent with a mechanism involving intramolecular C–H activation of a bound isocyanide in the indole-forming reaction.

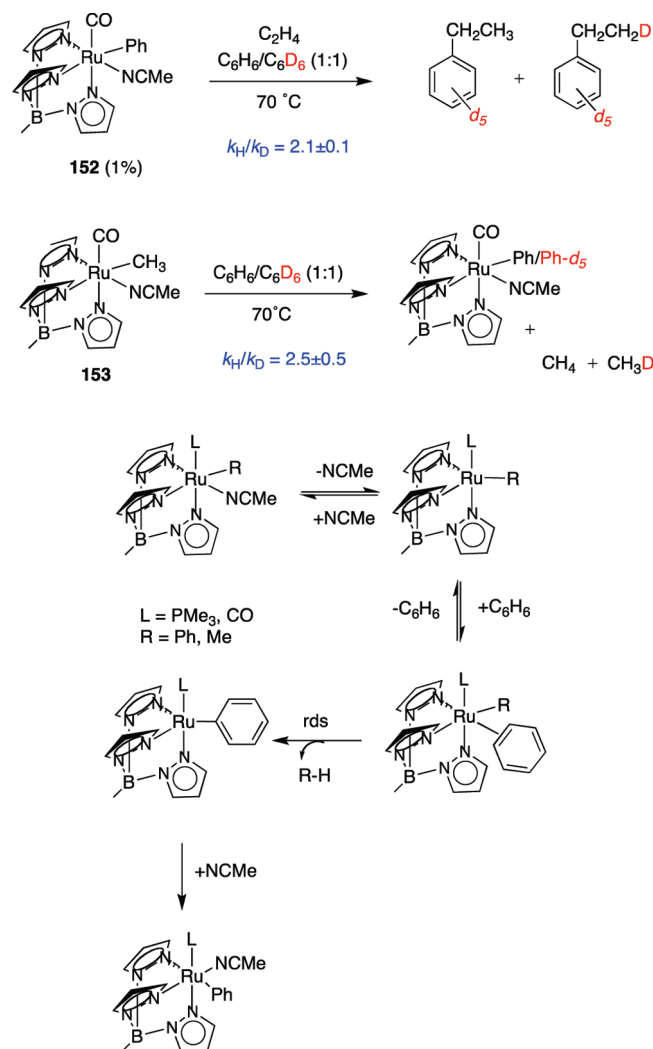
The cleavage and addition of *ortho*-C–H bonds in various aromatic compounds such as ketones, esters, imines, imidates, nitriles, and aldehydes, to olefins and acetylenes, can be achieved catalytically with the aid of ruthenium catalysts. The reaction is generally highly efficient and useful in synthetic methods. The coordination to the metal center by a heteroatom in directing groups such as carbonyl and imino groups is the key. The reductive elimination to form a C–C bond is the rate-determining step. This topic has been extensively studied by Murai's group.¹⁰⁷

The mechanism of the $\text{Ru}(\text{H})_2(\text{CO})(\text{PPh}_3)_3$ -catalyzed addition of C–H bonds in aromatic esters to olefins was studied by means of deuterium-labeling experiments and measurement of ^{13}C -KIEs (Scheme 75).¹⁰⁸ If a C–C bond-formation step was rate-determining, the relative intensity of the *ortho*-carbon in the starting material should be increased compared with those at natural abundance.¹⁰⁹ Thus, in reactions stopped at 64–79% conversions, the average KIE of the *ortho*-carbon in the recovered starting material was determined to be 1.033, while those of the remaining aromatic carbons had values near to 1.000 for each carbon atom. The same experiment was also applied to the reaction of aromatic ketones. In this case, the KIE of the *ortho*-carbon of the ketone was determined to be 1.023.¹⁰⁷ These results strongly suggest that, for both aromatic esters and ketones, the C–H bond-cleavage step is a rapid equilibrium prior to the rate-determining C–C bond-formation step

Scheme 70



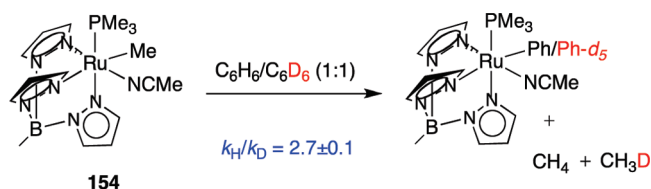
Scheme 71



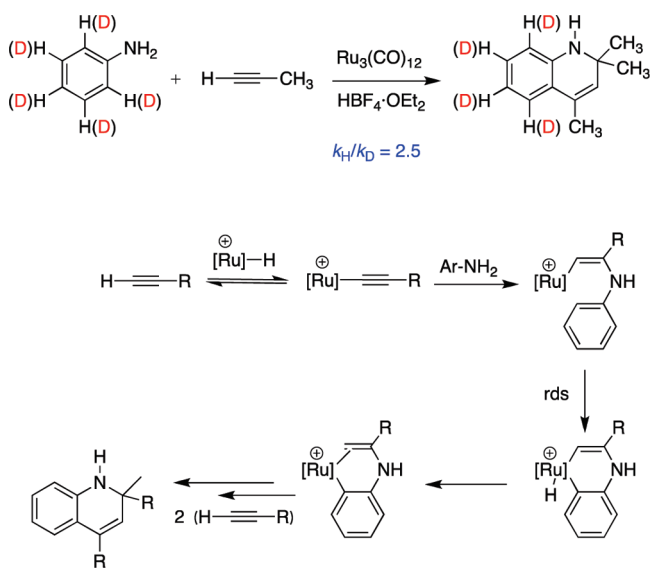
(reductive elimination). On the basis of these studies, the reaction pathway in Scheme 75 was proposed. However, the dramatic effect of the substituents on the aromatic ring in the ester coupling reactions suggests that different mechanisms for the reductive elimination step in aryl ketones and esters should be considered.

Yi and Lee have recently reported¹¹⁰ the formation of indene products **156** resulting from intermolecular coupling of arylketones **157** and 1-alkenes mediated by the cationic ruthenium hydride complex **158** formed in situ from the treatment of the tetranuclear Ru hydride complex $\{[(PCy_3)_2(CO)RuH]_4(\mu_4-O)(\mu_3-OH)(\mu_2-OH)\}$ with $HBf_4 \cdot OEt_2$ (Scheme 76). Preliminary mechanistic studies revealed a negligible KIE ($k_H/k_D = 1.13 \pm 0.05$ at $110^\circ C$) from the coupling reaction of acetophenone- d_0 /acetophenone- d_8 with 1-hexene, indicating a rapid and reversible *ortho*-C–H bond activation step. Additionally, the ^{13}C -KIE from the coupling reaction of 2-acetonaphthone and 1-hexene (70% conversion)¹⁰⁹ revealed a $^{12}C/^{13}C$ ratio at *ortho*-arene carbon atom of 2-acetonaphthone $C(3) = 1.020$ (with $C(7)$ as the internal reference). The observation of this significant ^{13}C -KIE supports the notion that the C–C bond-forming step involving the migratory insertion of the alkene to the *ortho*-metalated species **159** is the rds (Scheme 76).

Scheme 72



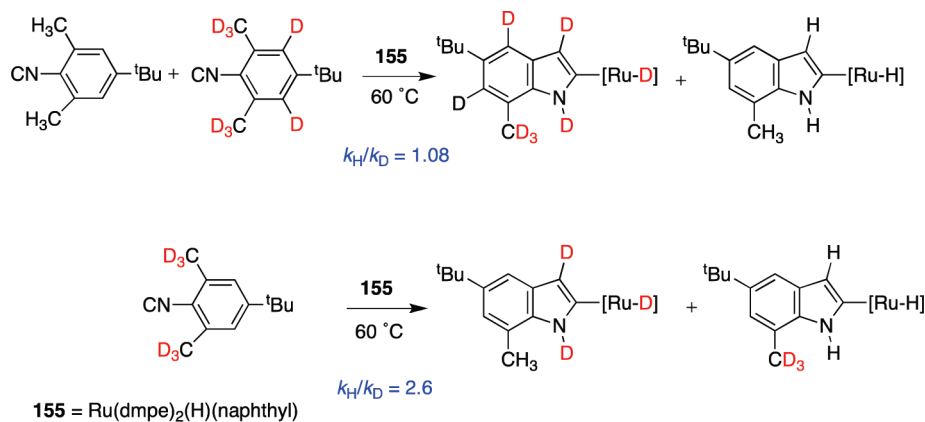
Scheme 73



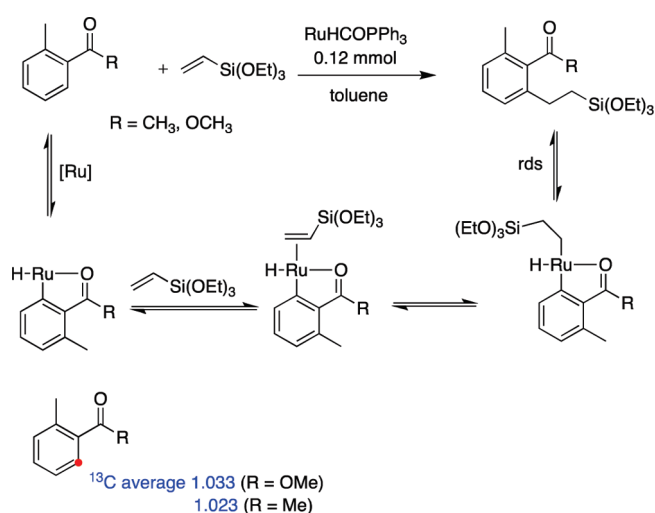
3.5.2. Hydroamination of Alkenes and Alkynes¹¹¹. Transition metal-catalyzed hydroamination of alkenes and alkynes is a highly effective method for forming new C–N bonds.¹¹² This fact makes this reaction a field of wide interest to develop mechanistic studies. Thus, the cationic ruthenium complex **160** $[(PCy_3)_2(CO)(Cl)Ru=CHCH=C(CH_3)_2]^+BF_4^-$ reacts with aniline and ethylene to form a 1:1 ratio of *N*-ethylaniline **161** and 2-methylquinoline **162** (Scheme 77). The analogous reaction with 1,3-dienes resulted in the preferential formation of Markovnikov addition products.¹¹³ A normal KIE ($k_H/k_D = 2.2 \pm 0.1$ at $80^\circ C$) was observed for the reaction of $C_6H_5NH_2$ and $C_6D_5ND_2$. In contrast, a negligible isotope effect of k_{CH}/k_{CD} was observed from $C_6H_5NH_2$ and $C_6D_5NH_2$ with ethylene at $80^\circ C$. These results indicate that the N–H bond activation is the rds of the catalytic reaction and the subsequent *ortho*-C–H bond and alkene insertion steps are relatively facile. The formation of a nearly equal ratio of products **161** and **162** is explained by an initial N–H bond-activation rate-limiting step followed by energetically compatible reductive elimination versus *ortho*-C–H bond activation for the catalytic reaction (Scheme 77).

Ruthenium–hydride complex $(PCy_3)_2(CO)RuHCl$ is an effective catalyst for the regioselective dehydrogenative coupling reaction of cyclic amines and alkenes. The formation of imine products **163** was rationalized by invoking the dehydrogenation of the amine and subsequent R–CH imine bond-activation/alkene-insertion sequence (Scheme 78).¹¹⁴ The observation of a normal KIE ($k_{NH}/k_{ND} = 1.9 \pm 0.1$) is consistent with a rate-limiting N–H bond-activation step. The formation of C–H

Scheme 74



Scheme 75



bond insertion products derived from **164** and even of *N*-alkylated amines depending on the structure of the reagents indicate that both the steric and electronic nature of alkenes are important for the product selectivity. An alternate mechanism involving the formation of a ruthenium–amide complex from the N–H bond activation would also be consistent with the observed *normal* isotope effect and cannot be ruled out.

The catalytic formation of bicyclic pyrroles **165** has been achieved from the direct coupling reaction of 2,5-dimethylpyrroles with terminal alkynes in the presence of $\text{Ru}_3(\text{CO})_{12}/\text{NH}_4\text{PF}_6$. Compounds **165** were obtained as single products or accompanied by coupling products **166** and **167** depending on the reaction conditions.¹¹⁵ The relatively small KIE ($k_{\text{H}}/k_{\text{D}} = 1.2$) observed for the reaction of 1,2,5-trimethylpyrrole with phenylacetylene- d_0 /phenylacetylene- d_1 supports a rapid H/D exchange between the two substrates. This result is an evidence in support of a mechanism involving three consecutive sp^2 C–H bond-activation and alkyne-insertion steps as outlined in Scheme 79.

A related example using $[\text{Ir}(\text{COD})\text{Cl}]_2$ as a highly effective precatalyst for the intramolecular addition of primary, as well as secondary, alkyl- or arylamines to tethered unactivated olefins at

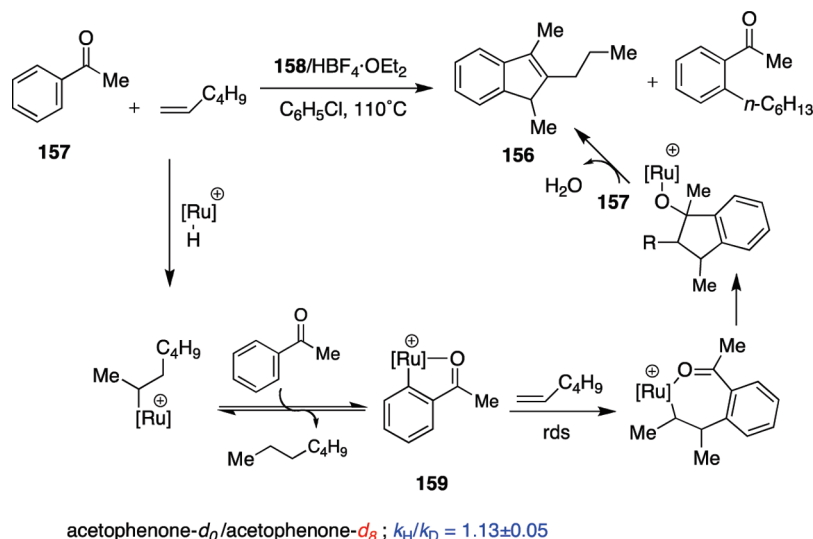
relatively low catalyst loading has been studied.^{116,117} Kinetic analysis of the hydroamination of **168** revealed that the reaction rate displays first-order dependence on the concentration of Ir and inverse-order dependence with respect to both substrate and product concentrations. Additionally, a primary KIE ($k_{\text{H}}/k_{\text{D}} = 3.4 \pm 0.3$) was observed in the cyclization of **168- d_0** and **168- d_1** in 1,4-dioxane at 110°C . These observations are compatible with an alkene activation mechanism involving nucleophilic attack of a tethered amine on a metalcoordinated alkene, followed by a rate-limiting protonolysis step (Scheme 80). However, alternative mechanisms, including those involving N–H oxidative addition, cannot be ruled out on the basis of these empirical data alone. A computational (DFT) study excluded these latter pathways and confirmed that reductive elimination involving a highly reactive Ir(III)–hydrido intermediate, and passing through a highly organized transition-state structure, is turnover-limiting.

A related hydroalkoxylation/cyclization of alkynyl alcohols mediated by lanthanide–organic complexes of the general type $\text{Ln}[\text{N}(\text{SiMe}_3)_2]_3$ ($\text{Ln} = \text{La}, \text{Sm}, \text{Y}, \text{Lu}$) has been reported (Scheme 81).¹¹⁸ KIE data obtained with internal alkynyl alcohol substrates **169** revealed an *inverse* KIE ($k_{\text{H}}/k_{\text{D}} = 0.95 \pm 0.03$), consistent with the alkyne insertion into Ln–O bonds (involving a highly organized transition state **170**) being the turnover-limiting step in the catalytic cycle, with subsequent, rapid Ln–C protonolysis.

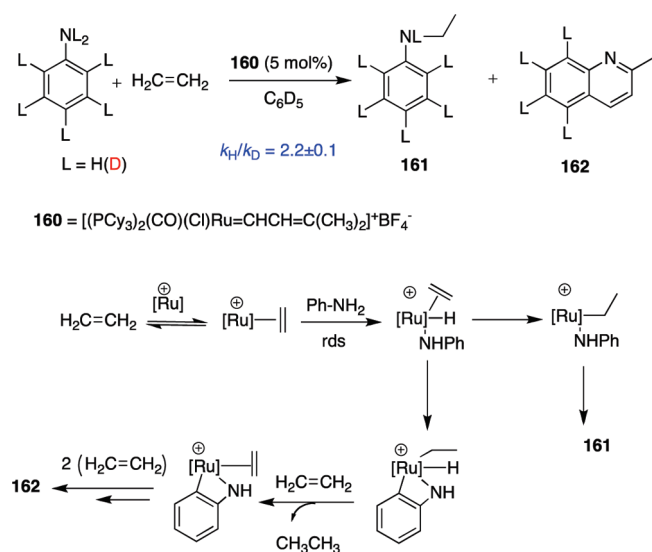
3.5.3. Other Ru-Catalyzed C–H insertions. The ruthenium–acetamido complex $[(\text{PCy}_3)_2(\text{CO})(\text{CH}_3\text{CONH})(^i\text{PrOH})\text{RuH}]$ **171** was found to be an effective catalyst for the conjugate addition of alcohols to acrylic compounds under mild reaction conditions to form β -alkoxynitrile compounds **172** (Scheme 82).¹¹⁹ Both the observation of a significant carbon isotope effect ($^{12}\text{C}/^{13}\text{C} = 0.979$) at the terminal carbon of acrylonitrile and the positive Hammett ρ value of +0.18 are consistent with the rate-limiting nucleophilic addition of alkoxide via the zwitterionic species **173** (Scheme 82).

Reaction of Ru(II) complexes $\text{TpRu}(\text{L})(\text{L}')(\text{R})$ ($\text{L} = \text{CO}$, $\text{L}' = \text{NCMe}$, and $\text{R} = \text{CH}_3$ or $\text{CH}_2\text{CH}_2\text{Ph}$; $\text{L} = \text{L}' = \text{PMe}_3$ and $\text{R} = \text{CH}_3$) with AgOTf leads to alkyl elimination reactions that produce $\text{TpRu}(\text{L})(\text{L}')(\text{OTf})$ and organic products that likely result from Ru–C_{alkyl} bond homolysis.¹²⁰ Analysis of several reactions of $\text{TpRu}(\text{CO})(\text{NCMe})(\text{Me})$ **174** with AgOTf in a 1:1 molar mixture of toluene- d_0 and toluene- d_8 revealed a kinetic isotope effect of $k_{\text{H}}/k_{\text{D}} = 5.9 \pm 0.7$ (Scheme 83). This result

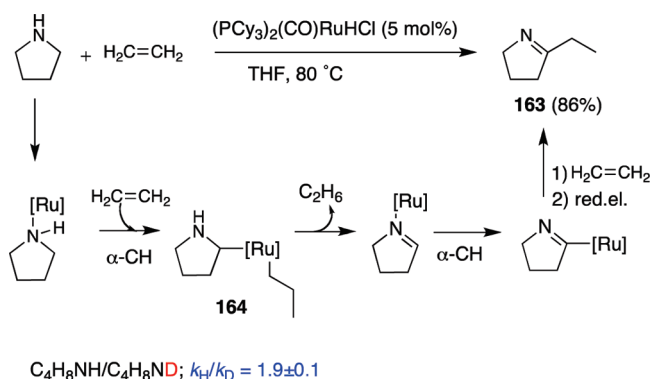
Scheme 76



Scheme 77



Scheme 78



together with DFT calculations on Ru(II) and Ru(III) $TpRu(CO)(NCMe)(Me)$ suggest a single-electron oxidation of the complex that favors the Ru–CH₃ homolytic bond dissociation.

To explore the influence of a trans ligand on a Ru center opposite an anchored tetradentate tripodal $[SiPPh_3]^-$ ligand, thermally unstable phosphide complex **175** was found to decay to the cyclometalated phosphine adduct **176** (Scheme 84).¹²¹ A study of the process using labeled **175** revealed a high KIE ($k_H/k_D = 5.5 \pm 0.3$), suggesting a highly ordered transition state with significant C–H bond cleavage.

The photochemical reaction of transition metal boryl complexes of the type $Cp^*M(CO)_nB(OR)_2$ ($M = Fe, Ru, W$) **177** with different alkanes has been explored.¹²² The metal boryl complexes reacted exclusively at the terminal C–H position of alkanes. Functionalization of 2-methylbutane occurred preferentially at the least sterically hindered terminal position with a selectivity of 10:1. These selectivity data, in addition to the

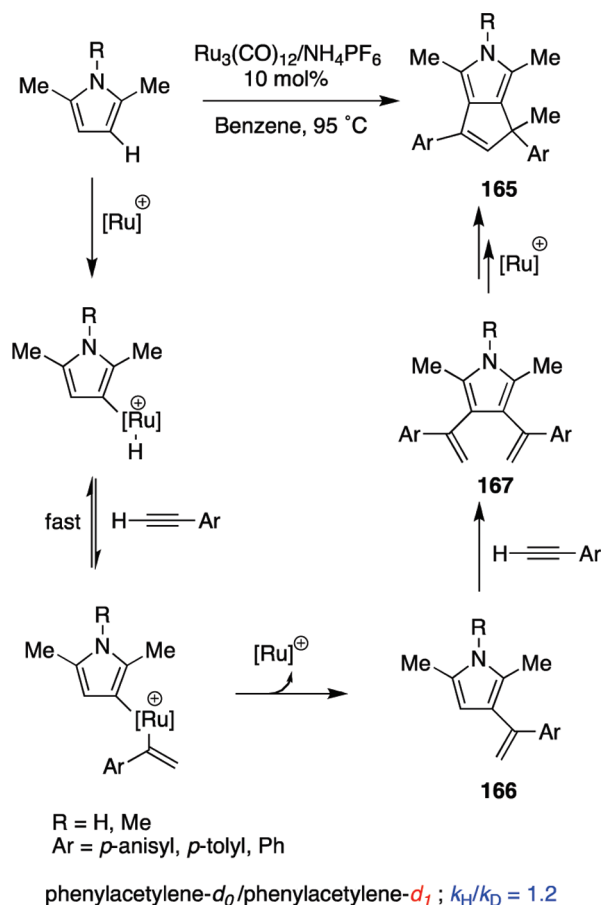
different KIEs measured for reaction of metal boryls **177** with a mixture of pentane- d_0 and pentane- d_{12} ($k_H/k_D = 1.9$ for $M = Fe$, 2.2 for $M = Ru$, 4.9–5.1 for $M = W$), indicate that the alkane functionalization does not occur by reaction of a free boryl radical with free alkane (Scheme 85).¹²³

3.6. KIEs in the Study of C–H Activation Mechanisms by Zr and Ti Complexes

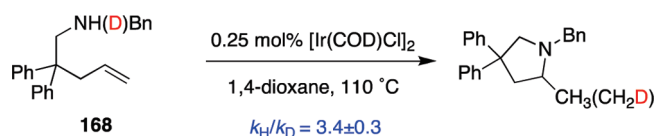
An alternative approach to the functionalization of unactivated hydrocarbons involves a 1,2-RH-addition across metal–heteroatom multiple bonds $[MX]$ ($M = \text{groups 4–6}$, $X = NR, CR_2, CR, O$) to afford products of general structure $[M(XH)(R)]$ (Scheme 86). Extensive selectivity studies have been performed on group 4 imido $[M=NR']$ systems that activate hydrocarbons under reversible conditions.

Several studies have been carried out on the thermal 1,2-RH-elimination in labeled $(t\text{-Bu}_3SiNH/D)_3ZrNR$ complexes **178–180** in methane or benzene to yield the addition products **181** (Scheme 87).¹²⁴ The large primary KIEs ($k_H/k_D = 6.27 \pm 0.09$)¹²⁵ and ($k_H/k_D = 7.3 \pm 0.4$)¹²⁶ reported for loss of CH_3H/D unlabeled/labeled **178** at 96 °C were consistent with a rate-determining 1,2-RH-elimination having a relatively linear H-atom transfer that implicated similar amounts of C–H bond making and N–H bond breaking in the transition state. The

Scheme 79



Scheme 80

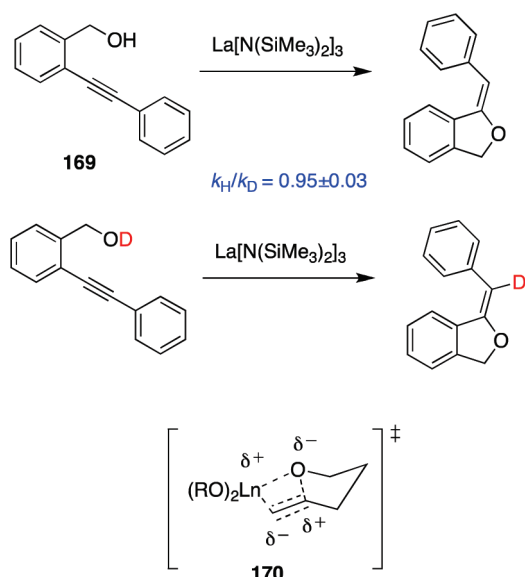


KIEs for PhCH_3 versus PhCH_2D loss from unlabeled/labeled **179** ($k_{\text{H}}/k_{\text{D}} = 7.1 \pm 0.6$, 96.8 °C), and PhH versus PhD loss from unlabeled/labeled **180** ($k_{\text{H}}/k_{\text{D}} = 4.6 \pm 0.4$, 96.7 °C),¹²⁵ supported similar contentions, although the latter number hinted at a significantly less symmetric transition state for phenyl elimination. Multiple deuteration of the products was not detected, excluding reversible elimination/addition prior to RH loss. Additionally a secondary KIE ($k_{\text{H}}/k_{\text{D}} = 1.32 \pm 0.08$) (or = 1.10 per D) was observed for CH_4 versus CD_3H loss from unlabeled/labeled **182** at 96.7 °C (Scheme 87).

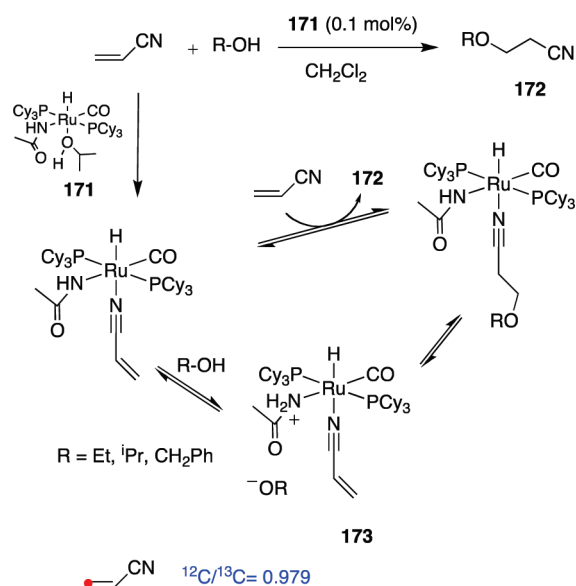
A mechanism involving rate-determining $\text{R}-\text{H}$ 1,2-elimination through a relatively linear H-atom transfer in a four-centered transition state to generate the three-coordinate $(^t\text{Bu}_3\text{SiNH})_2\text{Zr}=\text{NSi}^t\text{Bu}_3$ species **183** accounts for the experimental results. This intermediate can then select to activate RH or $\text{R}'\text{H}$ via 1,2- $\text{RH}/\text{R}'\text{H}$ addition across the $\text{Zr}=\text{N}$ bond (Scheme 88).

Analogous 1,2- RH -elimination processes have been reported for the thermolysis in benzene and 1,2- RH elimination/addition

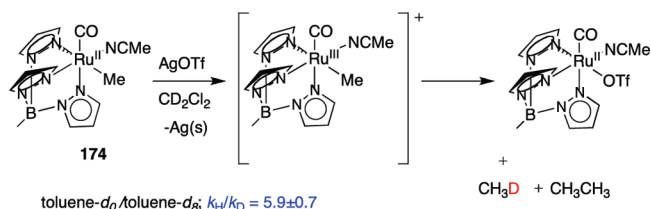
Scheme 81



Scheme 82



Scheme 83



in Ti complexes **184**,^{30c,127} the thermolysis of $(^t\text{Bu}_3\text{SiNH})_3\text{TiCl}$ **185** to form $(^t\text{Bu}_3\text{SiNH})(\text{THF})\text{ClTi}=\text{NSi}^t\text{Bu}_3$ **186**,¹²⁸ the thermolysis in benzene of Ta complexes **187**,¹²⁹ and the

transformation of the short-lived pentaneopentyl Ta complex **188** into the alkylidene derivative **189** (Scheme 89).¹³⁰ The primary KIEs observed were consistent with rate-limiting abstraction of the *N*-proton/deuterium and implicate the intermediacy of a three-coordinate intermediate rather than σ -bond metathesis or pathways initiated by amine elimination. As has been postulated for other proton-transfer reactions, the large KIE values could be attributable to tunneling effect, although it was not experimentally confirmed.

Hoyt and Bergman studied the selectivity of sp^3 , sp^2 , and sp C–H activation reactions by complex $[Cp^*CpZr=NCMe_3](THF)$ **190** and found higher relative selectivity for those substrates bearing C–H bonds with a greater degree of σ -character.¹³¹ Thermolysis of **190** forms the transient imido complex $[Cp^*CpZr=NCMe_3]$ **191** that in the presence of alkyl, alkenyl, alkynyl, and aryl C–H bonds forms the activation products $[Cp^*CpZr(Ph)-(NHCMe_3)]$ **192**. The nature of the transition state was examined by performing KIE studies. Measured at 45 °C, KIE values for reaction of **190** with unlabeled/labeled benzene, *n*-pentane, mesitylene, and (*E*)-neohexene were $k_H/k_D = 7.4, 8.9, 8.8,$ and 6.9 , respectively. These large positive values indicated a primary KIE consistent with a direct C–H bond-breaking event in the rate-determining step of the reaction, most likely occurring through a four-center transition state **193**, wherein transfer of H from R to N is relatively linear (Scheme 90).

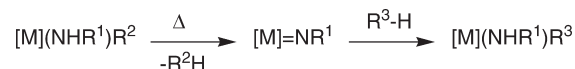
The high relative rate for activation of *tert*-butylacetylene led to speculate that complex **190** may activate alkynes by a different mechanism. In contrast with the large primary KIE values determined for the other substrates, for *tert*-butyl acetylene it was found to be $k_H/k_D = 0.8$. This small, *inverse* value indicated that a C–H bond was not broken in or before the rds (as in **193**). More likely, in analogy to a Ti=O system, alkynes may undergo rate-determining metallacycle formation with **191** to form intermediate metallacycle **194**, followed by rearrangement to provide **195** (Scheme 90).

Stable zirconium alkylidene complexes **196** are formed via the thermal decomposition of the corresponding dialkyl precursors **197**. Kinetic studies show that the decomposition of **197** follows

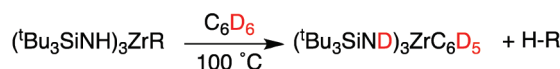
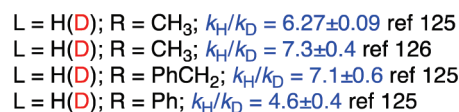
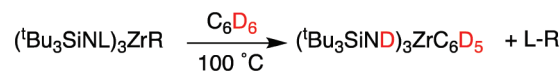
first-order kinetics, with activation parameters consistent with an intramolecular α -abstraction process.¹³² The kinetic isotope effect ($k_H/k_D = 3.0 \pm 0.5$) obtained for the benzyl perdeuterated analogue $[P_2Cp]ZrCl(CD_2C_6D_5)_2$ is in agreement with a four-centered transition state (Scheme 91). The reaction rates follow the order benzyl > neosilyl > neopentyl, exactly opposite to that found previously in other homoleptic $Ta(CH_2R)_5$ complexes ($R = Ph, SiMe_3, CMe_3$). These results reflect a subtle balance between the steric crowding imposed by the alkyl ligands and the side arm phosphines of the ancillary ligand.

The formation of η^2 -imine–zirconocene complexes (zirconaziridines) $(Cp_2Zr(NR^1CR^2R^3))$ **198** by elimination of R^4H from $Cp_2Zr(R^4)(NR^1CHR^2R^3)$ **199** has been investigated.¹³³ Hammett-type structure/rate correlations showed a marked dependency with the nature of the substituents; in particular, the reaction rate substantially increases when R^4 is an electron-rich aromatic ring. KIE studies carried out on complex **199** indicated that the elimination is first-order in the zirconocene complex, with a $k_H/k_D = 8.2$ at 20 °C. A concerted cyclometalation involving deprotonation α to nitrogen by R^4 via a four-member transition state **200** where the hydrogen moves as H^+ best fits the data (Scheme 92). A similar KIE ($k_H/k_D = 9.7$ at 25 °C) has been observed by Bercaw and co-workers¹³⁴ for the analogous formation of a tantalum η^2 -imine complex. A small

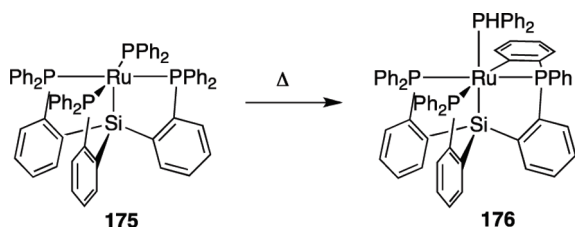
Scheme 86



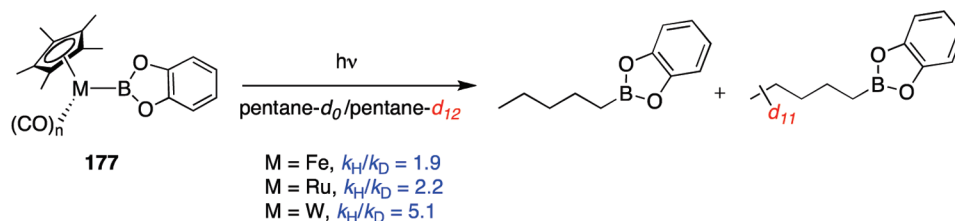
Scheme 87



Scheme 84

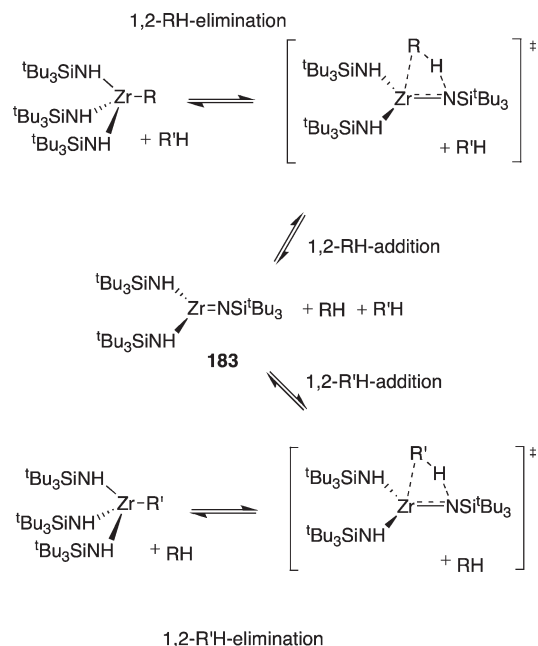


Scheme 85



inverse KIE ($k_{\text{H}}/k_{\text{D}} = 0.88 \pm 0.05$) with three deuteriums was observed for the elimination of CD_3H from $\text{Cp}_2\text{Zr}(\text{CD}_3)(\text{NPh}^i\text{Pr})$ compared with CH_4 from $\text{Cp}_2\text{Zr}(\text{CH}_3)(\text{NPh}^i\text{Pr})$ at

Scheme 88

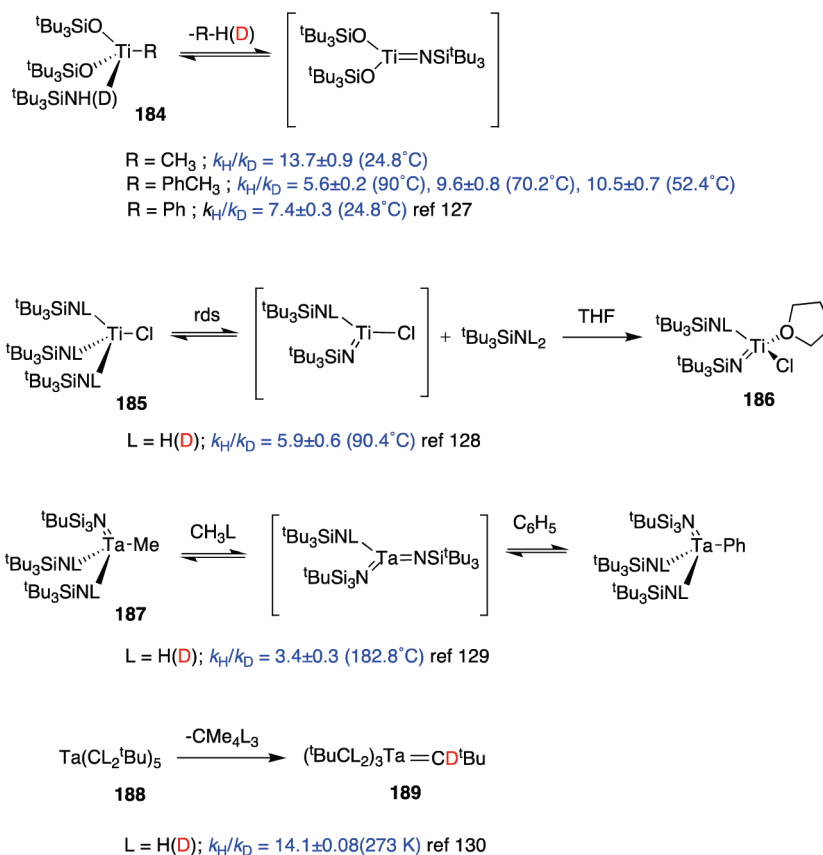


338 K. This is consistent with the methyl carbon bonding to both the zirconium and migrating H in the transition state (rehybridization decreases the strength of the C–D/H bonds).

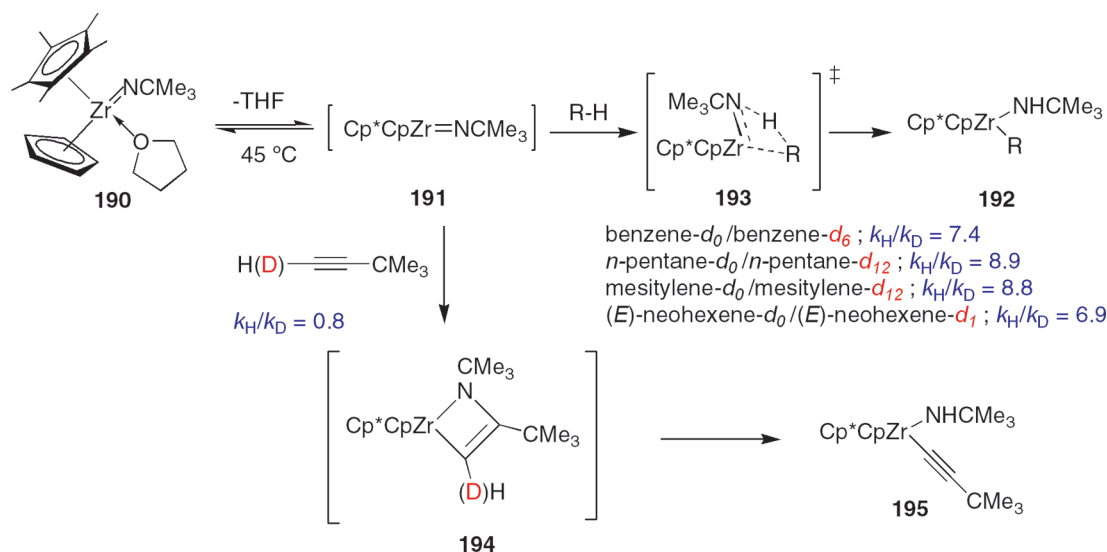
Chirik and Bercaw¹³⁵ have reported that group 4 metallocene dihydrides **201** (R_nCp)₂MH₂ (R_nCp = alkyl-substituted cyclopentadienyl; M = Zr, Hf) react with olefins to afford stable metallocene alkyl hydride complexes **202**. Kinetic studies on $\text{Cp}^*(\eta^5\text{-C}_5\text{Me}_4\text{H})\text{ZrX}_2$ (X = H, D) showed a primary KIE ($k_{\text{H}}/k_{\text{D}}$ of 2.4 ± 0.3 at 23 °C). This *normal*, primary isotope effect is consistent with an insertion into the Zr–H bond proceeding by a pre-equilibrium involving rapid coordination and dissociation of olefin, followed by rate-determining hydride transfer (Scheme 93). A similar kinetic profile has been proposed for reactions of olefins with $\text{Cp}^*_2\text{M}(\text{OR})(\text{H})$ (M = Th, U), where primary KIEs of 1.4 ± 0.1 and 1.3 ± 0.2 have been measured for the insertion of cyclohexene and 1-hexene at 60 °C,¹³⁶ and with hydridocyclization reactions in scandocene hydrides.¹³⁷

Zirconocene alkyl hydride complexes **203** react with alkynes¹³⁵ to form the alkenyl hydride complex **204** and free olefin. These products are consistent with a β -H elimination from the starting alkyl hydride **203** liberating free olefin and the zirconocene dihydride **205** that is subsequently trapped by the acetylene in solution to form **204**. The kinetic isotope effect (23 °C) for β -H/D elimination in a series of isobutyl hydride complexes ($\text{R}_n\text{-Cp}$)₂Zr($\text{CH}_2\text{CHR}'$)(H/D) were determined to be in the range $k_{\text{H}}/k_{\text{D}} = 3.9\text{--}4.5$ (Scheme 94). The rate of β -H elimination also slows with more substituted (hence, more sterically crowded) cyclopentadienyl ligands. These data suggest that β -H elimination proceeds via rate-determining C–H(D)

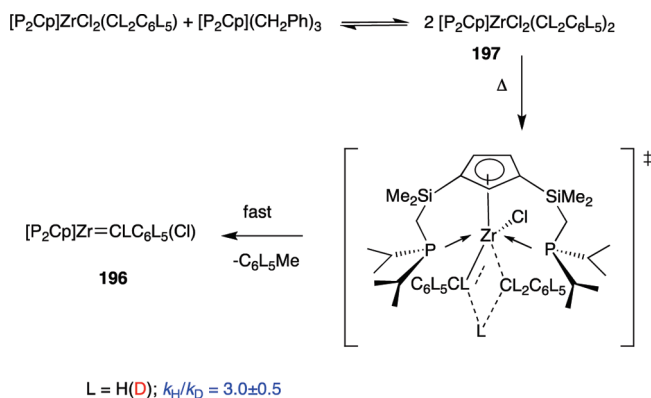
Scheme 89



Scheme 90



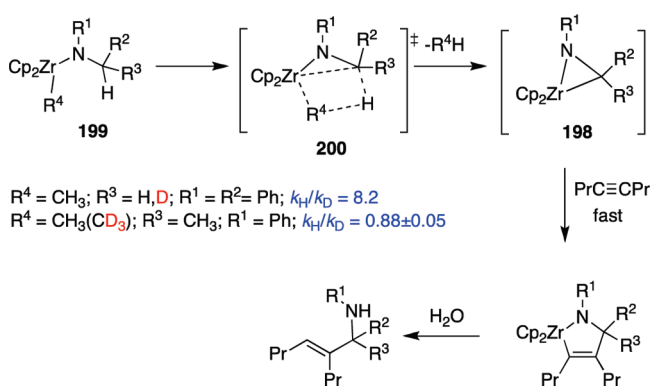
Scheme 91



bond cleavage followed by rapid dissociation of the coordinated olefin. The values obtained in this study ($k_H/k_D \approx 4$) are somewhat larger than those measured for related β -H elimination in $Cp^*2ScCH_2CH_2C_6H_5$ systems ($k_H/k_D = 2.0$).¹³⁸ Likewise, a smaller KIE ($k_H/k_D = 1.6$) has been measured for the β -H elimination in the polymerization of propene with $[(Me_2Si)_2\{\eta^5-C_5H-3,5-(CHMe_2)_2\}(\eta^5-C_5H_2-4-CHMe_2)]ZrCl_2$ /methyalumoxane mixtures.¹³⁹ The larger values for the alkyl hydrides in the current study may reflect a somewhat later transition state (more C–H bond breaking) for the less electrophilic, neutral group 4 metallocene derivatives.

The mechanism for C–O bond cleavage in dialkyl and cyclic ethers by η^9, η^5 -bis(indenyl)zirconium sandwich complexes has been established by means of experimental and computational studies.¹⁴⁰ Thus, treatment of the bis(indenyl)zirconium sandwich complex **206** with dialkyl ethers resulted in facile C–O bond scission furnishing a bis(indenyl)zirconium alkoxy hydride complex **207** (Scheme 95). Observation of *normal* primary KIEs for diethyl ether ($k_H/k_D = 5.0 \pm 0.5$ and $k_H/k_D = 4.7 \pm 0.4$) and for THF (k_H/k_D of 3.5 ± 0.3) indicate that a C–H bond-cleavage event precedes the C–O bond scission either in or prior to the rds. The proposed mechanism involves haptotropic

Scheme 92



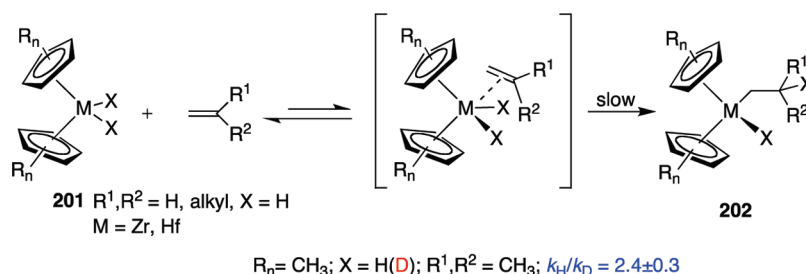
rearrangement to η^5, η^5 -bis(indenyl)zirconium intermediates that promote rate-determining C–H activation to yield an η^5, η^5 -bis(indenyl)-zirconium alkyl hydride intermediate, and ultimately C–O bond scission.

Zirconocene thioaldehyde complexes **209** have been prepared in high yield by heating (alkylthio)-methylzirconocenes **208** in the presence of PMe_3 . The large primary KIEs ($k_H/k_D = 5.2 \pm 0.2$, 80 °C) together with the first order kinetics, the Hammett value $\rho = 0.39$, and the negative entropy of activation ($\Delta S^\ddagger = -20.6$ (0.4) eu) observed for the formation of the thiobenzaldehyde complex $Cp_2Zr(Me)SCH_2Ph$, are consistent with a concerted four-center cyclometalation process.¹⁴¹ The rate-limiting step involves a transfer of hydrogen in a polarized transition state (Scheme 96).

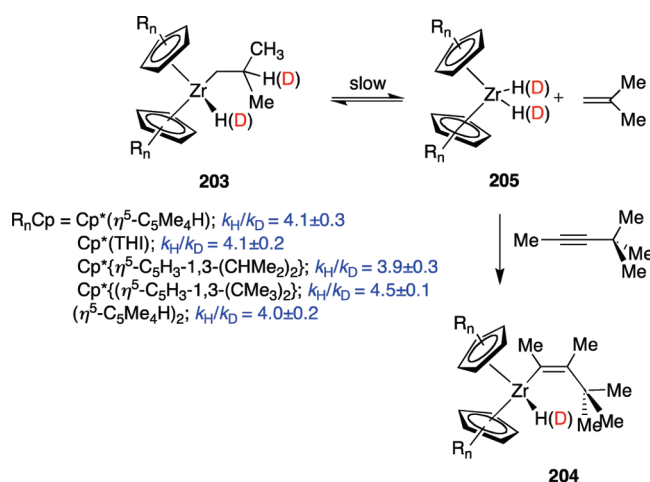
Complex **210** undergoes unimolecular thermolysis in solution to yield the ring-metallated complex **211** and benzene. A kinetic study carried out on labeled and unlabeled complexes revealed a substantial KIE ($k_H/k_D = 13.5 \pm 0.20$, 25 °C and $k_H/k_D = 6.5 \pm 0.10$, 70 °C). Hence, aryl rather than Cp^* methyl C–H bond scission is rate-limiting.¹⁴² The magnitude of the KIE at room temperature suggests a symmetrical transition state with possible tunneling contributions (Scheme 97).

Thermolysis of titanium tribenzyl complexes **212** yield titanium dibenzyl species with an *ortho*-cyclometallated pendant

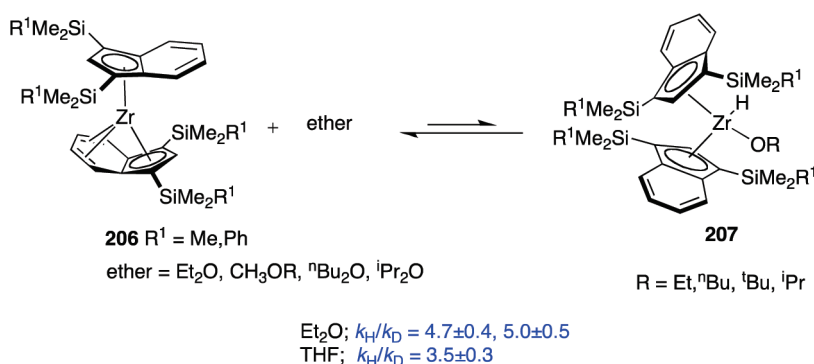
Scheme 93



Scheme 94



Scheme 95



arene group **213**.¹⁴³ Kinetic investigation of the thermolysis of **212-d₅** ($R = \text{D}$) revealed a small KIE ($k_H/k_D = 1.23 \pm 0.05$, 65°C) indicating that the aryl *ortho*-C–H/D bond is not broken in the transition state of the rds. The observations conclusively rule out a direct σ -bond metathesis pathway and confirm the involvement of a benzylidene intermediate **214** obtained after rate-determining toluene elimination in **212** (Scheme 98). Rapid intramolecular addition of the *ortho*-CH bond of the pendant arene group to the $\text{Ti}=\text{C}$ bond of the intermediate **214** yields cyclometalated compound **213**.

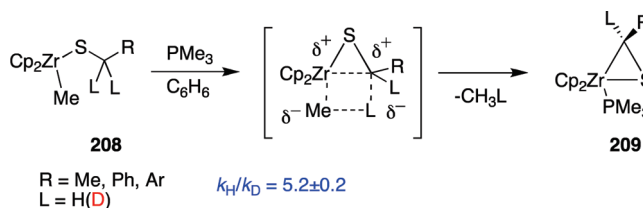
C–H bond activation of benzene by hafnium complex **215** occurs at room temperature to form compound **216** (Scheme 99).¹⁴⁴ The

kinetic studies indicate first-order dependence of the rate on benzene and a large primary KIE ($k_H/k_D = 6.9 \pm 0.7$), confirming that benzene is involved in the rate-determining step. These data are consistent with a σ -bond metathesis mechanism in which Hf–Si bond cleavage, Hf–Ph bond formation, and transfer of hydrogen from carbon to silicon in the β -position occur simultaneously on a four-centered transition state.

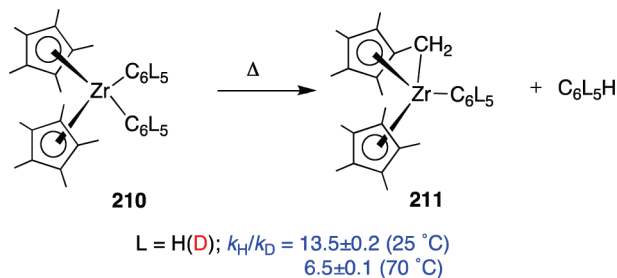
3.7. KIEs in the Study of C–H Activation Mechanisms by Other Transition Metal Complexes

Photolysis of the complexes $(\text{HBpz}_3)\text{ReO}(\text{I})\text{Cl}$ **217** and $(\text{HBpz}_3)\text{ReOI}_2$ in arene solvents results in replacement of the

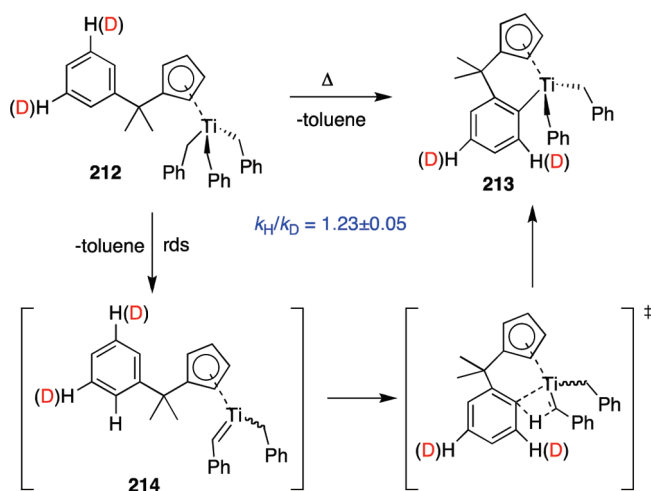
Scheme 96



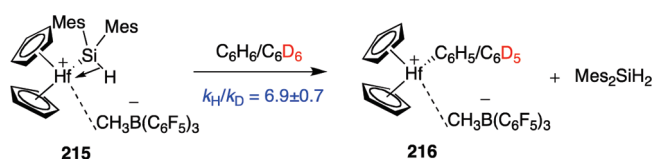
Scheme 97



Scheme 98

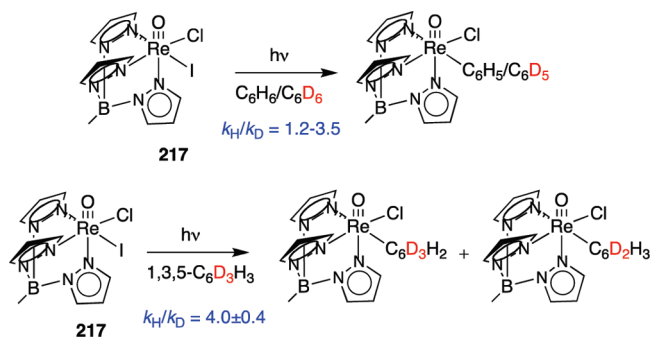


Scheme 99

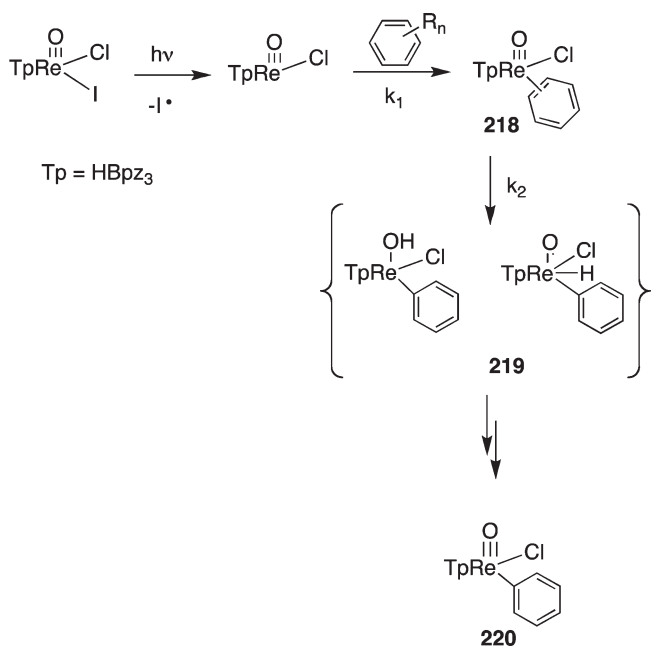


iodide ligand by an aryl group.¹⁴⁵ Arene activation occurs exclusively at aromatic rather than benzylic positions, has some functional group tolerance, and shows marked preference for reactions with electron-rich arenes (electron-deficient arenes react poorly). The intermolecular KIE observed on irradiation of **217** in mixtures of C_6H_6 and C_6D_6 ranges from $k_{\text{H}}/k_{\text{D}} = 1.2$ to 3.5, depending on the concentration of $[\text{Re}]$ and on the presence of other reagents such as

Scheme 100



Scheme 101



pyridine or I_2 . The isotope effect from intramolecular competition in 1,3,5- $\text{C}_6\text{H}_3\text{D}_3$ is larger ($k_{\text{H}}/k_{\text{D}} = 4.0 \pm 0.4$) and insensitive to the details of the reaction conditions (Scheme 100)

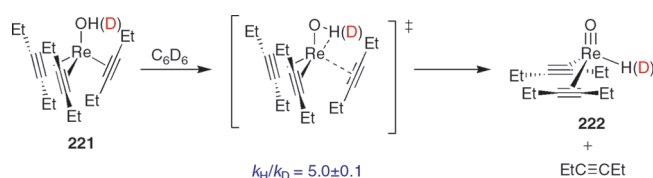
These data indicate a mechanism with two product-determining steps, such as in Scheme 101. Changing the photolysis conditions changes the amount that each step is product-determining, thus changing the (intermolecular) isotope effect. At low rhenium concentrations (or in the presence of pyridine), the product is determined by a step with a very low intermolecular KIE ($k_{\text{H}}/k_{\text{D}} = 1.2$), which is suggested to be arene coordination **218**. The subsequent C–H activation step **219** is more product-determining at higher rhenium concentrations and in the presence of added I_2 and is the source of the intramolecular isotope effect. The changing of the reaction conditions affects the rate of arene decooordination. In the absence of additives (particularly I_2), C–H activation is significantly faster than dissociation of the arene. C–H activation is proposed to take place by addition of the C–H bond across the ReO bond, with subsequent oxidation of the $\text{Re}-\text{OH}$ to give the final oxo–aryl product **220**.

The spontaneous isomerization of rhenium hydroxide complex **221** to the oxo–hydride complex **222** and 3-hexyne is a first-order

process.¹⁴⁶ There is a primary KIE ($k_{\text{OH}}/k_{\text{OD}} = 5.0 \pm 0.1$), and the rearrangement is unaffected by the presence of 1 M 3-hexyne. These data rule out a mechanism involving initial ligand loss followed by rearrangement. Instead, hydrogen migration from oxygen to rhenium occurs in the coordinatively saturated tris(alkyne) species **221**, either synchronously with or prior to the loss of alkyne (Scheme 102). The experimental data thus indicate that rearrangement occurs by rate-limiting hydrogen migration synchronously with or prior to loss of ligand. An alternative pathway of pre-equilibrium hydrogen migration followed by rate-limiting ligand loss was discarded based on the comparison between the calculated ($k_{\text{H}}/k_{\text{D}} = 2.4$) and the experimental KIEs.

Watson, Wu, and Richmond have reported¹⁴⁷ the first isotope study on *ortho*-metalation in a polynuclear system, in the reaction between the diphosphine ligand bpdc and $\text{Os}_3(\text{CO})_{10}$ - $(\text{MeCN})_2$ to give $1,2\text{-Os}_3(\text{CO})_{10}(\text{bpdc})$ **223** (bpdc = 4,5-bis-(diphenylphosphino)-4-cyclopentene-1,3-dione) as the kinetic

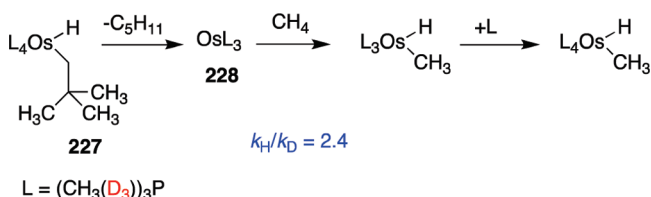
Scheme 102



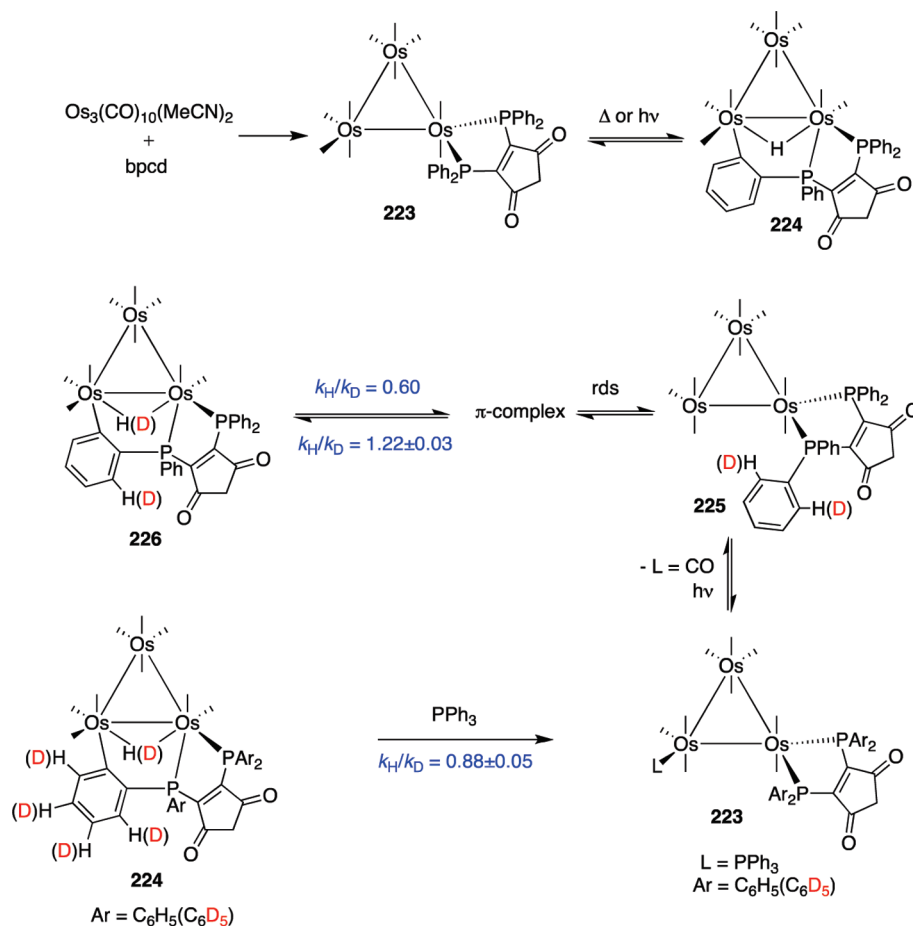
product of ligand substitution. Nondissociative ligand isomerization to the chelated cluster **223** occurs upon heating or UV-light irradiation, followed by the loss of CO and formation of the hydride cluster **224** (Scheme 103).

The mechanism of isomerization has been investigated. The *inverse* KIE ($k_{\text{H}}/k_{\text{D}} = 0.88 \pm 0.05$) observed in the reductive coupling of unlabeled/labeled **224** in the presence of PPh_3 has been interpreted as arising from a preequilibrium involving the hydride (deuteride) cluster and a transient arene-bound Os_3 species that precedes the rate-limiting formation of 1,1- $\text{Os}_3(\text{CO})_9(\text{bpdc})$ **225**. In parallel, the KIEs for the oxidative coupling of the C–H(D) bond in the *ortho*-metalation step ($k_{\text{H}}/k_{\text{D}} = 1.22 \pm 0.03$) and the reverse reductive coupling step ($k_{\text{H}}/k_{\text{D}} = 0.60$) were obtained from the irradiation of labeled **223** in toluene to yield cluster **226**. The data support a reversible *ortho*-metalation reaction that proceeds by way of a transient π -complex and

Scheme 104



Scheme 103



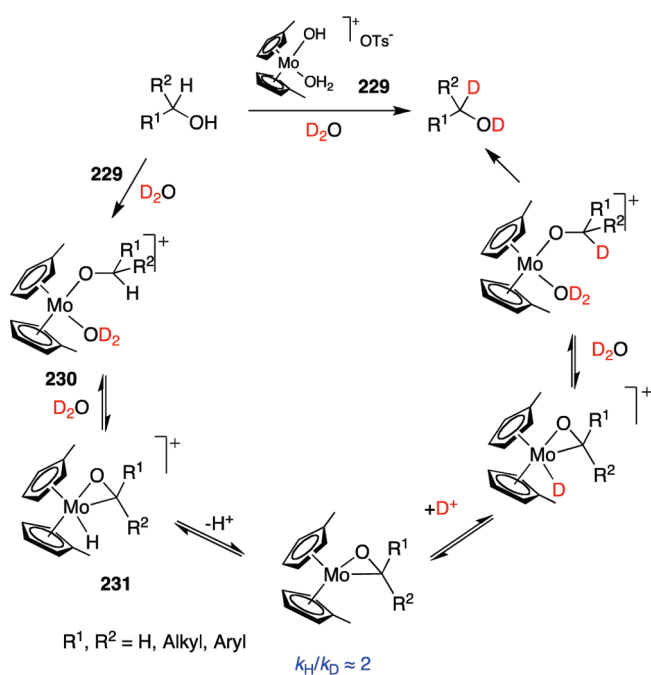
demonstrate the role of unsaturated cluster **225** as a precursor of **226** (Scheme 103).

The primary KIE ($k_{\text{H}}/k_{\text{D}} = 2.4$) obtained in the pyrolysis of neopentyl osmium hydride **227** in the presence of methane was considered a strong evidence in favor of the intermediacy of Os(0) reactive intermediate **228** as the key species in the C–H activation process (Scheme 104).¹⁴⁸

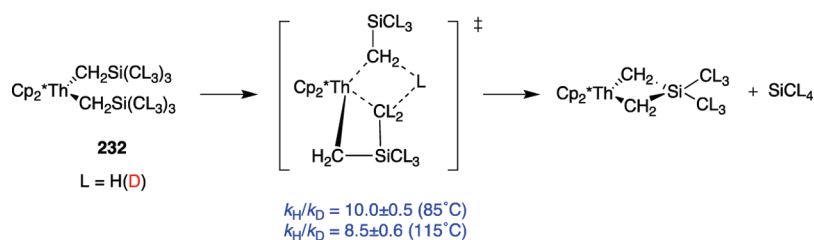
The mechanism of the catalytic α -H/D exchange in alcohols promoted by molybdocenes in D₂O was shown to occur by C–H bond activation.¹⁴⁹ The H/D exchange reaction proceeds stepwise (Scheme 105). Following the exchange of the aquo ligand in **229** and coordination of the alcoholic substrate, an alkoxide complex **230** is formed. Upon dissociation of the remaining aquo ligand, the coordinatively unsaturated molybdocene inserts into the R–C–H bond of the alkoxide, forming intermediate **231**, which can undergo reversible protonation. This key step leads to the observed isotope exchange upon dissociation of the coordinated alcohol and justifies the estimated primary KIE ($k_{\text{H}}/k_{\text{D}} \approx 2$) of the reaction.

The cyclometalation of bis(pentamethylcyclopentadienyl)-thorium dialkyl complexes has been reported.¹⁵⁰ The large KIEs obtained in different studies of thermolysis of **232** at 85 and 115 °C ($k_{\text{H}}/k_{\text{D}} = 5.0$ – 10.0) suggest that a mechanism involving rate-limiting γ -hydrogen abstraction is operative. The mechanism for cyclometalation is proposed to involve a concerted,

Scheme 105



Scheme 106



heterolytic process with hydrogen atom abstraction and metallacycle formation occurring in a four-center transition state (Scheme 106).¹⁵¹

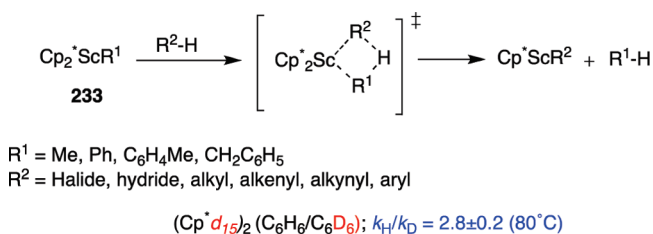
A σ -bond methathesis mechanism has been proposed for the C–H and H–H activation reactions reaction of organoscandium compounds **233** based on the $k_{\text{H}}/k_{\text{D}} = 2.8 \pm 0.2$, 80 °C, observed for the reaction of labeled **233** (Cp^*d_{15})₂Sc–CH₃ with C₆H₆/C₆D₆, together with the noticeable decrease in rate with decreasing σ -character of the reacting σ -bonds.¹⁵² The very small differences in the rates of vinylic and aryl C–H bond activation suggested that sp²-hybridized C–H bonds are activated without formation of a π -complex (Scheme 107).

KIEs were also used in the study of migratory insertion and elimination reactions of Cp^*_2TaXR (R = H, alkyl; X = olefin, alkylidene, NMe, O, S).¹⁵³ An *inverse* KIE value ($k_{\text{H}}/k_{\text{D}} = 0.46 \pm 0.03$) was reported for the thermolysis of hydrido η^2 -formaldehyde complex **234**, indicative of a stepwise process involving a preequilibrium with intermediate species **235** followed to rate-determining α -CH₃ elimination to form **236**, rather than cleavage of the C–O bond in concert with C–H bond formation. Similar reactivity is exhibited for thioaldehyde hydride complexes **237**^{153c} (Scheme 108).

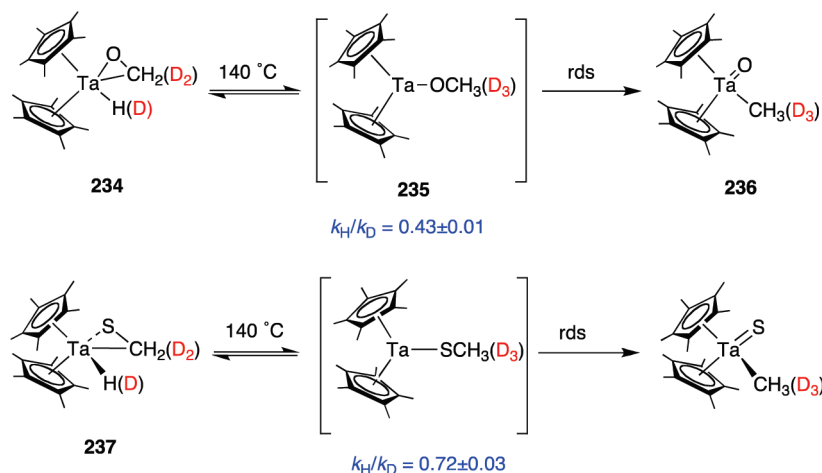
The study of KIEs has proven decisive in proposing a C–H activation mechanism for the methane loss and formation of metalated scandium borate **238** from the reaction between β -dikethyliminato scandium complex **239** and HB(C₆F₅)₂.¹⁵⁴ The reaction proceeds through an isolable ion pair **240**, which decomposes with loss of methane, giving a large primary KIE ($k_{\text{H}}/k_{\text{D}} = 8.7 \pm 0.6$). This data in conjunction with deuterium labeling studies is indicative of methane loss via cleavage of a borate methyl C–H/D bond, implicating a highly reactive four-membered scandocycle **241** as intermediate (Scheme 109). The KIE value is higher than others reported for σ -bond metathesis processes¹⁵² but similar to the value observed in another system in which a methane-eliminating σ -bond metathetical event was proposed ($k_{\text{H}}/k_{\text{D}} = 9.1 \pm 0.6$).¹⁵⁵

In synthesizing [Cp^*_2SmPh]₂ (**242**), Castillo and Tilley¹⁵⁶ discovered an intramolecular C–H activation that leads to the formation of $\text{Cp}^*_2\text{Sm}(\mu\text{-}1,4\text{-C}_6\text{H}_4)\text{SmCp}^*_2$ (**243**) and benzene. Two competitive pathways involving the C–H activation of a Cp* ring and a phenyl group, respectively, were identified for the

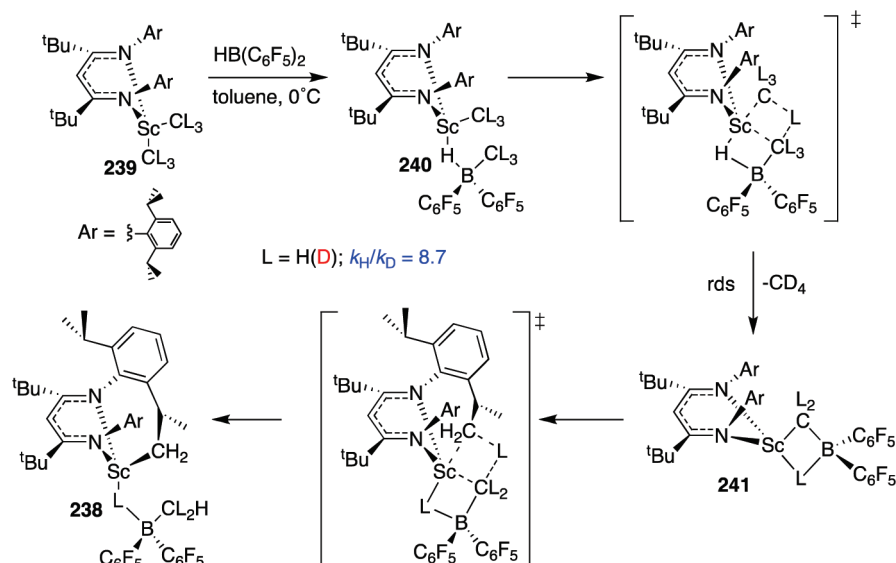
Scheme 107



Scheme 108



Scheme 109



thermal decomposition of **242**. One could occur by activation of the C–H bond of one of the phenyl groups at the para position, with concomitant loss of benzene in the rate-limiting step (**244**, Scheme 110). This would give rise to second-order rate behavior at high concentrations of **242** with a large KIE. The other, a unimolecular one, involving rate-limiting C–H activation of a Cp* ligand (**245**, Scheme 110), exhibits no kinetic isotope effect. In both cases, equilibrium between monomeric and dimeric species seems to be present, with the former being responsible for the σ -bond metathesis chemistry. The two competing pathways lead to a concentration-dependent KIE arising from the relative contributions of the two reaction manifolds at different concentrations. Thus, a small isotope effect ($k_{\text{H}}/k_{\text{D}} = 2.1 \pm 0.3$) was obtained from the low-concentration runs, whereas a much larger value of ($k_{\text{H}}/k_{\text{D}} = 5.3 \pm 0.7$) was obtained at high concentrations. The observed KIE is therefore a function of the concentration of $[\text{Cp}^*_2\text{SmC}_6\text{D}_5]_2$. Additional examples of determination of KIEs to study diverse processes in condensed and gas phase have been reported.¹⁵⁷

4. KIES IN THE STUDY OF SI–H ACTIVATION MECHANISMS

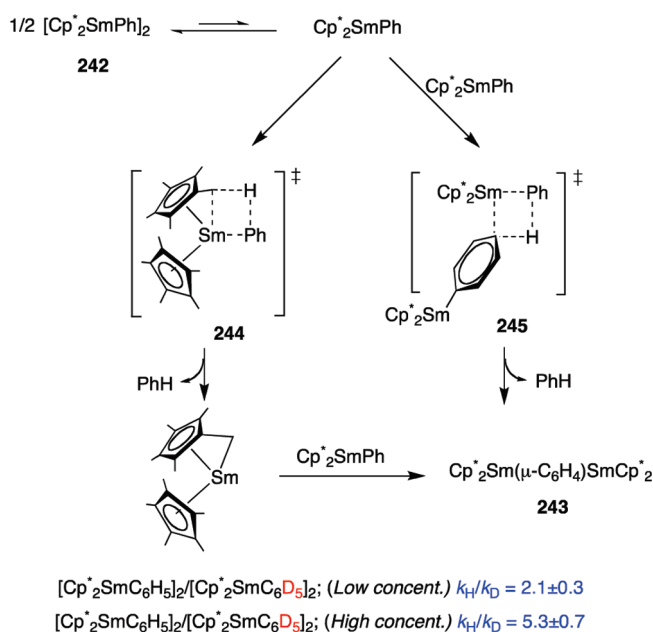
4.1. Si–H Activation

Albeit less studied than C–H insertion processes, there are significant KIE-based mechanistic studies for the Si–H bond activation by transition metal complexes. Thus, based on kinetic data, activation parameters, and a $k_{\text{H}}/k_{\text{D}} = 2.5 \pm 0.1$, Tilley and co-workers postulated¹⁵⁸ a four-center transition state for the σ -bond metathesis reactions of hafnium complexes **246** with hydrosilanes $\text{RR}'\text{SiH}_2$ to give the isolable metal silyl derivatives **247** (Scheme 111). These latter species were studied by the same research group in the context of the mechanisms for the dehydropolymerization of hydrosilanes to polysilanes, catalyzed by early transition metal metallocene derivatives.¹⁵⁹ The thermolytic decomposition of **247** to **248** results in Si–Si bond formation, with the production of polysilane oligomers. This second-order reaction exhibits a deuterium isotope effect of $k_{\text{H}}/k_{\text{D}} = 2.9 \pm 0.2$, consistent with the proposal of a four-center transition state in the process (Scheme 111).¹⁶⁰

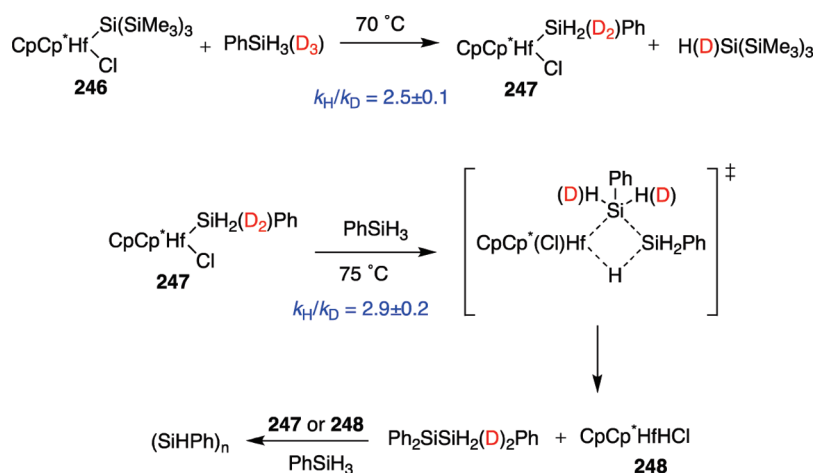
KIEs were also determined in the study of the reaction of Cp^*_2ScMe (**249**) with hydrosilanes in the context of hydrocarbon activation.¹⁶¹ For the reaction of **249** with $\text{Ph}_2\text{SiH}_2/\text{Ph}_2\text{SiD}_2$, a small primary KIE ($k_{\text{H}}/k_{\text{D}} = 1.15 \pm 0.05$) was determined. This small KIE is consistent with a σ -bond metathesis reaction with an early transition state in which the Si–H(D) bond is not significantly broken. This result is in agreement with the activation parameters. Additionally, the possible α -agostic assistance in the transition state of its reaction was discarded by the small *inverse* KIE ($k_{\text{H}}/k_{\text{D}} = 0.91 \pm 0.05$) observed in the reaction of $\text{Cp}^*_2\text{ScCH}_3/\text{Cp}^*_2\text{ScCD}_3$ (Scheme 112).

Klei, Tilley, and Bergman¹⁶² reported the study of the mechanisms of Si–H activation by iridium complex **250** and the rearrangements of the resulting silyliridium complexes (Scheme 113). Reaction of **250** and H_2SiMes_2 leads to cyclo-metallated iridium(V) complex **251**, obtained by intramolecular benzyl C–H bond activation in the iridium silyl complex

Scheme 110



Scheme 111

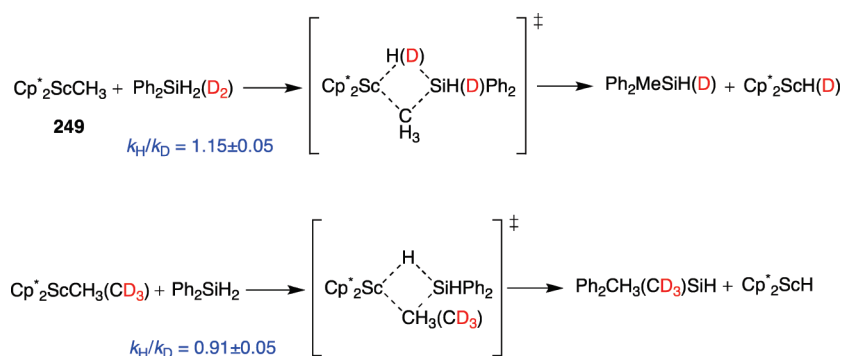


$[\text{Cp}^*(\text{PMe}_3)\text{Ir(SiHMe}_2)] [\text{OTf}]$ formed in the first instance. Complex **251** cleanly isomerizes to silylene complex $[\text{Cp}^*(\text{PMe}_3)\text{Ir(SiMe}_2)(\text{H})] [\text{OTf}]$ (**252**) over the course of 12 h. The primary KIE ($k_{\text{H}}/k_{\text{D}} = 1.6 \pm 0.1$) for Si–H versus Si–D migration in **251** points to a rate-limiting 1,2-H migration from silicon to the metal center.¹⁶³ Pt–silylene intermediates have also been proposed in the thermolytic rearrangements of *cis*- $\text{Pt}(\text{CH}_2\text{SiMe}_2\text{R})_2\text{L}_2$ (L = tertiary phosphine ligand).¹⁶⁴

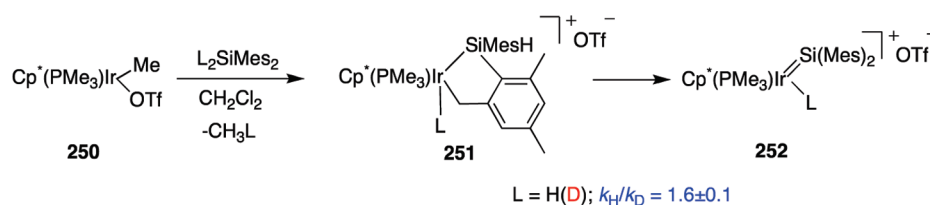
The mechanism of the $[\text{Cu}(\text{CH}_3\text{CN})_4](\text{PF}_6)$ -mediated asymmetric carbenoid insertion of aryl diazoesters into Si–H bonds was studied by means of kinetic isotope effects (Scheme 114).¹⁶⁵ A primary KIE has been determined by allowing intermolecular competition for carbenoid Si–H(D) insertion into $\text{PhMe}_2\text{Si–H/PhMe}_2\text{Si–D}$ at 0 °C. The value so obtained ($k_{\text{H}}/k_{\text{D}} = 1.29$) is relatively small but significant. No H/D scrambling is observed in the process, indicating that the insertion reaction takes place in a concerted fashion. In addition, the KIE value varies significantly with temperature (from $k_{\text{H}}/k_{\text{D}} = 2.12$, –40 °C to $k_{\text{H}}/k_{\text{D}} = 1.08$, 25 °C) in agreement with other small KIE values observed for processes in which Si–H activation is involved in the turnover-limiting step.^{86,87,166} These results are discussed in light of an early transition state, characterized by hydrogen-first penetration of the Si–H bond into the copper-carbenoid cavity, which is assumed to impart high levels of enantioselectivity due to intrinsic preorganization under the influence of the specific ligand and aryl diazoesters employed.

Bergman and co-workers¹⁶⁷ reported an accurate study of β -deuterium KIEs on the rate and equilibrium of the oxidative addition of silane $\text{Et}_3\text{SiH/Et}_3\text{SiD}$ to the iridium center in the heterodinuclear complex $\text{Cp}_2\text{Ta}(\mu\text{-CH}_2)_2\text{Ir(CO)}_2$ (**253-d₀**) and to its tetradeuterated analogue $\text{Cp}_2\text{Ta}(\mu\text{-CD}_2)_2\text{Ir(CO)}_2$ (**253-d₄**). The equilibrium isotope effect (EIE) of the process is *inverse* and the magnitude changes over the temperature range studied from $k_{\text{H}}/k_{\text{D}} = 0.54 \pm 0.04$ at 0 °C to $k_{\text{H}}/k_{\text{D}} = 0.76 \pm 0.06$ at 80 °C. The EIE values combine primary and secondary *equilibrium* isotope effect on the silane oxidative addition/reductive elimination equilibrium constant. With the EIE in hand, a detailed study was performed on the rate of oxidative addition of $\text{Et}_3\text{SiH/Et}_3\text{SiD}$ to **253** and **253-d₄** (Scheme 115). The rate constants gave an *inverse* secondary KIE ($k_{\text{H}}/k_{\text{D}} = 0.875 \pm 0.02$) for the bridging CH_2 groups. Hence, the calculated KIE from the Si–H(D) bond is *normal* but small ($k_{\text{H}}/k_{\text{D}} = 1.13 \pm 0.06$). For the reductive elimination of $\text{Et}_3\text{SiH(D)}$ from $\text{Cp}_2\text{Ta}(\mu\text{-CX}_2)_2\text{Ir(X)(SiEt}_3)(\text{CO}_2)$ (X = H, D), the Si–H(D)

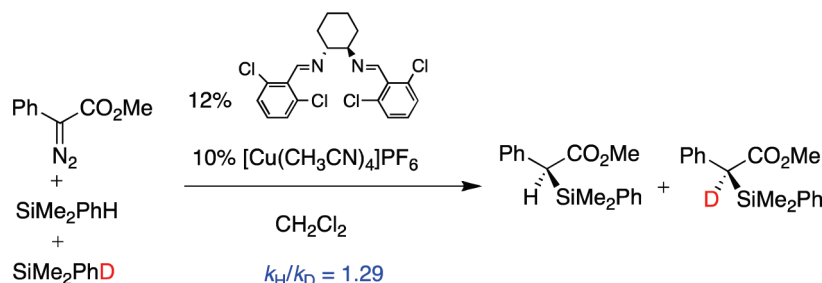
Scheme 112



Scheme 113



Scheme 114

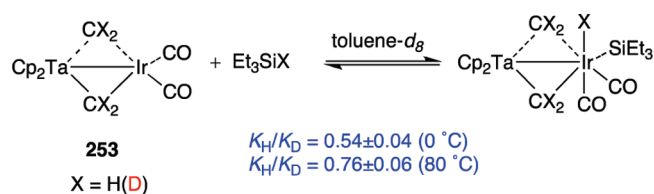


normal KIEs were obtained for both the primary Si–H(D) contribution ($k_{\text{H}}/k_{\text{D}} = 1.45 \pm 0.08$) and the secondary isotopic CH_2 substitution ($k_{\text{H}}/k_{\text{D}} = 1.25 \pm 0.03$). As the KIE on the rate of reductive elimination is larger than the KIE on the rate of oxidative addition, it was inferred that the transition state resembles the silane and Ir(I) reactants more than does the Ir(III) oxidative addition product.

4.2. Hydrosilylation of Ketones

The work by Zheng and Chan¹⁶⁸ in the mechanism of the Rh-catalyzed hydrosilylation of ketones was seminal to establish a mechanistic pathway for this reaction. Studies carried out with acetophenone in the presence of hydridotetrakis(triphenylphosphine)rhodium(I) as catalyst showed a primary KIE ($k_{\text{H}}/k_{\text{D}} = 2$) but no isotope effect in an analogous experiment with dimethylphenylsilane. Additionally, the hydrosilylation of α,β -unsaturated ketone **254** did occur with the absence of any significant KIEs, although the reaction was remarkably regioselective: diphenylsilane was found to give the 1,2-hydrosilylation product **255**, whereas dimethylphenylsilane and other monohydrosilanes gave 1,4-addition product **256** (Scheme 116).

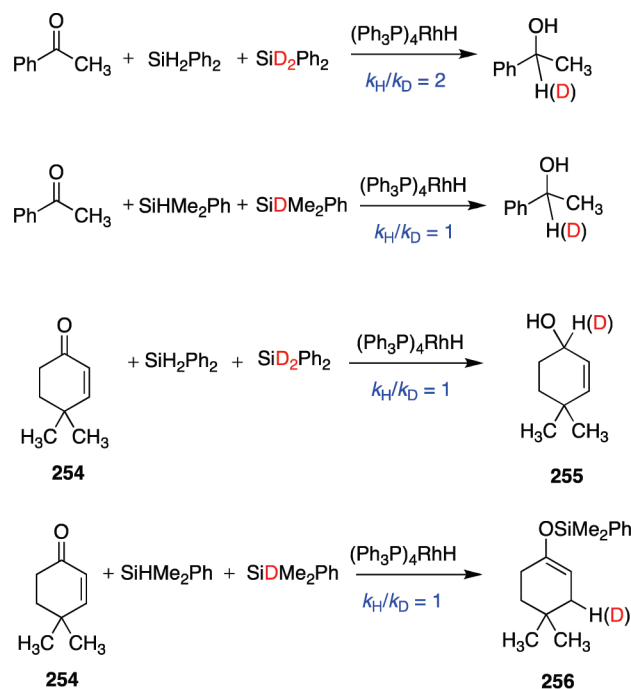
Scheme 115



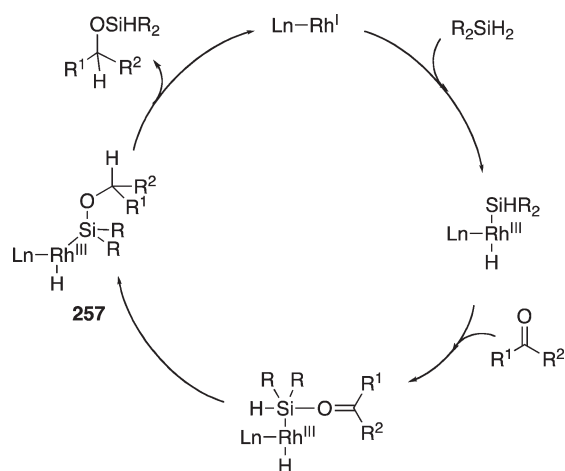
These results were compatible with the catalytic cycle in Scheme 117 in which the ketone interacts with the metal-bonded silicon atom and inserts into the Si–H bond to give an alkoxysilylrhodium intermediate **257** in the key step. The mechanism of Chan improves the early mechanistic proposal raised by Ojima in 1976.¹⁶⁹

A recent study by Hofmann, Gade, and co-workers¹⁷⁰ has reevaluated the KIEs in the hydrosilylation of acetophenone with rhodium catalyst **258**, finding out that, whereas the reaction with PhMe_2SiH and PhMe_2SiD displayed no kinetic isotope effect, the same reaction with Ph_2SiH_2 and Ph_2SiD_2 was found to be

Scheme 116



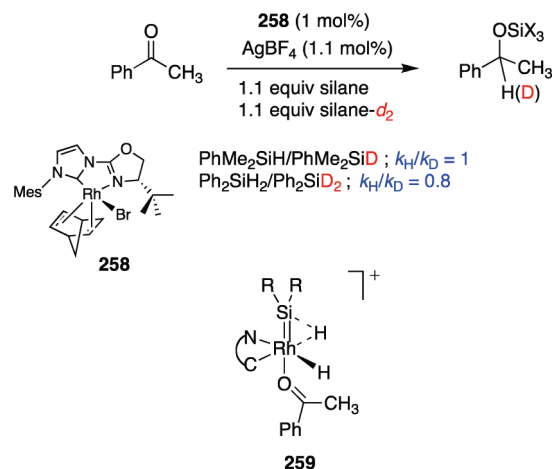
Scheme 117



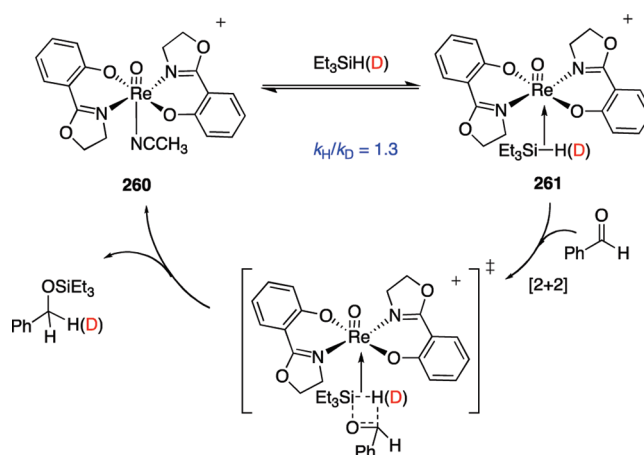
characterized by an *inverse* KIE of $k_{\text{H}}/k_{\text{D}} = 0.8$. The different mechanistic pathways were evaluated by DFT calculations,¹⁷¹ and the latter observations were rationalized by considering a new mechanistic pathway, which involves a silylene intermediate **259**. Formation of rhodium silylene requires a double Si–H activation and, therefore, is only accessible when a secondary silane is used (Scheme 118).

The hydrosilylation of aldehydes and ketones has been also reported using monooxorhenium(V) catalyst **260**.¹⁷² The proposed mechanism would involve organosilane activation through formation of $\eta^2\text{-Et}_3\text{SiH}$ complex **261** (Scheme 119), with the rds being the formation of the organosilane–Re adduct. The observed KIEs for $\text{Et}_3\text{SiH}/\text{Et}_3\text{SiD}$ ($k_{\text{H}}/k_{\text{D}} = 1.3$) and benzaldehyde–H/benzaldehyde–D ($k_{\text{H}}/k_{\text{D}} = 1.0$) are also consistent with the proposal raised.

Scheme 118



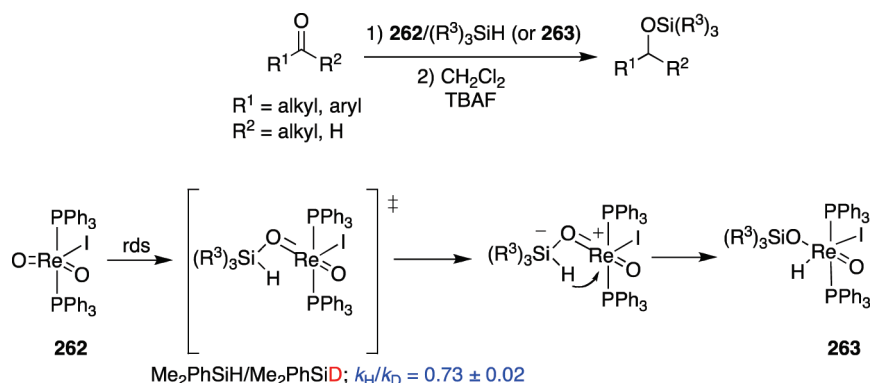
Scheme 119



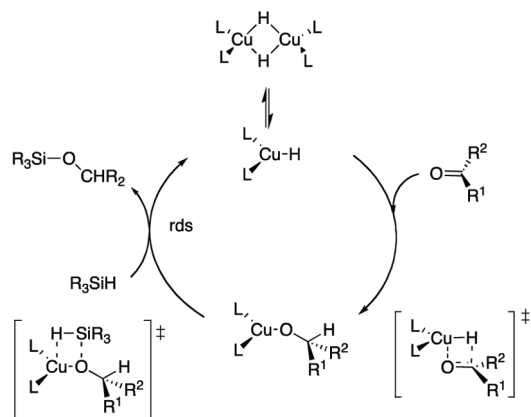
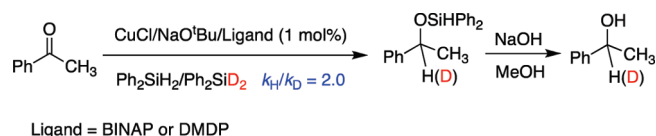
Toste and colleagues¹⁷³ reported a mechanistic study for the hydrosilylation of carbonyl compounds catalyzed by $(\text{PPh}_3)_2\text{Re}(\text{O})_2\text{I}$ **262**. The reaction proceeds via an unprecedented mechanism that begins with addition of a silane Si–H bond across one of the rhenium–oxo bonds and formation of a siloxyrhenium hydride complex **263**, which is stabilized by the presence of a spectator oxo ligand. This intermediate was isolated, identified crystallographically, and shown to be the true active species of the process. The *inverse* secondary KIE observed for the reactions of Me_2PhSiH and Me_2PhSiD ($k_{\text{H}}/k_{\text{D}} = 0.73 \pm 0.02$) is most consistent with rate-determining formation of a Si^-/Re^+ zwitterion prior to hydride transfer and formation of **263** (Scheme 120).

The copper-catalyzed hydrosilylation of ketones has been investigated by combining DFT calculations, kinetic, KIE, and isotope labeling studies.¹⁷⁴ The KIE observed in the hydrosilylation of acetophenone using either Ph_2SiH_2 or Ph_2SiD_2 as a silane source was similar to that observed by Chan and Zheng in rhodium-catalyzed hydrosilylation ($k_{\text{H}}/k_{\text{D}} = 2$).¹⁶⁸ The combination of theoretical and experimental studies provides the mechanistic proposal for the enantioselective hydrosilylation of ketones catalyzed by copper diphosphane shown in Scheme 121. The data are consistent with the rds being the reaction of the

Scheme 120



Scheme 121



copper alkoxide with the silane to form the silyl product and concomitant regeneration of copper hydride species.

4.3. Hydrosilylation of C=C Bonds

Rhenium(I) complexes of the type $[\text{ReBr}_2(\text{L})(\text{NO})(\text{PR}_3)_2]$ ($\text{L} = \text{H}_2, \text{CH}_3\text{CN, ethylene}$; $\text{R} = \text{}^i\text{Pr}$ and cyclohexyl (Cy)) catalyze dehydrogenative silylation of alkenes in a highly selective manner to yield silyl alkenes and the corresponding alkanes.¹⁷⁵ To gain further insight into the rate-determining steps of the catalytic cycle, deuterium isotope kinetics of the dehydrogenative silylation of *p*-methylstyrene with Et_3SiH and Et_3SiD catalyzed by Re(I) hydride complex **264** (one of the species involved in the initiation pathway of the catalysis) were pursued. The *inverse* KIE ($k_{\text{H}}/k_{\text{D}} = 0.84$) excludes the reductive elimination of alkenes as rate-limiting, pointing to phosphine dissociation as the slow step of the cycle (Scheme 122).

Lloyd-Jones and co-workers¹⁷⁶ have investigated the mechanism of intermolecular chirality transfer in Pd-catalyzed hydrosilylation of norbornene derivative **265** with chiral silanes **266** by means of catalytic crossover experiments. The process involves a complex two-silicon catalytic cycle in which the chirality transfer from silicon to carbon likely occurs in a C–H bond-forming

σ -bond metathesis step. The magnitude of the primary KIE ($k_{\text{H}}/k_{\text{D}} = 3.0 \pm 0.5$) is fully consistent with this proposal (Scheme 123).

5. HYDROGEN ADDITION AND HYDRIDE TRANSFER

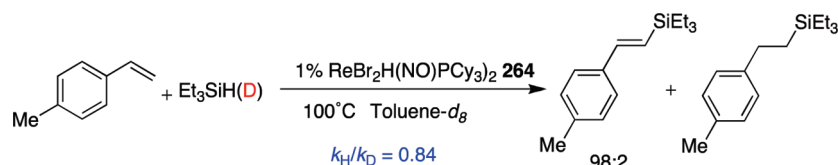
5.1. Hydrogen Addition Mediated by Ru Catalysts

The hydrogenation and dehydrogenation processes promoted by transition metals have been profusely studied, due to their synthetic and economic relevance.¹⁷⁷ Within these classes of reactions, those mediated by Shvo's catalyst **267** (Figure 7) deserve a special treatment, because their mechanisms have been extensively studied using KIE data among other kinetic and thermodynamic parameters. Shvo's catalyst was the first ligand–metal bifunctional catalyst, and it was reported in the mid-1980s.¹⁷⁸ The first attempts to determine KIEs in the reduction of deuterated aldehydes or imines resulted in null values.¹⁷⁹ These results, even though they were preliminary, opened a vivid debate about the mechanism of these reactions.

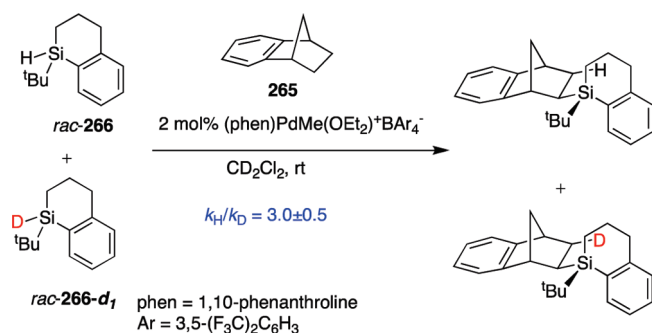
Tolyl-substituted complex **268** was used to determine KIEs in the reduction of benzaldehyde.¹⁸⁰ The observation of primary KIEs for both Ru–D and OH positions ($k_{\text{RuH}}/k_{\text{RuD}} = 1.5 \pm 0.2$ and $k_{\text{OH}}/k_{\text{OD}} = 2.2 \pm 0.1$, THF, 0 °C) provided the strongest evidence for a concerted hydrogen transfer mechanism involving both Ru–H and O–H bond breaking in the transition state to form an intermediate **269** together with the benzylic alcohol. Simultaneous deuteration in both positions gave a combined KIE of ($k_{\text{RuHOH}}/k_{\text{RuDOD}} = 3.6 \pm 0.3$), which is in agreement with the product of the two individual values ($1.5 \times 2.2 = 3.3$). All the experimental results are in concordance with a concerted reaction (Scheme 124).

Samec and Bäckvall reported an analogous study in the reduction of imines by the complex **270** and $\text{}^i\text{PrOH}$.¹⁸¹ The reaction shows an interesting solvent effect, where polar solvents decrease the reaction rate (Scheme 125). The substrate itself had a significant influence on the process. Ketimines react faster than aldimines. Electron-donating groups increase the rate, while electron-withdrawing groups decrease the rate. The deuterium KIE for the catalytic hydrogen transfer reaction of imine **271** and complex **272** was $k_{\text{H}}/k_{\text{D}} = 2.4 \pm 0.25$. Complex **272** was thought to be an intermediate in the catalytic cycle, and it was isolated by reaction of complex **273** and α -phenylethyl amine. The isolation of complex **272**, together with the effect of the substituents in the imine reduction, pointed to a nonconcerted reaction, as in the mechanism originally proposed by Menashe and Shvo¹⁷⁹ for the

Scheme 122



Scheme 123



Scheme 125

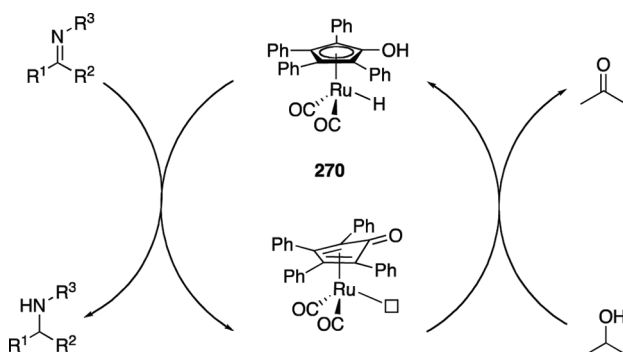
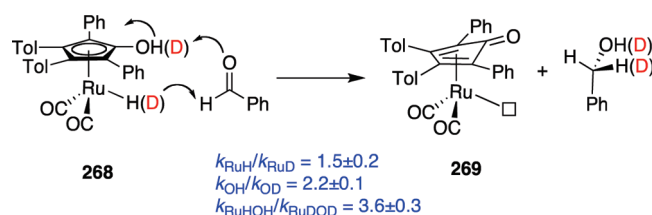


Figure 7

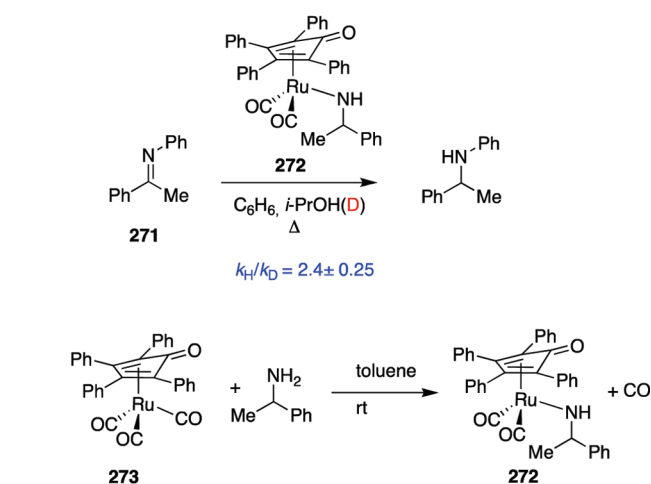
Scheme 124



reduction of carbonyl compounds, that is, coordination to ruthenium, followed by migratory insertion of hydrogen.

Subsequently, Bäckvall and co-workers reported the dynamic kinetic resolution of amines using a combination of complexes analogous to **272** and enzymes¹⁸² and taking into account the ability of these complexes to racemize through the imine formed by β -hydrogen elimination, and the subsequent reduction of the enzyme. KIEs in the range of $k_H/k_D = 3.53 \pm 0.62$ and $k_H/k_D = 1.70 \pm 0.12$ were determined for this rate-determining β -hydrogen elimination.

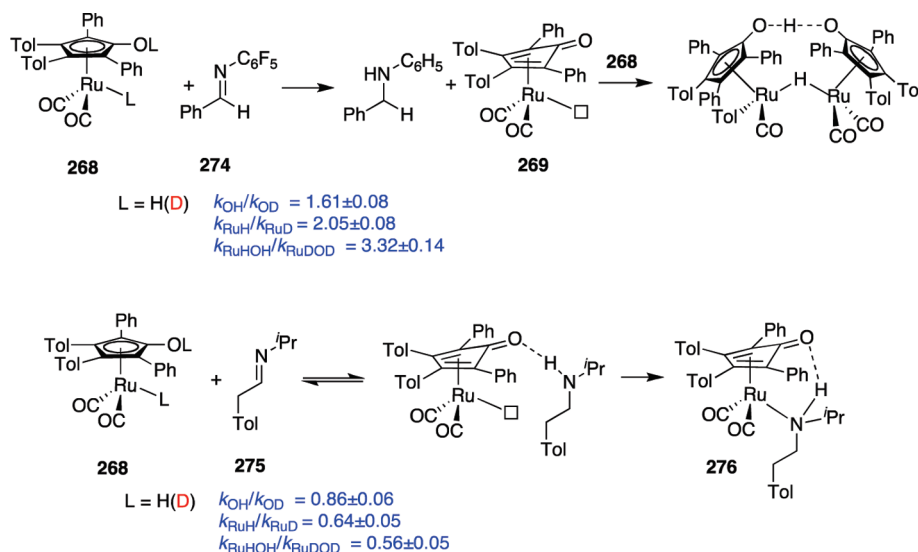
Casey and Johnson¹⁸³ concluded that the concerted or stepwise nature of the mechanism of reduction of imines by Shvo complexes depended fundamentally on the electronic nature of the amine, and therefore, on the basicity of the imine. These studies show that the reaction begins by net trans addition of proton and hydride from the complex **268** to the imine and formation of coordinatively unsaturated intermediate **269**



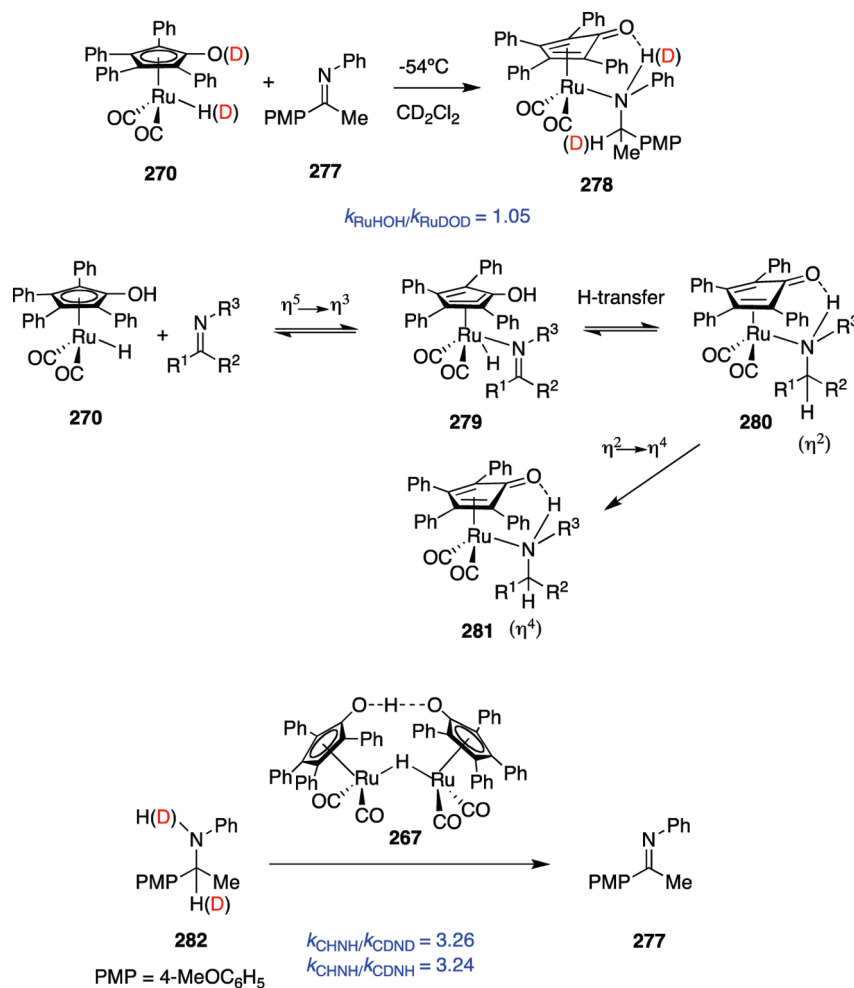
(Scheme 126). In the case of the electron-deficient C_6F_5 -substituted imines **274**, this step is rate-limiting. For electron-rich alkyl-substituted imines **275**, back hydrogen transfer to ruthenium occurs at a rate competitive with (or faster than) the coordination of nitrogen. In these cases, the rds becomes the coordination of nitrogen to ruthenium, to form the complexes **276** (isomerization of imines is also observed for these substrates). This mechanism was supported by the fact that KIEs for electron-poor imines **274** were very similar to those observed in the reduction of aldehydes and ketones (initial H-transfer: $k_{\text{OH}}/k_{\text{OD}} = 1.61 \pm 0.08$, $k_{\text{RuH}}/k_{\text{RuD}} = 2.05 \pm 0.08$, and $k_{\text{RuHOH}}/k_{\text{RuDOD}} = 3.32 \pm 0.14$). However, for electron-rich alkyl-substituted imines, inverse KIEs ($k_{\text{OH}}/k_{\text{OD}} = 0.86 \pm 0.06$, $k_{\text{RuH}}/k_{\text{RuD}} = 0.64 \pm 0.05$, and $k_{\text{RuHOH}}/k_{\text{RuDOD}} = 0.56 \pm 0.05$) for reversible hydrogen transfer were obtained. The inverse KIE values are compatible with an initial reversible H-transfer.

Soon after the study reported by Casey and Johnson,¹⁸³ Bäckvall and co-workers reported a different interpretation for

Scheme 126



Scheme 127

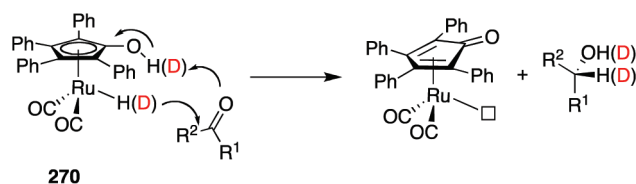


the reduction of imines by Shvo's catalyst.¹⁸⁴ Again, clear differences between electron-rich and electron-poor imines were

observed, especially in the temperature dependence of the coordination of the resulting amine to the Ru complex

Scheme 128

Outer Sphere Mechanism



270

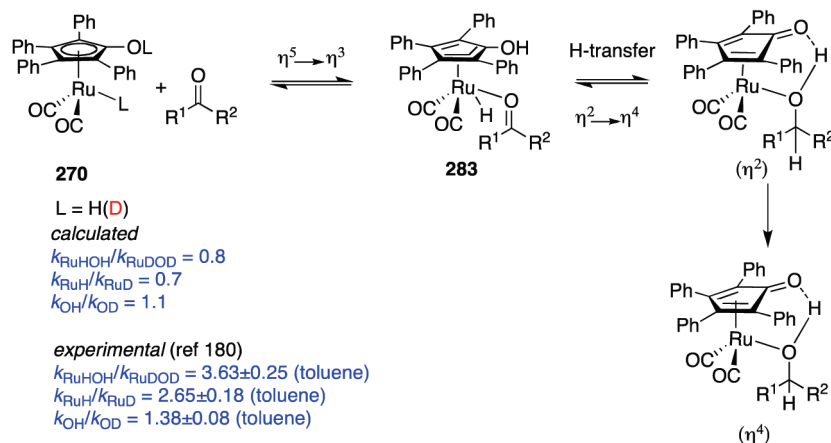
calculated

$$k_{\text{RuHOH}}/k_{\text{RuDOD}} = 3.5$$

$$k_{\text{RuH}}/k_{\text{RuD}} = 1.3$$

$$k_{\text{OH}}/k_{\text{OD}} = 2.8$$

Inner Sphere Mechanism



270

L = H(D)

calculated

$$k_{\text{RuHOH}}/k_{\text{RuDOD}} = 0.8$$

$$k_{\text{RuH}}/k_{\text{RuD}} = 0.7$$

$$k_{\text{OH}}/k_{\text{OD}} = 1.1$$

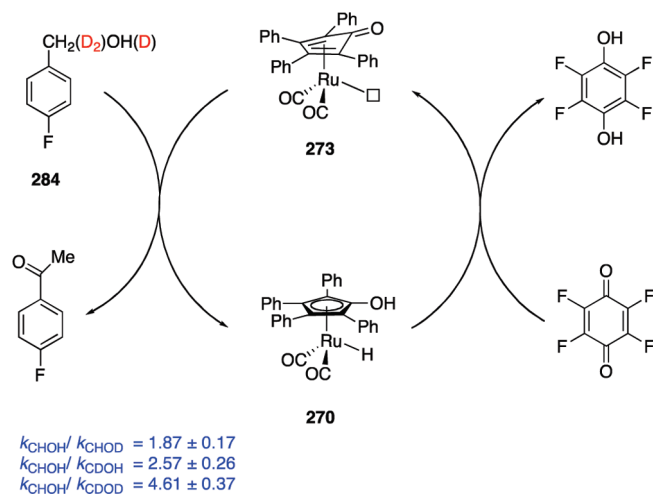
experimental (ref 180)

$$k_{\text{RuHOH}}/k_{\text{RuDOD}} = 3.63 \pm 0.25 \text{ (toluene)}$$

$$k_{\text{RuH}}/k_{\text{RuD}} = 2.65 \pm 0.18 \text{ (toluene)}$$

$$k_{\text{OH}}/k_{\text{OD}} = 1.38 \pm 0.08 \text{ (toluene)}$$

Scheme 129



270

$$k_{\text{CHOH}}/k_{\text{CHOD}} = 1.87 \pm 0.17$$

$$k_{\text{CHOH}}/k_{\text{CDOH}} = 2.57 \pm 0.26$$

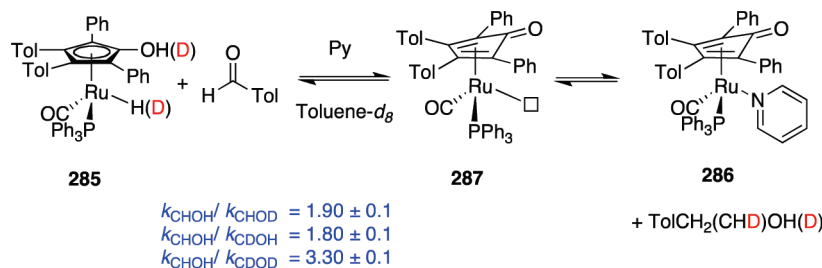
$$k_{\text{CHOH}}/k_{\text{CDOD}} = 4.61 \pm 0.37$$

(Scheme 127). Hydride 270 forms amine complexes with electron-rich imines at lower temperatures than with electron-deficient imines. Furthermore, the negligible KIE ($k_{\text{H}}/k_{\text{D}} = 1.05$)¹⁸⁴ observed in the reaction of 270 with ketimine 277 to form complex 278 excludes a rate-determining hydrogen transfer in contrast with the reaction with ketones/aldehydes. The KIE

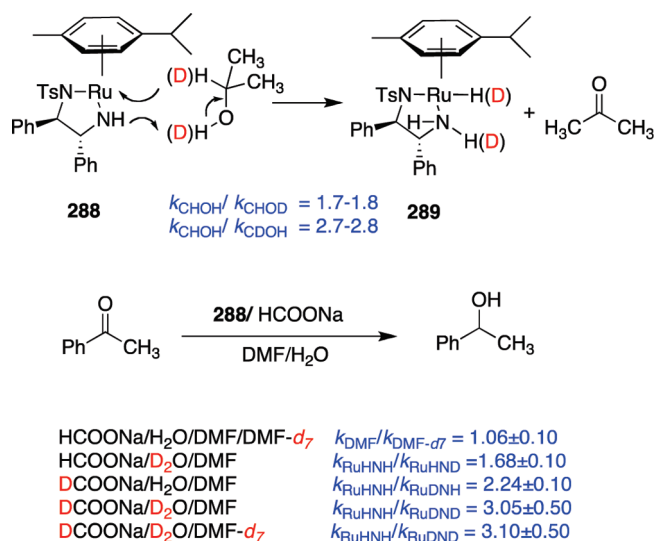
values observed clearly show that the hydride transfer alone is not rate-limiting, which requires, in principle, a stepwise mechanism (Scheme 127). On the basis of these and additional experimental data, an inner-sphere mechanism where the imine coordinates to ruthenium to form complex 279 via an η^5 - η^3 ring slippage, prior to the intramolecular hydrogen transfer step to form 280 and finally 281, was proposed. Interestingly, the reverse reaction, namely, the catalytic dehydrogenation of amine 282 in the presence of 267 to form imine 277, has a large KIE for the cleavage of the C–H bond of the amine ($k_{\text{CHNH}}/k_{\text{CDNH}} = 3.24$). This KIE value for the C–H cleavage is equal within experimental error to the combined isotope effect for C–H and N–H cleavages ($k_{\text{CHNH}}/k_{\text{CDND}} = 3.26$). These facts point to a rate-determining C–H bond cleavage and suggest that the hydrogen transfer from the amine to the complex cannot be a concerted process.

Taking into account the experimental data, there are two possibilities for the hydrogen transfer from Shvo's catalysts to carbonyl and imine groups. For the sake of clarity, we will denote both pathways as *outer-sphere* H-transfer and *inner-sphere* pathway (Scheme 128). In both mechanisms, the hydride migrates to the carbonylic carbon atom. Nevertheless, whereas in the *inner-sphere* mechanism it is supposed that a metal alkoxide intermediate 283 is formed (therefore, the substrate must become coordinated to the catalyst), in the *outer-sphere* mechanism the hydrogen transfer may proceed in a concerted manner (without the coordination of the substrate to the catalyst). Comax-Vives,

Scheme 130



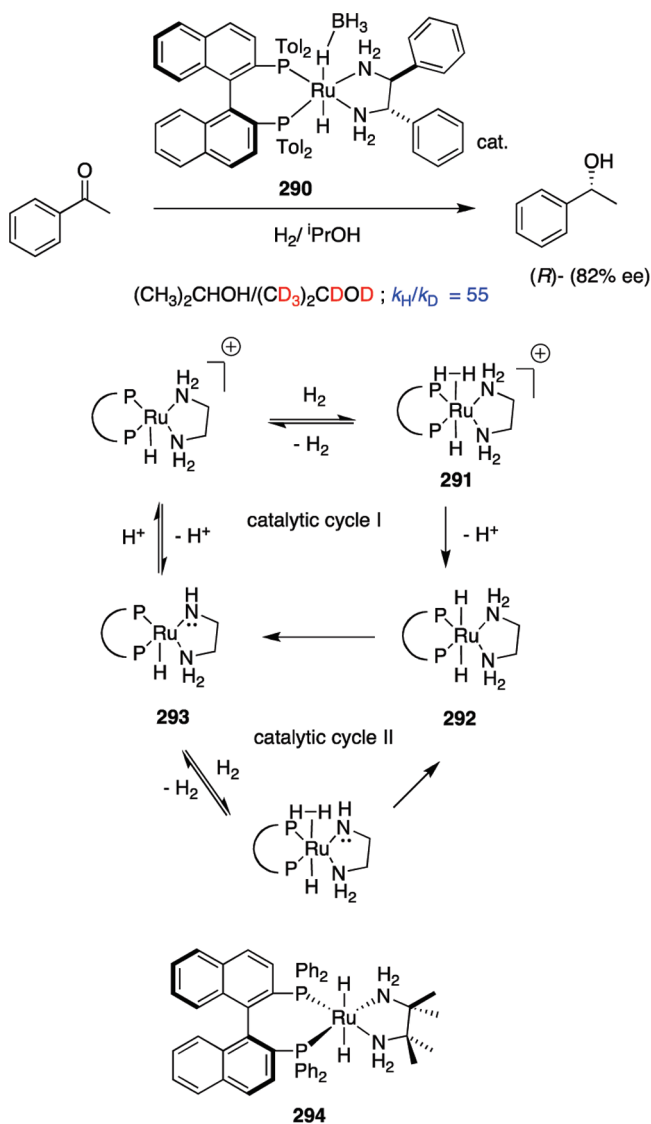
Scheme 131



Ujaque, and Lledós¹⁸⁵ computationally studied both mechanisms for the reaction of **270** and formaldehyde (Scheme 128). In the *outer-sphere* mechanism, the combined isotope effect is very close to the experimental one (3.5 versus 3.63 ± 0.25). However, there are noticeable differences between the calculated and experimental individual KIEs. Considering solvent effects, the theoretical values turned out to be closer to the individual KIE values reported in THF with a small amount of added water than to those obtained in dry THF or toluene.¹⁸⁶ In the case of the concerted *inner-sphere* mechanism, the value for the combined KIE is quite different from the experimental value in toluene (0.8 versus 3.63 ± 0.25), and there are also differences with the calculated and the individual values in toluene. Considering these facts, the authors concluded that the calculated combined isotope effect for the outer-sphere mechanism is in better agreement with the experimentally reported values.

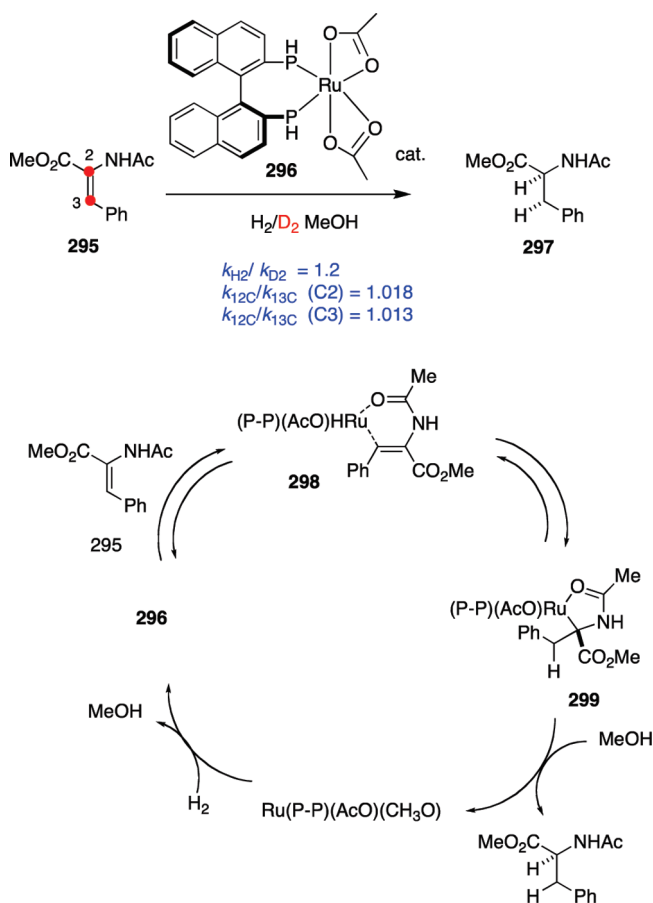
The KIEs in the alcohol dehydrogenation (the opposite to carbonyl group hydrogenation) have been also studied.¹⁸⁷ Thus, values of $k_{\text{H}}/k_{\text{D}} = 1.8-1.9$ for the breaking of the OH bond of the alcohol **284** and of $k_{\text{H}}/k_{\text{D}} = 2.5-2.6$ for the breaking of the CH bond were found in the reaction depicted in Scheme 129. The doubly labeled alcohol **284** showed a $k_{\text{H}}/k_{\text{D}} = 4.61 \pm 0.37$. These KIE values were consistent with a mechanism involving concerted transfer of both hydrogens of the alcohol to ruthenium species **273**. Additionally, the use of iron complexes analogous to the Shvo's complex in double H-transfer has been also reported, but no KIE studies have been effected to date.¹⁸⁸

Scheme 132



Casey et al.¹⁸⁹ reported the effect of CO substitution in Shvo's catalyst by PPh_3 in the reduction of aldehydes and ketones. Thus, **285** was reacted with tolualdehyde in the presence of pyridine to yield *p*-methylbenzylalcohol and complex **286** through intermediate **287**. The product of each individual isotope effect for substitution of the hydroxyl proton or the hydride proton is $1.8 \times 1.9 = 3.4 \pm 0.2$, which is, within error, the KIE obtained for the doubly labeled compound

Scheme 133

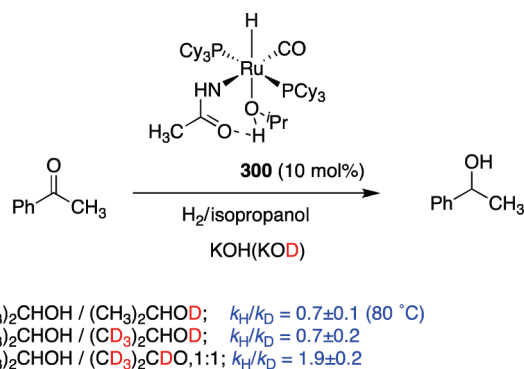


(3.3 ± 0.1). This indicates that reduction of *p*-tolualdehyde by **285** occurs by a mechanism involving transfer of the hydroxyl proton and hydride in a concerted fashion (Scheme 130). Additional experiments showed that **285** has slower stoichiometric reduction, faster catalytic hydrogenation, and higher chemoselectivity for hydrogenation of aldehydes over ketones than the dicarbonyl Shvo catalyst **270**.

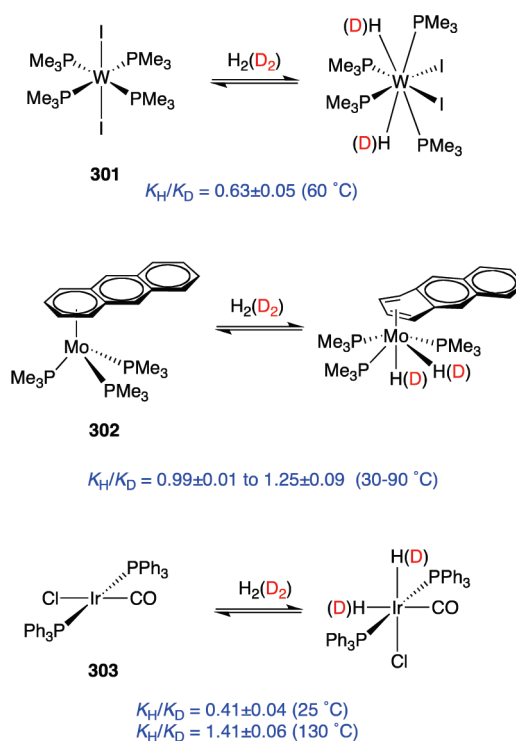
The asymmetric transfer of hydrogen (ATH) to carbonyl and imine groups has been thoroughly and repeatedly reviewed.^{177,190} The mechanisms of these reactions are related to the processes depicted for Shvo's catalyst. The Noyori–Ikariya Ru–TsDPEN catalytic system **288** has received the most attention among a large number of catalysts employed for ATH of ketones and imines.¹⁹¹ For the reduction of ketones with Ru–TsDPEN in isopropanol, Noyori and co-workers proposed a concerted pathway for the hydrogen transfer process, that is, the hydridic hydrogen on RuH and the protonic hydrogen on the NH₂ moiety are transferred simultaneously to the carbon and oxygen atom of the carbonyl group, respectively. This concerted mechanism is supported by KIE studies from Casey's group,¹⁸³ which demonstrated a reversible, concurrent hydride and proton transfer from isopropanol to the complex **288** to form the Ru–hydride **289** and acetone (Scheme 131). Primary KIEs ($k_H/k_D = 2.7$ – 2.8 for breaking the CH bond of isopropyl alcohol and $k_H/k_D = 1.7$ – 1.8 for breaking the OH bond of isopropyl alcohol) were found. These KIE values are consistent with a mechanism involving concerted transfer of hydrogen from carbon to ruthenium and from oxygen to nitrogen.

Xiao and co-workers¹⁹² presented further evidence for the asymmetric reduction of ketones by complex **288**. The reaction

Scheme 134



Scheme 135



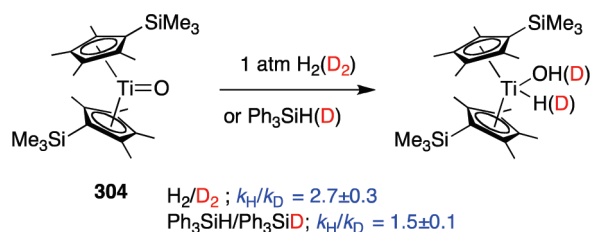
of **288** and acetophenone in the presence of HCOONa was studied in homogeneous H₂O/DMF media under neutral to basic conditions (under such conditions, the acetate acts as hydride donor and the water acts as the proton source). Significant KIEs were measured for RuH₂NH/RuHND, RuH₂NH/RuD₂NH, and RuH₂NH/RuDND (Scheme 131), which appear to be consistent with the hydrogen transfer to acetophenone as the rds in the aqueous ATH. The individual values are similar to those observed by Casey¹⁸³ for stoichiometric hydrogen transfer from **289** to acetone. However, the product of the individual KIEs ($k_{RuH_2NH}/k_{RuHND} \times k_{RuH_2NH}/k_{RuDNH} = 3.76$) deviates significantly from the measured $k_{RuH_2NH}/k_{RuDND} = 3.05$ when using DCOONa/D₂O as hydrogen source. Although this partly could arise from extensive H–D scrambling in the process, the DFT calculations suggest that the hydrogen transfer in water is actually not entirely concerted.

Noyori and co-workers studied the ATH¹⁹³ from the chiral diphosphine/1,2-diamine-Ru(II) combination in 2-propanol.¹⁹⁴ In the absence of base, a large KIE ($k_{\text{H}}/k_{\text{D}} = 55$) was observed in the reaction of **290** and acetophenone using *i*PrOH (or the perdeuterated alcohol) as the solvent (Scheme 132). This value is much larger than that obtained in the presence of KO^{*t*}Bu ($k_{\text{H}}/k_{\text{D}} = 2$). These findings indicate that dual mechanisms were in operation, both dependent on reaction conditions and involving heterolytic cleavage of H₂ to form a common reactive intermediate. The two catalytic cycles are depicted in Scheme 132, both involving the deprotonation of the η^2 -H₂ Ru complex **291** as the turnover-limiting step (catalytic cycle I). Under base-free conditions, 2-propanol acts as the base that deprotonates **291**, giving **292** by a bimolecular process. The small KIE observed with KO^{*t*}Bu reflects the dominance of the catalytic cycle II, where H₂(D₂) heterolysis is induced by the amido nitrogen in **293**.

The work by Sandoval, Noyori, and co-workers¹⁹⁴ has been recently supported by the KIE ($k_{\text{H}}/k_{\text{D}} = 2.0 \pm 0.1$) observed by Zimmer-De Iuliis and Morris¹⁹⁵ for the homogeneous hydrogenation of acetophenone catalyzed by *trans*-RuH₂(NH₂CMe₂CMe₂NH₂) ((*R*)-binap) **294** in benzene under 8 atm of gas (H₂ or D₂), at room temperature. The experimental data is in concordance with the calculated (DFT) value ($k_{\text{H}}/k_{\text{D}} = 2.1$) obtained on the basis of a mechanism involving the turnover-limiting, heterolytic splitting of dihydrogen or dideuterium across the ruthenium–amido bond. Thus, the experiment and theory agreement might indicate a similar transition state for the Noyori system.

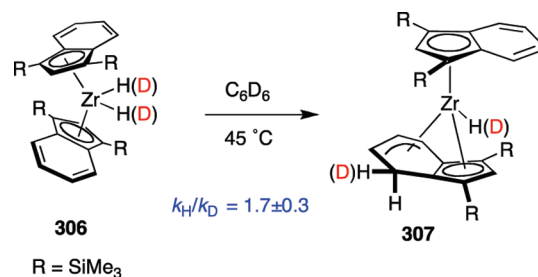
Kitamura, Noyori, and co-workers¹⁹⁶ have studied extensively the mechanism of asymmetric hydrogenation of α -(acylamino)acrylic esters catalyzed by BINAP–ruthenium(II) diacetate. KIEs played a key role in elucidating the origin of the asymmetric induction. Thus,

Scheme 136

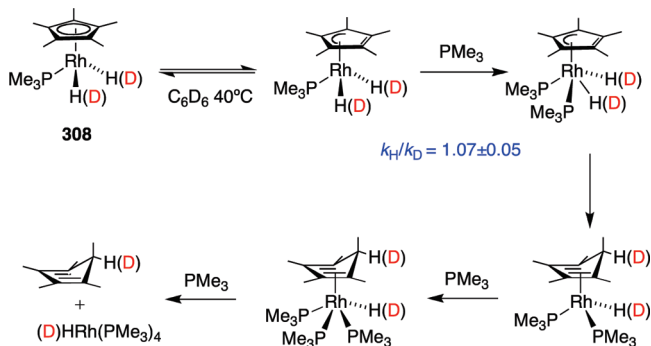


consistent with this view, when (*Z*)-**295** was reduced in MeOH using BINAP–ruthenium(II) diacetate **296** separately using H₂ and D₂ gas, a normal $k_{\text{H}}/k_{\text{D}} = 1.2$ was observed in the formation of **297**. The ¹²C/¹³C isotope effects (1.018 at C(2) and 1.013 at C(3) in **295**, respectively) agree with a mechanistic picture in which the olefin/Ru–H migratory insertion from intermediate **298** is reversible. The repeated bond reorganization is expected to display cumulative equilibrium isotope effects at both C(2) and C(3). In addition, if the migratory insertion in **298** were irreversible, a ¹²C/¹³C KIE would be expected only at C(2). The observation of isotope effects at both of the olefinic carbons is consistent with turnover-limiting hydrogenolysis of the Ru–C(2) in intermediate **298** to form **299** (Scheme 133).

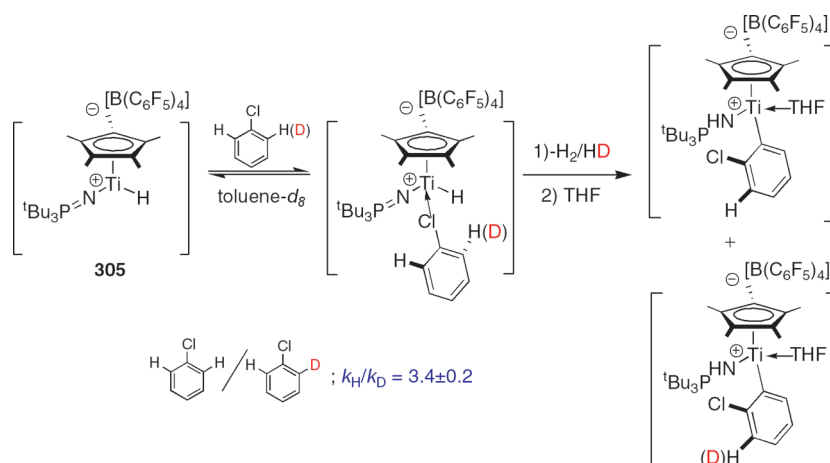
Scheme 138



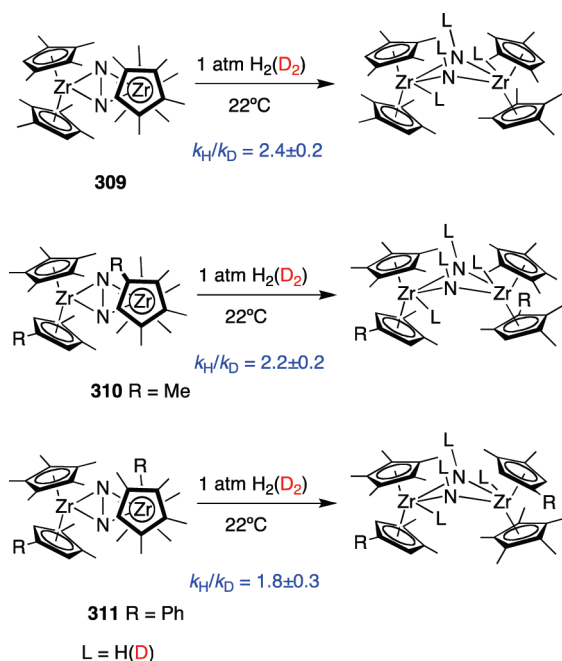
Scheme 139



Scheme 137



Scheme 140



Scheme 141



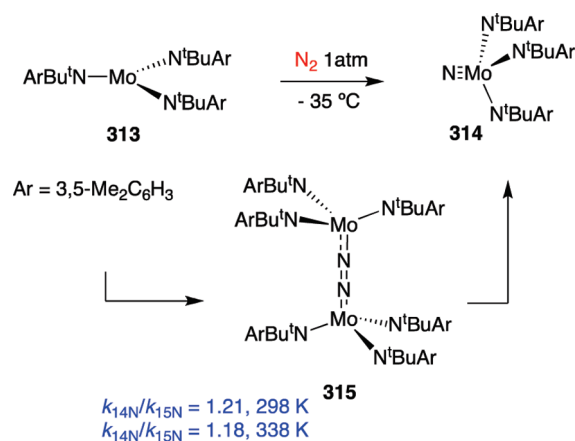
The ruthenium–acetamido complex **300**¹⁹⁷ was found to be an effective catalyst for the transfer hydrogenation of carbonyl compounds and imines. Although a detailed reaction mechanism still remains to be established, the observation of both *inverse* and *normal* deuterium KIEs in the hydrogenation of acetophenone in the presence of KOH/KOD, and the competitive inhibition by added phosphine, provided strong evidence for a stepwise mechanism of proton and hydride transfer via a coordinatively unsaturated ruthenium–amido species (Scheme 134).

Kinetic and mechanistic studies of the homogeneous hydrogenation of benzaldehyde were carried out using the cationic complex $[\text{RuH}(\text{CO})(\text{NCMe})_2(\text{PPh}_3)_2]\text{BF}_4$ as the catalyst precursor, which was very efficient under mild reaction conditions in 2-methoxyethanol as the solvent.¹⁹⁸ Also, studies on $\text{Ru}(\text{OH})_x/\text{Al}_2\text{O}_3$ as an efficient heterogeneous catalyst for hydrogen-transfer reactions were reported.¹⁹⁹

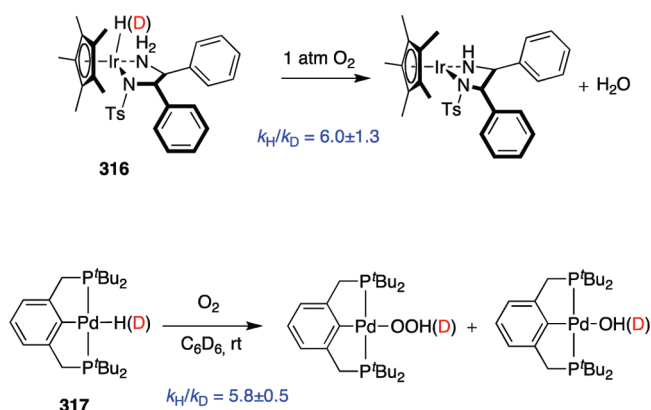
5.2. Interaction of H–H Bonds with Other Transition Metal Centers

The oxidative addition of dihydrogen is an important elementary transformation that plays a critical role in many processes involving H_2 (i.e., metal-catalyzed hydrogenation and hydroformylation). In close parallelism with the C–H activation reactions, the process involves coordination of H–H and oxidative addition of dihydrogen, the position of the equilibrium

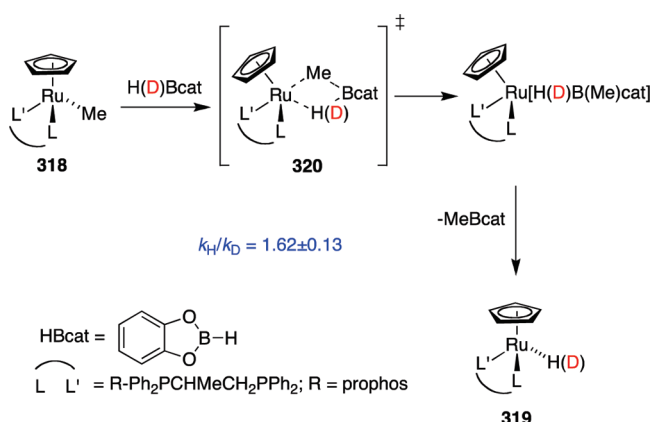
Scheme 142



Scheme 143



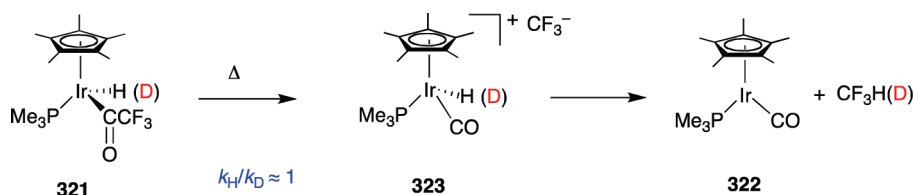
Scheme 144



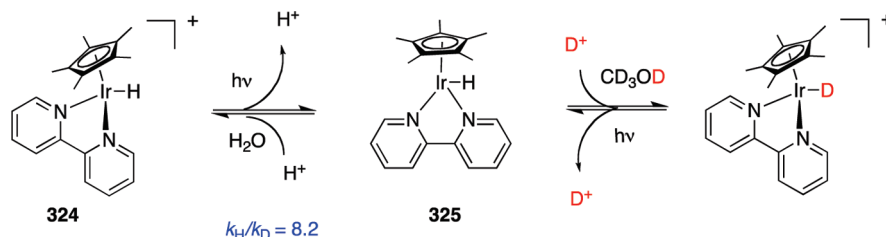
being highly dependent on the system. Hence, experimental and computational EIEs studies have resulted in being relevant in the elucidation of the reaction mechanisms, and some effort has been devoted to the question of their predictability.^{18,200}

Both *normal* and *inverse* EIEs have been reported in H_2 additions. Relevant examples are the substantial *inverse* EIE ($k_{\text{H}}/k_{\text{D}} = 0.63 \pm 0.05$, 60 °C) observed in the oxidative addition of H_2 and D_2 to

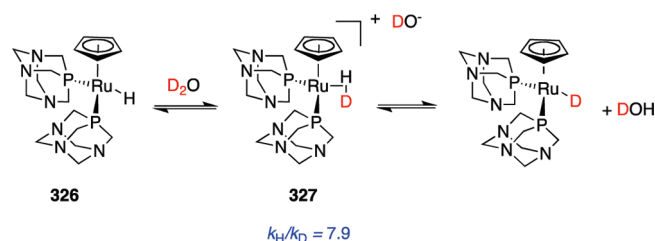
Scheme 145



Scheme 146



Scheme 147



W(PMe₃)₄I₂ (**301**)²⁰¹ and the *normal* EIEs ($k_H/k_D = 1.03$ – 1.27) reported for the oxidative addition of the molybdenum complex **302** at relatively low temperatures (30–90 °C)²⁰² (Scheme 135). Interestingly, the EIEs in H₂ additions can be affected by changes in the temperature, as in the *inverse* to *normal* temperature-dependent transition reported for the Vaska system, Ir(PMe₂Ph)₂(CO)Cl **303**,²⁰³ for which the strongly *inverse* EIE of $k_H/k_D = 0.41 \pm 0.04$ at 25 °C became *normal* at temperatures > 90 °C and reached a value of $k_H/k_D = 1.41 \pm 0.06$ at 130 °C (Scheme 135).²⁰⁴ The experimental results are in full agreement with the early computational study of the process.^{30b,205}

A thorough analysis to rationalize the origin of the *inverse* EIEs in these processes, as well as the study of the variation of the EIEs with temperature, has been recently reported by Parkin and co-workers.^{18,31,206} The activation of H₂ by Ti complexes has been studied by several groups. Thus, Chirik and co-workers reported the addition of H₂(D₂) to Ti–oxo complex **304**, which exhibited a *normal*, primary KIE ($k_H/k_D = 2.7 \pm 0.3$, 23 °C) consistent with a 1,2-addition pathway. Isotope effects of the same direction but with smaller magnitudes were determined for silane addition to the same system (Scheme 136).²⁰⁷

The titanium methyl cation [Cp*(^tBu₃P=N)TiCH₃]⁺ [B(C₆F₅)₄][−] reacts rapidly with H₂ to give the analogous cationic hydride **305**, which can be trapped and isolated as its THF adduct.²⁰⁸ When generated in the presence of chloro- or bromobenzene, **305** undergoes C–X activation or *ortho*–C–H activation, depending on the amount of H₂ present in the

reaction medium. Mechanistic studies of the C–H activation pathway in the generation of **305** with an excess of Cl–C₆H₄ and *ortho*–1–Cl–C₆H₄D indicate a high KIE ($k_H/k_D \approx 3.4 \pm 0.2$) that supports a σ -bond metathesis reaction between Ti–H and an *ortho*–C–H bond of the haloarene substrate to eliminate hydrogen, which, if not removed, can render this transformation reversible (Scheme 137).

A *normal*, primary KIE ($k_H/k_D = 1.7 \pm 0.3$) has been measured for the isomerization of **306** to **307**, which is consistent with a pathway involving regio- and stereoselective insertion of a benzo–C=C bond into a zirconium hydride. The stereochemistry of the insertion reaction, and hence the η^5 , η^3 –4,5-dihydroindenyl product, is influenced by the presence of donor ligands and controlled by the preferred conformation of the indenyl rings (Scheme 138).²⁰⁹

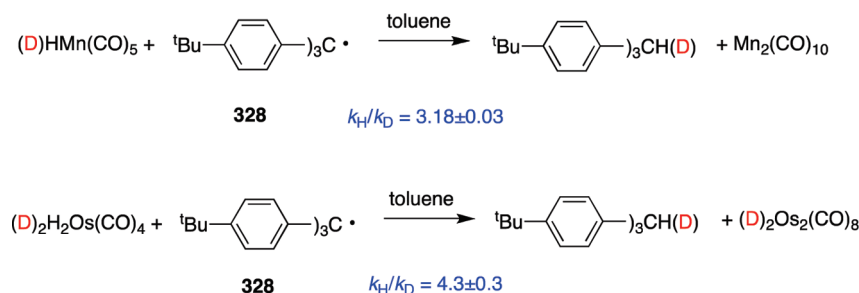
Evidence for ring slippage was reported by Jones et al.²¹⁰ in the reaction of Rh complexes **308**/**308-d**₂ with excess of PMe₃. The lack of any significant KIE ($k_H/k_D \approx 1.07 \pm 0.05$) is consistent with the η^5 – η^3 ring slip mechanism shown in Scheme 139, because the Rh–H and Rh–D bonds remain intact in both the preequilibrium and rate-determining step involving PMe₃.

The measured $k_H/k_D = 1.3$ was decisive to determine that the Pt₃Re₂(CO)₆(^tBu₃P)₃ cluster system was able to add H₂ to form the series of compounds Pt₃Re₂(CO)₆(^tBu₃P)₃(μ -H)₂, Pt₃Re₂(CO)₆(^tBu₃P)₃(μ -H)₄, and Pt₃Re₂(CO)₆(^tBu₃P)₃(μ -H)₆ without ligand dissociation or without the presence of an obvious “vacant site” by utilizing multiple metal atom hydrogen activation pathways.²¹¹

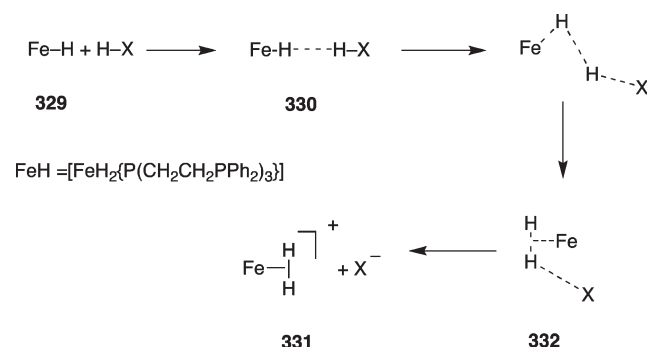
5.3. Hydrogen Addition to Dinitrogen Compounds

Within the context of the fundamental process of N₂ fixation,²¹² the advent of well-defined transition metal complexes that coordinate and functionalize dinitrogen offers the opportunity to elucidate the mechanisms and possibly establish structure–reactivity relationships for N–H bond formation. Chirik and co-workers²¹³ studied the H₂ addition to *ansa*-zirconocene dinitrogen complexes **309**–**311** in Scheme 140. Experimental k_H/k_D determination was accomplished by comparing the observed pseudofirst-order rate constants obtained at 23 °C for H₂

Scheme 148



Scheme 149



versus D_2 addition. In each case, *normal*, primary KIEs were observed. These results were consistent with H–H bond breaking in the rds of N_2 hydrogenation. KIE values together with entropy of activation suggested an ordered, four-centered transition structure with synchronous H–H cleavage concomitant with Zr–H and N–H bond formation.

KIEs were also determined for the dehydrogenation of *ansa*-complexes **312** (Scheme 141).²¹⁴ A $k_{\text{H}}/k_{\text{D}}$ value of 3.6 ± 0.1 was consistent with N–H or Zr–H bond breaking in or prior to the rds. Both kinetic and isotopic labeling experiments for the subsequent diazene dehydrogenation are consistent with a rapid preequilibrium involving reversible dihydrogen loss and readition, followed by rate-determining β -hydrogen elimination.

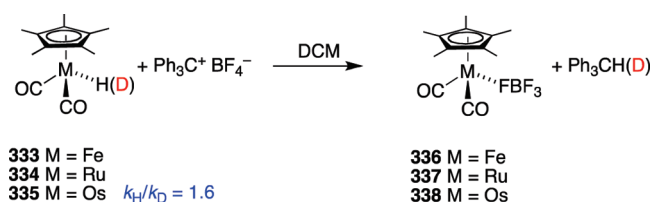
Molybdenum complex **313** is amenable to molecular N_2 cleavage to yield nitrene complexes **314**. This fact renders complex **313** unique among nitrogenase models. The evolution from **313** to **314** occurs through a dinuclear μ -dinitrogen complex **315**. The calculated $^{14}\text{N}/^{15}\text{N}$ KIEs (Raman spectroscopy) for the thermal dissociation of complex **315** were $k_{14\text{N}}/k_{15\text{N}} = 1.21$ at 298 K and $k_{14\text{N}}/k_{15\text{N}} = 1.18$ at 338 K, which is in agreement with the experimental data and supports the mechanism proposed in Scheme 142.²¹⁵

The transfer of H_2 from Ir complexes **316** to oxygen has been also studied.²¹⁶ Thus, a dramatic isotope effect ($k_{\text{H}}/k_{\text{D}} = 6.0 \pm 1.3$) was obtained for the reduction of O_2 . A KIE of similar magnitude ($k_{\text{H}}/k_{\text{D}} = 5.8 \pm 0.5$) was observed by Goldberg and co-workers for the oxygenation of an organopalladium hydride **317** with dioxygen²¹⁷ (Scheme 143).

5.4. Hydride Transfer

The nature of the hydride transfer (both from a transition metal to an organic substrate or from a main group hydride to a transition metal nucleus) is an excellent playground to determine the reaction

Scheme 150



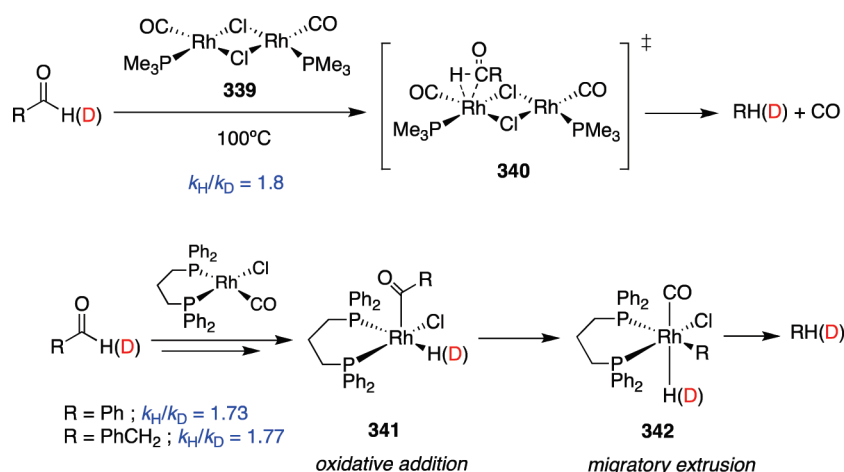
mechanism using KIEs. Let us first consider the transfer from a main group hydride to a transition metal (the C–H and Si–H may be included in this class of reactions; however, for the purposes of this review, they have been treated separately). Hartwig et al.²¹⁸ determined that an oxidative step is not involved in the reaction of the borane B–H bond with $\text{CpRu}(\text{PPh}_3)_2\text{Me}$ **318** leading to **319**. Thus, a comparison of pseudofirst-order rate constants for B–H–catecholborane and B–D–catecholborane provided a $k_{\text{H}}/k_{\text{D}} = 1.62 \pm 0.13$. Although small for a primary KIE, this value would be considered large for a secondary KIE. This interpretation suggests the importance of a bridging hydride during the exchange process and led to a proposed transition state represented by **320** (Scheme 144).²¹⁹

The transfer of H-group from metal–hydride complexes has been much studied.²²⁰ The relevance of M–H hydride complexes in processes such as the preparation of metal acyl complexes from oxidative addition of aldehydes, decarbonylation reactions, and reductive elimination reactions makes these products suitable for the use of KIEs in their mechanistic studies. Cordaro and Bergman²²¹ used Ir–acyl hydride **321** to study the dissociation of carbanions from acyl iridium complexes. The absence of KIE indicates that deprotonation of **321** is not rate-determining, and is consistent with a mechanism involving dissociation of the CF_3^- moiety being the rds to form **323** with the subsequent hydride abstraction rendering the final product **322** (Scheme 145).

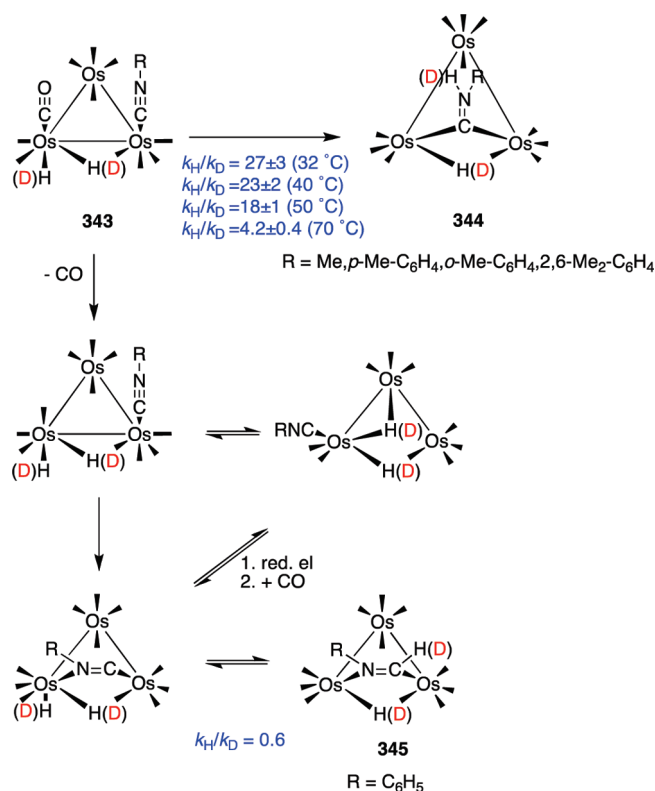
In parallel, Guldi, Fukuzumi, and co-workers²²² investigated the photochemical H/D exchange of the Ir–H complex **324**. A large KIE value ($k_{\text{H}}/k_{\text{D}} = 8.2$) was measured, which pointed to a H/D interchange through an Ir(I) complex **325** (Scheme 146).

Frost and Mebi²²³ studied the protonation of Ru–hydride **326**. The measured primary KIE ($k_{\text{H}}/k_{\text{D}} \approx 7.9$), together with additional kinetic and thermodynamic parameters, allowed them to propose an associative mechanism with little Ru–H (or Ru–D) bond cleavage at the transition state. The reaction was postulated to occur via protonation of the hydride ligand of **326** by water to form a dihydride complex **327**, followed by deprotonation by the resultant hydroxide (Scheme 147).

Scheme 151



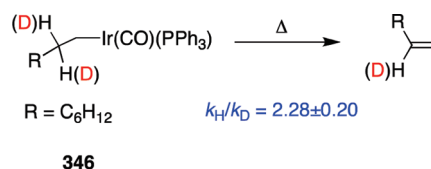
Scheme 152



Norton and co-workers²²⁴ studied the H-transfer from two hydride complexes, HMn(CO)_5 having a relative soft Mn–H bond and $\text{H}_2\text{Os(CO)}_4$ having a stronger Os–H bond, to organic radicals (trityl radicals **328**). A $k_{\text{H}}/k_{\text{D}} = 3.18 \pm 0.03$ was determined for the reaction of **328** with HMn(CO)_5 , while $k_{\text{H}}/k_{\text{D}} = 4.3 \pm 0.3$ was determined in the reaction with $\text{H}_2\text{Os}_2(\text{CO})_8$. It was not clear how much of the increased isotope effect in the osmium system was due to the more symmetric transition state expected in that case (Scheme 148).²²⁵

The interest in the preparation of metal-bound dihydrogen complexes by the protonation of M–H complexes has translated

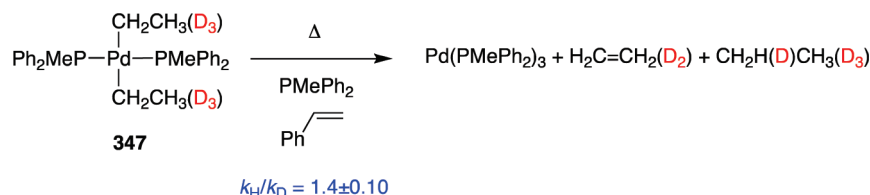
Scheme 153



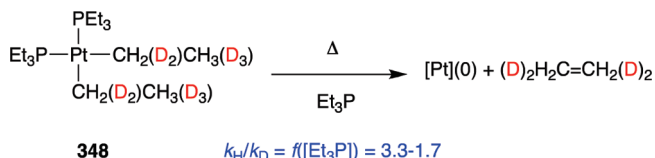
in some studies in the mechanism of this reaction using KIEs. Protonation of $\text{cis-[FeH}_2\{\text{P}(\text{CH}_2\text{CH}_2\text{PPh}_2)_3\}]$ **329** with acids can be formally considered acid–base equilibria involving proton transfer from HX to a coordinated hydride.²²⁶ The $k_{\text{HX}}/k_{\text{DX}}$ values for these reactions oscillate between 0.45 ± 0.2 for CF_3COOH to 0.64 ± 0.4 for HBr. These *inverse* KIEs were interpreted either as the *inverse* KIE on an elementary single-step reaction with a late transition state, or as the result of an *inverse* preequilibrium EIE. Protonation of metal hydrides with HX involves the breaking of the H–X bond and the formation of H–H and Fe–(H₂) bonds. The mechanism in Scheme 149 was proposed. Electrostatic interaction between the partially negative metal-bound hydride and the partially positive proton of the acid leads initially to adduct **330**. As the H–H interaction increases, there is a weakening of the Fe–H and H–X bonds that becomes more and more important, leading to the reaction products **331**. The KIE values for the different acids would indicate transition states with structures close to that represented by **332** because KIEs for very early transition states are expected to be substantially higher. However, the alternative interpretation of the *inverse* KIE as the result of an *inverse* preequilibrium EIE is difficult to differentiate from the previous and cannot be ruled out. KIEs were also used by Henderson and Oglieve²²⁷ to study the mechanisms of protonation of $[\text{M}\eta^5\text{-(C}_5\text{H}_5)_2\text{H}_2]$ (M = Mo or W) with an excess of anhydrous HCl.

Cheng and Bullock²²⁸ studied the abstraction of H from the M–H (M = Fe, Ru, Os) complexes **333–335** by Ph_3C^+ to form complexes **336–338**. In these studies, a primary KIE ($k_{\text{H}}/k_{\text{D}} = 1.6$) was determined for the reaction of Os complex **335** with Ph_3CBF_4 to yield **338**. This value was similar to those found for hydride transfers from $\text{Cp}^*(\text{CO})_3\text{MoH}$, $\text{Cp}(\text{CO})_3\text{MoH}$, $\text{Cp}^*(\text{CO})_3\text{WH}$, and *trans*- $\text{Cp}(\text{CO})_2(\text{PCy}_3)\text{MoH}$ ($k_{\text{H}}/k_{\text{D}} = 1.7\text{--}1.8$),²²⁹ which

Scheme 154



Scheme 155



argues in favor of a common, single-step hydride transfer mechanism for all of these reactions (Scheme 150).

The study of KIE in M–H associated with their role as intermediates in the catalytic decarbonylation processes has been also reported. Thus, Goldman and co-workers²³⁰ reported the decarbonylation of aldehydes by $\text{Rh}_2(\text{PMe}_3)_2(\text{CO})_2\text{Cl}_2$ **339**. A significant KIE ($k_{\text{H}}/k_{\text{D}} = 1.8$) was observed in the reaction of **339** with dodecanal and octanal, which was consistent with an associative pathway with partial or complete cleavage of the aldehyde C–H bond in the transition state (**340**) (Scheme 151). In a recent report, the mechanism for the rhodium-catalyzed decarbonylation of benzaldehyde and phenyl acetaldehyde was investigated to see if there was a change in the rds between the two substrates and to get a better idea whether the oxidative addition **341** or the migratory extrusion **342** was the slow step of the process.²³¹ The KIEs obtained for both substrates were close to that reported above by Goldman and co-workers²³⁰ and similar for both aldehydes ($k_{\text{H}}/k_{\text{D}} = 1.73$ and 1.77 for benzaldehyde and phenyl acetaldehyde, respectively), indicating that the same mechanisms were operating. These values suggested that the C–H bond had been broken in going from the resting state to the selectivity-determining step, although they did not reveal the exact nature of the transition state. However, the DFT studies showed theoretical KIE values in excellent agreement with the experimental ones but *only* when migratory extrusion of CO was selected as the rate-determining step (Scheme 151).

Rosenberg and co-workers reported the thermal rearrangements of triosmium complexes **343**.²³² The mechanistic studies indicate that the metal-to-nitrogen **344** and metal-to-carbon **345** hydrogen transfer reactions proceeded by distinctly different mechanisms (Scheme 152). The very large H/D KIEs, in the temperature range 32–70 °C, obtained for the transformation of **343** to **344**, indicate that the reaction proceeds with a significant proton barrier tunneling component and suggests that the intramolecular hydrogen transfer from osmium to nitrogen involves a proton rather than a hydrogen atom or a hydride. Additionally, the observed $k_{\text{H}}/k_{\text{D}}$ values are quenched if the reaction is carried out in the presence of base. These data are in agreement with previous studies of the same research group in the intramolecular ligand to metal hydrogen transfer of $[(\mu\text{-H})\text{M}_3(\text{CO})_{11}]^-$ (M = Fe, Ru, Os).²³³ However, for the metal to carbon hydrogen-transfer product **345**, only a small

inverse KIE ($k_{\text{H}}/k_{\text{D}} = 0.6$), suggestive of reversible hydrogen transfer, was observed. On the basis of the isotope effects and the dependence of the formation of **345** on CO, a mechanism proceeding via rate-limiting decarbonylation was suggested (Scheme 152).

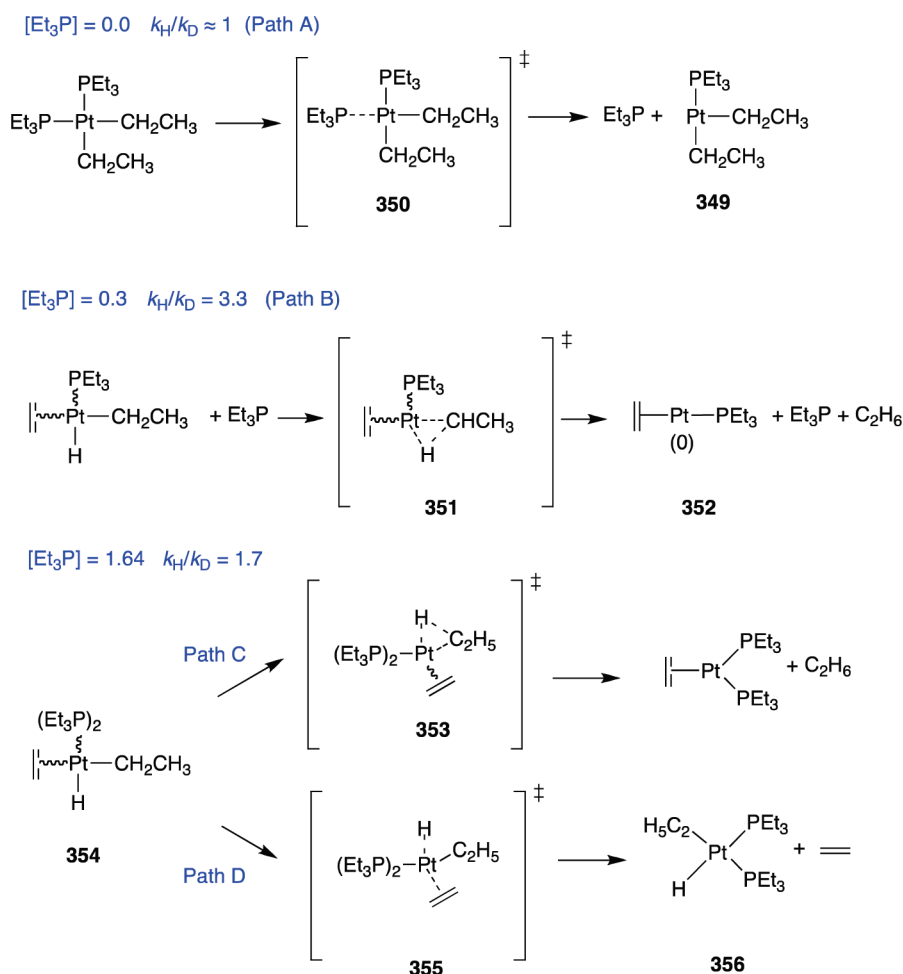
6. β -ELIMINATION/MIGRATORY INSERTION

Tracing back the study of these essential organometallic reactions, the paper by Schwartz and co-workers²³⁴ in 1974 summarizes in a few words the situation of the research in the field using KIEs and the challenges to be faced: “Although β -elimination from metal alkyls and addition of metal hydrides to olefins are central processes in many organic transformations involving transition metal complexes, very little is known about this process mechanistically. The kinetic deuterium isotope effect $k_{\text{H}}/k_{\text{D}}$ for β -hydride elimination can clearly provide useful mechanistic information, and several studies concerning it have been reported.²³⁵ These determinations have not, however, afforded readily interpretable values for $k_{\text{H}}/k_{\text{D}}$, due either (1) to β -hydride elimination not being rate determining in the process studied, (2) to equilibrium effects which scramble deuterium labels, or (3) to an inability to rule out special cluster effects which may be important in β -elimination from clustered transition metal alkyls.” Subsequently, these authors stated that alkyl(I)iridium complexes were excellent substrates to determine KIEs and, thence, to study the β -hydride elimination reaction. Thus, a $k_{\text{H}}/k_{\text{D}} = 2.28 \pm 0.20$ was determined for the β -hydride elimination in Ir complex **346**. This result suggested a transition state for β -elimination in which the iridium atom inserts into the β -C–H bond of the alkyl group (or C–Ir and H–Ir bond formation are both important in the transition state). This interpretation is formally an oxidative addition of C–H to Ir(I) (Scheme 153).

The steric effects by tertiary phosphine ligands on the decomposition of diethylpalladium complexes through a β -hydride elimination reaction was studied by Yamamoto and co-workers.²³⁶ A kinetic isotope effect of $k_{\text{H}}/k_{\text{D}} = 1.4 \pm 0.10$ was obtained in the thermolysis of complex **347**, a value too high to be considered a secondary KIE but smaller than that reported for the iridium complex **346** (Scheme 153) or for the complex $[\text{Co}(\text{CH}_2\text{CD}_3)_2\text{acac}(\text{PMe}_2\text{Ph})_2]$ ($k_{\text{H}}/k_{\text{D}} = 2.30 \pm 0.05$).²³⁷ These data together with the absence of H/D scrambling in the remaining ethyl groups of $\text{Pd}(\text{PMePh}_2)_3$ and in the evolved gases suggested that β -elimination was an irreversible process (Scheme 154).²³⁸

Whitesides and co-workers²³⁹ reported a detailed study on the thermal decomposition of diethylbis(triethylphosphine)platinum(II), **348**. Previous studies in these reactions⁷⁶ had shown that, for the thermal decomposition of **348**, when the concentration of free triethylphosphine in solution was low, the overall rds was the generation of an additional vacant coordination site on platinum. At higher concentrations, phosphine dissociation was reversible, and

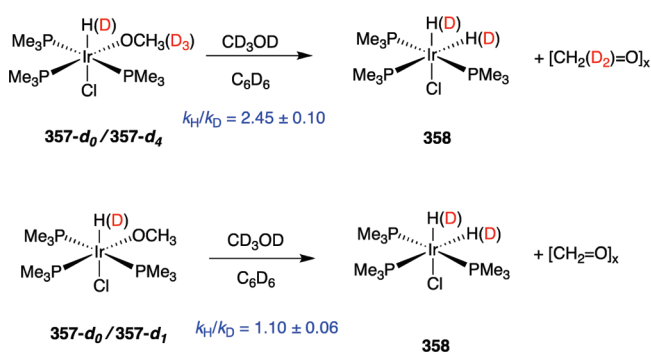
Scheme 156



reductive elimination of alkane from an intermediate hydridoalkyl-(triethylphosphine)platinum(II) complex of undefined composition and stereochemistry was rate-limiting. H/D KIEs were obtained by comparing the rates of decomposition of $(\text{Et}_3\text{P})_2\text{Pt}(\text{CH}_2\text{CH}_3)_2$ and $(\text{Et}_3\text{P})_2\text{Pt}(\text{CD}_2\text{CD}_3)_2$. The value of $k_{\text{H}}/k_{\text{D}} = 3.3$ obtained for $[\text{Et}_3\text{P}] = 0.3$ M indicates C–H(D) bond making or breaking in the transition state and is compatible with rate-limiting reductive elimination of alkane from the $\text{Pt}(\text{H},\text{D})\text{Et}$ group (Scheme 155).²⁴⁰ The decrease in the value of $k_{\text{H}}/k_{\text{D}}$ from 3.3 to 1.7 as $[\text{Et}_3\text{P}]$ increases from 0.3 to 1.64 reflects a change in mechanism. Furthermore, decomposition of $\text{dmpePt}(\text{CH}_2\text{CH}_3)_2$ and $\text{dmpePt}(\text{CD}_2\text{CD}_3)_2$ resulted in an observed KIE of $k_{\text{H}}/k_{\text{D}} = 1.6 \pm 0.3$. This value is (perhaps coincidentally) similar to that observed for $(\text{Et}_3\text{P})_2\text{Pt}(\text{CH}_2\text{CH}_3)_2$ for $[\text{Et}_3\text{P}] = 1.64$ M ($k_{\text{H}}/k_{\text{D}} = 1.7$).

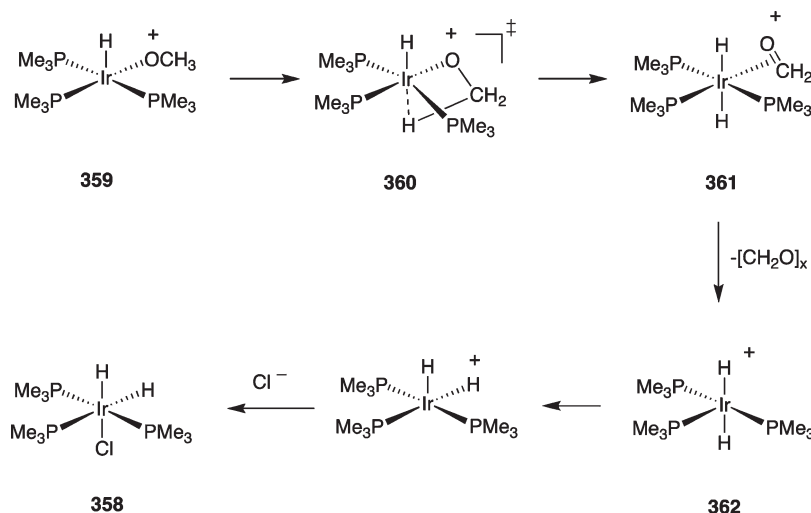
These KIE values coupled to extensive isotope scrambling and kinetic measurements resulted in the proposal of external ligand-dependent mechanisms. For low ligand concentration in solution, all observations are consistent with rate-limiting Et_3P dissociation (Scheme 156, path A). The absence of KIE indicates that β -hydride elimination is not concerted with Et_3P loss and occurs as a separate step from an intermediate, three-coordinate species, $\text{Et}_3\text{PPtEt}_2$, **349** through a transition state **350**. Increasing the concentration of external ligand produced a mechanism in which phosphine dissociation and β -hydride elimination/readdition are fully or partially

Scheme 157

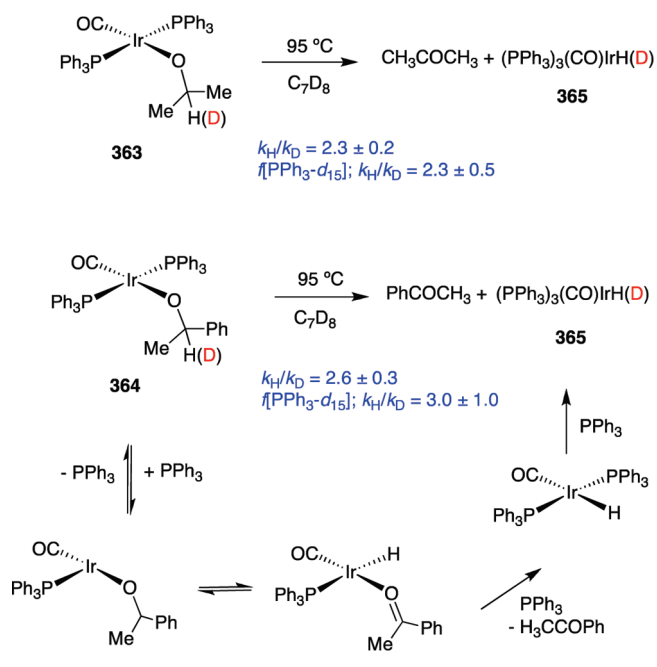


reversible ($k_{\text{H}}/k_{\text{D}} = 3.3$). The KIE value is similar to that observed by Halpern and co-workers.²¹ In these conditions, the overall rds is reductive elimination of ethane from an intermediate $(\text{Et}_3\text{P})(\text{ethylene})\text{ethylhydridoplatinum(II)}$, **351** to form a $\text{Pt}(0)$ complex **352** (Scheme 156, path B). Finally, for high external ligand concentrations, there are two plausible transition states. The transition state **353** involves reductive elimination of ethane from **354** as the rate-limiting step (Scheme 156, path C). The second transition state **355** (Scheme 156, path D) would invoke ethylene loss from **354** as

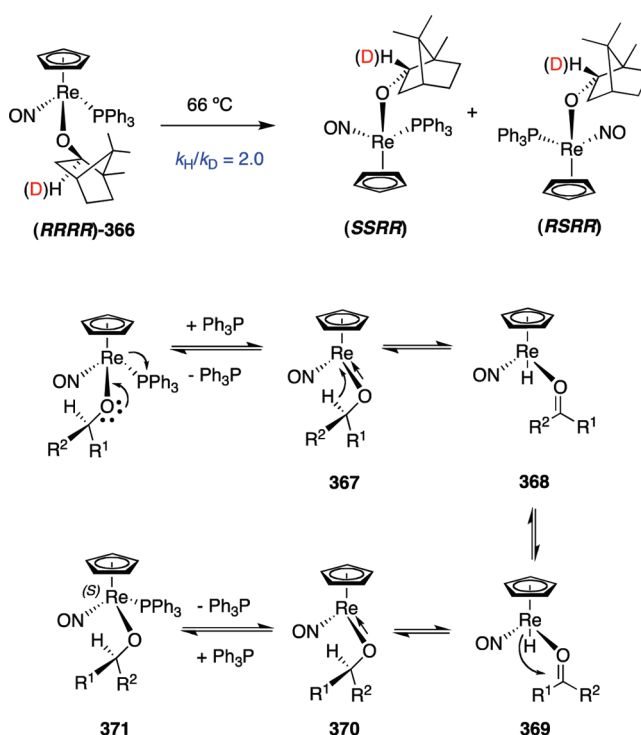
Scheme 158



Scheme 159



Scheme 160



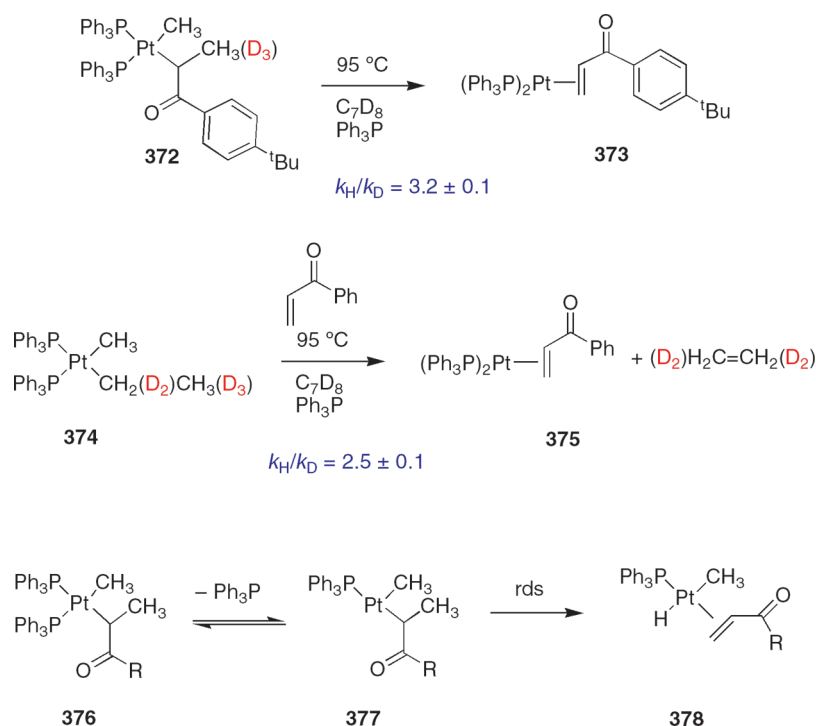
the overall rds, followed by a fast post-rate-determining reductive elimination of ethane to form **356**. In the first of these mechanisms, the low value of $k_{\text{H}}/k_{\text{D}} = 1.4\text{--}1.7$ (relative to the value of $k_{\text{H}}/k_{\text{D}} = 3$ observed for $[\text{Et}_3\text{P}] = 0.3\text{ M}$) would be rationalized on the basis of an early transition state; in the second, it would be rationalized as a combination of secondary isotope effects reflecting changes in force constants for $\text{Pt}(\text{H})$ and $\text{C}_2\text{H}_4(\text{D}_4)$ bonds on dissociation of ethylene and small preequilibrium isotope effects.²⁴¹

Yamamoto and co-workers²⁴² presented further support for the nonconcerted pathway for the β -H elimination on Pt complexes. These authors reported the absence of KIEs in the decomposition of $\text{Pt}[\text{CH}_2\text{CH}_3(\text{D}_3)][(n\text{-Pr}(\text{PPh}_3)_2)]$, which is compatible with the results reported by Whitesides and Halpern.^{76e,239}

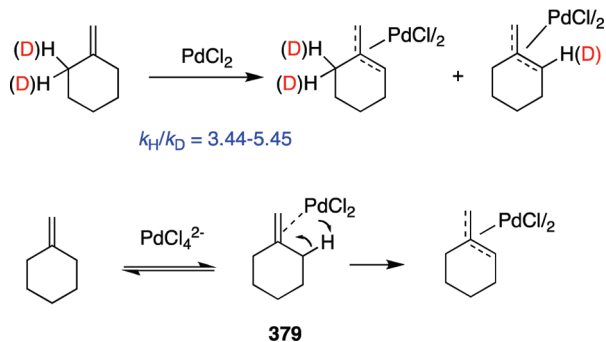
Blum and Milstein²⁴³ studied the β -H elimination from iridium alkoxo complexes **357** to *mer-cis* isomers **358** to compare the analogies and differences between the β -H elimination from metal-alkyls and metal-alkoxides.^{244,245} The KIE obtained for the decomposition of **357-*d*₀**/**357-*d*₄** combined primary and secondary effects ($k_{\text{H}}/k_{\text{D}} = 2.45 \pm 0.10$), and the secondary KIE obtained in the decomposition of **357-*d*₀**/**357-*d*₁** was $k_{\text{H}}/k_{\text{D}} = 1.10 \pm 0.06$ under the same conditions (Scheme 157). This result strongly implies that the C–H bond cleavage is either involved in the rds or precedes it.²⁴⁶

On the basis of the KIE values and additional experimental data, it was established that the initial step for the β -H elimination is the

Scheme 161



Scheme 162



generation of a free coordination site by a methanol-assisted dissociation of a chloride. The pentacoordinate dissociation product **359** experiences the rate-determining irreversible scission of the β -C–H bond, which has a relatively early transition state, **360**. The unstable η^2 -formaldehyde *trans*-dihydrido intermediate formed **361** and undergoes a facile product release process, which includes detachment of the aldehyde, fast isomerization within the pentacoordinate intermediate **362**, and irreversible reassociation of the chloride to obtain **358**. Although the product release was found to be the slowest step in the β -hydride elimination from most transition metal–alkyls studied, the C–H scission from alkoxo complexes is rate-controlling (Scheme 158).

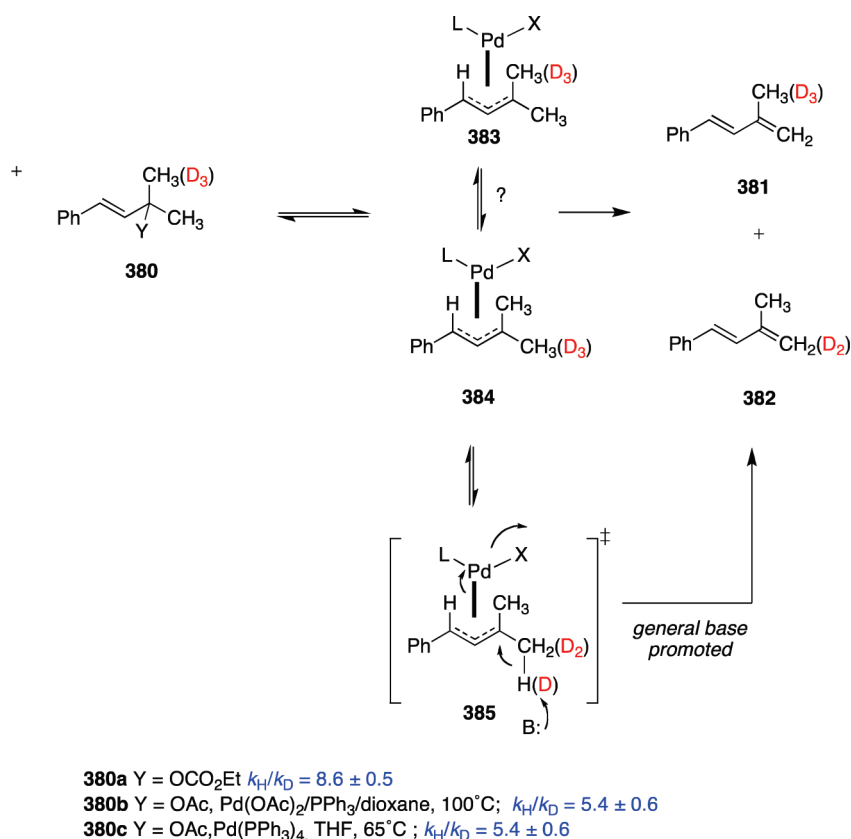
Hartwig and co-workers²⁴⁷ investigated the mechanism of β -H elimination from square-planar iridium(I) alkoxide complexes **363**–**364** having labile dative ligands to yield **365** and acetone or acetophenone, respectively. KIE values of $k_{\text{H}}/k_{\text{D}} = 2.3 \pm 0.2$ and $k_{\text{H}}/k_{\text{D}} = 2.6 \pm 0.3$ were obtained for **363** and **364**, respectively (Scheme 159). The deuterium isotope effect on the thermolysis of

363–**364** was also evaluated as a function of phosphine concentration. This measurement was conducted as a function of $[\text{PPh}_3\text{-}d_{15}]$ because the kinetic importance of the C–H bond cleavage step depends on whether dissociation of $\text{PPh}_3\text{-}d_{15}$ and β -hydrogen elimination are reversible, which may render the reversibility of these steps dependent on $[\text{PPh}_3\text{-}d_{15}]$. The observed data revealed a significant KIE ($k_{\text{H}}/k_{\text{D}} = 2.3 \pm 0.5$ for **363** and $k_{\text{H}}/k_{\text{D}} = 3.0 \pm 1.0$ for **364**) as a function of $[\text{PPh}_3\text{-}d_{15}]$. The combination of KIEs and phosphine dependence on the k_{obs} and on stereochemical integrity of the starting complexes led them to propose a reaction pathway involving reversible phosphine dissociation and reversible β -hydrogen elimination (Scheme 159). This pathway contrasts with previously reported solvent-assisted ligand dissociation,²⁴⁸ direct elimination,²⁴⁶ and bimolecular hydride abstraction.²⁴⁹

The mechanism depicted in Scheme 159 is fully compatible with the dissociative pathway previously proposed by Saurallamas and Gladysz²⁵⁰ for the catalytic epimerization of secondary alcohols by Re-alkoxyde complexes. The KIE value ($k_{\text{H}}/k_{\text{D}} = 2.0$) observed in the isomerization of enantiopure complex **366**, together with an extensive stereochemical and kinetic study, allowed these authors to propose an epimerization mechanism in which the extrusion of phosphine from the initial complex forms an intermediate **367** that experiences a β -hydrogen elimination to yield **368**. Hydride **368** has a flat carbonyl group that may rotate and accept the hydride for the opposite enantioface leading to **369**. Finally, **370** forms the complex **371** having the epimeric alcohol configuration (Scheme 160).

Alexanian and Hartwig²⁵¹ studied the β -H elimination in organoplatinum(II) enolate complex **372**. The thermal decomposition in the presence of added phosphine led to coordinated enone complex **373** with a noticeable KIE ($k_{\text{H}}/k_{\text{D}} = 3.2 \pm 0.1$). Also a high KIE value ($k_{\text{H}}/k_{\text{D}} = 2.5 \pm 0.1$) was determined for the thermal

Scheme 163



reaction of complex 374 with phenylvinyl ketone to yield complex 375 (Scheme 161). These KIEs coupled to an exhaustive analysis of the electronic effects on the reactions of alkyl and enolate complexes allowed the proposal of a mechanism involving initial ligand dissociation from the starting complex 376 to form intermediate 377, followed by rate-determining β -H elimination to form 378. The rate was retarded by the presence of electron-withdrawing groups on the enolate. This electronic effect can be attributed to both increased stabilization of the enolate complex 377 and decreased stabilization of the η^2 -bound alkene products 378 due to the electron-withdrawing group attached to the R group.

The primary KIEs in the β -H elimination from {H/D-C-C-Pd} have been employed to distinguish between *syn*- ($k_H/k_D \approx 2$ –3) and *anti*- ($k_H/k_D \approx 5$ –7) elimination mechanisms.²⁵² Consistent with *syn* processes were the above-mentioned KIE values reported for alkyliridium(I) complexes 346 (Scheme 153) ($k_H/k_D = 2.28 \pm 0.20$),²³⁴ Pd complexes 347 (Scheme 154) ($k_H/k_D = 1.4 \pm 0.10$),²³⁶ or the $k_H/k_D = 2.5 \pm 0.2$ observed by Brainard and Whitesides²⁵³ during the thermolysis of complex L₂PtClC₂H₅(D₅) and by Romeo et al. ($k_H/k_D \approx 2.55$) in the *syn*- β -hydride elimination from monoalkyl solvento complexes of Pt(II) of formula *trans*-[Pt(PET₃)₂(R)(S)]⁺ (S = solvent).²⁵⁴

The much higher KIE values associated to *anti*- β -H eliminations were initially reported by Chrisope, Beak, and Saunders.²⁵⁵ The reaction of methylenecyclohexane with PdCl₂ under several reaction conditions produced values of $k_H/k_D = 3.44$ –5.45 that were consistent with a fast, reversible complexation prior to rds C–H bond cleavage. The noticeable KIE value of $k_H/k_D = 5.4 \pm 0.1$ confirms that C–H bond breaking is rate-determining for the entire process. The identical product isotope effect indicates the ratio of

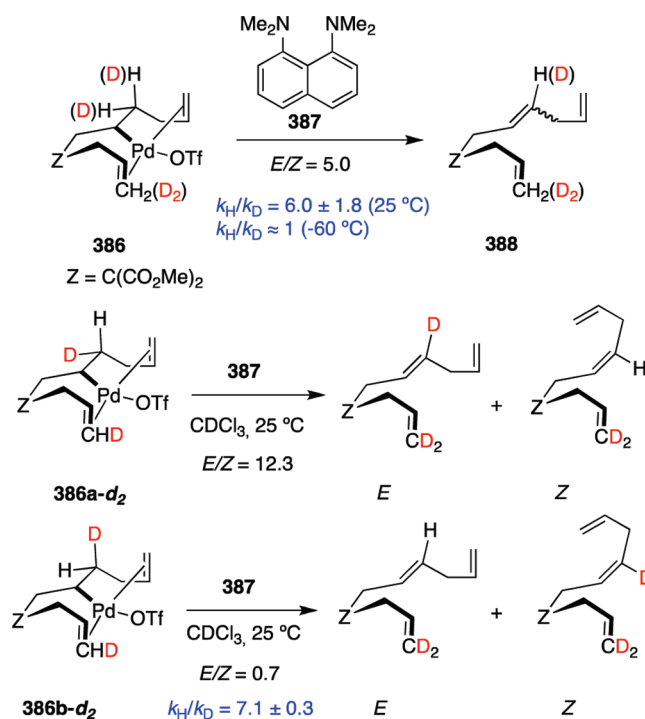
products is established in the same elementary reaction. On the basis of these and additional kinetic data and calculations, a mechanism consisting of deprotonation of the initially formed complex 379 by a basic internal ligand was proposed (Scheme 162).

Takacs and co-workers²⁵⁶ found that the Pd-catalyzed elimination of 380 to give 381 and 382 had very high KIE values ($k_H/k_D = 5.4$ –8.6) (Scheme 163). These results together with additional stereochemical data were not consistent with the commonly accepted mechanism where hydrogen is lost via β -elimination. However, they were compatible with a stereospecific anti-addition of LnPd(0) to the allylic carbonate to form 383 and 384 followed by stereospecific base-promoted anti-elimination of the elements LnPd(X)–H through a transition state 385.

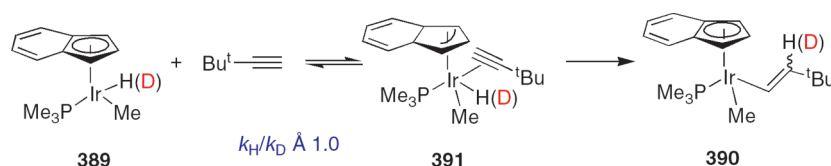
Lloyd-Jones and Slatford²⁵⁷ claimed that the presence of a large KIE may not involve an *anti*- β -H elimination mechanism. These authors found a $k_H/k_D = 6.0 \pm 1.8$ in the reaction of σ -alkyl–palladium complex 386-*d*₀/386-*d*₄ with proton sponge 387 to form *E/Z*-trienes 388 at 25 °C. Independent experiments with labeled complexes 386a-*d*₂ and 386b-*d*₂ to study both the stereochemistry of the β -H elimination process and the *E/Z* partitioning through KIEs demonstrated that the reaction follows a *syn*- β -H elimination process, not a base-mediated *anti*-elimination. The KIE values observed result from a complex interplay of three primary KIEs (β -H elimination, hydropalladation, and Pd–H deprotonation) and are larger than those usually associated with *syn*- β -H elimination (Scheme 164).

Small KIE values were observed in the β -elimination of groups other than H, such as on ligand substitution W(CO)₃(PCy₃)₂L [L = H₂, N₂, py, POME₃] complexes ($k_H/k_D = 1.20$)²⁵⁸ or in the Si–C scission of ((trimethylsilyl)methyl)platinum complexes

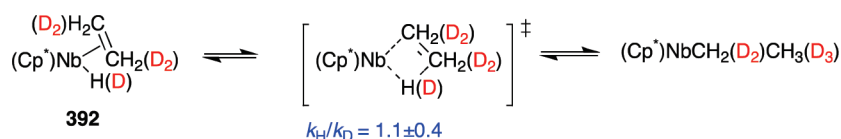
Scheme 164



Scheme 165



Scheme 166



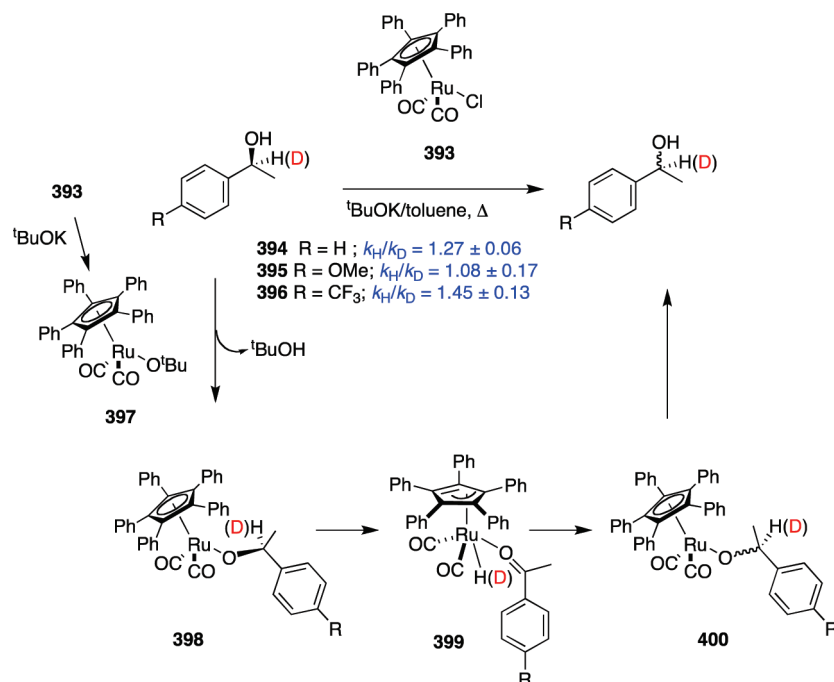
reported by Young and co-workers¹⁶⁴ ($k_{\text{H}}/k_{\text{D}} = 2.1\text{--}1.4$). In these cases, the involvement of agostic interactions was claimed.

The KIEs in the reverse to β -elimination, namely, the migratory insertion, have also been determined for several systems. Foo and Bergman²⁵⁹ determined the KIE in the insertion of (η^5 -Ind) (PMe_3)Ir(CH₃)(H) **389** with *tert*-butylacetylene to yield complex **390**. The negligible KIE values of these reactions are most consistent with a mechanism involving initial reversible coordination of alkyne to the metal center (probably with concurrent η^5 - η^3 isomerization of the indenyl ligand to yield the intermediate **391**) followed by irreversible migration of the metal-bound hydrogen to the *tert*-butyl-substituted carbon of the alkyne and then rapid recoordination of the indenyl group. The coordination of the alkyne to the Ir center

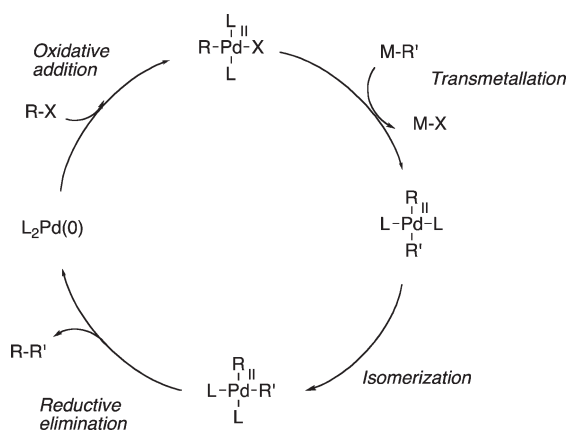
should be rate-determining because no KIE was observed (Scheme 165).

Mechanistic studies of olefin insertion into the niobium hydride bond of Cp^{*}Nb(III)(olefin)(H) complex **392** support the generally proposed picture for olefin insertion and β -H elimination, with insertion and elimination proceeding through a relatively nonpolar, cyclic transition state with concerted bond making and bond breaking (Scheme 166). The measured KIE value ($k_{\text{H}}/k_{\text{D}} = 1.1 \pm 0.4$) on hydride-olefin insertion for **392-d₀**/**392-d₅** is a composite isotope effect, which is the product of a normal primary and four inverse secondary KIEs, the latter involving sp² to sp³ hybridization changes of the two methylene carbons. Considering these facts, an estimated range for the primary isotope effect for hydride-olefin insertion in **392** could

Scheme 167



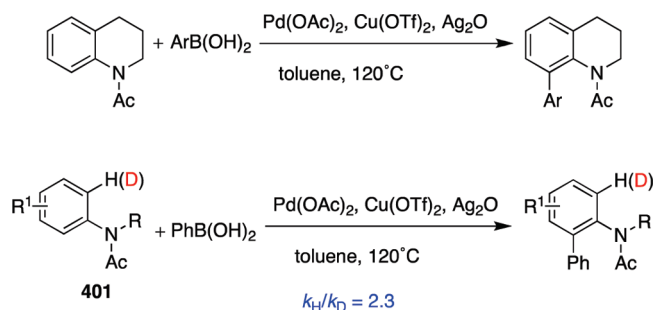
Scheme 168



be $1.7 \pm 0.6 < k_H/k_D < 2.7 \pm 1.0$.²⁶⁰ β -hydride eliminations on Fe-cluster surfaces have been also reported.²⁶¹

Bäckvall and co-workers²⁶² studied the racemization of *sec*-alcohols catalyzed by pentaphenylcyclopentadienyl–Ru complex 393. This racemization occurs at the migratory insertion step. Evidence for an alkoxide pathway by a β -elimination/migratory insertion was obtained from the moderate KIEs ($k_H/k_D = 1.08$ – 1.45) observed by racemizing the alcohols 394–396 in the presence of complex 393 as the catalyst (Scheme 167). The more electron-rich alcohol 395 showed no isotope effect, which suggests that the relative rate of β -hydride elimination has increased compared to the unsubstituted case. For the electron-deficient alcohol 396, the isotope effect was larger. This shows that, for the more electron-deficient alcohol, the β -hydride elimination step becomes more rate-determining than for the more electron-rich ones. From these and additional

Scheme 169



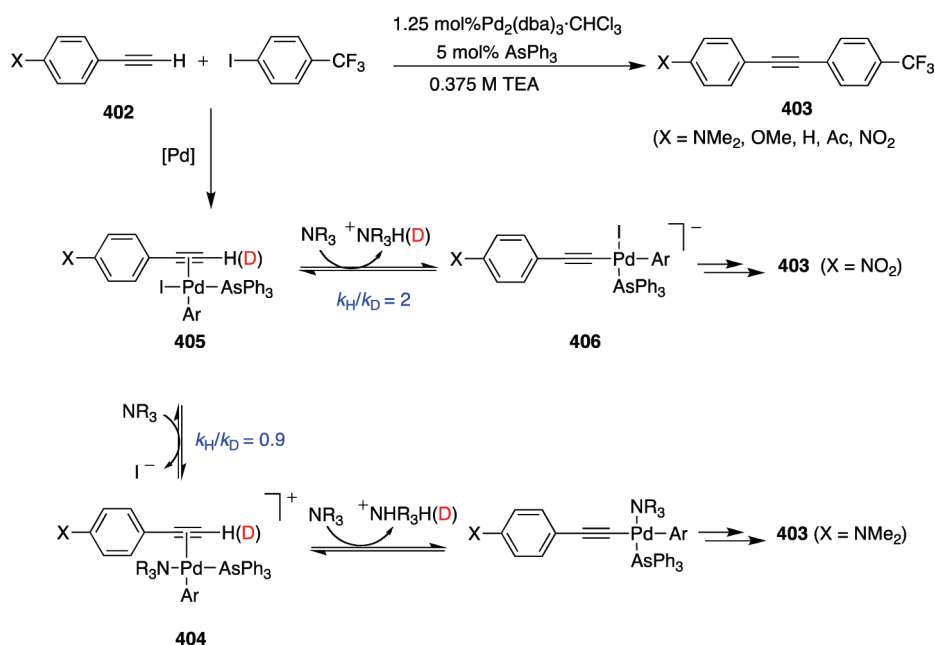
kinetic data, a mechanism involving ruthenium–alkoxide intermediates 398 formed by the reaction of *tert*-butoxide ruthenium complex 397 with alcohols 394–396. β -Elimination from the *sec*-alkoxide complex 398 forms a hydride ketone intermediate 399, in which the cyclopentadienyl ligand coordinates in a η^3 -mode to the Ru center. This intermediate undergoes a fast reversible migratory insertion to yield complex 400 in which the alcohol chiral center is racemized (Scheme 167).

7. KIES IN THE STUDY OF C–C COUPLINGS MEDIATED BY TRANSITION METAL COMPLEXES

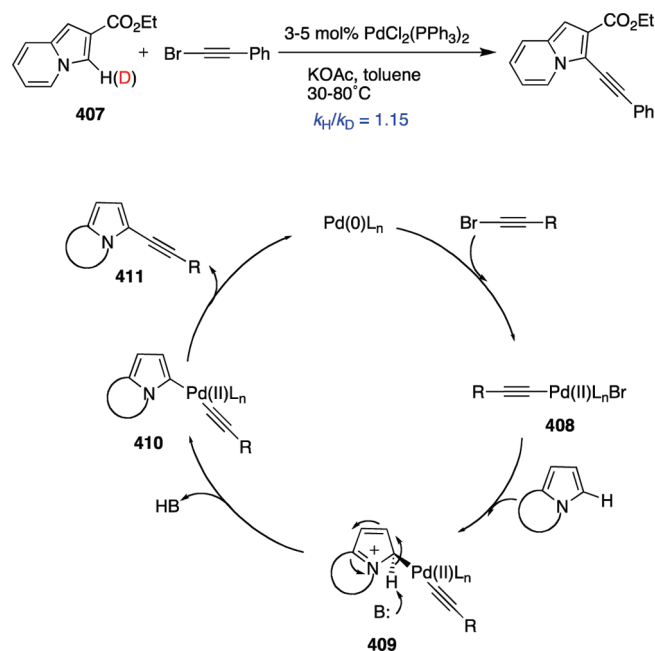
7.1. Sequence Ad–Ox–Transmetalation

The standard three-step catalytic cycle consisting of (i) *oxidative addition* of a Pd(0) complex with an organic electrophile, (ii) *transmetalation* to generate diorganopalladium derivatives, and (iii) their *reductive elimination* to produce the desired coupled product with concomitant regeneration of the Pd(0) complex described in textbooks (Scheme 168) is profitably used as a basis for discussions and predictions of four of the

Scheme 170



Scheme 171



cornerstone processes in the field of organic synthesis, namely, the palladium-catalyzed coupling reaction between aryl or alkynyl halides (or triflates), zincates and stannanes, boranes, or terminal alkynes.²⁶³ The synthetic relevance of these metal-mediated coupling reactions has motivated the interest for their mechanistic insights, but although different studies of these processes have been reported,^{263a} the use of KIEs is very limited.

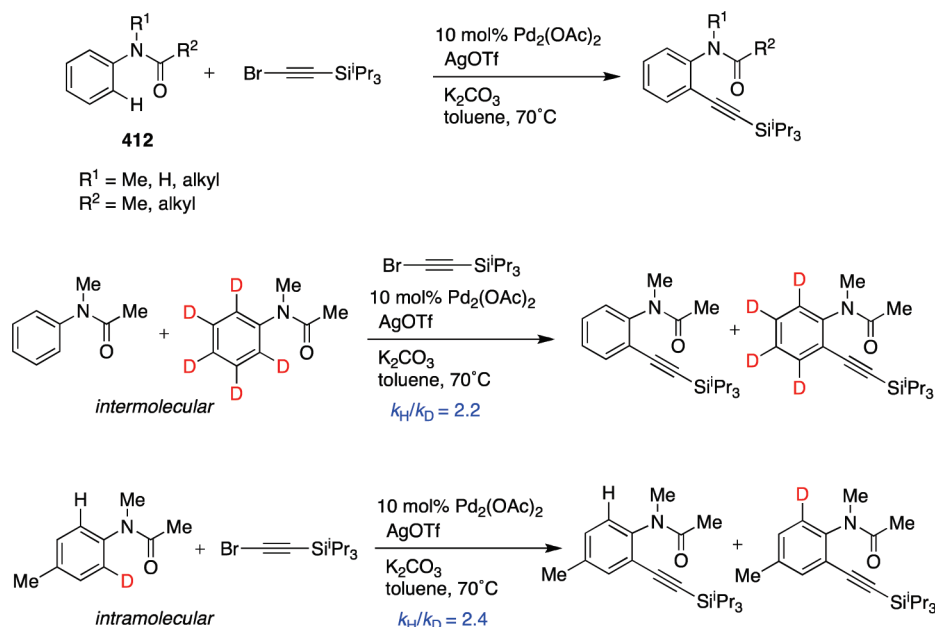
Shi and co-workers²⁶⁴ reported the use of KIEs in the study of an efficient Suzuki–Miyaura-type coupling of aryl boronic acids and cyclic and acyclic *N*-alkyl acetanilides in the presence of

Cu(OTf)₂. The intramolecular isotopic effect ($k_H/k_D = 2.3$) obtained in the reaction of **401** and phenylboronic acid indicated that the cleavage of a C–H bond was involved in the rds. Although considering the experimental data, a mechanism based on the initial aryl C–H activation followed by transmetalation and reductive elimination seems to be likely, the authors were not able to discard other mechanistic alternatives (Scheme 169).

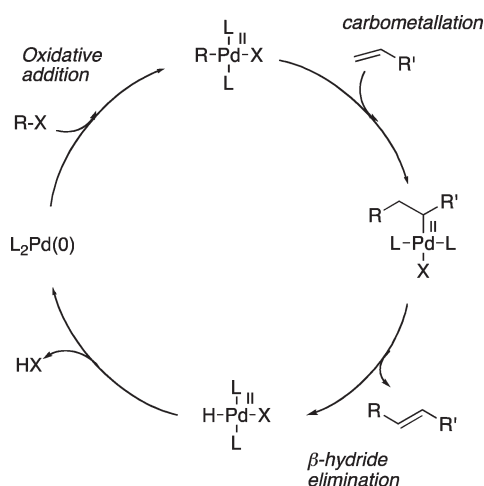
A recent study revealed a mechanistic changeover for the copper-free Sonogashira cross-coupling of *para*-substituted phenylacetylenes **402** with 4-iodobenzotrifluoromethane when going from electron-poor to electron-rich alkynes (Scheme 170).²⁶⁵ To test whether or not the acetylenic C–H bond was broken in a step strongly influencing the reaction rate, a KIE study was performed in cross-coupling reactions using normal and deuterated phenylacetylenes. The substantial KIE observed for the electron-withdrawing substrate (EWG) ($k_H/k_D = 2$ for X = NO₂) supports the assumption of a rate-influencing C–H bond breaking. The significant difference between the KIE observed for the EWG and the electron-donating (EDG)-substituted phenylacetylenes, respectively ($k_H/k_D \approx 0.9$ for X = NMe₂), corroborated the mechanistic changeover indicated by the Hammett plots. Furthermore, there was a pronounced base dependence for the couplings with electron-rich substrates, suggesting that the amine was acting not only as a base but also as a nucleophile in the reactions involving EDG-substituted alkynes.

Considering these results, the preferred pathway for electron-rich alkynes is hypothesized to include a slow formation of a cationic Pd–alkyne complex **404**, via an iodide–amine exchange. This proposition is supported by the negative slope of the Hammett plot for the EDG-substituted alkynes and the increasing reaction rate with increasing nucleophilicity of the applied amine. The electron-poor alkynes are hypothesized to react via a pathway in which the key step is proton transfer from an uncharged complex **405** to produce the Pd–acetylide intermediate **406**. This is corroborated by the positive slope of the Hammett plot for EWG-substituted

Scheme 172



Scheme 173



alkynes, as well as by the primary KIE observed. The changeover point is dependent on the nature of the amine base and its concentration. The mechanistic proposals were supported by theoretical calculations.

Gevorgyan and co-workers reported²⁶⁶ the palladium-catalyzed alkynylation of a series of electron-rich *N*-fused heterocycles, from indolizines to pyrroloisoquinolines, pyrrolooxazoles, and pyrroloquinolines. The authors propose that the reaction operates via an electrophilic substitution pathway. The electrophilic nature of the process is supported by a low KIE ($k_{\text{H}}/k_{\text{D}} = 1.15$) observed in the alkynylation of the deuterium-labeled indolizine **407**. This KIE value is in the range of those reported in the Pd-catalyzed arylation of electron-rich heterocycles proceeding through an electrophilic pathway (Scheme 171).²⁶⁷ The mechanism involves a nucleophilic attack of the most electron-rich C3 position of the heterocycle at alkynyl-palladium intermediate **408** to form iminium intermediate **409**.

Deprotonation of the latter furnishes the Pd(II) intermediate **410**, which upon reductive elimination produces alkynyl heterocycle **411**.

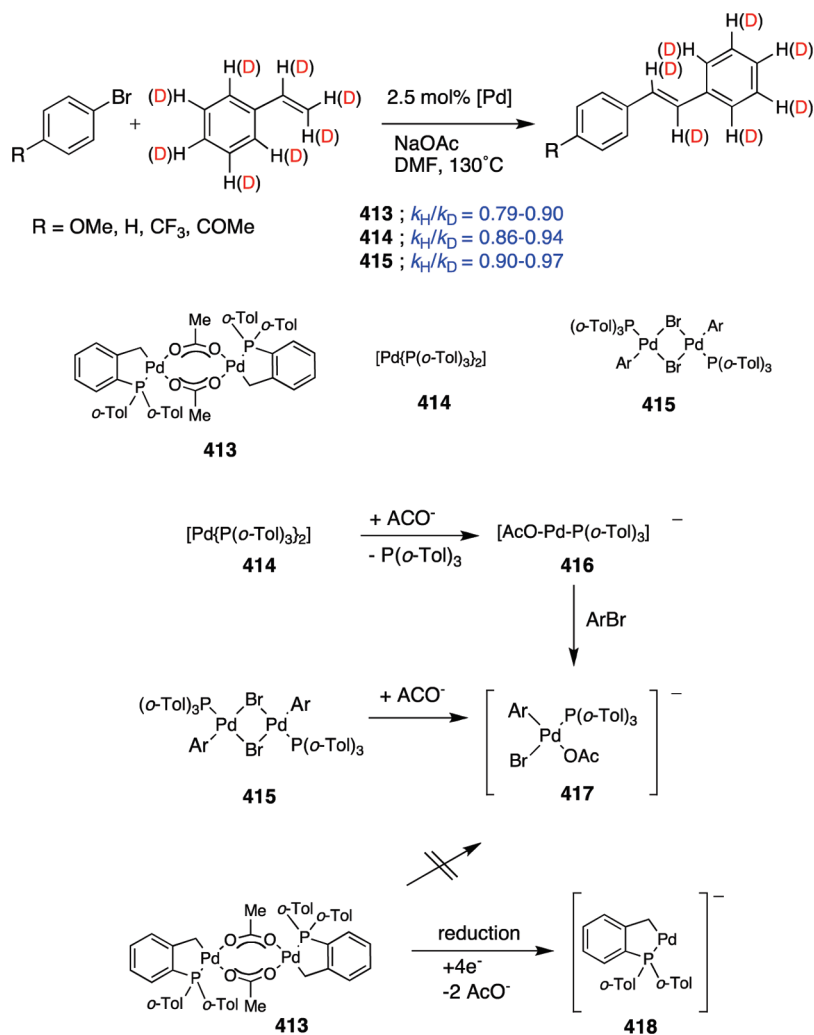
Chatani and co-workers reported²⁶⁸ the alkynylation of aromatic C—H bonds of anilides **412**. To probe the nature of the C—H bond cleavage, they made inter- and intramolecular competitive KIE experiments that indicate clear primary $k_{\text{H}}/k_{\text{D}}$ values of 2.2 and 2.4, respectively (Scheme 172). Both results indicated that the cleavage of an *ortho*-C—H bond was involved in the rds and excluded an alkynylpalladium electrophilic aromatic substitution pathway.

7.2. Heck Coupling

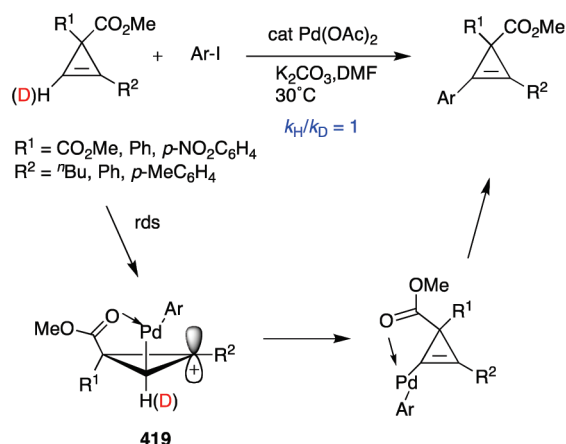
The Heck reaction (Scheme 173),²⁶⁹ having no organometallic reagent involved in the step subsequent to the oxidative addition, does not include a transmetalation step in its mechanism. The absence of the transmetalation step makes it probable that the oxidative-addition step is not rate-determining.²⁷⁰

Among the mechanistic details about the Heck reaction, the question of whether the stable palladium(II) complexes allow palladium(IV) intermediates to be formed in an alternative catalytic cycle has attracted substantial interest, as this potential mechanism would complement the classical catalytic cycle involving a palladium-(II) intermediate. Hermann and co-workers investigated the mechanism of the Mizoroki–Heck vinylation of aryl bromides catalyzed by the phosphapalladacycle **413** in comparison with other classical catalysts such as **414** and **415**.²⁷¹ Complex **415** is the product of the oxidative addition of ArBr to complex **414**. Under the conditions of the Heck reaction, that is, an excess of NaOAc, catalysts **414** and **415** should form the same anionic 14-electron palladium(0) intermediate species **416** and **417**. The noticeable differences found within palladacycle **413** and the others in the Hammett studies for the reaction of styrene with aryl bromides pointed to a different mechanism cycle in the former case. However, the competition experiments between styrene-*d*₀ and styrene-*d*₈ revealed similar *inverse* secondary KIEs for all three catalysts (Scheme 174). These results led to the conclusion that the classic mechanism through

Scheme 174



Scheme 175



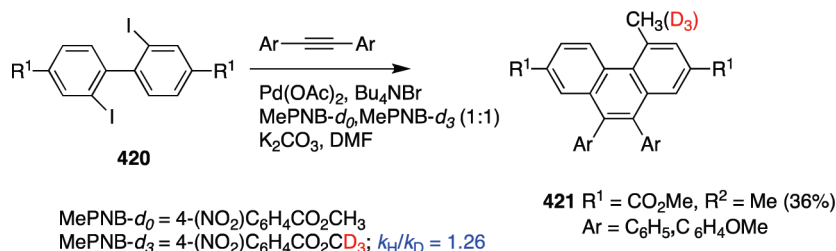
Pd(0) intermediates must be operative in all cases. The differences found in the experiments with palladacycle **413** could be explained by a modified classical catalytic cycle involving a novel, cyclometalated, anionic palladium(0) species **418** rather than palladium(IV)

intermediates. Species **418** could account for the observed high activity and stability of palladacycle catalysts such as **413** in the Heck reaction. Palladium(IV) intermediates can be ruled out by taking into account the experiments performed.

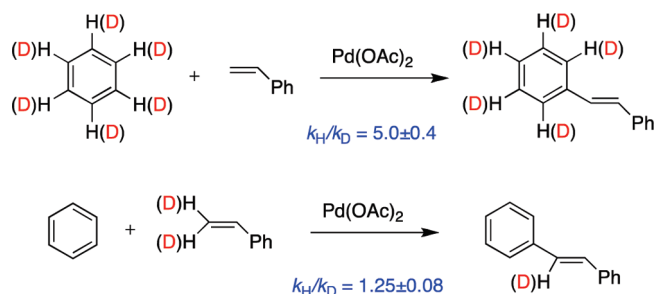
The absence of KIEs proved to be decisive in the discussion of the different mechanistic proposals for the palladium-catalyzed arylation and heteroarylation of cyclopropenes reported by Gevorgyan and co-workers (Scheme 175).²⁷² The mechanism of this reaction can be rationalized via several alternative pathways including Heck-type, C–H activation, or cross-coupling protocols. However, the absence of KIEs ruled out all the alternatives excepting a cationic path involving electrophilic addition of ArPd⁺ species to cyclopropene to form cyclopropyl cation **419** (R² = Ar) is additionally stabilized by interaction with the *d*-orbitals of Pd. The dependence of the process on the electronic nature of R² is in agreement with this proposal.

The Heck-like Pd-catalyzed annulation of dimethyl 2,2'-diiodo-4,4'-biphenyldicarboxylate **420** with internal alkynes yields 4-methylphenanthrenes **421** as the main products.²⁷³ To establish the origin of the methyl group in the annulation product **421**, the reaction of **420** and diphenyl acetylene was successfully

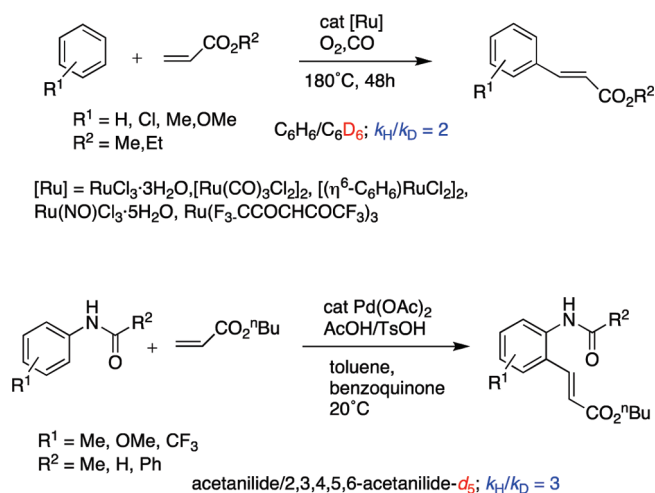
Scheme 176



Scheme 177



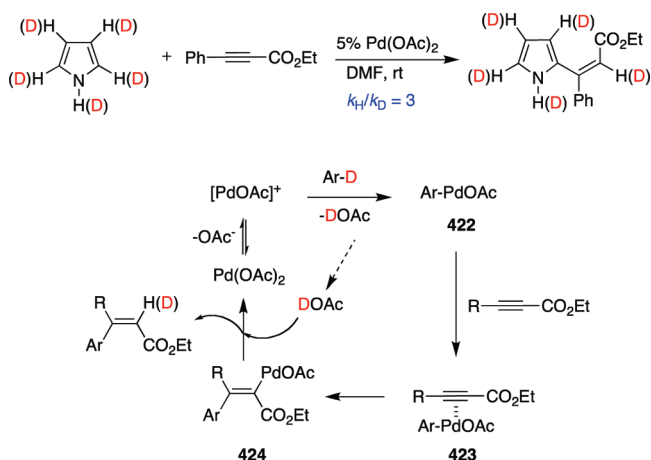
Scheme 178



carried out in the presence of methyl carboxylates such as 4-(NO₂)C₆H₄CO₂Me (MePNB) as methyl transferring agents. Additionally, a competitive KIE study using a 1:1 mixture of MePNB-*d*₀ and MePNB-*d*₃ led to a secondary kinetic isotope effect of $k_H/k_D = 1.26$. This value suggested that the methyl transferring process may play an important role in the rate-determining step (Scheme 176).

In an early article, Shue²⁷⁴ reported a significant KIE in the phenylation of styrene with benzene-*d*₀ and benzene-*d*₆ ($k_H/k_D = 5.0 \pm 0.4$) but a secondary KIE in the reaction of benzene and β,β-*d*₂-styrene ($k_H/k_D = 1.25 \pm 0.08$). The results were consistent with a rate-determining Pd–aryl σ-bond formation and not with a slow Pd–olefin σ-bond formation as had been postulated (Scheme 177).²⁷⁵

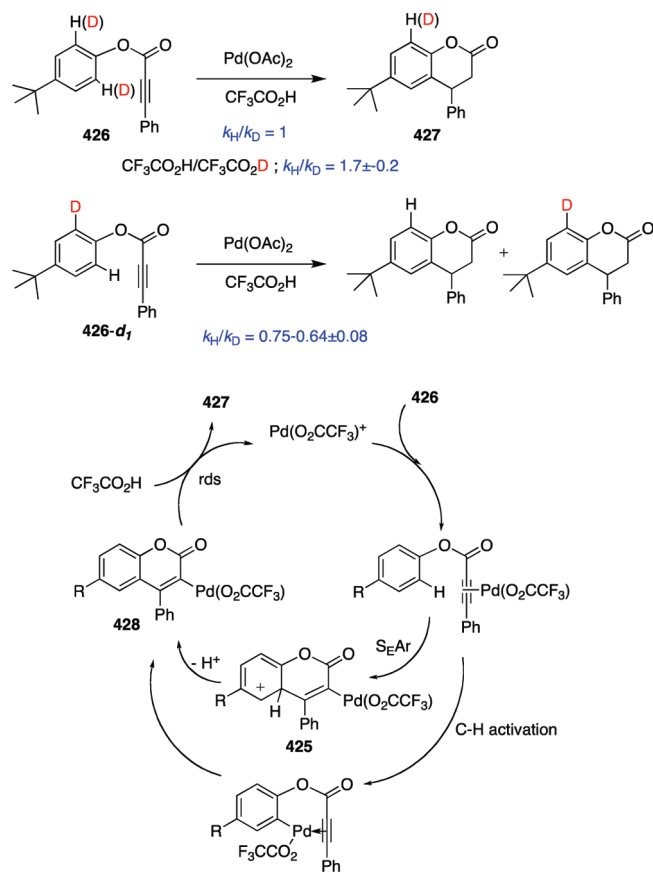
Scheme 179



Milstein and co-workers reported the Heck-type coupling of arenes and acrylates in the presence of Ru catalysts and O₂ as oxidant.²⁷⁶ The reaction takes place with moderate selectivity and requires high temperatures. van Leeuwen and co-workers²⁷⁷ reported the coupling of acetanilides with *n*-butyl acrylate using 2 mol % Pd(OAc)₂ and benzoquinone (BQ) as oxidant (Scheme 178). In both cases, the reactions are sensitive to electron-donating substituents in the arene, which is consistent with a reaction pathway via electrophilic attack of cationic [PdOAc]⁺ species and formation of a σ-aryl–[Pd] complex and shows primary KIEs ($k_H/k_D = 2$ and $k_H/k_D = 3$) indicating slow *ortho*-C–H bond activation.

Pd-catalyzed coupling of arenes and alkynes has been a subject of additional mechanistic debate. Fujiwara and co-workers studied the coupling of arenes and heteroarenes (pyrroles, furans, indoles) with alkynes in the presence of catalytic Pd(OAc)₂ to form *cis*-aryl and heteroarylalkenes.²⁷⁸ Independent experiments carried out with pyrrole-*d*₀ and pyrrole-*d*₅ with ethyl phenylpropionate showed a large primary KIE ($k_H/k_D = 3$), indicating that the cleavage of the pyrrol C–H/C–D bonds was rate-determining. On the basis of KIEs and deuterium labeling experiments, a mechanism involving the [PdOAc]⁺ species was proposed (Scheme 179). Thus, electrophilic substitution of the aromatic C–H bond by cationic Pd(II) species would result in the formation of a σ-arylpalladium complex 422, which is followed by coordination of alkyne to give 423. *trans*-Insertion of C–C triple bonds to the σ-aryl–Pd bond would afford vinyl–Pd complexes 424; upon protonation, a 1/1 arene/alkyne adduct would be released from the Pd(II) species. The presence of acid (AcOH) as solvent should favor the formation of the

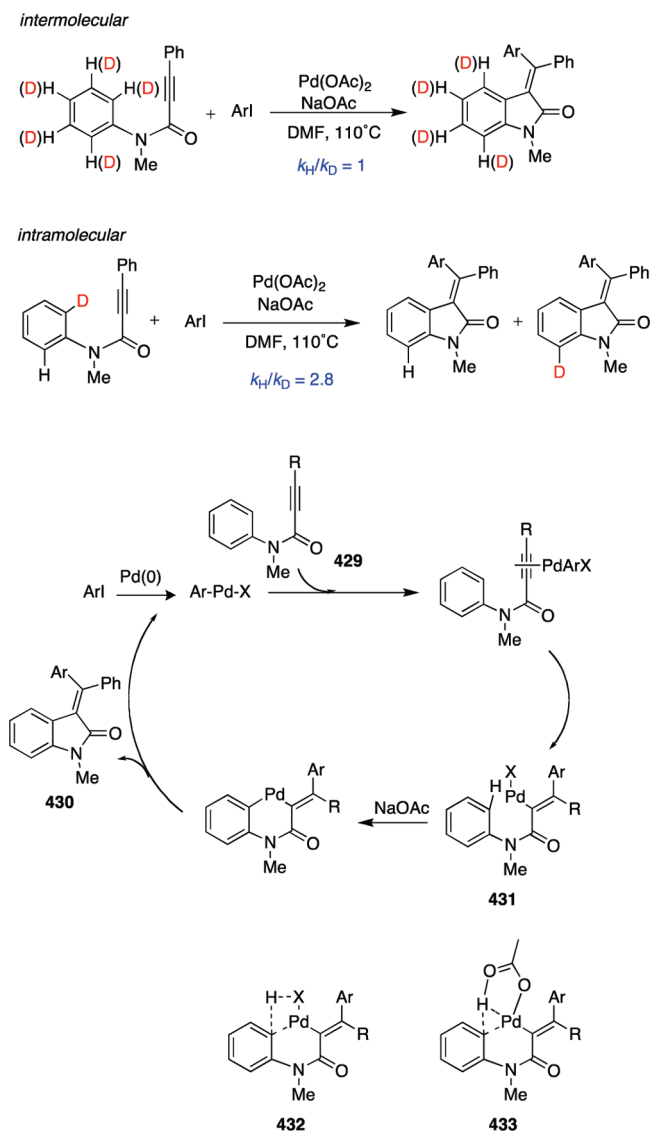
Scheme 180



cationic Pd species. Indirect evidence for the intermediacy of Pd–vinylidene intermediates also supported this proposal.^{278b}

However, in a more recent study, Tunge and Foresee²⁷⁹ used the intramolecular Fujiwara coupling reaction as a model to raise the question of whether the addition of the C–H bonds of arenes across alkynes in the presence of $\text{Pd}(\text{OAc})_2$ proceeds through C–H activation or follows an electrophilic aromatic substitution ($\text{S}_{\text{E}}\text{Ar}$) pathway through the intermediacy of a Wheland-type intermediate **425** (Scheme 180). The key experiments were inter-/intramolecular deuterium KIEs in the hydroarylation of alkynyl ester **426** to coumarin **427**. The lack of an intermolecular primary KIE in the reactions with **426-d₀**/**426-d₂** clearly indicates that the C–H/C–D bond breaking is not involved in the rds. Additionally, the solvent KIE observed when the reaction was carried out with $\text{CF}_3\text{CO}_2\text{H}$ and $\text{CF}_3\text{CO}_2\text{D}$ (1.7 ± 0.2) is consistent with rate-limiting protonolysis of the palladium–carbon bond present in intermediate **428**. Although C–H bond breaking is not involved in the rate-limiting step, if the arene is selectively *ortho*-monodeuterated, then the substrate will be able to partition between reaction at the C–D bond and reaction at the C–H bond, making it possible to measure the level of deuterium incorporation in the product. This intramolecular KIE would be noticeable in the case of a C–H activation process and negligible for the $\text{S}_{\text{E}}\text{Ar}$ pathway, as the product-determining cyclization does not involve C–H/C–D bond breaking. The *inverse* KIEs ($k_{\text{H}}/k_{\text{D}} = 0.64-0.75$) observed in the reaction with **426-d₀**/**426-d₁** were interpreted by Tunge and Foresee as evidence against a C–H activation mechanism, as they were far from the range reported for other C–H activations

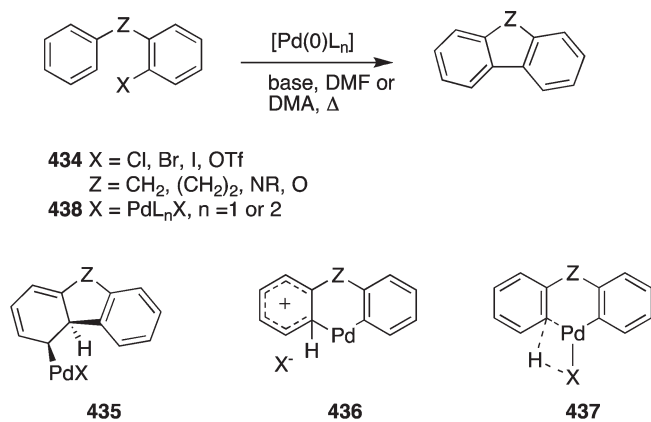
Scheme 181



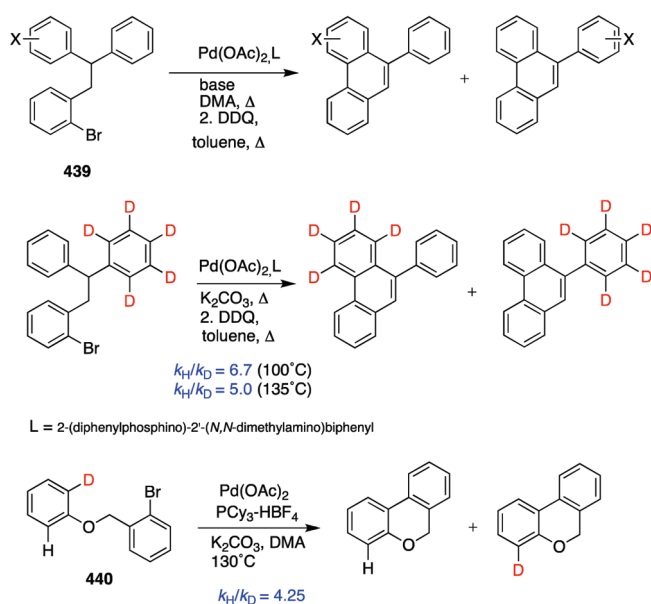
by similar Pd and Pt compounds ($k_{\text{H}}/k_{\text{D}} = 2-5$).²⁸⁰ Considering these results, they suggested that the reaction proceeds by electrophilic aromatic substitution rather than Fujiwara's proposal.

Inter- and intramolecular KIEs were also used by Zhu and co-workers in the study of the mechanism of the formation of oxindoles **430** from alkynyl anilides **429** and aryl iodides.²⁸¹ The reaction proposal, a palladium-mediated *syn*-carbopalladation/C–H activation/C–C bond-formation sequence, is depicted in Scheme 181. A competitive experiment of **429-d₀**/**429-d₅** provided an intermolecular $k_{\text{H}}/k_{\text{D}}$ value of 1. This result indicated that the C–H functionalization (from intermediate **431** to product **430** in Scheme 181) is not the rds of this domino process. On the other hand, a high intramolecular KIE ($k_{\text{H}}/k_{\text{D}} = 2.8$) was obtained in the cyclization of **429-d₁**, indicating that the cyclization of **431** is incompatible with a $\text{S}_{\text{E}}\text{Ar}$ mechanism.²⁸² On the basis of the experimental results, proton abstraction via either σ -H bond metathesis **432** or formation of an agostic C–H intermediate **433** followed by acetate-mediated H-transfer, provided the best explanation for the C–H activation step.

Scheme 182



Scheme 183



Echavarren and co-workers studied the mechanism of intramolecular palladium-catalyzed arylation of arenes **434**. In these processes, the direct (Heck-like) insertion into the arene leading to **435**, the electrophilic aromatic substitution (S_EAr) via intermediates **436**, and even a σ -bond metathesis involving intermediates **437** were considered as possible alternatives for the evolution of the initially formed oxidative addition complex **438** (Scheme 182).²⁸³

The mechanism has been studied on a variety of bromobenzyl diarylmethane systems **439** (Scheme 183).²⁸⁴ Electron-withdrawing substituents favor the reaction on the substituted ring. Electronegative methoxy groups that are electron-releasing in electrophilic aromatic substitutions behave similarly to chlorine substituents, which indicates that the main effect of substituents in this reaction is inductive. Electron-releasing substituents drive the reaction toward the unsubstituted ring. These results together with the substantial intramolecular KIEs observed in the cyclization of labeled **439** ($k_H/k_D = 6.7$, 100 °C; $k_H/k_D = 5.0$, 135 °C) are incompatible with the S_EAr mechanism and, at the

same time, are consistent with the intramolecular KIEs observed in other related Pd(OAc) mediated cyclizations such as the arylation of bromides **440** ($k_H/k_D = 4.25$ –5.4) reported by Fagnou and co-workers (Scheme 183).²⁸⁵

All the experimental results would fit better in a mechanism where the hydrogen from the phenyl is transferred as a proton in the step deciding the selectivity. In fact, pronounced KIEs are compatible with mechanisms where C–H bond cleavage is occurring simultaneously with carbon–palladium bond formation.^{282a}

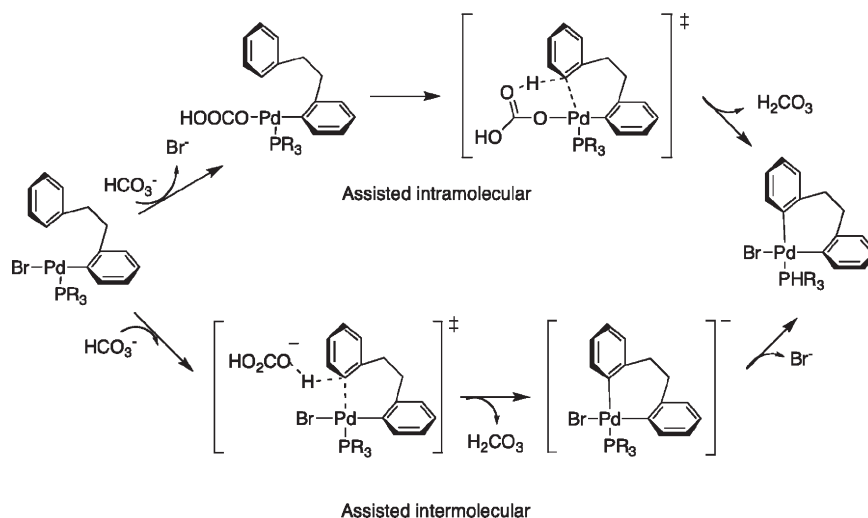
On the basis of DFT calculations, Echavarren and co-workers²⁸⁴ proposed that the key step is the abstraction of a proton from the aryl ring by carbonate, hydrogenocarbonate, or a related basic ligand present in the reaction medium (Scheme 184). Although the calculations reproduce well the experimental KIEs, both the inter- or intramolecular base-assisted versions are likely. As a recent study by the same group has pointed out, the nature of the substrate and the ligand could be determinant for the mechanism of the reaction, and for example, arylations carried out in the presence of bidentate phosphines²⁸⁶ such as dppm, dppe, dppf, and Xantphos proceed by an intermolecular proton abstraction.²⁸⁴ These proposals are also in agreement with Fagnou's results.

The mechanism of the efficient catalytic Pd *ortho*-arylation of free benzoic acids **441** with aryl chlorides was also studied by inter-/intramolecular KIEs, which in this case were found to have the same magnitude ($k_H/k_D = 4.4$) (Scheme 185).²⁸⁷ This result was close to those in Scheme 183 and pointed toward C–H bond breaking as the rds of the process. Given the magnitude of the KIE, the insensitivity of the reaction to electronic properties of benzoic acid, and the lack of selectivity in the monoarylation of 3-fluorobenzoic acid, the authors propose the mechanism in Scheme 185 as the most likely for the C–H bond cleavage. The sequence of events is similar to that proposed above^{284a} and consists of the reduction of Pd(II) to Pd(0), oxidative addition of aryl chloride to Pd(0) (facilitated by an electron-rich, bulky ligand), replacement of the halide in the coordination sphere of palladium by the benzoate, and rate-limiting C–H bond-cleavage step. The formation of an agostic complex **442** is favored by electron-rich C–H bonds, and the deprotonation step, on the other hand, may be more facile for more acidic protons allowing the arylation of electron-poor benzoic acids. As a consequence, it appears that the deprotonation of the agostic complex **442** is the overall rds. Finally, reductive elimination followed by fast ligand exchange affords the product.

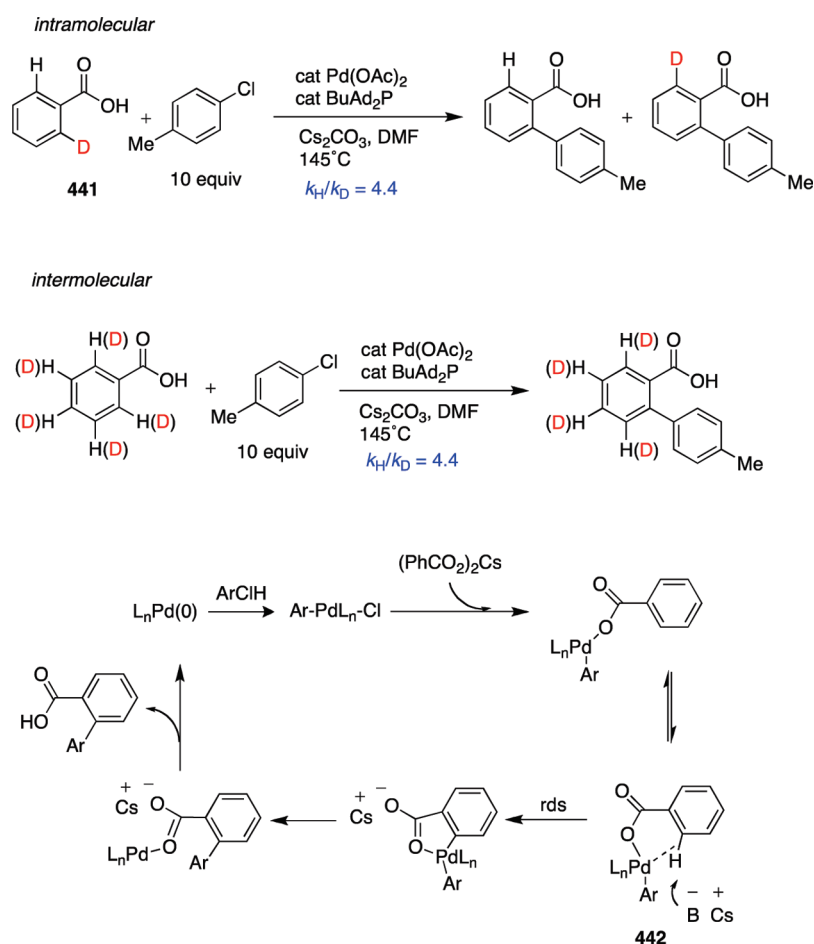
High KIEs were also measured in other palladium-mediated intermolecular arylation reactions, such as the arylation of perfluorobenzenes **443** ($k_H/k_D = 3.0$),²⁸⁸ or the direct arylation of completely unactivated arenes in the presence of pivalic acid as cocatalyst ($k_H/k_D = 5.5$) (Scheme 186).²⁸⁹ The experimental results and selectivities obtained in these studies are in line with those reported for concerted metalation-deprotonation mechanistic proposal, indicating that the base is directly involved in C–H bond cleaving, and that C–H acidity is an important reaction parameter to be considered. The proposals have been examined by DFT calculations.²⁸⁸

The Heck-type reactions of mono and bicyclic heteroarenes have been a subject of interest for several research groups, and different mechanisms were proposed depending on substitution patterns and reaction conditions. Fagnou and co-workers²⁹⁰ reported the efficient arylation of a series of electron-rich heteroarenes with Pd(OAc)₂ in the presence of pivalic acid,

Scheme 184



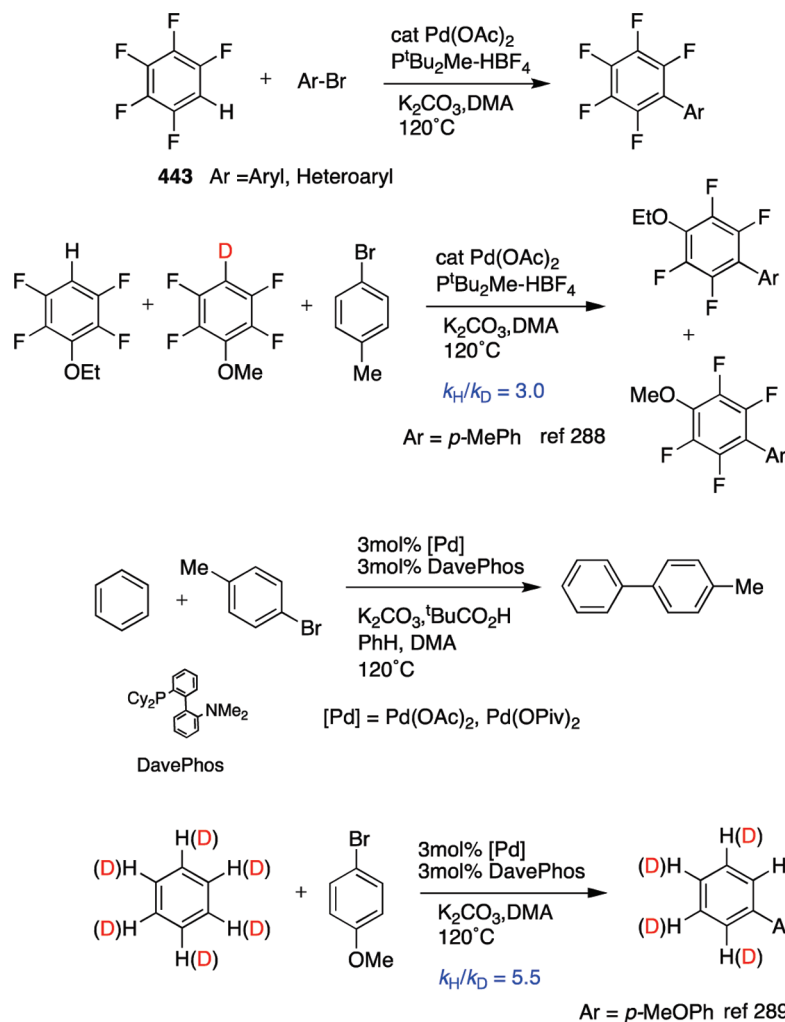
Scheme 185



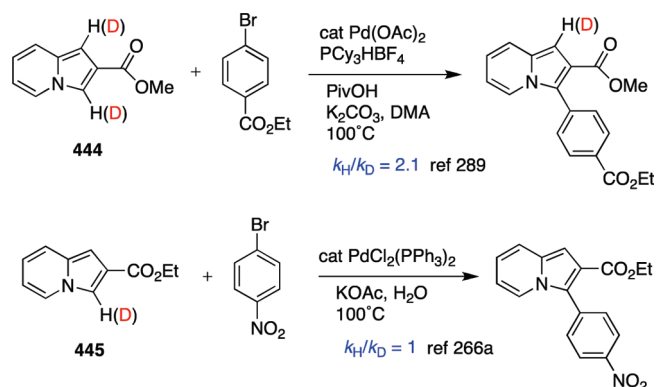
and Gevorgyan and co-workers studied the arylation/heteroarylation of substituted indolizines with PdCl₂(PPh₃)₂.^{267a} Surprisingly, in these studies, the kinetic isotope experiments led to contradictory conclusions about the reaction mechanism.

Thus, whereas Fagnou found a clear primary KIE ($k_H/k_D = 2.1$) in the arylation of unlabeled/labeled indolizines **444**, Gevorgyan reported the absence of KIEs in the arylation of the analogous indolizine **445**. The KIE value observed for

Scheme 186

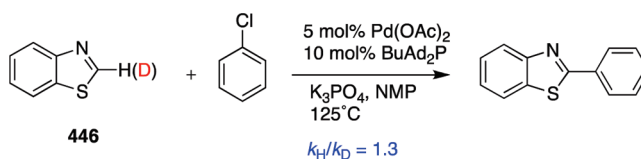


Scheme 187



444 was interpreted as evidence for a mechanism involving a concerted metalation–deprotonation, whereas the lack of KIE obtained in the coupling of **445** was believed to support an electrophilic substitution mechanism, analogous to that earlier proposed for the arylation of thiazoles and imidazoles (Scheme 187).²⁹¹

Scheme 188

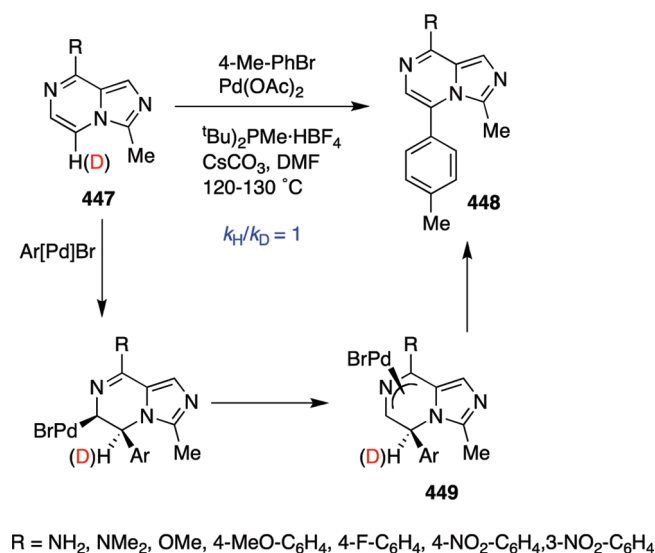


The electrophilic substitution mechanism was also considered the best alternative to explain the arylation of different electron-rich mono- and bicyclic heterocycles with aryl chlorides.^{267b} In this study, the deuterium KIE for the arylation of benzothiazole **446** was found to be $k_{\text{H}}/k_{\text{D}} = 1.3$ (Scheme 188).

However, the absence of a KIE together with the lack of electronic effects were clues to propose a Heck-like mechanism for the efficient synthesis of 5-aryl imidazo[1,5-*a*]pyrazines **448** by palladium-catalyzed coupling of the corresponding 8-substituted derivatives **447** with aryl halides.²⁹² The lack of electronic effects on the reactivity ruled out an electrophilic palladation mechanism, frequently suggested to rationalize arylations of this type. Additionally, the lack of a primary KIE is

inconsistent with C–H oxidative addition, proton abstraction, or σ -bond metathesis. In addition, an electrophilic substitution mechanism, which would be expected to give an *inverse* secondary KIE, is ruled out. The results are consistent with a Heck-type mechanism consisting of rate-determining carbopalladation followed by formation of an unprecedented π -azaallyl intermediate **449** and rapid reductive elimination to product **448** (Scheme 189).

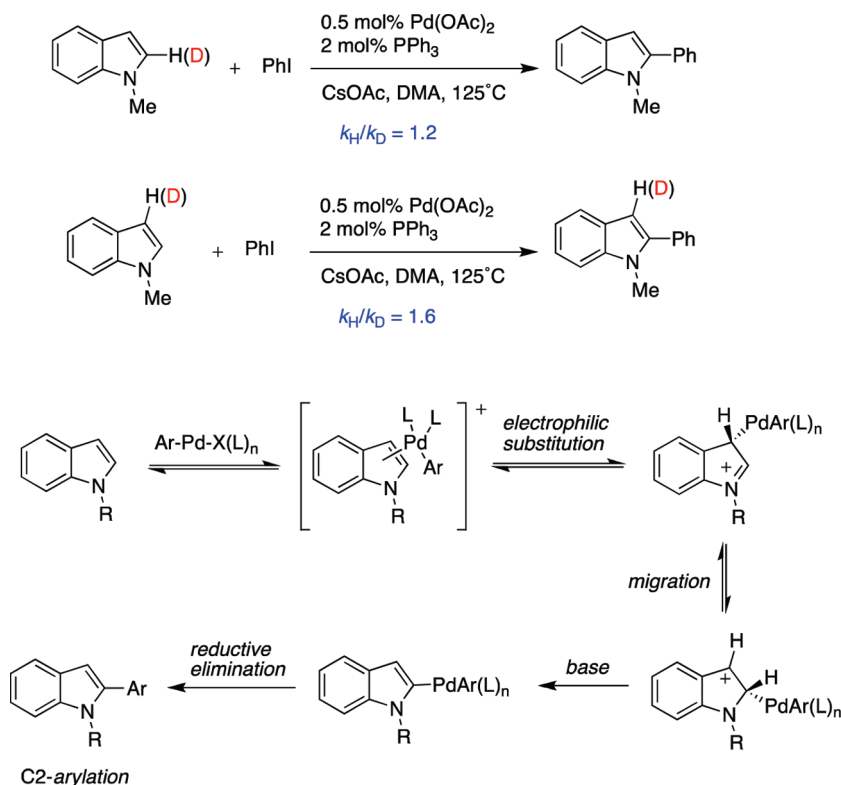
Scheme 189



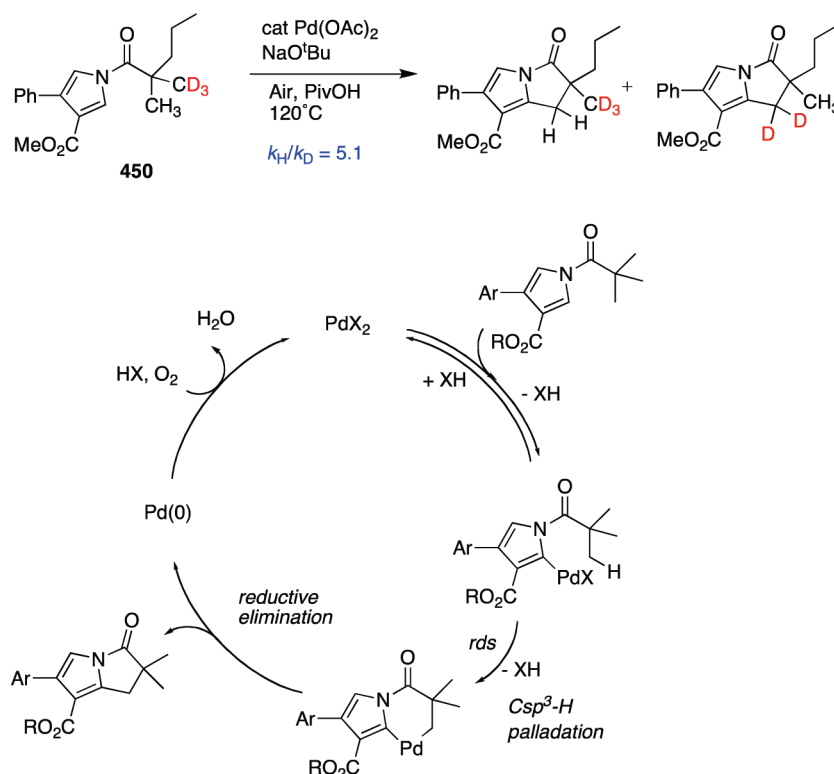
The mechanism of palladium-catalyzed arylation of indoles and the C2 selectivity of the reaction were studied by determining the KIEs for both C2- and C3-positions of indole (Scheme 190).²⁹³ The larger KIE value ($k_{\text{H}}/k_{\text{D}} = 1.6$) was obtained for the C3-position, where the substitution does not occur, and thereby represents a secondary KIE. The $k_{\text{H}}/k_{\text{D}} = 1.2$ obtained for C2 (apparent primary KIE) is too small for this bond to be broken in the slow step of the reaction. These kinetic studies, together with the Hammett plot, support an electrophilic substitution mechanism that features a 1,2-migration of palladium. The electrophilic attack of the arylpalladium species on indole and (or) the migration of palladium represent the slow step(s) of the catalytic cycle. This mechanism has a close parallel in classical electrophilic substitution reactions of indoles substituted in the C3-position.

Metal-mediated C–C bond formation occurring at sp^2 C–H bonds are more prevalent and widespread than those at C(sp^3)–H bonds. A recent example is the intramolecular palladium-catalyzed Csp^2 – Csp^3 bond formation between an azole ring and an unactivated methyl substituent, employing air as the terminal oxidant.²⁹⁴ The reaction with labeled pyrrole **450** showed a large primary KIE ($k_{\text{H}}/k_{\text{D}} = 5.1$) at the methyl group, consistent with a reversible pyrrole palladation–proto-(deuterio)depalladation step that is followed by an irreversible alkane C–H bond-cleavage step, leading to product formation (Scheme 191). Considering this proposal, the regioselectivity and reactivity with respect to the pyrrole moiety may be governed not by the ability of the catalyst to induce selective C–H bond cleavage but by the persistence of one of the aryl–palladium intermediates, allowing a slower aliphatic C–H bond cleavage to occur.

Scheme 190



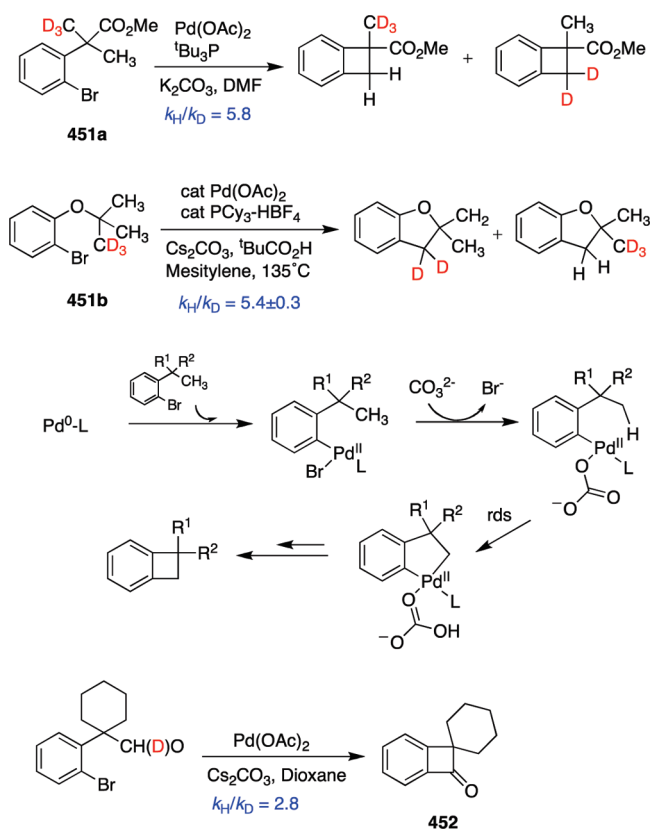
Scheme 191



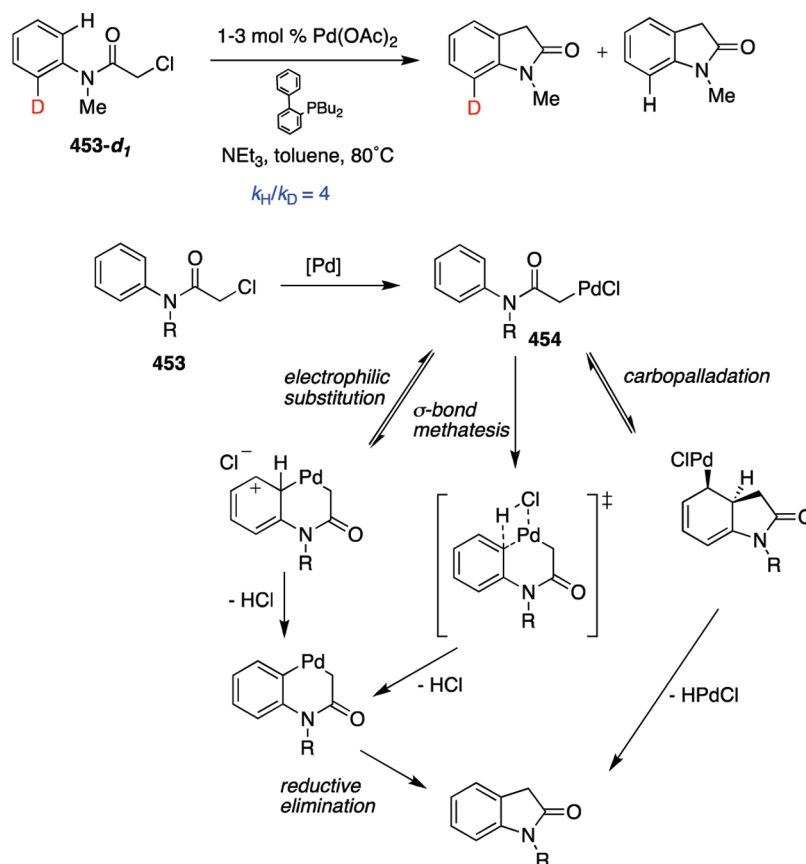
Other $\text{Csp}^2\text{--Csp}^3$ couplings have been reported in the efficient synthesis of benzocyclobutenes from the aryl derivatives **451a**²⁹⁵ and the preparation of 2,2-dialkyldihydrobenzofurans from aryl ethers **451b**.²⁹⁶ The determination of primary intramolecular isotope effects on these substrates resulted in high KIEs at the methyl groups ($k_H/k_D = 5.8$ and $k_H/k_D = 5.4$, respectively), in agreement with $\text{Csp}^3\text{--H}$ activation being the *rds*. The experimental data were rationalized by DFT calculations that supported a process involving oxidative addition, ligand exchange, and rate-determining C--H activation by ligand (base) proton abstraction as the key steps (Scheme 192). Also a primary KIE value ($k_H/k_D = 2.8$) was consistent with a mechanism based on C--H bond functionalization for the intramolecular acylation of aryl bromides to benzocyclobutanones **452**.²⁹⁷

Hennessy and Buchwald reported the synthesis of substituted oxindoles from α -chloroacetanilides **453**.²⁹⁸ To probe the mechanism of this transformation, they conducted inter-/intramolecular experiments with isotopically labeled substrates (Scheme 193). No KIE was observed in the competitive reaction of *N*-methyl chloroacetanilide and the corresponding pentadeuterated substrate. However, an intramolecular primary KIE ($k_H/k_D = 4$) was observed in the cyclization of the *ortho*-monodeuterated substrate **453-d₁**. On the basis of these findings, the authors propose a process most likely initiated by oxidative addition of the α -chloroamide to Pd(0) , resulting in a Pd(II) enolate **454**. The formation of the C--C bond may proceed by an electrophilic aromatic substitution to give a six-membered palladacycle, by carbopalladation of the aromatic ring followed by anti-elimination of HPdCl , or even by σ -bond metathesis. The observed intramolecular KIE implies that either palladation

Scheme 192



Scheme 193



process would be reversible and rapid relative to C–H bond cleavage.

8. CYCLOISOMERIZATIONS: DIENES, ENYNES, ENEDIINES

The interest in the study of the mechanisms of metal-mediated cycloisomerizations of dienes and enynes relies on their wide synthetic applications. These processes take place with a large number of transition metal complexes, generate a great diversity of compounds, and, in consequence, the understanding of their mechanistic insights would lead them to control the selectivity of the products formed. Dienes are less reactive toward transition metals than enynes but, in the presence of the appropriate catalyst, 1,6-dienes afford cyclopentenes with structures **I**, **II**, or **III** depending on the metal complex (Pd, Pt, Ru, Rh, Ni), and the reaction conditions (Scheme 194). Of the three types of products, most catalysts generate **I** and/or **III**. Catalysts for the selective generation of **II** are less common and all are based on Pd.²⁹⁹

The preliminary work in the mechanisms of metal-mediated carbocyclizations was performed by Grigg et al.,³⁰⁰ but the extensive studies by Lloyd-Jones's^{4b,301} and Widenhoefer's groups³⁰² have definitively shed light into the mechanisms of the reactions. Most of the mechanistic investigations to date have been based on deuterium labeling, crossover experiments, and the detection of intermediates. Hence, the kinetic isotope studies reported are scarce.

Widenhoefer's group studied the mechanism of the cycloisomerization of dimethyl diallylmalonate **455** catalyzed by the cationic palladium phenanthroline complex **456**. Heating a solution of **455** and **456** (5 mol %) in dichloroethane at 40 °C led to the formation of a 27:2.2:1.0 mixture of cyclopentenes **457**, **458**, and **459**. Cyclopentenes **457** and **458** were formed both kinetically and via secondary isomerization of **459**. Extensive labeling and crossover experiments, and the lack of KIEs in the cycloisomerization of **455-2,6-d₂** and **455-3,3,5,5-d₄** (Scheme 195), were consistent with a mechanism involving hydrometalation of a C=C bond, intramolecular carbometallation, isomerization via reversible β -hydride elimination/addition, and turnover-limiting displacement of the cyclopentenes from palladium (Scheme 196).³⁰³

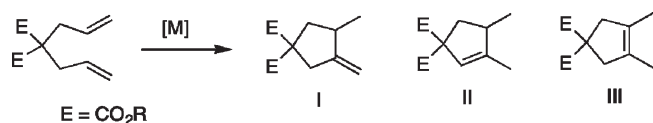
Thus, by coordination of the catalyst to the alkene and β -migratory insertion into the Pd–H bond, intermediate **460** would be formed. Coordination of the pendant olefin in complex **460** followed by β -migratory insertion would form the palladium cyclopentylmethyl complexes **461** and **462**. The high trans selectivity in the carbocyclization step is one of the keys of the process and explains the formation of cyclopentene **458** as a secondary product in the reaction. By a sequence of reversible β -hydride eliminations/additions, a mixture of complexes **461**, **463**, and **464** could be formed. Primary KIEs ($k_H/k_D = 2.5–3$) are expected for rate-limiting C–H bond scission in β -hydride eliminations of alkyl or alkoxy groups,^{234,237,243,253,254,304} while rapid and reversible C–H bond scission followed by rate-limiting dissociation of the unsaturated fragment should lead to a

negligible KIE.^{245,305} This latter alternative is more consistent with the experimental results.

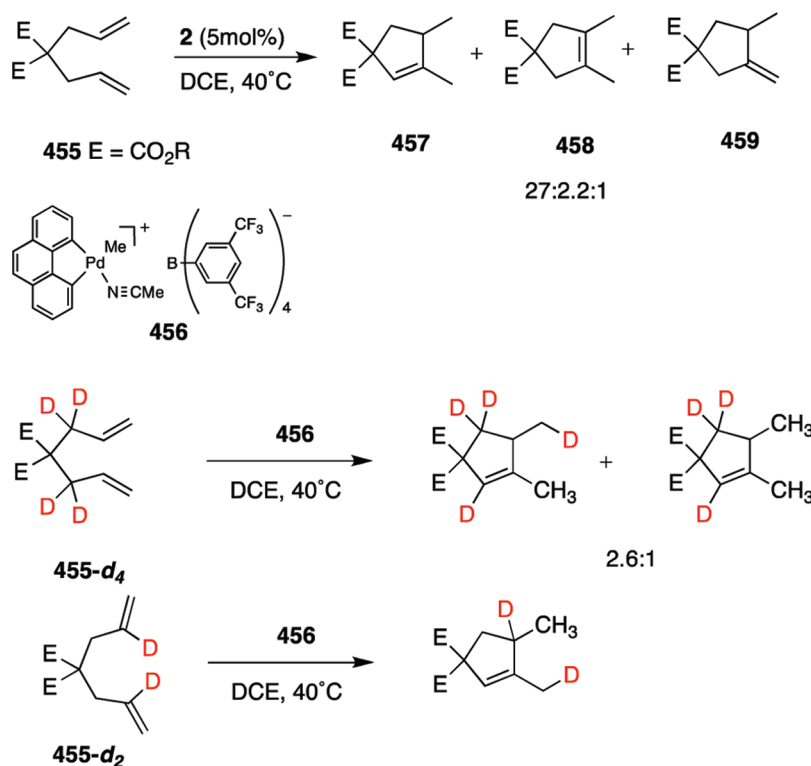
In the case of bisdienes, the cycloisomerization with Pd(II) catalysts yields enedienes with high *trans* selectivity (Scheme 197).³⁰⁶ Deuterium labeling experiments carried out with enedienne **465** in the presence of CD₃OD and KIE studies with labeled substrates **466a–b** provided valuable mechanistic information. Labeled **466a–b** did not form deuterated enedienes analogous to **467**, suggesting a mechanism in which the hydrogen is not transferred intramolecularly. Instead, the reaction with bisdienes **466** yielded compounds **468–469** exhibiting a large deuterium KIE ($k_{\text{H}}/k_{\text{D}} > 5$) for the step involving loss of the hydrogen. Hydrogen can be lost from either methyl substituent (R^1 or R^2), but there must be a small inherent preference for loss of hydrogen from the substituent labeled R^2 , which is superimposed on the isotope effect to account for the higher selectivity for the formation of **468** from **467b** than **467a**.

The proposed sequence of events is shown in Scheme 198. The incorporation of the label observed in **467** should occur during the protonation of intermediate **470** ($\text{S}_{\text{E}}2'$ deuteration). The large KIE observed for the **470**-to-**471** transformation step is not fully in agreement with a β -hydride elimination (typical KIEs $\approx 2.5\text{--}3$),^{235,238,243,253,254,304} and a base-promoted deprotonation is proposed instead.

Scheme 194



Scheme 195

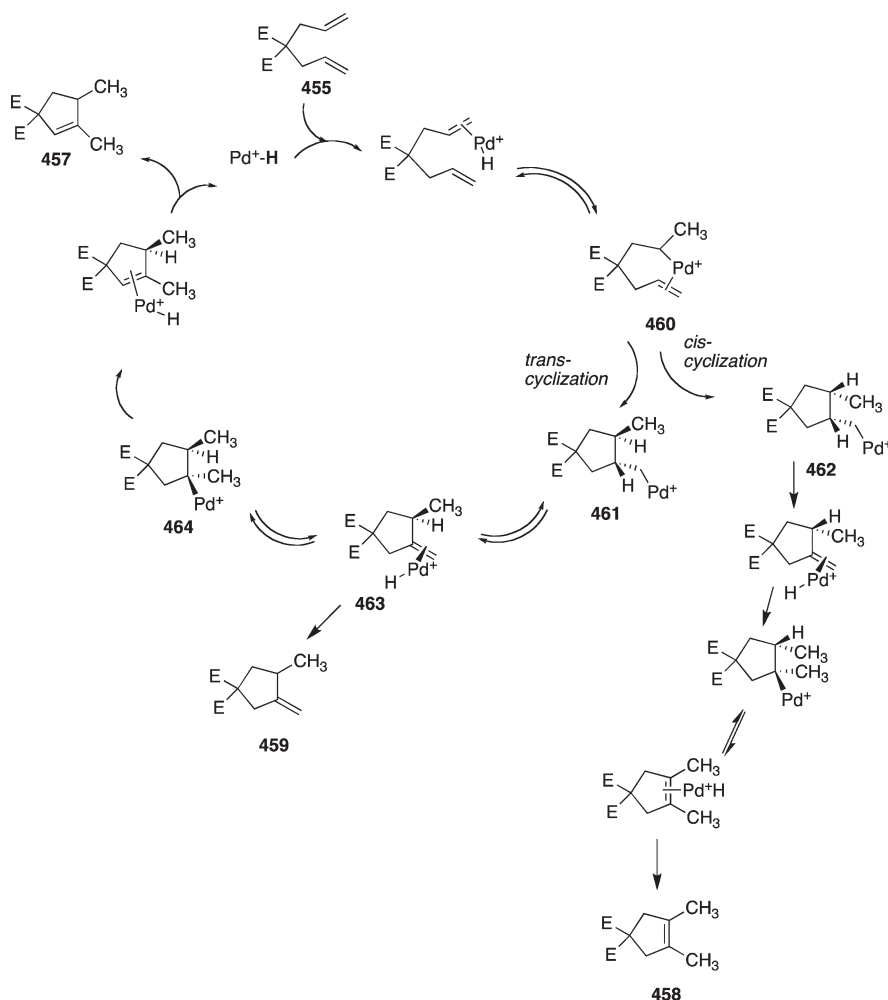


The transition metal cyclization of 1,*n*-enynes is a powerful strategy for the synthesis of functionalized cyclic molecules. Starting from rather simple substrates and under experimentally simple conditions, a great diversity of products can be obtained, from five-membered dienes to bicycloalkenes and six-membered compounds (Scheme 199). The subject has been the focus of several research groups, and excellent reviews, which compile the different aspects of the advances in these cyclizations, have been published.³⁰⁷

Cyclizations of 1,*n*-enynes have been achieved with a wide range of transition metal complexes either in a catalytic or in a stoichiometric manner. A recent report by Toste, Houk, and co-workers³⁰⁸ reported an experimental-computational study of Au(I)-catalyzed rearrangement of allenynes to cross-conjugated trienes. Kinetic isotope experiments performed with substrates **472** and **473** indicated essentially identical KIEs ($k_{\text{CD}_3}/k_{\text{CH}_3} = 1.89 \pm 0.02$ and $k_{\text{H}}/k_{\text{D}} = 1.84 \pm 0.15$), suggesting that the formal 1,5-sigmatropic shift is responsible for the measured values (Scheme 200). Among the several alternatives studied computationally, a mechanism involving nucleophilic addition of an allene double bond to a phosphine–gold-complexed phosphine–gold acetylide is more likely than oxidative cyclization or simple nucleophilic addition to phosphine–gold-complexed substrate. The computed KIE values of the proposed mechanism were in excellent agreement with those experimentally observed.

Toste and co-workers also studied the Au(I)-catalyzed sequential cycloisomerization/ sp^3 C–H bond functionalization of 1,5-enynes **474** and 1,4-enallenes **475** to provide tetracyclododecane and tetracyclotridecane derivatives **477**, respectively.³⁰⁹ The process was believed to occur by initial complexation of the cationic Au(I) complex to the alkyne or allene moiety and intramolecular addition of the alkene, leading to key cationic stabilized Au(I)

Scheme 196



carbene intermediate **476** that underwent a sp^3 C–H bond insertion to generate the tetracyclic products (Scheme 201).

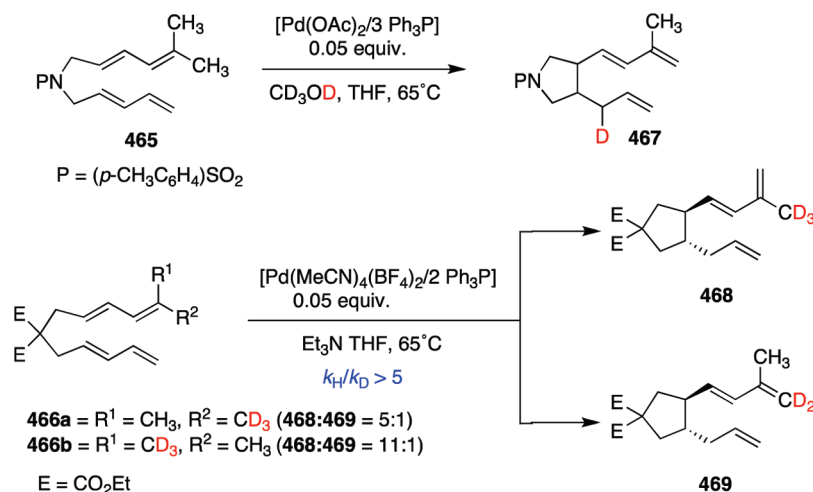
To obtain experimental evidence for the C–H insertion step, a series of inter- and intramolecular KIE experiments were designed (Scheme 202).³⁰⁹ In all cases, small *normal* or *inverse* KIEs were observed. Particularly relevant were the *inverse* KIEs obtained in the intramolecular KIE experiments carried out with labeled enyne **478** and allene **479** because, in both cases, the cationic gold intermediate-formed **480** necessarily requires a C–H or C–D bond-cleavage step. Intramolecular C–H insertion reactions of metal–carbenoid complexes typically exhibit primary KIEs ($k_H/k_D = 1.1–3.1$),³¹⁰ which was inconsistent with the experimental values. Thus, the measured *inverse* KIEs for the C–H insertion suggest that a mechanism different from a simple hydride-to-carbocation-like intermediate is operative in this case. As the isotope effects require that the transition state for hydride transfer have larger force constants for the C–H bond than for cationic intermediate **480**, formation of a σ -complex between the hydrogen atom and cationic Au(I) preceding the C–H activation may account for the experimental results.¹¹

The mechanism of the C2–C6 (Schmitt)/ene cyclization of enyne–allenes was studied by a combination of KIEs, theoretical calculations, and dynamics trajectories.³¹¹ The KIE observed for the cyclization of allenol acetate **481** ($k_H/k_D \approx 1.43$) is too large

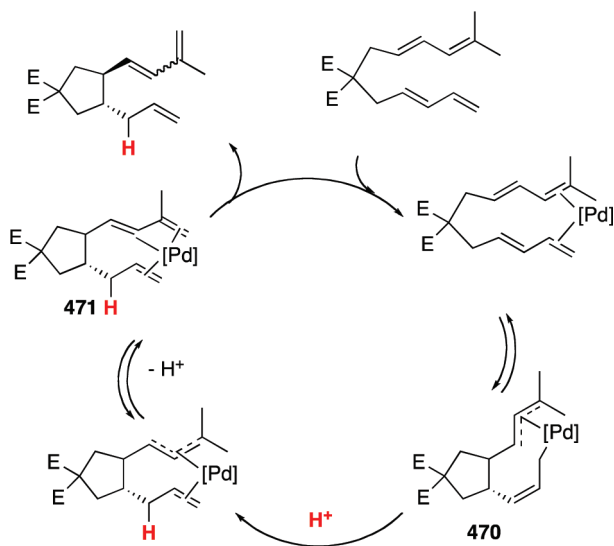
for a secondary KIE that would support a diradical intermediate **482**. However, this value is also too small for the primary KIE expected for a concerted ene reaction. DFT calculations predict a theoretical $k_H/k_D = 1.54$, roughly consistent with the experimental value and based on a highly asynchronous ene transition state **483**, in which hydrogen transfer has progressed to a minimal extent (Scheme 203).

Chatani and co-workers reported a study of the cycloisomerization of 1-alkyl-2-ethynylbenzenes in the presence of $PtCl_2$, $PtCl_4$, and $[RuCl_2(CO)_3]_2$ as catalysts.³¹² A mechanistic study based on kinetic isotope effects revealed an intermolecular KIE of $k_H/k_D = 1.1$ for the alkynic hydrogen and an intramolecular KIE of $k_H/k_D = 1.9$ for the benzylic hydrogen. On the basis of these experiments, labeling studies, and substituent effects, the authors proposed a mechanism involving an alkyne 1,2-hydrogen shift to form a vinylidene intermediate followed by a 1,5-shift of the benzylic hydrogen. The transference of the benzylic hydrogen as a hydride to the most electrophilic vinylidene α -carbon results in the formation of a benzyl cation intermediate, which will finally lead to the indene product as shown in Scheme 204. Although the observed KIE was relatively small, all of the experimental data can be rationalized with certainty by assuming the 1,5-hydride shift as the rds of this catalytic cycloisomerization. The possible concerted benzylic hydrogen shift was discarded by the

Scheme 197



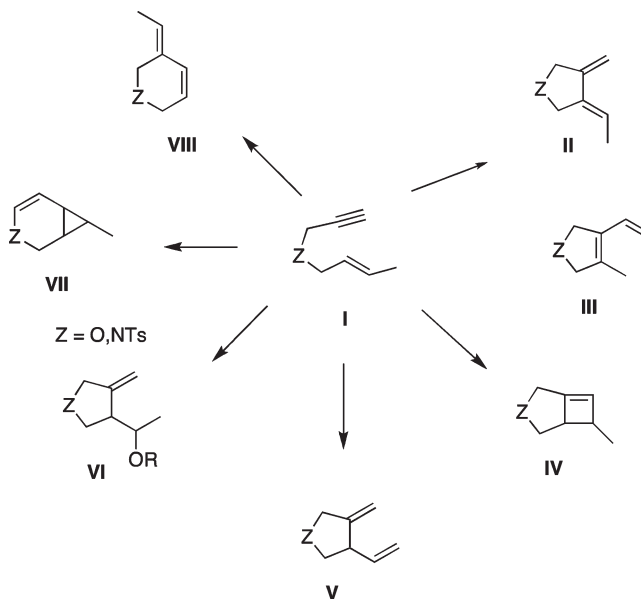
Scheme 198



racemization observed when the reaction was carried out with a chiral substrate.

To delineate the mechanism of the preparation of 2,3-substituted quinolines from diallylanilines **484** and $\text{Co}_2(\text{CO})_8$ as catalyst, isotopic labeling experiments and steric and electronic effects studies were performed.³¹³ Steric effects predominate over electronic effects, and electron-withdrawing groups inhibit the reaction. An experiment carried out with a 1:1 mixture of **484-*d*₀**/**484-*d*₅** showed a large KIE ($k_{\text{H}}/k_{\text{D}} = 5.4 \pm 0.1$), indicating that the cleavage of the *ortho*-aryl C–H/C–D bond occurs during (or before) the rds and very likely must be one of the first steps in the reaction sequence. Although the complex mechanism proposed by the authors is speculative, the KIE experiments point to the initial cleavage of the *o*-aryl C–H bond, which might be assisted by coordination of a $\text{Co}_2(\text{CO})_7$ fragment to the nitrogen. The reaction is favored carrying the process under CO atmosphere, which helps the generation of a vacant coordination site in the $\text{Co}_2(\text{CO})_8$ by the loss of a labile CO ligand (Scheme 205).

Scheme 199



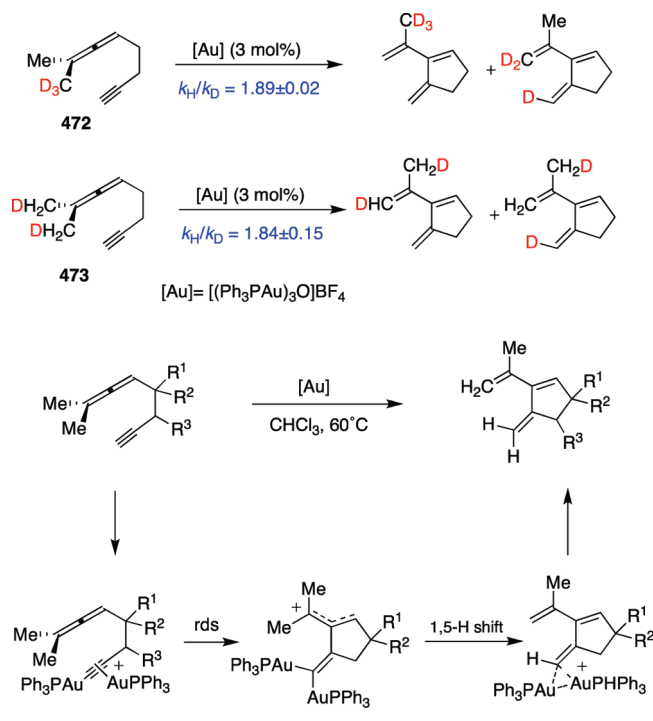
9. KIES IN THE STUDY OF TRANSITION METAL-MEDIATED CYCLOADDITIONS³¹⁴ AND SIGMATROPIC SHIFTS

The mechanisms of transition metal-mediated cycloadditions have been established mainly by deuterium labeling experiments, capture of intermediates, and theoretical calculations, and hence, the references of KIE studies are scarce.

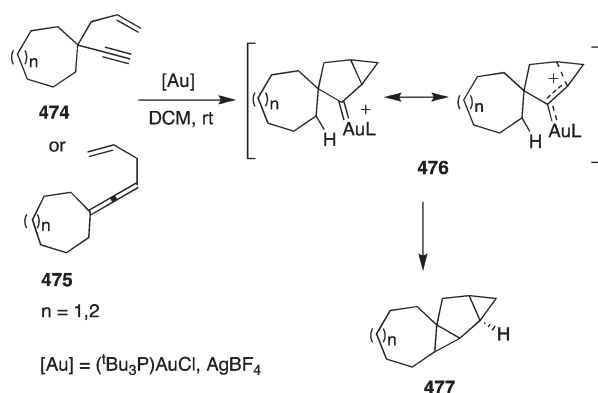
9.1. [*n* + *m*]-Cycloadditions

9.1.1. [2 + 1]-Cycloadditions³¹⁵. The mechanism of the copper-catalyzed cyclopropanation of alkenes with diazo compounds has been studied by experimental (Hammett, deuterium labeling, and isotope effects) and computational methods to determine the nature of the step that controls the stereochemistry of the reaction and the participation of a metallacyclobutane intermediate in the process.³¹⁶ The KIE value obtained in the cyclopropanation of β -deuterated styrene **485** indicated that the β -carbon was somewhat rehybridized in the transition state

Scheme 200



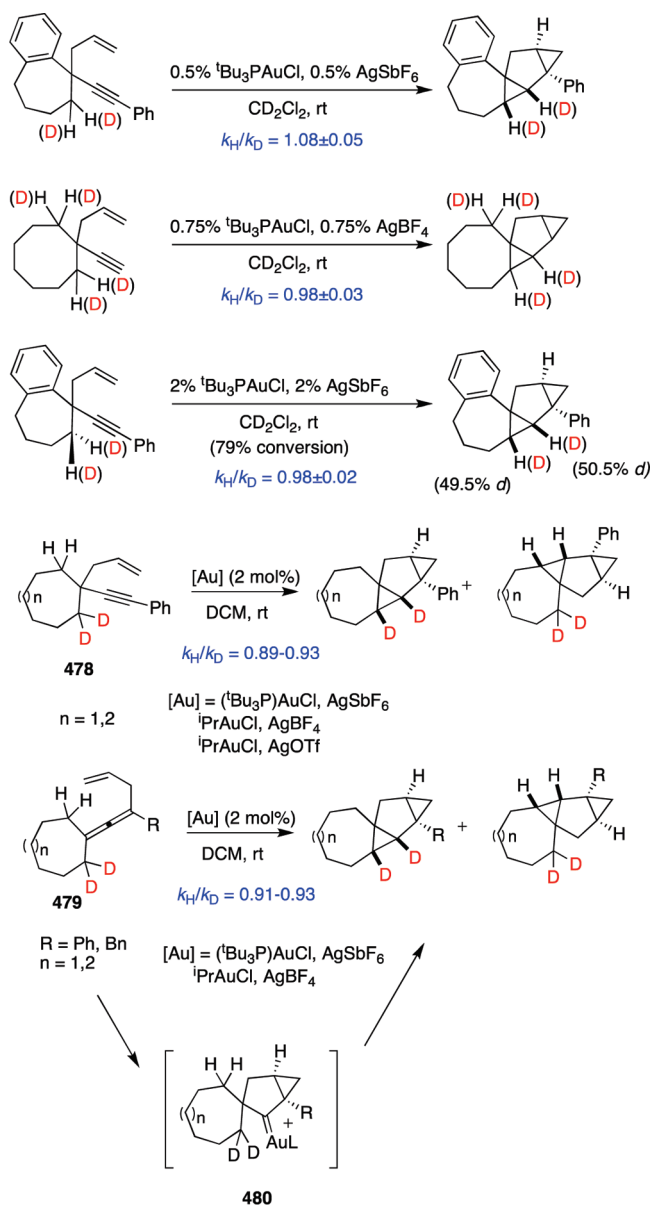
Scheme 201



($k_{\text{H}}/k_{\text{D}} = 0.95$ per deuterium). This data, together with the negligible isotope effect observed in the α -deuterated styrene **486** ($k_{\text{H}}/k_{\text{D}} = 1.02$) were consistent with a concerted but very asynchronous addition of the metallacarbene to the alkene (Scheme 206). For styrene substrates, the bond to the β -carbon is formed early in the reaction, with final ring closure to the cyclopropane product occurring late, but still in a concerted manner, as in transition state **487**. Experimental and computational data indicated that the formation of a metallacyclobutane intermediate by a $[2 + 2]$ -addition is kinetically disfavored.

Using the reaction of styrene with methyl phenyldiazoacetate and ethyl diazoacetate as a model, Singleton and co-workers have combined experimental ^{13}C KIEs and DFT calculations to study the mechanism of $\text{Rh}_2(\text{L})_4$ -catalyzed cyclopropanation of alkenes (Scheme 207).³¹⁷ The ^{13}C KIEs for this reaction were determined from analysis of recovered styrene by natural

Scheme 202

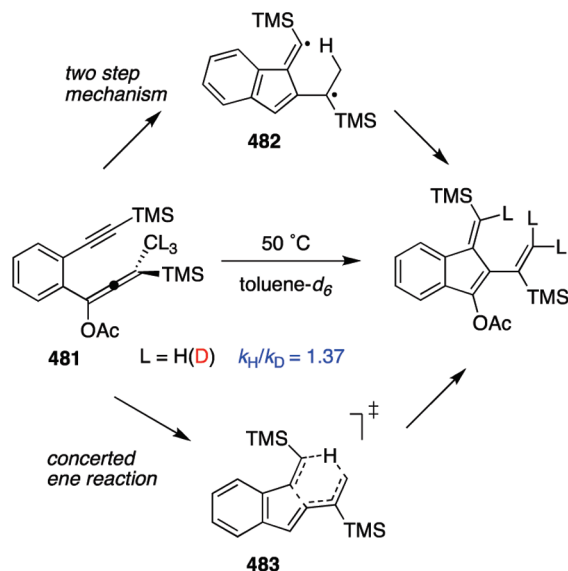


abundance NMR measurements.¹⁰⁹ The reaction of styrene and methyl phenyldiazoacetate catalyzed by $\text{Rh}_2(\text{octanoate})_4$ exhibited a substantial ^{13}C KIE at the terminal olefinic carbon (1.024), a smaller but consistently significant KIE at the internal olefinic carbon (1.003–1.004), and small or negligible KIEs at the aromatic ring carbons. These results suggest substantial bond formation to the terminal carbon in a highly asynchronous cyclopropanation transition state. The similar ^{13}C isotope effects observed for the same reaction catalyzed by the bulky bisrhodium tetrakis[(*S*)-*N*-(dodecylbenzenesulfonyl)proline] ($\text{Rh}_2(\text{S-DOSP})_4$) suggest that the chiral catalyst engages in a very similar cyclopropanation transition-state geometry in both cases. However, cyclopropanation of styrene with $(\text{Rh}_2(\text{S-DOSP})_4)$ and ethyl diazoacetate showed a much smaller ^{13}C KIE at the terminal olefinic carbon (1.012–1.015). Because the reactions of both methyl phenyldiazoacetate and ethyl diazoacetate are highly exothermic (and hence, both should have a relatively early

transition state), the ^{13}C KIEs would be qualitatively interpreted as implying a significantly earlier transition state with the first of the two azo-compounds.

These experimental results were nicely supported by DFT calculations that predicted a reaction pathway involving complexation of the diazoesters to rhodium, loss of N_2 to afford a rhodium carbenoid, and an asynchronous but concerted cyclopropanation transition state. The theoretical studies not only were in agreement with the measured ^{13}C KIEs but also

Scheme 203

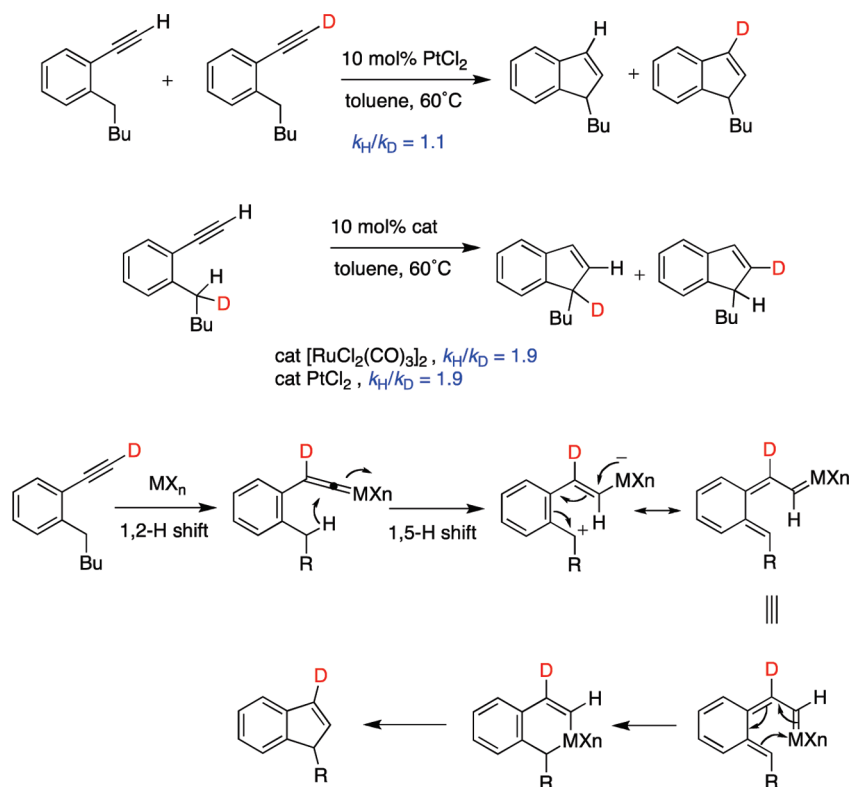


discarded other mechanistic alternatives, including stepwise cyclopropanations and mechanisms not involving discrete rhodium carbenoids, that could not be excluded only with the experimental KIE values. The calculations also allow interpretation of the nature of alkene selectivity and diastereoselectivity effects.

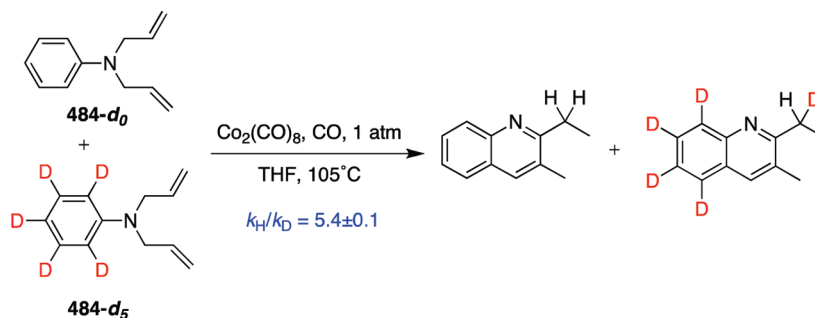
The same experimental and theoretical combination methodology was used in the study of the mechanism of the $\text{Rh}_2(\text{OAc})(\text{DPTI})_3$ -catalyzed cyclopropanation of alkynes (DPTI = diphenyltriflylimidazolidinone), particularly focusing on the involvement of tribridged or tetrabridged rhodium structures in the process (Scheme 208).³¹⁸ The experimental ^{13}C KIEs for cyclopropanations of 1-pentyne or 1-hexyne with ethyl diazoacetate catalyzed by $\text{Rh}_2(\text{OAc})(\text{DPTI})_3$ **488** (0.2 mol %) or $\text{Rh}_2(\text{OAc})_4$ (0.1 mol %) at 25°C indicated significant *normal* KIEs for the terminal acetylenic carbon (slightly larger for $\text{Rh}_2(\text{OAc})_4$ than for $\text{Rh}_2(\text{OAc})(\text{DPTI})_3$) but only a slight effect for the internal acetylenic carbon. KIEs at C3 were negligible. These KIE values qualitatively suggest an early, asynchronous transition state in which bond formation to the terminal carbon is proceeding, but with little bond formation occurring at the internal acetylenic carbon. Additionally, the similarity of KIEs for the two catalysts suggests analogous mechanisms in both cases. The experimental conclusions were confirmed by DFT calculations, which were entirely consistent with the conventional cyclopropanation through intact tetrabridged rhodium carbenoids and discarded the $[2+2]$ -cycloaddition mechanism. On the basis of the theoretical data, the authors suggest an explanation for the enantioselectivity of the reaction with DPTI ligands.

By means of secondary KIEs, Kodadek, Woo, and co-workers³¹⁹ proved that iron porphyrin complexes are active catalysts for the cyclopropanation of alkenes by ethyl

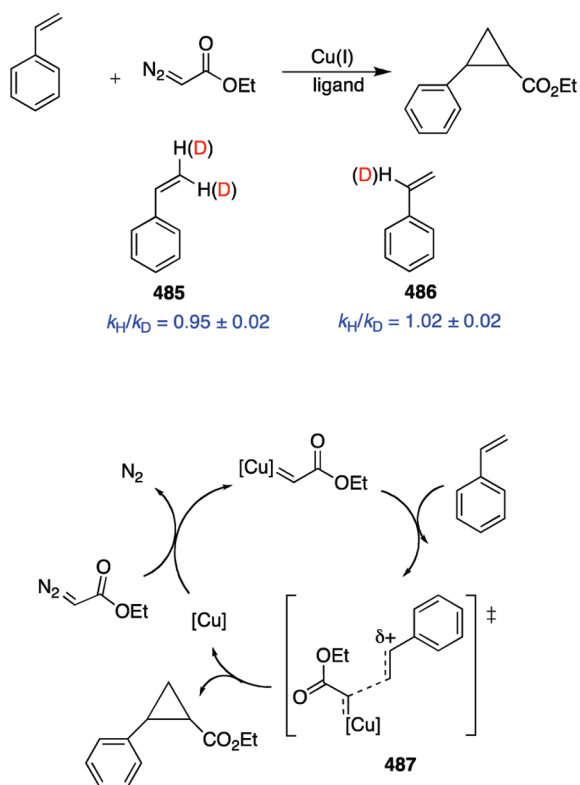
Scheme 204



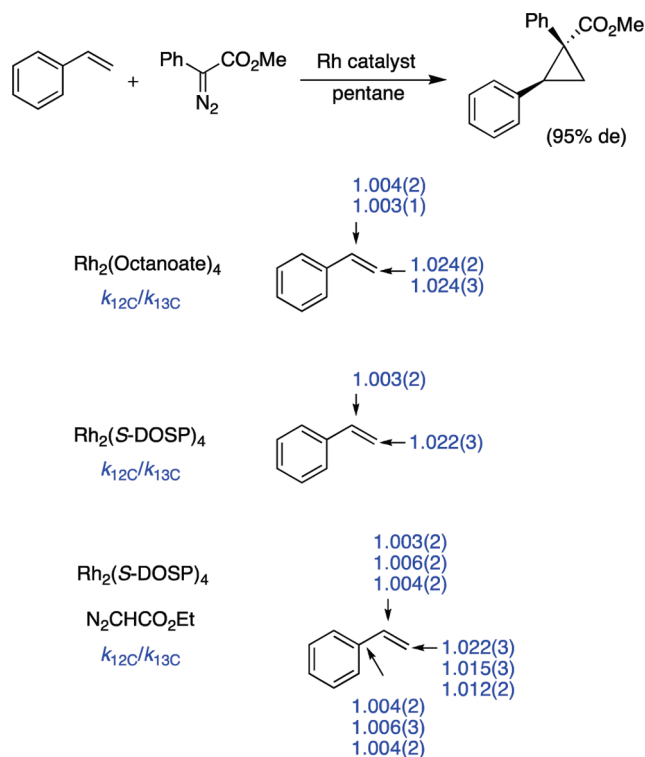
Scheme 205



Scheme 206



Scheme 207



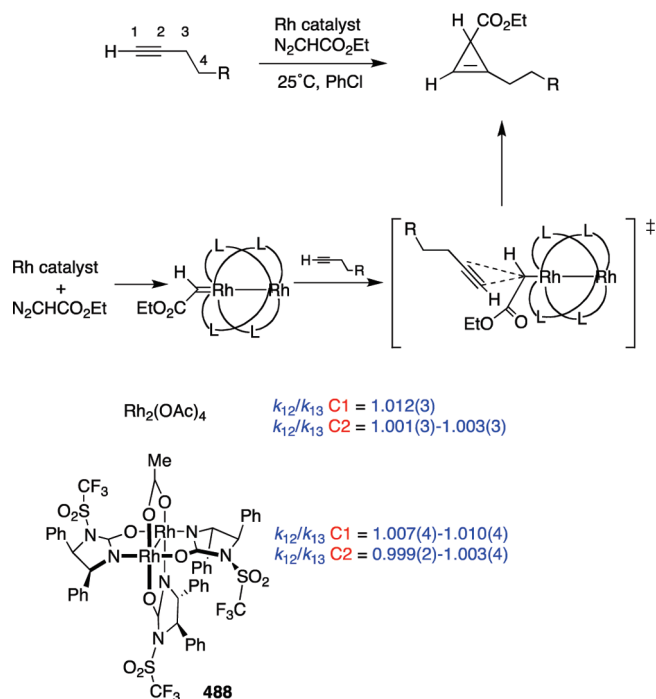
diazoacetate. The nature of the transition state of the iron-mediated cyclopropanation was determined in a competitive reaction between styrene- d_0 and styrene- d_8 using $\text{Fe}(\text{PFP})\text{Cl}$ (PFP = *meso*-tetrakis(pentafluorophenyl)porphyrin) as the catalyst. A modest, but significant, *inverse* KIE ($k_{\text{H}}/k_{\text{D}} = 0.87 \pm 0.07$) was observed, indicating that there is some rehybridization of the olefin in the transition state of the iron-mediated reaction, and pointing to a more productlike transition state than that of the rhodium-mediated reactions (Scheme 209).³²⁰

A recent study demonstrated this latter point, showing also the effect of an axial ligand in the iron porphyrin on the nature of the transition state³²¹ by examining the $k_{\text{H}}/k_{\text{D}}$ values obtained with and without axial ligand in styrene cyclopropanation catalyzed by $\text{Fe}(\text{II})$ porphyrin 489. An *inverse* secondary KIE ($k_{\text{H}}/k_{\text{D}} = 0.87 \pm 0.01$) was observed in the absence of axial ligand. Interestingly,

the KIE value was lowered to $k_{\text{H}}/k_{\text{D}} = 0.81 \pm 0.01$ in the presence of methylimidazole (MeIm). This result indicated that a higher degree of rehybridization from sp^2 to sp^3 of styrene in the transition state occurred in the case of adding an axial ligand. The difference between $k_{\text{H}}/k_{\text{D}} = 0.87$ and $k_{\text{H}}/k_{\text{D}} = 0.81$ is significant enough to indicate the direction of the shift of transition state toward the product side. In other words, a more productlike transition is developed in the presence of axial ligand. This mechanistically explains the improvements of trans/cis ratio in cyclopropanation of styrenes upon adding axial ligands.

9.1.2. [2 + 2]-Cycloadditions. Ti(IV) oxo complex 490 reacts with terminal alkynes to form oxametallacyclobutenes 491 in a [2 + 2]-process.³²² After thermolysis, compounds 491 efficiently rearrange to the corresponding hydroxoacetylide complexes 492. To investigate the mechanism of the oxametallacycle-to-hydroxoacetylide rearrangement, deuterium KIEs were

Scheme 208



measured at 101°C for the reaction with labeled and unlabeled oxametallacyclobutene **491** ($\text{R}^1 = \text{Ph}$, $\text{R}^2 = \text{H}$, D) (Scheme 210). The EIE ($k_{\text{H}}/k_{\text{D}} = 0.781 \pm 0.014$) is consistent with the conventional prediction that the deuterium should favor a location at the higher frequency $\text{O}-\text{H}$ over the $\text{C}-\text{H}$ bond of the metallacycle. The *normal* KIE for the forward reaction ($k_{\text{H}}/k_{\text{D}} = 2.94 \pm 0.06$) indicates that $\text{C}-\text{H}$ bond cleavage takes place before or during the rds. From the equilibrium and forward reaction KIEs, the authors calculate an isotope effect for the reverse reaction of $k_{\text{H}}/k_{\text{D}} = 3.77 \pm 0.28$. These results together with the profound effect of the substituents on the rate of the rearrangement ($\text{Ph} \approx \text{Tol} < \text{Me} \ll \text{tBu}$) are consistent with the initial cycloreversion to generate $\text{Cp}^*\text{Ti}=\text{O}$ and phenylacetylene, followed by proton transfer and $\text{Ti}-\text{C}$ bond formation in a concerted step.

9.1.3. [3 + 2]-Cycloadditions. Singleton studied the $\text{Pd}-\text{TMM}$ ($\text{TMM} = \text{trimethylenemethane}$) $[3 + 2]$ -cycloaddition on alkene **493**, obtaining evidence for a concerted reaction.³²³ The process proceeded with substantial ^{13}C KIEs in the C3- and C4-positions of the product **494** (the former α - and β -carbons in **493**). A previous experiment revealed that rate-limiting nucleophilic Michael addition to **493** (step 1) occurs with any significant ^{13}C KIE at $\text{C}\alpha$. Even if considering that ring closure (step 2) was the slow step, this could not account for the high KIE observed in C4 of the product **494**. The experimental KIEs together with the stereospecificity of the reaction were considered strong evidence for a concerted cycloaddition. These results, however, do not mean that all $\text{Pd}-\text{TMM}$ -mediated cycloadditions can occur through concerted mechanisms (Scheme 211).

Palladium–phenanthroline ($\text{Pd}(\text{Phen})_2$) complexes efficiently catalyze the reaction of nitroarenes **495** with arylalkynes and CO to give 3-arylindoles **496** by an *ortho*- $\text{C}-\text{H}$ functionalization of the nitroarene ring.³²⁴ Although kinetic studies indicated that the rds of the cycle is the initial nitroarene

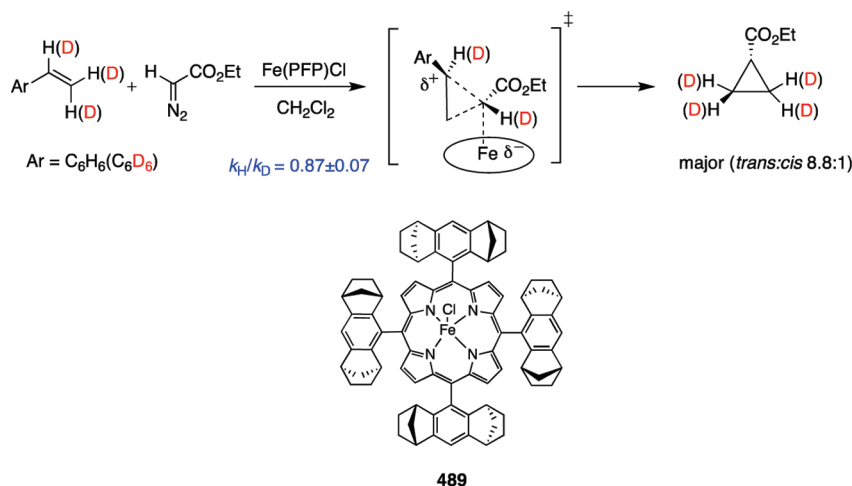
reduction, the authors investigate whether the cyclization step was important in determining the selectivity of the reaction, running three parallel reactions employing either pure $\text{C}_6\text{H}_5\text{NO}_2$ and $\text{C}_6\text{D}_5\text{NO}_2$ or a 1:1 mixture of the two as substrates. The secondary KIEs of around $k_{\text{H}}/k_{\text{D}} = 1.08-1.15$ indicated that the cyclization step is fast and does not determine the selectivity of the process (Scheme 212).

The study of KIEs was decisive in the history of mechanistic investigation of osmylation and related reactions that could be rationalized by both a concerted $[3 + 2]$ -process and a stepwise mechanism proceeding via a metallaoxetane.³²⁵ The issue was apparently resolved in 1997 by the observation that oxidation of *tert*-butylethylene showed, within experimental error, identical primary and secondary KIEs at the two olefinic positions. The results supported a very symmetrical transition state and a rate-limiting $[3 + 2]$ -cycloaddition step. A similar $[3 + 2]$ -mechanism also has been proposed for the reduction of OsO_4 by molecular hydrogen (Scheme 213).³²⁶

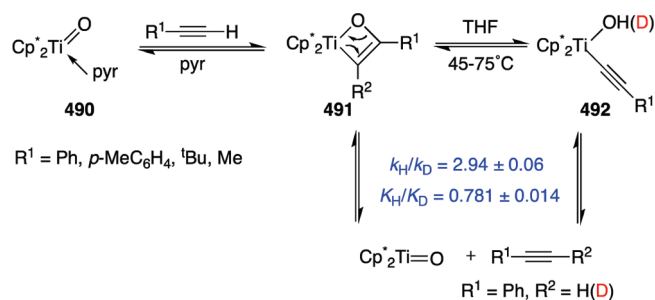
cis-Dioxoruthenium(VI) complex **497** reacts with alkenes **498** to afford *cis*-dihydroxylation and oxidative $\text{C}=\text{C}$ bond-cleavage reactions depending on the reaction conditions. The process, a formal $[3 + 2]$ -cycloaddition, was studied by Che and co-workers to establish the concerted/stepwise nature of the reaction (Scheme 214).³²⁷ In the reactions with cyclooctene and *trans*- β -methylstyrene, the corresponding $\text{Ru}(\text{III})$ cycloadducts **499** were isolated and structurally characterized by X-ray crystal analyses. Additionally, the synchronicity of the $\text{C}-\text{O}$ bond formation was examined by measuring secondary KIEs. A concerted reaction pathway involving synchronous $\text{C}-\text{O}$ bond formation would require a simultaneous sp^2 to sp^3 rehybridization of the alkenic α - and β -carbon atoms in the rate-determining step, resulting in similar *inverse* secondary KIEs for both atoms. The secondary KIEs observed for the oxidation of β - d_2 -styrene ($k_{\text{H}}/k_{\text{D}} = 0.83 \pm 0.04$; 0.92 ± 0.02 per deuterium) and α -deuteriostyrene ($k_{\text{H}}/k_{\text{D}} = 0.96 \pm 0.03$), together with the stereoselectivity of *cis*-alkene oxidation by **497**, were in favor of a concerted mechanism. The observed KIEs were also comparable to those reported for the OsO_4 -mediated *cis*-dihydroxylation reaction ($k_{\text{H}}/k_{\text{D}}$ per deuterium of 0.91 and 0.93 for $\text{C}\alpha$ and $\text{C}\beta$ atoms of alkenes, respectively), which is proposed to proceed by a synchronous transition state involving formation of two $\text{C}-\text{O}$ bonds.³²⁵

Secondary KIEs were also key in the study of the mechanism of extrusion of alkenes from $\text{Re}(\text{V})$ diolates **500** (the microscopic reverse of the alkene addition to Cp^*ReO_3).³²⁸ Analysis of the extrusion of different alkenes revealed little or no effect of the alkene strain in the enthalpies of activation, as well as entropies of activation lower than zero. These data are not easily interpreted through a concerted $[3 + 2]$ -cycloreversion mechanism. Even considering a very early transition state for the concerted process, with little reorganization of bonding, it should require a low KIE, which is not in agreement with the noticeable secondary KIE ($k_{\text{H}}/k_{\text{D}} = 1.32 \pm 0.06$) measured for extrusion of ethylene- d_4 (Scheme 215). Taken together, these data are inconsistent with a concerted $[3 + 2]$ -mechanism for interaction of alkenes with Cp^*ReO_3 but are consistent with a stepwise mechanism with a metallaoxetane intermediate, where the migration of carbon between rhenium and oxygen is rate-limiting. The hybridization of the reacting carbons in the intermediate is sp^3 , and because the strain associated with the sp^2 hybridization of the eventual product is not yet present at the transition state, there should

Scheme 209



Scheme 210



be little structural effect on the activation barrier. Although there is no net change in hybridization during the rate-determining transition state, the migrating carbon has increased its coordination number in the transition state and thus achieved a de facto change in hybridization, leading to the significant *normal* secondary KIE observed.

A further study by the same research group combined ¹³C, deuterium KIEs, Hammett studies, and DFT calculations to delve into the structure of the transition state, using the cycloreversion of 4-methoxystyrene from the corresponding Tp'Re(O)(diolato) complex **501** as model reaction.³²⁹ Noticeable primary KIEs were observed at both the α- (average $k_{12C}/k_{13C} = 1.041 \pm 0.005$) and β-positions (average $k_{12C}/k_{13C} = 1.013 \pm 0.006$). Also, secondary KIEs were observed at the α- (average $k_H/k_D = 1.076 \pm 0.005$) and β-positions (average $k_H/k_D = 1.017 \pm 0.005$) (Scheme 216). Primary ¹³C and secondary deuterium KIEs are consistent with the computational models that locate a concerted, although highly asynchronous, transition state for the cycloreversion process and point to significantly more bond breaking to the α-carbon than to the β-carbon. This picture does not fully agree with the Hammett behavior that suggests a more flexible structure for the transition state depending on the substituents that can induce shifts in the direction of electron flow during initial bond-cleavage step.

9.1.4. [3 + 3]-Cycloadditions. The zirconium imido complex Cp₂(THF)Zr=NSi(^tBu)Me₂ **502** reacts with allylic ethers and halides to give exclusively the products of the apparent the

S_N2' reaction.³³⁰ However, several experimental features such as the regio- and stereospecificity of the reaction, or the higher reactivity of allylic fluorides relative to other halides, could not be easily explained by a simple direct substitution. The *inverse* secondary KIE ($k_H/k_D = 0.88 \pm 0.01$), together with a DFT study of the substitution reaction, is more consistent with a concerted asynchronous [3,3]-sigmatropic rearrangement. The process involves initial dissociation of THF and binding of the substrate, followed by the formation of a six-membered closed transition state in the rate-determining step (Scheme 217).

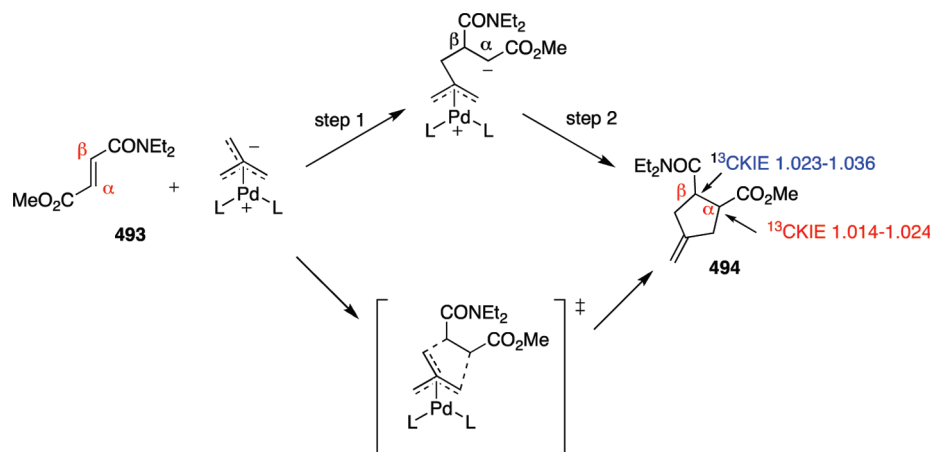
The reaction has been explored with zirconium oxo complexes and *E*-allylic chlorides to produce the expected S_N2' substitution derivatives in a regio- and stereospecific manner.³³¹ Kinetic, isotope labeling, and stereochemical experiments allowed the authors to propose a mechanism for the overall reaction. The secondary KIEs ($k_H/k_D = 1.16$, 1.055, and 0.571, respectively), obtained in the competition experiments between *E*-1-chloro-2-hexene **503** and deuterated analogues **504**, **505**, and **506** (Scheme 218), were consistent with the hybridization changes produced involving a concerted *closed* transition state for the rate-determining C–O bond formation.

9.2. [4 + 2 + 2]-Cycloadditions

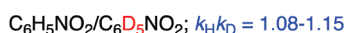
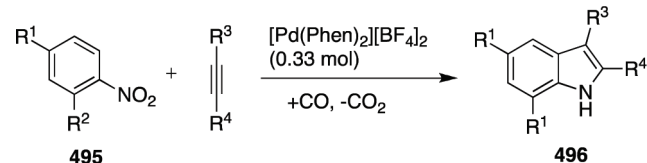
The mechanism of catalytic platinum(PtCl₂)-mediated cyclopropane opening of [4 + 2 + 2]-homo-Diels–Alder cycloadducts has been probed through deuterium labeling and KIE studies.³³² Although three different mechanistic alternatives were considered for this process (α-elimination, endocyclic β-elimination, and exocyclic β-elimination), deuterium labeling experiments pointed to the α-elimination followed by Puddephatt rearrangement as the most likely (Scheme 219). The process begins with a platinum(IV)cyclobutane **507**, which after α-hydride transfer from C3 to the platinum leads to the platinum(IV) carbene **508**, which after a 1,2-hydride shift and decomplexation leads to the final product.

KIE experiments supported the proposed mechanism. The rates of olefin formation of labeled compounds **509** and **510** compared with the nondeuterated analogue revealed isotope effects of $k_H/k_D = 5.44$ and $k_H/k_D = 1.54$, respectively (Scheme 220). The high primary KIE observed for the **509** to **511** transformation suggested that the rds is most likely the α-

Scheme 211



Scheme 212



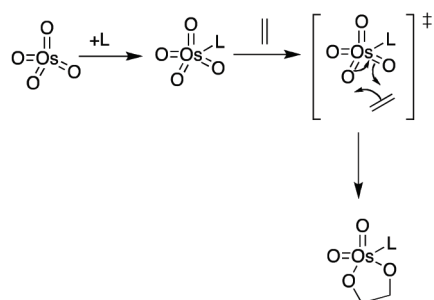
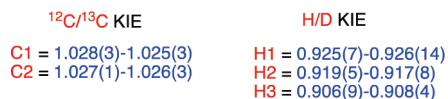
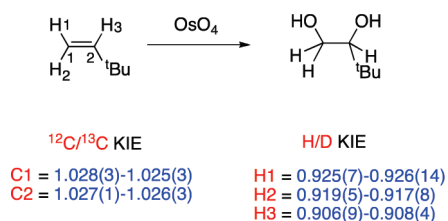
$\text{R}^1 = \text{H, Cl, Me, OMe, CO}_2\text{Me, NO}_2, \text{CN}$

$\text{R}^2 = \text{H, Cl, Me}$

$\text{R}^3 = \text{Et, Ph, Ar, CO}_2\text{Me, TMS}$

$\text{R}^4 = \text{H, Me, Et, Ph, CO}_2\text{Me, TMS}$

Scheme 213



hydride transfer. On the other hand, the much smaller KIE ($k_{\text{H}}/k_{\text{D}} = 1.54$) observed in the opening of **510** to yield **512** is consistent with a relatively large secondary KIE caused by the

significant σ -donation from C7-H/C7-D into the developing electron-deficient center at C3 during the hydride transfer to the platinum. Additional evidence was obtained in the transformation of C1,C2-dideuterated **513** to C2,C3-dideuterated **514** with a high KIE value ($k_{\text{H}}/k_{\text{D}} = 11.3$) that combined primary and secondary isotope effects.

9.3. [1,*n*]-Sigmatropic Shifts

An early work by Paquette reported mechanistic studies of $\text{Mo}(\text{CO})_6$ -promoted skeletal rearrangement of unsaturated [4.4.2]propellanes **515** to unsaturated bicyclo [6.4.0]-dodecane derivatives **516**, a process that requires a [1,5]-sigmatropic shift proceeding necessarily with migration of an sp^2 - or sp^3 -hybridized carbon of the four-membered ring. The reaction presumably takes place through a $\text{Mo}(\text{CO})_4$ intermediate complex **517**, which could be obtained from the stable Mo complex **518**, used in the study along with its deuterated analogues **519** and **520**.³³³ The results obtained in the rearrangement of **519** to **521** indicated that labeling of C2 and C5 with deuterium introduced minimal (if any) KIE on the isomerization rate. On the other hand, a noticeable *inverse* KIE ($k_{\text{H}}/k_{\text{D}} = 0.92$) was observed with C11,C12-dideuterated **520**. Additional information was provided by an intramolecular KIE experiment carried out with monodeuterated propellane **522**. In the presence of $\text{Mo}(\text{CO})_6$ in refluxing benzene, **522** produced a mixture of the cyclooctatetraenes **523** and **524** (which were not isolated but treated directly with *N*-phenyltriazolinedione to form the stable adducts) with a KIE ($k_{\text{H}}/k_{\text{D}} = 0.93 \pm 0.05$) almost identical to that determined previously for **520** (Scheme 221).

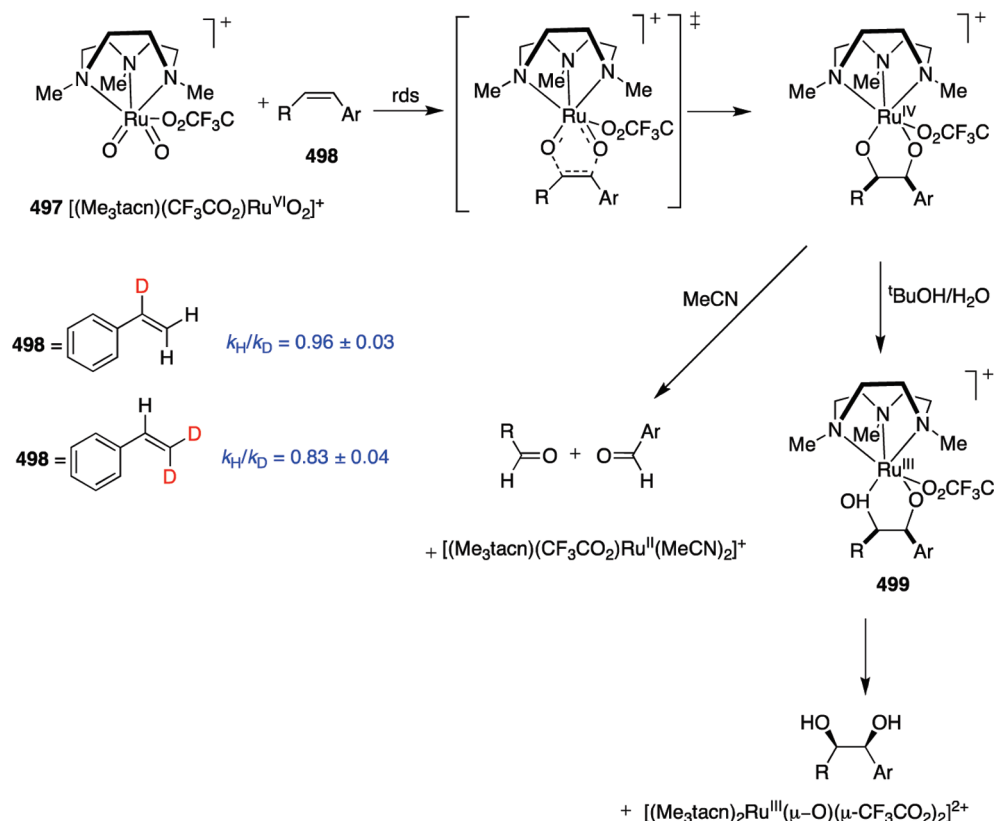
The magnitude and *inverse* nature of these secondary KIEs was interpreted to be compatible with a transition state model involving complexation of the propellatriene anti to the cyclobutene bridge and suprafacial [1,5]-sigmatropic carbon migration on that molecular face opposite to the site of molybdenum coordination (Scheme 222).

10. REACTIONS OF METAL–CARBENE COMPLEXES

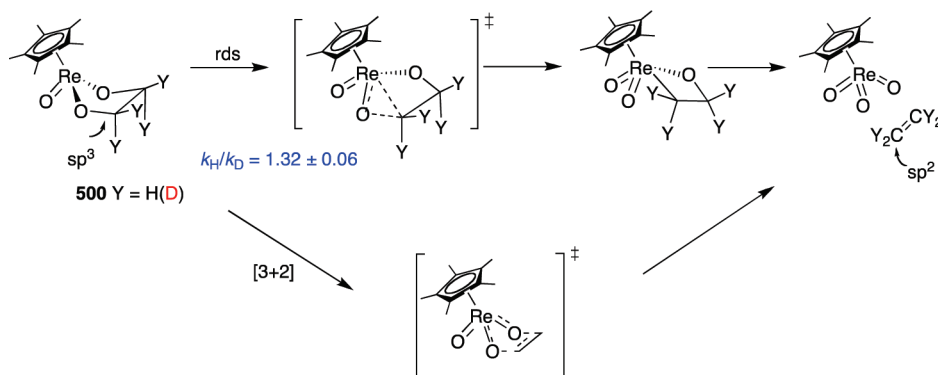
10.1. Fischer Carbene Complexes

The mechanisms of hydrolysis of Fischer carbene complexes have been extensively studied by the group of Bernasconi.³³⁴ Kinetic studies carried out with carbene complexes with ionizable

Scheme 214



Scheme 215



α -carbons **525**, **526**,³³⁵ **527**, **528**,³³⁶ **529**,³³⁷ and **530**³³⁸ revealed that the hydrolysis (50% MeCN–50% water) is pH dependent (a general base-catalyzed reaction) and is subject to a substantial kinetic solvent isotope effect (k_{H_2O}/k_{D_2O}) larger in magnitude as the pH of the medium increases, which is consistent with a rate-limiting proton transfer (Figure 8).

The mechanism that accounts best for all experimental observations involves rapid deprotonation to **531** that could follow two possible, stepwise or concerted, evolution pathways. The stepwise pathway entails rate-limiting protonation on the metal to form **532** followed by rapid reductive elimination to **533**, while the concerted pathway involves protonation on the carbene carbon with simultaneous M–C bond cleavage

(Scheme 223). Complexation of the enol ether in **533** with $(CO)_5M$ makes it more reactive toward basic hydrolysis, leading to the vinyl alcohol and finally to the aldehyde.

In turn, the hydrolysis of aryl carbene complexes **534**–**537** occurs in two stages (Scheme 224). The first one is similar to the nucleophilic addition–elimination mechanism of esters and leads to the formation of carbene complex **538**, and the second, much slower stage is the decomposition of **538** to the observed reaction products ($ArCHO$ and $(CO)_5MOH^-$). A kinetic investigation of the first stage (50% MeCN–50% water (v/v) at 25 °C)³³⁹ revealed that nucleophilic attack by OH^- at high pH and by water at low pH (presumably to form a tetrahedral intermediate) is rate limiting. This intermediate is not detectable

even though the equilibrium for its formation is probably favorable at high pH. Solvent kinetic isotope effects (KSIEs) close to or slightly lower than unity were obtained for the OH^- pathway in line with KSIE values for the reaction of OH^- with esters or amides. On the other hand, large $k_{\text{H}_2\text{O}}/k_{\text{D}_2\text{O}}$ values (2.9–4.7) were observed for the water pathway, suggesting a mechanism where *two* water molecules are involved, probably one acting as nucleophile and the other acting as base catalyst.

KIEs were also used in the studies of acidity of α -ionizable metal carbene complexes **539** and **540**.³⁴⁰ Clear primary KIE values in the range $k_{\text{H}}/k_{\text{D}} = 2.60$ – 2.98 were observed for the

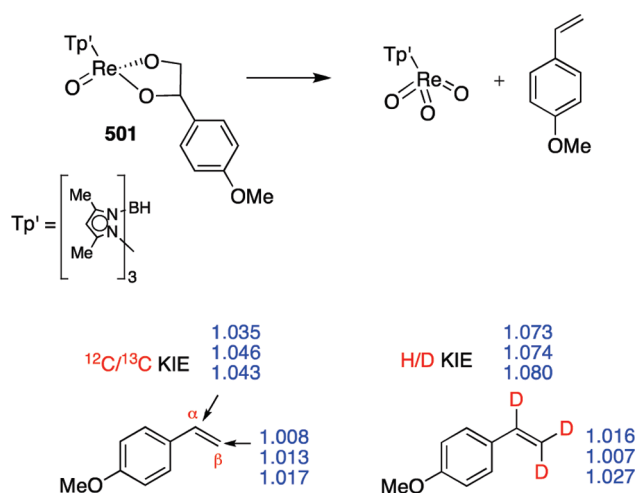
deprotonation of **539** by HO^- and of $k_{\text{H}}/k_{\text{D}} = 2.53$ and $k_{\text{H}}/k_{\text{D}} = 5.51$ for the reaction of **540** with OH^- and piperidine, respectively. However, although noticeable, the KIE values were rather low for a deprotonation. The influence of the pH of the medium, the electrostatic effects, and the possible coupling of proton transfer to heavy atom motion in the transition state could explain the experimental data (Scheme 225).

Pipoh and van Eldik studied the mechanism of addition of pyrrolidine, imidazoles, and anilines to pentacarbonyl alkynyl carbene complexes. The experimental data support a two-step process in which a zwitterionic intermediate is produced in the rds. The absence of a primary KIE for the reaction of tungsten complex **541** with deuterated pyrrolidine³⁴¹ and imidazole³⁴² together with the negligible KIE ($k_{\text{H}}/k_{\text{D}} = 1.2$) observed in the reaction of chromium complex **542** with deuterioaniline³⁴³ support this proposal (Scheme 226).

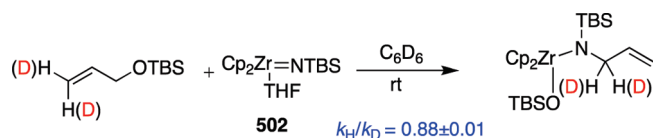
10.2. Vinylidene Complexes

The mechanism of the η^2 -alkyne to η^1 -vinylidene rearrangement has been extensively studied both experimentally and

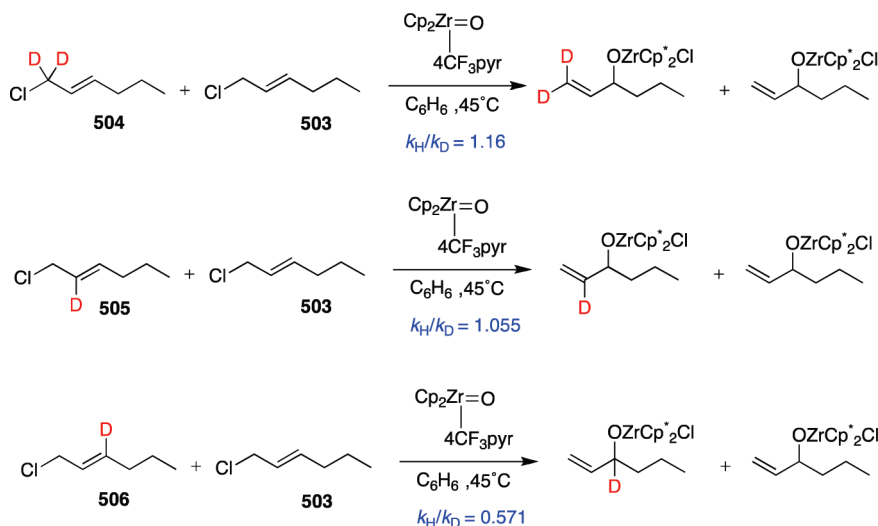
Scheme 216



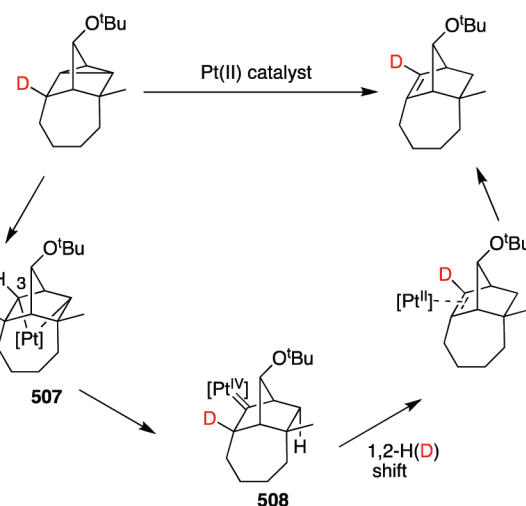
Scheme 217



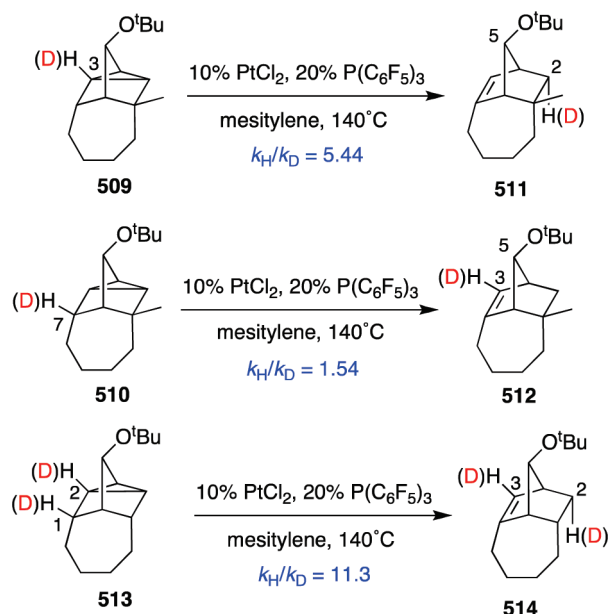
Scheme 218



Scheme 219



Scheme 220

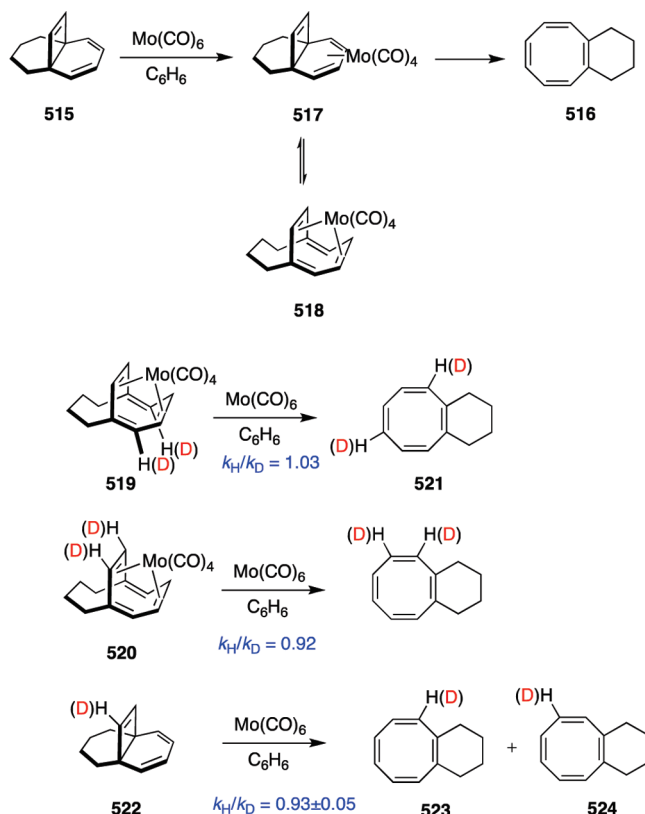


theoretically.³⁴⁴ Two alternative pathways are discussed so far in the literature (Scheme 227): either by an intramolecular 1,2-hydrogen shift (path A) or by the formation of a hydride alkynyl species and concomitant 1,3-hydrogen shift (path B) (Scheme 227). Generally, electron-rich metal complexes favor path A, whereas electron-poor complexes prefer path B. In some cases, KIEs have been of great use to gain insight into the process.

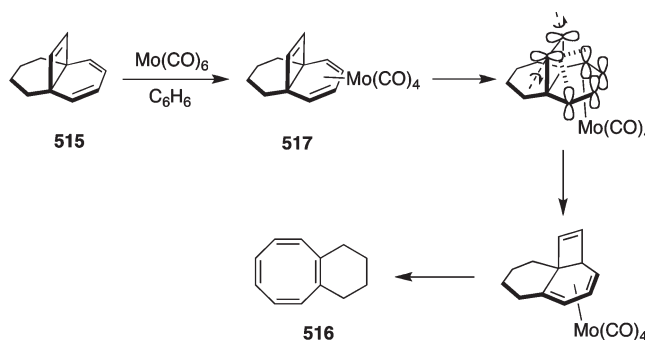
The reaction order (bimolecular/unimolecular) for the 1,3-hydrogen shift has also been a matter of active debate. Recently, Grothjan et al. studied³⁴⁵ the unimolecular versus bimolecular transformation of terminal alkyne–Rh(I) complexes **543** into vinylidenes **544** by experimental and computational studies. Lack of isotopic scrambling in double-crossover experiments carried out with labeled/unlabeled complexes **543** was inconsistent with alkyne activation on Rh(I) and transformation to vinylidene by a bimolecular pathway. The results were more consistent with the intermediacy of an $\eta^2\text{-(C–H)}$ intermediate such as **545**. The $k_{\text{H}}/k_{\text{D}} = 1.67$ obtained for the rearrangements of complexes **543** were in the range of those observed in analogous Ru(II) complexes ($k_{\text{H}}/k_{\text{D}} = 1.69 \pm 0.5$)³⁴⁶ and were considered as indirect support for this assessment (Scheme 228).

Ozawa and co-workers reported³⁴⁷ a study for alkyne–vinylidene interconversion on ruthenium complexes in the reaction of Ru(II) complex **546** with terminal alkynes to form vinylidene complexes **547** in quantitative yields. Although the reactivity is affected by both the electronic and steric nature of the R groups, the kinetic data observed for arylacetylene derivatives revealed that the more electron-donating substituent tends to give the higher reaction rate. Kinetic data together with the moderate KIE ($k_{\text{H}}/k_{\text{D}} = 1.69 \pm 0.05$) observed in the reaction with deuterated phenylacetylene suggested significant contribution of the rate of phenylacetylene–phenylvinylidene tautomerization, even though the dissociation of MeCN from **546** constitutes the slowest step in the overall process. The experimental data are consistent with a sequence of three elementary

Scheme 221



Scheme 222



processes: reversible dissociation of the MeCN ligand in coordinatively saturated complex **546** to form the five-coordinate intermediate **548**, coordination of alkyne, and tautomerization of alkyne ligand into vinylidene ligand (Scheme 229).

The mechanistic studies of the isomerization of η^1 -vinylidene transition metal complexes into the corresponding η^2 -alkyne complexes are, in turn, scarce. Studies on the thermal isomerization of W and Mo η^1 -vinylidene complexes **549** and **550** to the corresponding η^2 -alkyne tautomers **551** and **552** revealed that they followed different pathways.³⁴⁸ Normal secondary KIEs in the range of $k_{\text{H}}/k_{\text{D}} = 1.17\text{--}1.22$ for the isomerization of tungsten complexes **549** in aprotic solvents were in good agreement with a hybridization change from sp^2 to sp of the $\text{C}\beta$ of the η^1 -vinylidene ligand in the transition state during the migration

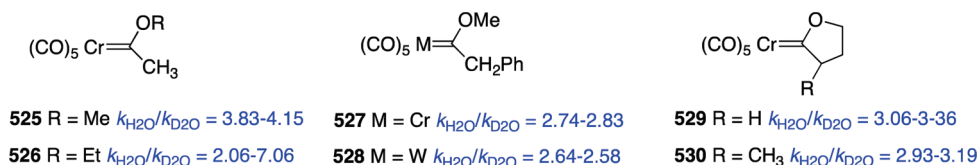
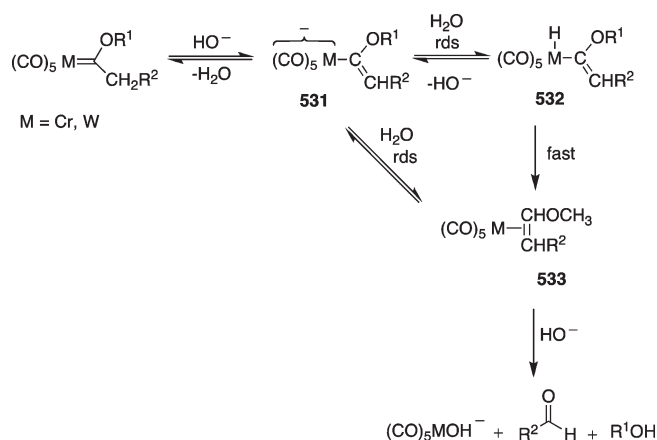
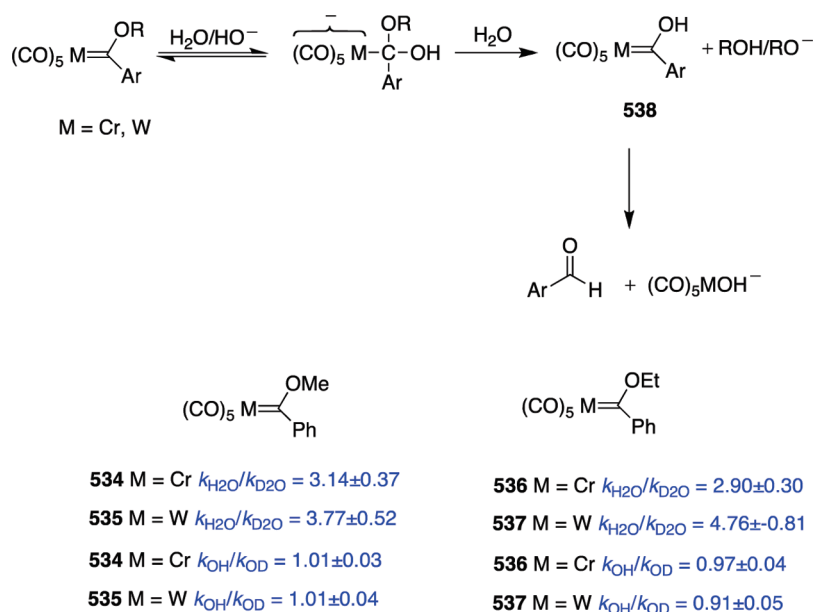


Figure 8

Scheme 223



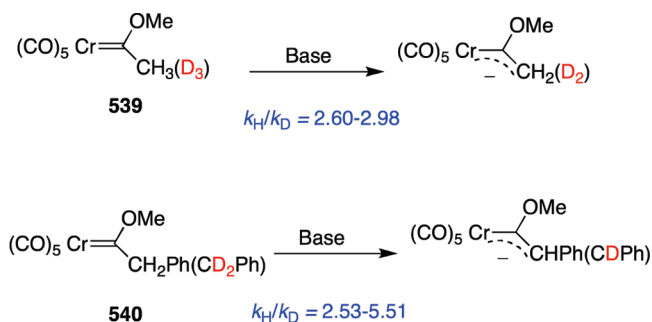
Scheme 224



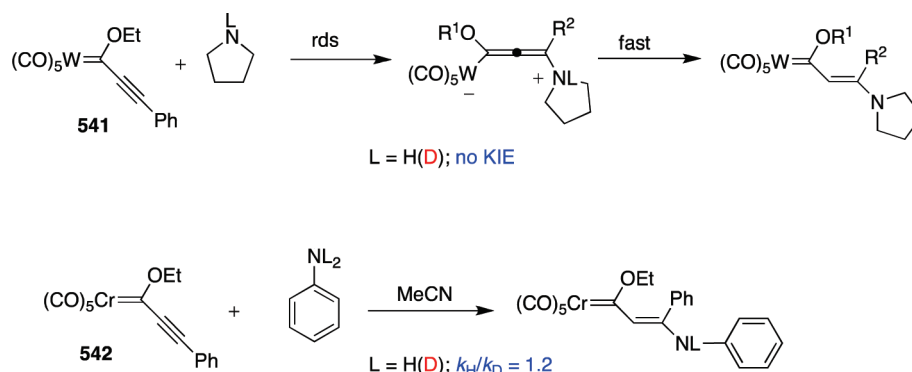
of the silyl group. On the contrary, Mo complexes **550** showed a dichotomous behavior. In toluene, $k_{\text{H}}/k_{\text{D}}$ values from 1.9 to 2.2 were observed with little temperature dependence, but KIEs in the range $k_{\text{H}}/k_{\text{D}} = 15.7$ at 60 °C and $k_{\text{H}}/k_{\text{D}} = 7.1$ at 100 °C were obtained for the isomerization in ethanol- d_0 /ethanol- d_6 (Scheme 230). To account for these experimental results, two different mechanistic pathways were proposed. In nonpolar solvents, a concerted 1,2-shift of the silyl group would lead to the transition state **553** for tungsten complexes

549, whereas 1,2-migration of the H atom should lead to transition state **554** for Mo complexes **550**. Slippage of the metal and π -coordination would yield the η^2 -alkyne complexes. In ethanol, however, the KIE data are more in agreement with a two-step dissociation–addition process through a deprotonation step generating the η^1 -alkynyl complex **555** followed by the protonation on molybdenum to the hydrido–alkynyl complex **556**, which undergoes reductive elimination to the η^2 -1-alkyne isomer **552**.

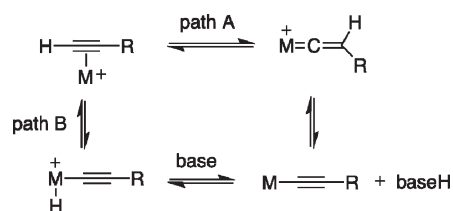
Scheme 225



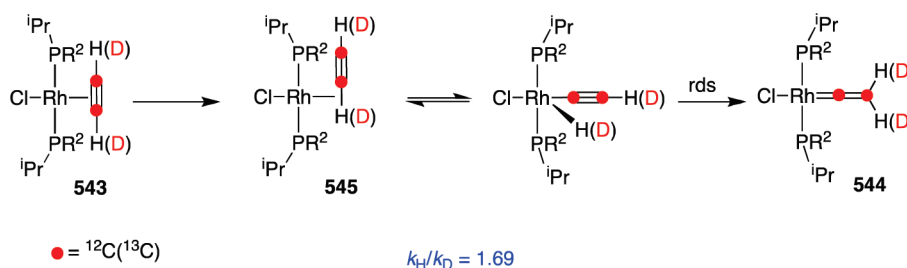
Scheme 226



Scheme 227



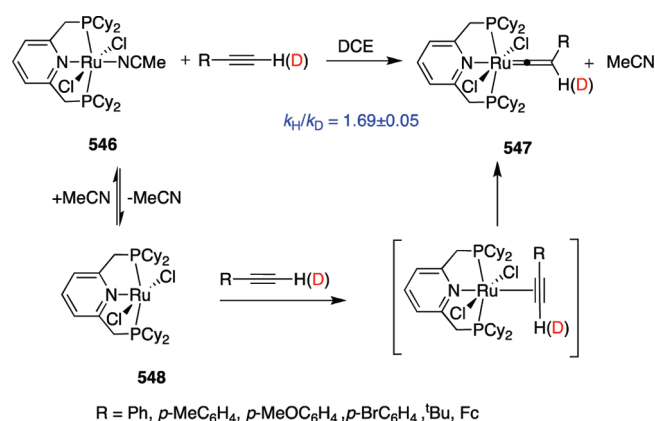
Scheme 228



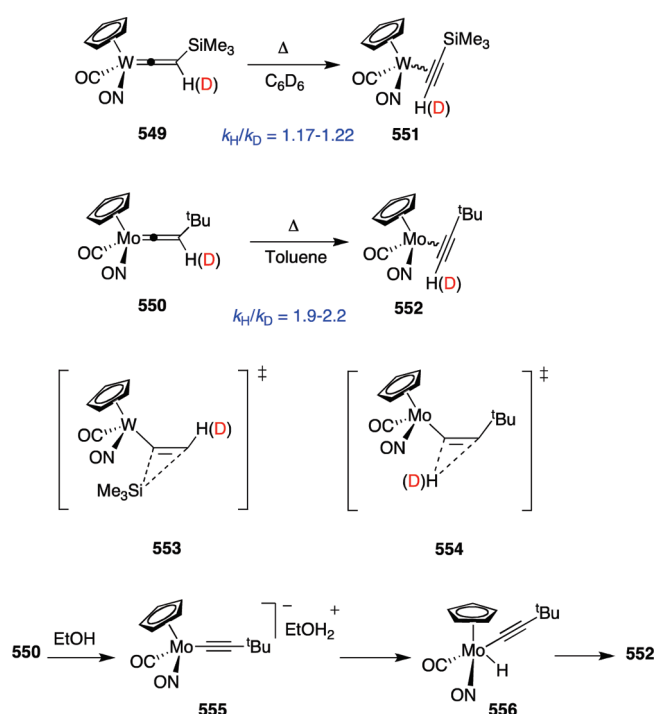
An experimental study for the η^1 -vinylidene to η^2 -alkyne tautomerization in indenylruthenium(II) vinylidene complexes has been recently reported.³⁴⁹ Reaction order, entropy of activation, Hammett studies, and the primary KIEs obtained in the isomerization of complexes **557** in acetonitrile- d_3 /

$\text{H}_2\text{O}(\text{D}_2\text{O})$ mixtures ($k_H/k_D = 1.17-1.88$) support an intramolecular 1,2 hydrogen shift mechanism in which the rearrangement of the $\text{C}=\text{CHR}$ moiety is the slow step of the process. This assessment is based also on theoretical calculations (Scheme 231).

Scheme 229



Scheme 230

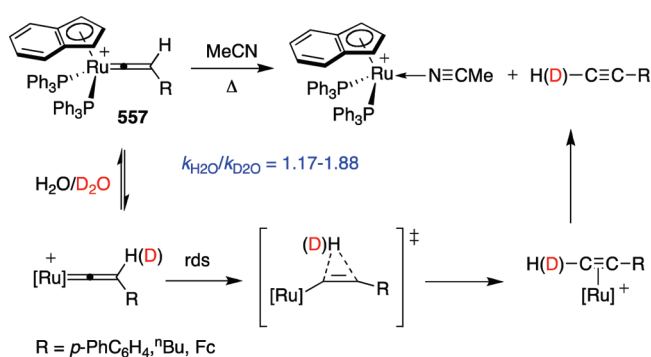


The reactions of *trans*-Re(dppe) complexes **558** with [NHEt₃][BPh₄] to form the carbyne complexes **559** were reported by Pombeiro and colleagues.³⁵⁰ The kinetic studies indicate that the process proceeds via three possible pathways whose relative contribution depends on the nature of the substituents R and X. The observation of marked primary KIEs in the reactions of **558** and [NDEt₃][BPh₄] were decisive in establishing that steps *k*₄ and *k*₆ involved rate-limiting proton transfer: intramolecular migration of the hydrido ligand for *k*₄ and slow H(D)-transfer to the β-carbon of the vinylidene ligand in the case of *k*₆ (Scheme 232).

10.3. Non-Stabilized Metal Carbene Complexes, Metallacycles, Carbynes, and Nitrenes

The strongly electrophilic carbene complexes **560** react with the transition metal hydrides [(CO)₅MnH] and

Scheme 231



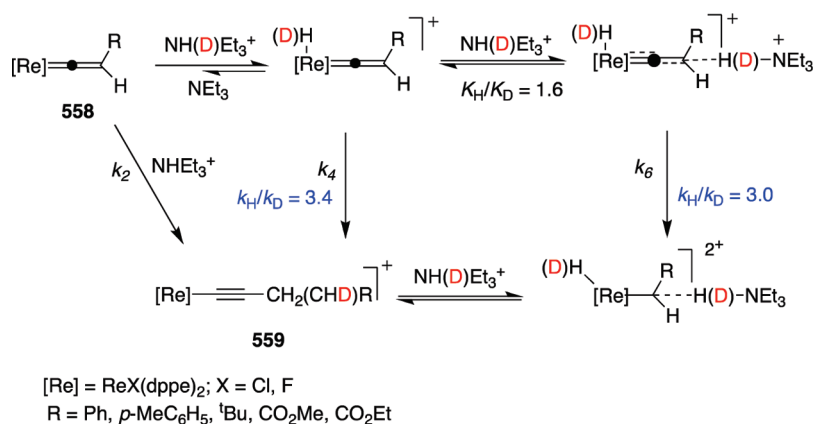
[Cp(CO)₃WH] by a formal transfer and insertion of the carbene ligand into the M–H bond to give benzyl complexes [(CO)₅MnCH₂Ar] and [Cp(CO)₃WCH₂Ar].³⁵¹ The reaction rate increases with increasing electrophilicity of the carbene carbon atom and with decreasing steric demand of the ligands at the metal hydride. Additionally, the KIE observed in the reaction of [Cp(CO)₃WH(D)] **561** (*k*_H/*k*_D = 2.6 ± 0.4) is consistent with an associative process with significant M–H(D) bond breaking and still less developed C–H(D) bond formation in the transition state (early transition state) (Scheme 233).

An early study by Gladysz and co-workers of the mechanism of the isomerization of propylidene complexes **562** to propene complexes **563** showed modest primary KIEs slightly varying with the temperature (*k*_H/*k*_D = 1.95–1.40) and in the range for 1,2-migrations, but a considerable *inverse* secondary KIE (*k*_H/*k*_D = 0.50–0.58).³⁵² These data, together with others confirming that the rearrangements are intramolecular and occur without PPh₃ ligand dissociation and with retention of the configuration at rhenium, suggest a stepwise mechanism that bears many similarities to 1,2-hydride shifts or Wagner–Meerwein rearrangements (Scheme 234).

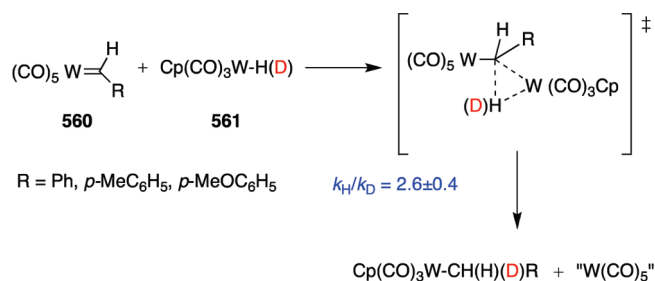
α-Hydrogen atoms in tungsten complexes **564** are found to migrate to the α-carbon atom of the alkylidene ligand, leading to the equilibrium **564**–**565** (Scheme 235).³⁵³ The isomerization showed large primary KIEs (*k*_H/*k*_D = 5.1 ± 0.3 for (Me₃CCH₂(D₂))₃W=CSiMe₃) and (*k*_H/*k*_D = 3.0 ± 0.2 for (Me₃CCH(D))₃W=CSiMe₃) suggestive of a symmetrical (linear) transition state for the transfer of hydrogen between the carbon atoms. The KIE data, activation parameters, and crossover experiments were consistent with consecutive α-hydrogen transfer through a concerted four-center transition state leading to a bis(alkylidene) activated complex or reactive intermediate **566**.

The thermal decomposition of Ti complex **567** produces complex **568** and methane through the reactive species Cp*₂Ti=CH₂ **569**.³⁵⁴ The KIE observed in the reaction with methyl-labeled **567** (*k*_H/*k*_D = 2.92 ± 0.01) suggested an intramolecular process in which a methyl C–H bond is being broken in the slow step of the process. However, while the isotopic labeling indicates that a Cp* methyl C–H bond is broken in the formation of the product, the negligible KIE (*k*_H/*k*_D = 1.03 ± 0.04) observed on the thermolysis of Cp*-d₆/Cp*-d₁₅ substrates suggests that this step must occur after the slow step. On the basis of these facts, one of the Ti–CH₃ groups obtains a hydrogen from its neighbor Ti–CH₃ group to form

Scheme 232



Scheme 233



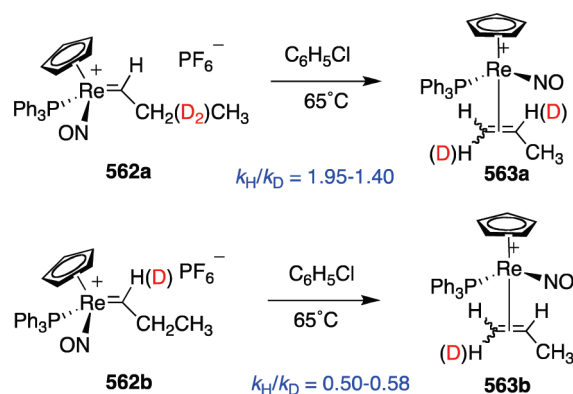
569 and methane (slow), and the reactive species rearranges (fast) to 570 by hydrogen migration from a Cp^*-CH_3 group to the methyldiene ligand. Both an α -hydrogen abstraction and an α -hydrogen elimination were considered for the formation of 569 (Scheme 236).

Diketimate Zr complex 571 eliminates toluene upon heating to form the *ortho*-metalated product 572. Isotopic labeling experiments and a large KIE ($k_{\text{H}}/k_{\text{D}} = 5.2 \pm 0.5$) were consistent with unimolecular rate-limiting direct C–H activation through a four-centered transition state 573 (Scheme 237).³⁵⁵ The magnitude of the primary KIE is slightly smaller than that reported by Wolczanski and co-workers for toluene loss from $\text{Zr}(\text{NHR})_3-(\text{CH}_2\text{Ph})$ and $\text{Zr}(\text{NDR})_3(\text{CH}_2\text{Ph})$ ($\text{R} = \text{Si}^t\text{Bu}_3$, $k_{\text{H}}/k_{\text{D}} = 7.1 \pm 0.6$).¹²⁵

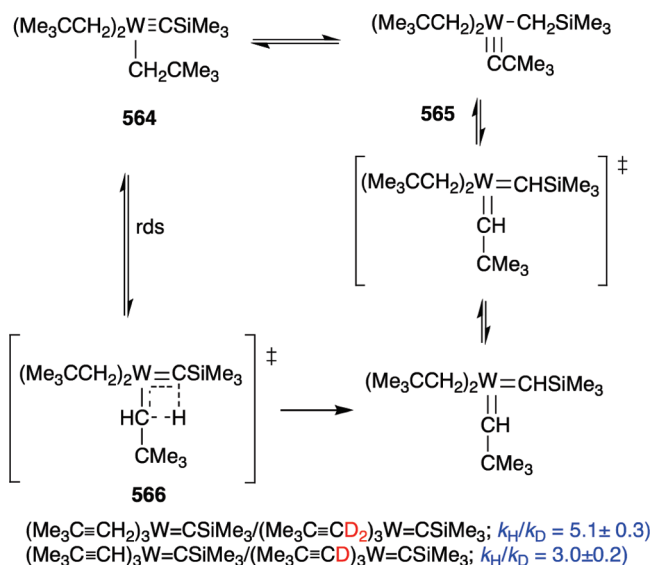
By a series of labeling studies, the same research group³⁵⁶ has determined the rds in the sequence of at least three separate C–H activation steps involved in the thermal conversion hafnium complex 574 to hafnabenzocyclobutene 575. As evidenced by the KIE observed ($k_{\text{H}}/k_{\text{D}} = 3.1 \pm 0.2$) when α -deuterated benzyl ligands 574– CD_2Ph were used, the slow step involves rate-limiting benzyl abstraction to form permethylhafnocene benzylidene intermediate 576. *ortho*-Metalation of the benzyl ligand occurs after the rds, as evidenced by the lack of KIE observed when labeled 574– $\text{CH}_2\text{C}_6\text{D}_5$ was used ($k_{\text{H}}/k_{\text{D}} = 1.1 \pm 0.1$) (Scheme 238).

This group³⁵⁷ has recently reported the generation of a stable benzylidene complex 578 by heating of a bis-(phenolate)pyridine tantalum tribenzyl species 577 in the presence of dimethylphenylphosphine. The process was

Scheme 234

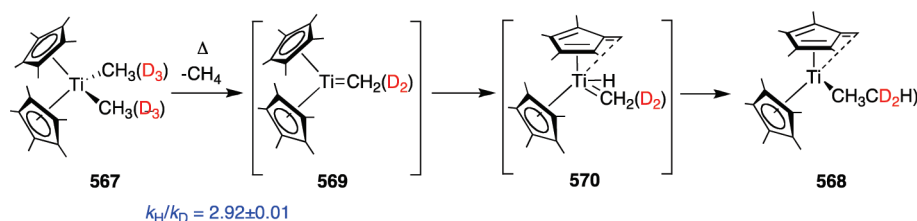


Scheme 235

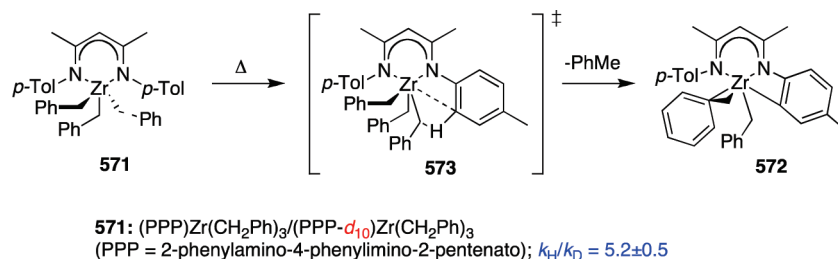


found to be first-order rate for the disappearance of the trialkyl species 577, independent of PMe_2Ph concentration, and showed a KIE ($k_{\text{H}}/k_{\text{D}} = 4.9 \pm 0.4$) consistent with a mecha-

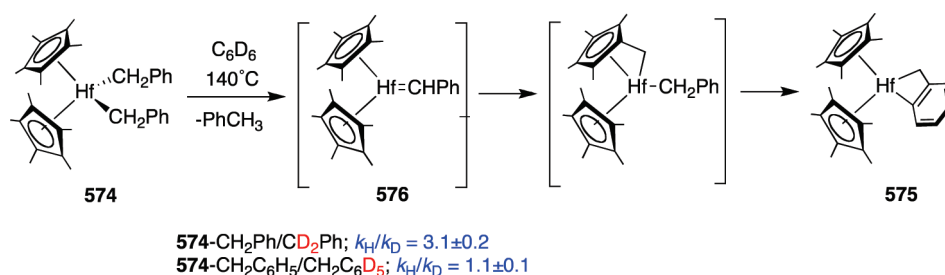
Scheme 236



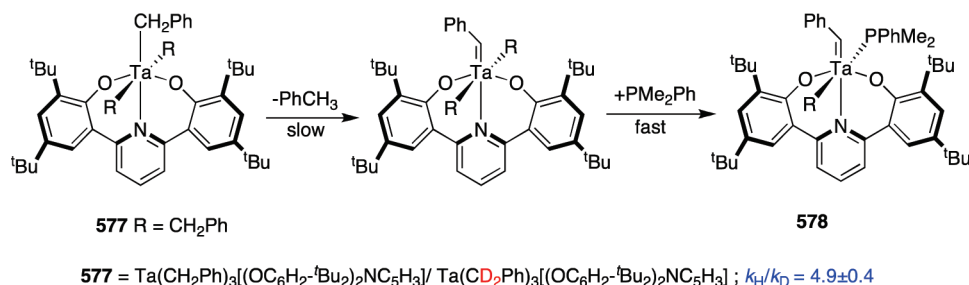
Scheme 237



Scheme 238



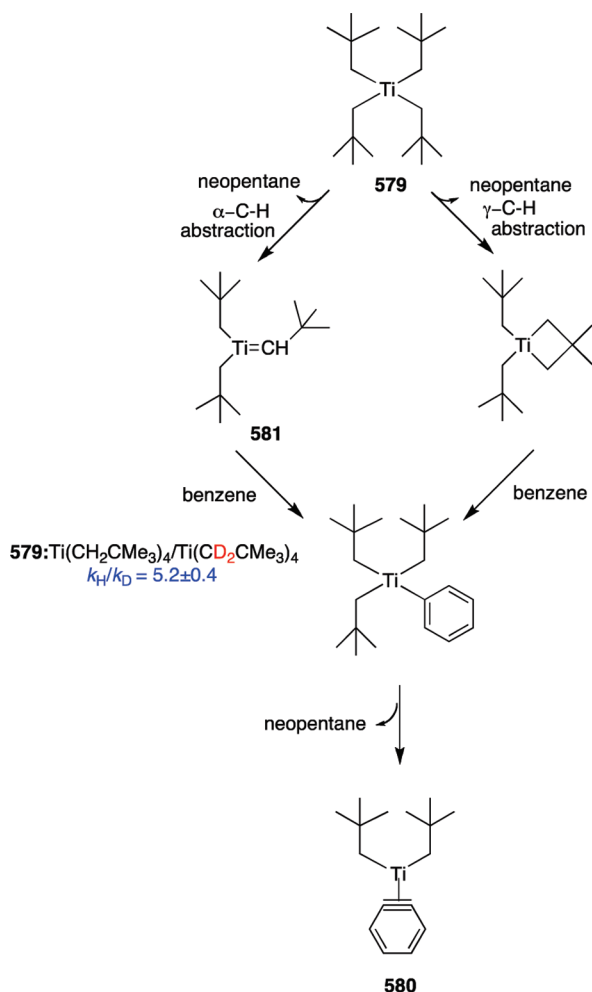
Scheme 239



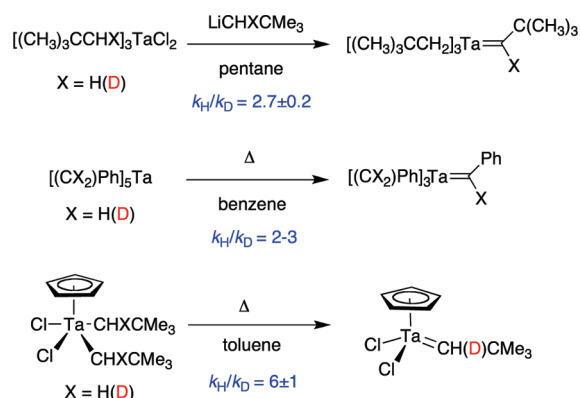
nism involving rate-determining C–H bond cleavage. Among the different proposals raised, this experimental evidence was only consistent with the mechanism in Scheme 239: α -hydrogen abstraction with loss of toluene, followed by fast phosphine coordination to the resulting benzyldiene species. An X-ray structure determination revealed that the benzyldiene π -bond in **578** is oriented perpendicular to the oxygen–oxygen vector, in accord with the prediction of DFT calculations.

Girolami and co-workers³⁵⁸ reported a mechanistic study of the thermolysis in solution of Ti(CH₂CMe₃)₄ **579** to obtain information about its conversion to titanium carbide **580** under chemical vapor decomposition (CVD) conditions. Experiments carried out with complexes Ti(CH₂CMe₃)₄ (**579-d**₀) and Ti(CD₂CMe₃)₄ (**579-d**₈) in hydrocarbon solution showed elimination of neopentane at significantly different rates and a noticeable KIE ($k_{\text{H}}/k_{\text{D}} = 5.2 \pm 0.4$). This result clearly indicated that a methylene α -C–H bond was broken in

Scheme 240

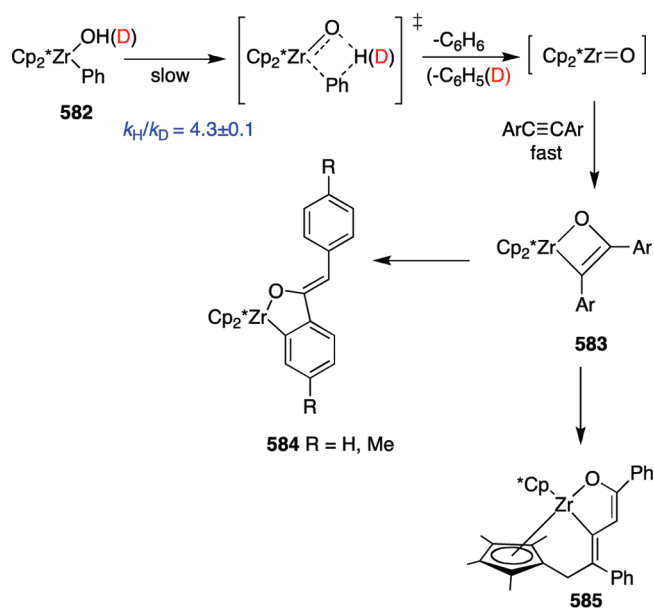


Scheme 241

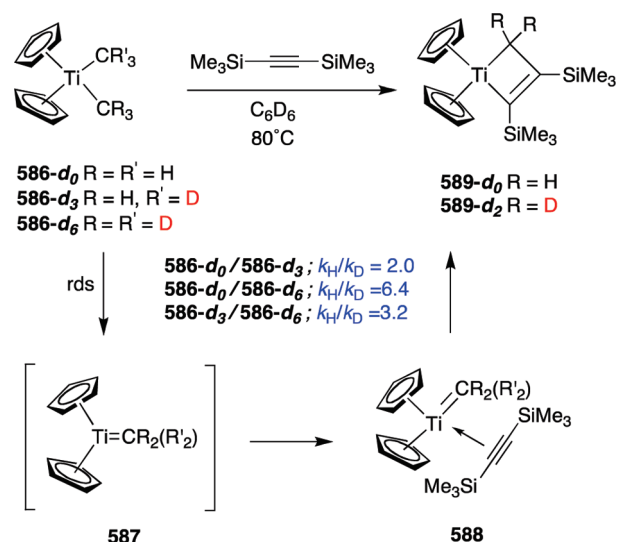


the rds, ruling out other pathways involving the γ -hydrogen abstraction. The observed KIE supports a thermolysis sequence that generates the titanium alkylidene intermediate **581** in the first step. In reactive solvents such as benzene (and to some extent in cyclohexane), the alkylidene intermediate activates solvent C–H bonds intermolecularly by addition

Scheme 242



Scheme 243

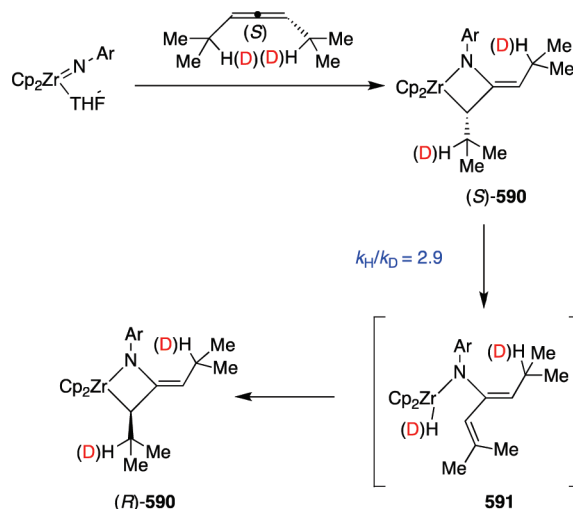


across the $\text{Ti}=\text{C}$ bond in **581**. Although in some circumstances the γ -hydrogen activation is considered as a second thermolysis pathway for **579**, this route is estimated to be 25 times slower than the α -hydrogen abstraction process (Scheme 240).

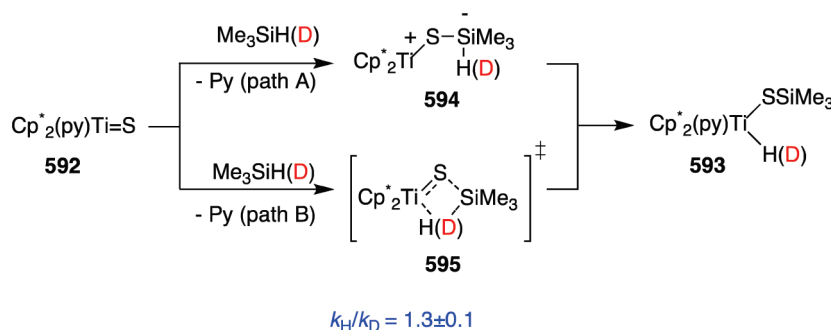
The KIE observed for $\text{Ti}(\text{CH}_2\text{CMe}_3)_4$ **579** is larger than most of those measured for other α -hydrogen abstraction processes in structurally related Ta complexes (Scheme 241).³⁵⁹

Bergman and co-workers³⁶⁰ reported the generation of the oxo complex $[\text{Cp}^*_2\text{Zr}=\text{O}]$ and its sulfur analogue $[\text{Cp}^*_2\text{Zr}=\text{S}]$, two unsaturated intermediates unusually reactive toward organic compounds. The generation of $[\text{Cp}^*_2\text{Zr}=\text{O}]$ was accomplished at 160°C by α -elimination of benzene from $\text{Cp}^*_2\text{Zr}(\text{Ph})(\text{OH})$ **582**, and after reaction with diarylacetylenes,

Scheme 244



Scheme 245



oxametallacyclobutenes of type **583** or their rearrangement products *ortho*-metalated oxametallacycles **584** and **585** were obtained (Scheme 242). To gain insight into the mechanism of the thermal decomposition, the reaction rates of **582-*d*₀**/**582-*d*₁** in the presence of the trapping agents were examined.³⁶¹ Separate thermolyses at 160 °C in the presence of excess diphenylacetylene indicated that C_6H_6 and $\text{C}_6\text{H}_5\text{D}$, respectively, were the exclusive (>97%) elimination products. The process also showed a KIE $k_{\text{H}}/k_{\text{D}} = 4.3 \pm 0.1$ indicating that an O–H (or O–D) bond undergo cleavage in the rds transition state. The above findings are most consistent with the mechanism shown in Scheme 242, proceeding by first-order, rate-determining elimination of benzene, leading to the transient species $[\text{Cp}^*_2\text{Zr}=\text{O}]$.

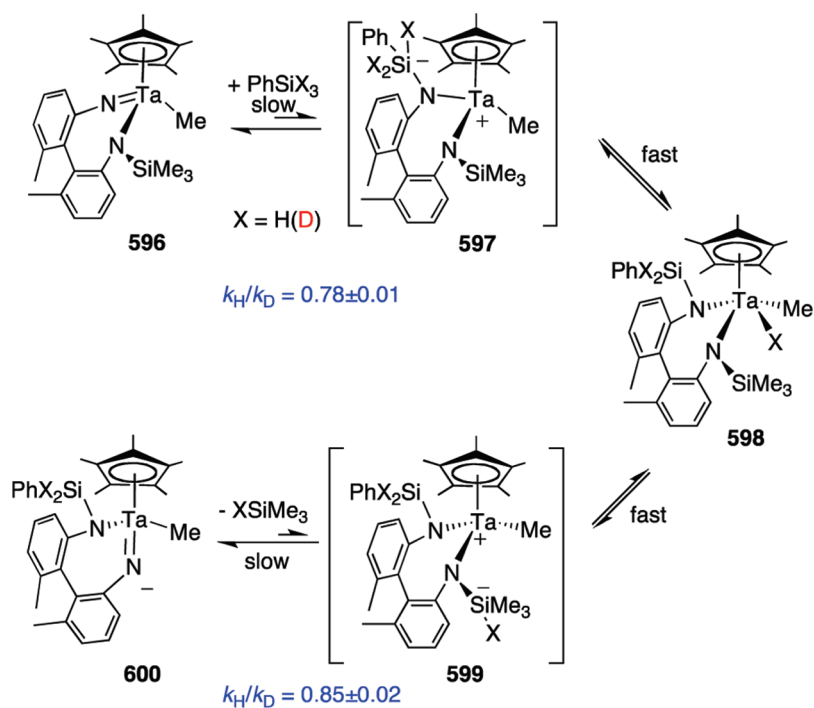
The mechanism of the efficient thermolysis of dimethyltitanocene in the presence of internal alkynes was reported by Petasis and Fu.³⁶² The reaction between titanocenes **586-*d*₀**, **586-*d*₃**, and **586-*d*₆** with bis(trimethylsilyl)acetylene was shown to be first order in dimethyltitanocene with primary KIEs of $k_{\text{H}}/k_{\text{D}} = 2.0$, $k_{\text{H}}/k_{\text{D}} = 6.4$, and $k_{\text{H}}/k_{\text{D}} = 3.2$, respectively (Scheme 243). The kinetic studies were consistent with an α -abstraction step taking place on the free dimethyltitanocene, which is converted to the methylenetitanocene **587**. This highly reactive species reacts rapidly with the alkyne to

form a labile alkyne complex **588**, which is finally transformed to the titanacyclobutene **589**. The high **583-*d*₀**/**583-*d*₆** KIE value presumably includes both a primary and a secondary component. The primary KIE results from the breaking of the C–H bond during the rds, while the change in hybridization from sp^3 in **586** to sp^2 in **587** is responsible for the secondary isotope effect.

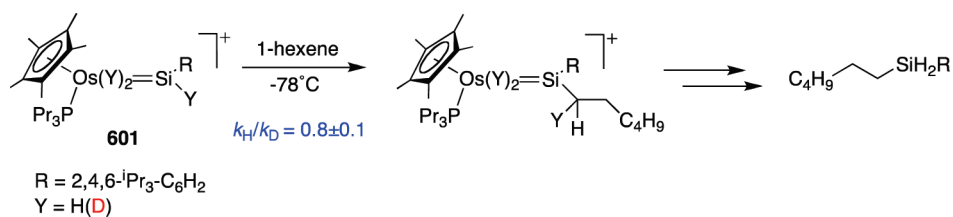
KIEs were used by Bergman's group to study the racemization of alkylazirconacyclobutenes **590**.³⁶³ The rapid reversible β -hydrogen elimination was probed with chiral **590-*d*₂**. The process followed clean first-order kinetics, and a *normal* primary KIE ($k_{\text{H}}/k_{\text{D}} = 2.9$) was observed in agreement with a reversible β -hydride elimination, formation of intermediate **591**, and hydrosilylation of the opposite enantioface of the newly formed olefin (Scheme 244). This pathway is available only to dialkylallene-derived metallacycles, which explains the large difference in racemization rate between dialkyl- and diarylallene metallacycles.

In the context of the study of the mechanisms of activation and hydrogenation of organosulfur species on surfaces, Bergman, Andersen, and their co-workers³⁶⁴ studied KIEs of the H_2 activation by Ti–disulfide complexes using the reaction of complex **592** with trimethylsilane to form complex **593** (Scheme 245). Rate-determining formation of a pentacoordinate

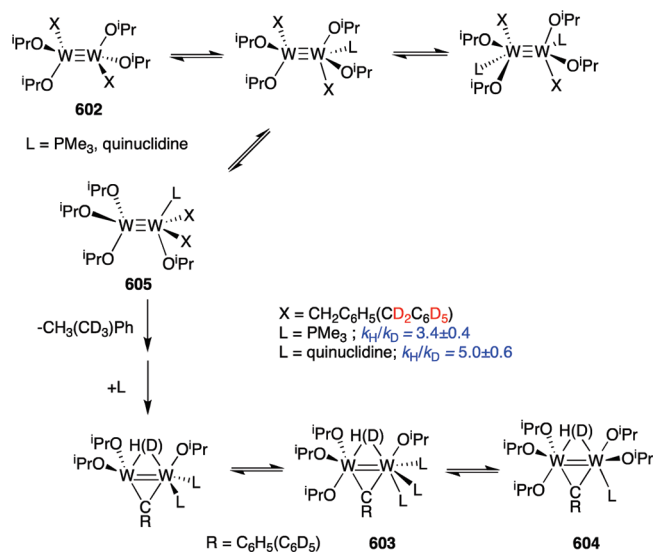
Scheme 246



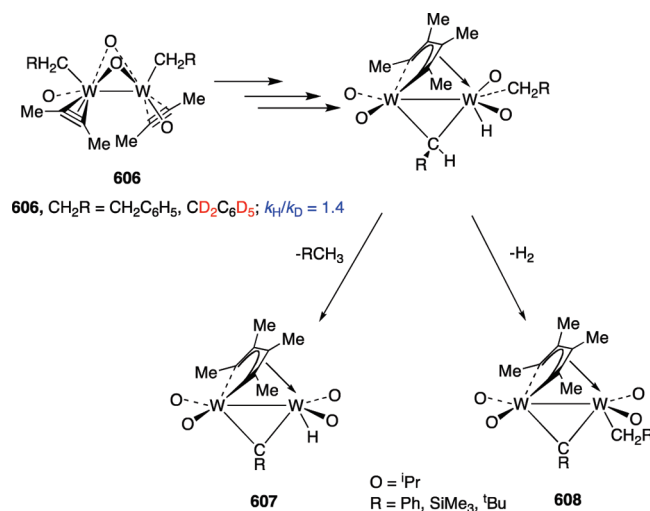
Scheme 247



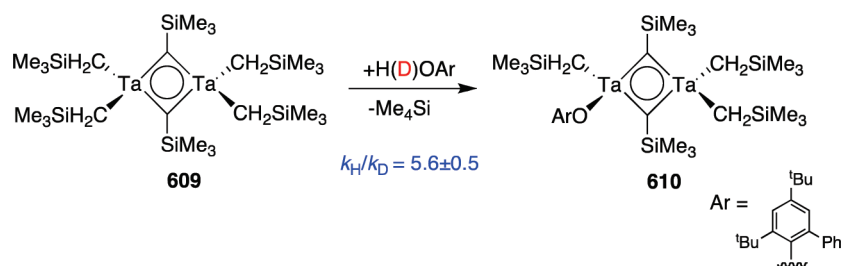
Scheme 248



Scheme 249



Scheme 250



silicon intermediate **594** (path A) should result in an *inverse* KIE, whereas a *normal* value would be expected for the process shown in path B, since the Si–H bond should be considerably weakened in the transition state. The observation of a normal KIE ($k_{\text{H}}/k_{\text{D}} = 1.3 \pm 0.1$, 298 K) in the reaction of **592** with HSiMe_3 suggests that the rds involves a concerted $[2 + 2]$ -addition.

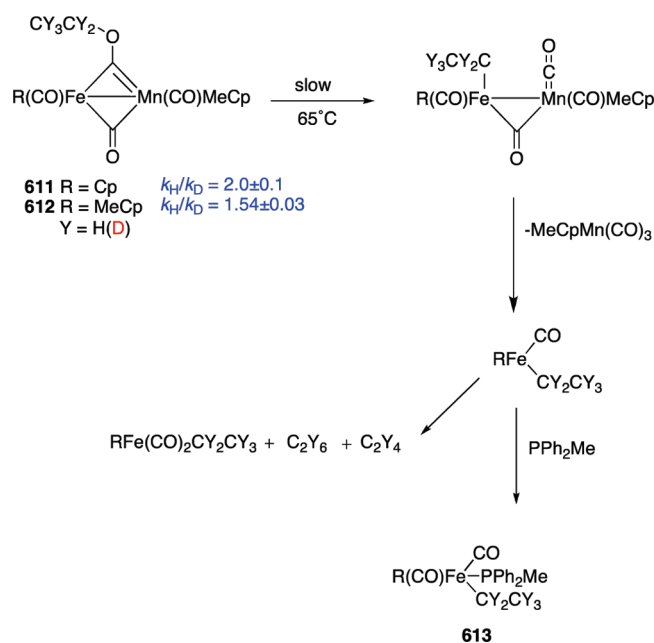
The highly bent tantalum imido complexes **596** react with silanes by an interesting two-step process involving an intermediate featuring a pentacoordinate silicon center.³⁶⁵ The mechanism of these transformations appears to reflect the tendency of silicon to easily expand its coordination sphere and is thus rather different from that of C–H bond activations by zirconium or tantalum imido complexes.^{125,129} Reactions of $\text{PhSiH}_3/\text{PhSiD}_3$ with **596** follow second-order kinetics and show an *inverse* KIE ($k_{\text{H}}/k_{\text{D}} = 0.78 \pm 0.01$), suggesting that the rds transition state does not involve significant breaking or making of bonds to hydrogen. The proposed mechanism involves the formation of a pentacoordinate silicon intermediate **597** coupled with a fast hydride shift between Ta and Si (Scheme 246). The *inverse* KIE obtained for the elimination of DSiMe_3 from **598-d**₃ ($k_{\text{H}}/k_{\text{D}} = 0.85 \pm 0.02$) is consistent with this hypothesis. Intermediate **599** is likely formed in a pre-equilibrium with **598** by a rapid hydride shift from Ta to Si, and a slow cleavage of the N–Si bond would liberate HSiMe_3 , leading finally to product **600**.

Finally, the reaction of the Si-related cationic complex $[\text{Cp}^*(\text{}^i\text{Pr}_3\text{P})(\text{H})_2\text{Os}=\text{SiH}(\text{trip})][\text{B}(\text{C}_6\text{F}_5)_4]$ ($\text{trip} = 2,4,6\text{-iPr}_3\text{-C}_6\text{H}_2$) **601** with alkenes at -78°C was used by Tilley's group as a model to study the key insertion into the Si–H bond previously proposed for the catalytic hydrosilylation of alkenes by $[\text{Cp}^*(\text{}^i\text{Pr}_3\text{P})(\text{H})_2\text{Ru}=\text{SiHPh}]^+$.³⁶⁶ The kinetic isotope effect was determined by a competition experiment involving reaction of **601-d**₀/**601-d**₃ with 0.5 equiv of 1-hexene. This experiment established an *inverse* KIE ($k_{\text{H}}/k_{\text{D}} = 0.8 \pm 0.1$), which indicates significant sp^2 to sp^3 hybridization at silicon during approach to the transition state for insertion into the Si–H bond (Scheme 247).

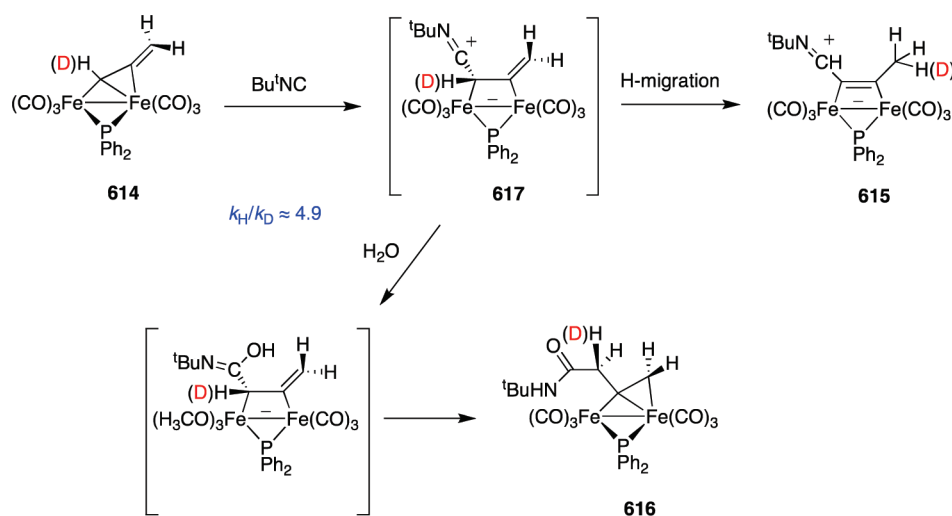
10.4. Bridging Carbene Complexes

Chisholm and colleagues reported the reaction of Lewis bases such as PMe_3 or quinuclidine and $1,2\text{-W}_2(\text{CH}_2\text{Ph})_2\text{-(O-}^i\text{Pr)}_4$ **602** in toluene and hexane, at room temperature, to give benzyldiene hydrido compounds **603** and **604** by way of a double $\alpha\text{-CH}$ activation and elimination of toluene.³⁶⁷ KIEs in toluene- d_8 , for **602-d**₀/**602-d**₂ with PMe_3 ($k_{\text{H}}/k_{\text{D}} = 3.4 \pm 0.4$) and with quinuclidine ($k_{\text{H}}/k_{\text{D}} = 5.0 \pm 0.6$), implied that C–H/C–D bond breaking was rate-determining. These data were consistent with the mechanism depicted in Scheme 248. The proposed $\alpha\text{-CH}$ activation pathway involves the 1,2-migration of $\text{CH}_2\text{R/O-}^i\text{Pr}$ ligands and the formation of **605**, which experiences C–H activation. The authors speculate

Scheme 251



Scheme 252



that the much larger quinuclidine plays a similar role in promoting the alkyl group migration. A large KIE ($k_{\text{H}}/k_{\text{D}} = 3.5 \pm 0.1$) was also observed in the thermal evolution of $\text{W}_2(\text{O}^i\text{Bu}^t)_7^-$ to form isobutene.³⁶⁸

Compounds $1,2\text{-W}_2(\text{R}_2)(\text{O}^i\text{Pr})_4$ react with internal alkynes to form bisalkyne adducts of formula $1,2\text{-W}_2(\text{R}_2)(\text{alkyne})_2(\text{O}^i\text{Pr})_4$ having a dimeric structure. Chisholm's group³⁶⁹ studied the thermolysis of bis(alkyne) adducts $\text{W}_2(\text{CH}_2\text{R})_2(\text{MeCCMe})_2(\text{O}^i\text{Pr})_4$ (**606** (R = Ph, SiMe₃, and ^tBu) in hydrocarbon solutions to produce alkylidyne-bridged compounds **607** and **608** by competitive double α -hydrogen activation reactions that liberate molecular H₂ and RCH₃, respectively. The small KIE ($k_{\text{H}}/k_{\text{D}} = 1.4$) observed and the associative activation parameters of the reaction are most consistent with

a rate-determining alkyne-coupling step that is followed by the α -C–H activation processes (Scheme 249).

The reaction of a series of phenols and naphthylphenol counterparts with the compound $\text{Ta}_2(\mu\text{-CSiMe}_3)_2(\text{CH}_2\text{SiMe}_3)_4$ **609** has been investigated. This reaction produces the mono-substitution products **610** at rates that are strongly dependent on the nature of the phenol substituents. A kinetic study of the reaction of **609** with bulky 2-phenyl-4,6-di-*tert*-butylphenol indicated that the reaction was first order in both **609** and phenol and showed a noticeable primary KIE ($k_{\text{H}}/k_{\text{D}} = 5.6 \pm 0.5$, 30°C), suggesting that the final step of the reaction involves proton transfer to the alkyl leaving group (Scheme 250).³⁷⁰

On the basis of secondary KIEs, a unimolecular mechanism was proposed for the thermal decomposition of the

iron–manganese ethoxycarbonyl **611** to give $\text{MeCpMn}(\text{CO})_3$ and (in the presence of PPh_3Me) $\text{CpFe}(\text{CO})(\text{PPh}_2\text{Me})\text{-CH}_2\text{CH}_3$ **613**.³⁷¹ The reaction is first order in carbonyl and zero order in phosphine, and the KIEs for the ethoxycarbonyl decomposition were $k_{\text{H}}/k_{\text{D}} = 2.0 \pm 0.1$ for **611** and $k_{\text{H}}/k_{\text{D}} = 1.54 \pm 0.03$ for **612**. Since $\text{C-H}(\text{C-D})$ bond cleavage does not occur in this reaction, both are *normal* secondary KIEs associated with sp^3 to sp^2 rehybridization at the cleavage site. The reaction is an interesting example of a β -elimination from an alkoxycarbonyl in which an alkyl group migrates from oxygen to iron. The observed secondary KIE shows that ethyl migration occurs in the rds and suggests an “electrophilic” migration mechanism by which a metal electron pair attacks the alkyl group (Scheme 251).

The nucleophilic addition of *tert*-butyl isonitrile to σ - η binuclear allenyl complex **614** yields the parallel alkyne-bridged complex **615** and the α,β -unsaturated amide **616**.³⁷² The mechanism of this unusual carbon nucleophile addition at a $\text{C}\alpha$ -coordinated allenyl ligand was studied by means of labeling experiments. The large primary KIE for the transfer of hydrogen between $\text{C}\alpha$ and $\text{C}\gamma$ ($k_{\text{H}}/k_{\text{D}} \approx 4.9$) and the product distribution obtained in competitive experiments with labeled/unlabeled **614** support the authors’ proposal of an initial nucleophilic attack at $\text{C}\alpha$ to give an unstable zwitterionic allene-bridged intermediate **617**, which subsequently undergoes either a 1,3-hydrogen migration to give **615** or hydrolysis to give the α,β -unsaturated amide **616**. The large KIE value also suggested a rather symmetrical transition state for the transfer of hydrogen between $\text{C}\alpha$ and $\text{C}\gamma$. The alternative pathway involving nucleophilic addition to $\text{C}\alpha$ followed by 1,3-hydrogen migration and migration of isonitrile could not be unequivocally excluded (Scheme 252).

11. CONCLUDING REMARKS

Among the classical tools of physical organic chemistry, deuterium labeling and isotope effects have been demonstrated to be, by far, the most valuable in the study of reaction mechanisms mediated by transition metals. In particular, H/D and, to a lesser extent, $^{12}\text{C}/^{13}\text{C}$ KIEs have proved to be essential in disentangling the mechanistic insights of some of the most relevant metal-mediated transformations known, the C–H activation processes and the C–C (C–heteroatom) coupling reactions. The *in depth* knowledge of these mechanisms has allowed the synthetic chemists to afford many new types of transformations that are currently being used in industry and academy. In the age of computation, many voices have claimed that physical organic chemistry is old history. Even more, parallel to the appearance of new, more accurate computational tools, many chemists had predicted the death of the field, as the scientists were gradually replacing in their published papers the experimental mechanistic studies by the theoretical calculations. In this scenario, isotope effects have experienced a renaissance. H/D KIEs are simple to interpret, do not require complex experimental support, and also are the perfect bench test for the computational data. Their values can be predicted with a minimal computational cost, and the comparison of the theoretical/experimental data is a strong support for/against a calculated pathway. Progress in science needs experimental substantiation for theories, and in this regard, the use of isotope effects in the study of organometallic reactions through the last 30 years is an example of how it is possible to employ the classical tools in new approaches to the study of reaction mechanisms.

AUTHOR INFORMATION

Corresponding Author

*E-mail: (M.G.-G.) margg@quim.ucm.es, (M.A.S.) sierraor@quim.ucm.es.

BIOGRAPHIES



Mar Gómez Gallego obtained her Ph.D. in Organic Chemistry (Cum Laude) in the UCM (Madrid, 1986). After a postdoctoral stay in Scotland (Dundee University, Prof. W. M. Horspool, Fleming Award), she obtained a permanent position at the UCM as Profesor Titular of Organic Chemistry in 1992. From 2002 she is advisor of the Energetic Materials Laboratory (LME) of the Spanish Ministry of Defense and simultaneously develops joint research projects with this laboratory, as well as with several agrochemical companies. Her current research interests are focused on the synthesis of bio-organometallic compounds, the development of new processes based on transition metal complexes, and the study of their reaction mechanisms as well as in the development of new iron chelating agents and the study of their mechanisms of action and their environmental impact.



Miguel A. Sierra was born in Villamiel (Toledo), studied Chemistry at the UCM (Madrid), and received his Ph.D. in 1987 (Honors). After a postdoctoral stay at Colorado State University (Prof. Louis Hegedus), he was promoted to Profesor Titular in 1990, and Catedrático in 2005 (UCM). He is consultant of the NBQ and Energetic Materials laboratories of the Spanish Defense Ministry, as well as the Secretary of the Spanish Organic Section of the Spanish Chemical Society and a member of its Board. Among other awards, he received (2002) the Military Cross (white ribbon) for his work for the Organization for the

Prohibition of Chemical Weapons (OPCW). His research encompasses the development of new processes based on transition metal complexes, the study of organometallic reaction mechanisms, the preparation of new bioorganometallic compounds, and the design and synthesis of new energetic materials.

ACKNOWLEDGMENT

Financial support by the Spanish Ministerio de Ciencia e Innovación (MCINN), grants CTQ2010-20714-C02-01 and Consolider-Ingenio 2010 (CSD2007-0006), and by the Comunidad de Madrid (CAM), grant P2009/PPQ1634-AVAN-CAT, is acknowledged. We thank Dr. Santiago Romano for his valuable suggestions and the thorough revision of the manuscript.

REFERENCES

- (1) The relevance of the use of Transition Metal Complexes in Organic Synthesis has been recognized with three Chemistry Nobel Prizes in the past decade. In 2001 for the developments in chirally catalyzed oxidation reactions: Knowles, W. S. *Angew. Chem., Int. Ed.* **2002**, *41*, 1998. Noyori, R. *Angew. Chem., Int. Ed.* **2002**, *41*, 2008. and Sharpless, K. B. *Angew. Chem., Int. Ed.* **2002**, *41*, 2024. In 2005 for the development of the metathesis method in organic synthesis: Chauvin, Y. *Angew. Chem., Int. Ed.* **2006**, *45*, 3740. Grubbs, R. H. *Angew. Chem., Int. Ed.* **2006**, *45*, 3760. and Schrock, R. R. *Angew. Chem., Int. Ed.* **2006**, *45*, 3748. In 2010 for the palladium-catalyzed cross-couplings in organic synthesis: Heck, R. F.; Negishi, E. I.; Suzuki, A.
- (2) Some recent monographies: (a) Anslyn, E. V.; Dougherty, D. A. *Modern Physical Organic Chemistry*; University Science Books: Sausalito, CA, 2006. (b) *The Investigation of Organic Reactions and their Mechanisms*; Maskill, H., Ed.; Blackwell: Oxford, U.K., 2006. (c) Maskill, H. *The Physical Basis of Organic Chemistry*; Oxford University Press: New York, 1995. (d) Gómez-Gallego, M.; Sierra, M. A. *Organic Reaction Mechanisms, 40 solved cases*; Springer Verlag: Berlin, 2003.
- (3) Classical references: (a) Halpern, J.; Okamoto, T.; Zakhariyev, A. *J. Mol. Catal.* **1976**, *2*, 65. (b) Halpern, J. *Acc. Chem. Res.* **1982**, *15*, 332. (c) Halpern, J. *Pure Appl. Chem.* **1983**, *55*, 99. For a recent article about the application of kinetic treatment to catalytic cycles, see: (d) Blackmond, D. G. *Angew. Chem., Int. Ed.* **2005**, *44*, 4302. For a revision on the application of electrochemistry to organometallic catalysis, see: (e) Jutand, A. *Chem. Rev.* **2008**, *108*, 2300.
- (4) For excellent revisions on the applications of the tools of physical organic chemistry to the investigation of organometallic reaction mechanisms, see: (a) Blum, S. A.; Tan, K. L.; Bergman, R. G. *J. Org. Chem.* **2003**, *68*, 4127. (b) Lloyd-Jones, G.; Muñoz, M. P. *J. Labelled Compd. Radiopharm.* **2007**, *50*, 1072.
- (5) Melander, L. C. S.; Saunders, W. *Reaction Rates of Isotopic Molecules*; Krieger: Malabar, FL, 1987.
- (6) KIE values greater than 10 at room temperature have been observed and are generally taken to indicate significant contribution of quantum mechanical tunnelling in proton transfer reactions, see: (a) Bell, R. P. *Chem. Soc. Rev.* **1974**, *4*, 513. (b) Bell, R. P. *The Proton in Chemistry*; Cornell University Press: Ithaca, NY, 1973. (c) Bell, R. P. *The Tunnel Effect in Chemistry*; Chapman and Hall: London, 1980. (d) Caldin, E. F. *Chem. Rev.* **1969**, *69*, 135. (e) Kwart, H. *Acc. Chem. Res.* **1982**, *15*, 401. (f) Limbach, H.; Lopez, J. M.; Kohen, A. *Philos. Trans. R. Soc., B* **2006**, *361*, 1399.
- (7) Goldshleger, N. F.; Tyabin, M. B.; Shilov, A. E.; Shteinman, A. A. *Russ. J. Phys. Chem.* **1969**, *43*, 1222.
- (8) Crabtree, R. H.; Mihelcic, J. M.; Quirk, J. M. *J. Am. Chem. Soc.* **1979**, *101*, 7738.
- (9) Selected references in C–H insertion: (a) Ryabov, A. D. *Chem. Rev.* **1990**, *90*, 403. (b) Arndtsen, B. A.; Bergman, R. G.; Mobley, T. A.; Peterson, T. H. *Acc. Chem. Res.* **1995**, *28*, 154. (c) Shilov, A. E.; Shul'pin, G. B. *Chem. Rev.* **1997**, *97*, 2879. (d) Sen, A. *Acc. Chem. Res.* **1998**, *31*, 550. (e) Guari, Y.; Sabo-Ennenne, S.; Chaudret, B. *Eur. J. Inorg. Chem.* **1999**, 1047. (f) Jones, W. D. *Science* **2000**, *287*, 1942. (g) Crabtree, R. H. *J. Chem. Soc., Dalton Trans.* **2001**, 2437. (h) Labinger, J. A.; Bercaw, J. E. *Nature* **2002**, *417*, 507. (i) Crabtree, R. H. *J. Organomet. Chem.* **2004**, *689*, 4083. (j) Jones, W. D. *Inorg. Chem.* **2005**, *44*, 4475. (10) Balcells, D.; Clot, E.; Eisenstein, O. *Chem. Rev.* **2010**, *110*, 749. (11) Jones, W. D. *Acc. Chem. Res.* **2003**, *36*, 140. (12) Churchill, D. G.; Janak, K. E.; Wittenberg, J. S.; Parkin, G. J. *Am. Chem. Soc.* **2003**, *125*, 1403. (13) Reviews: (a) Makhaev, V. D. *Russ. Chem. Rev.* **2003**, *72*, 257. (b) Hall, C.; Perutz, R. N. *Chem. Rev.* **1996**, *96*, 3125. (c) Crabtree, R. H. *Chem. Rev.* **1995**, *95*, 987. (d) Crabtree, R. H. *Angew. Chem., Int. Ed.* **1993**, *32*, 789. (e) *Metal Dihydrogen and σ -Bond Complexes: Structure, Theory, and Reactivity*; Kubas, G. J., Ed.; Kluwer Academic/Plenum Publishers: New York, 2001. (14) Selected references: (a) Janowicz, A. H.; Bergman, R. G. *J. Am. Chem. Soc.* **1983**, *105*, 3929. (b) Hackett, M.; Ibers, J. A.; Whitesides, G. M. *J. Am. Chem. Soc.* **1988**, *110*, 1436. (c) Hackett, M.; Whitesides, G. M. *J. Am. Chem. Soc.* **1988**, *110*, 1449. (d) Xie, X.; Simon, J. D. *J. Phys. Chem.* **1989**, *93*, 291. (e) Weiller, B. H.; Wasserman, E. P.; Bergman, R. G.; Moore, C. B.; Pimentel, G. C. *J. Am. Chem. Soc.* **1989**, *111*, 8288. (f) Whittlesey, M. K.; Mawby, R. J.; Osman, R.; Perutz, R. N.; Field, L. D.; Wilkinson, M. P.; George, M. W. *J. Am. Chem. Soc.* **1993**, *115*, 8627. (g) Geftakis, S.; Ball, G. E. *J. Am. Chem. Soc.* **1998**, *120*, 9953. (h) Schultz, R. H.; Bengali, A. A.; Tauber, M. J.; Weiller, B. H.; Wasserman, E. P.; Kyle, K. R.; Moore, C. B.; Bergman, R. G. *J. Am. Chem. Soc.* **1994**, *116*, 1369. (i) Bernskoetter, W. H.; Schauer, C. K.; Goldberg, K. I.; Brookhart, M. *Science* **2009**, *326*, 553. (15) (a) Stahl, S. S.; Labinger, J. A.; Bercaw, J. E. *Angew. Chem., Int. Ed.* **1998**, *37*, 2180. (b) Chin, R. M.; Dong, L.; Duckett, S. B.; Jones, W. D. *Organometallics* **1992**, *11*, 871. (c) Chin, R. M.; Dong, L.; Duckett, S. B.; Partridge, M. G.; Jones, W. D.; Perutz, R. N. *J. Am. Chem. Soc.* **1993**, *115*, 7685. (d) Jones, W. D.; Feher, F. J. *J. Am. Chem. Soc.* **1986**, *108*, 4814. (16) (a) Vigalok, A.; Uzan, O.; Shimon, L. J. W.; Ben-David, Y.; Martin, J. M. L.; Milstein, D. *J. Am. Chem. Soc.* **1998**, *120*, 12539. (b) Johansson, L.; Tilset, M.; Labinger, J. A.; Bercaw, J. E. *J. Am. Chem. Soc.* **2000**, *122*, 10846. (c) Reinartz, S.; White, P. S.; Brookhart, M.; Templeton, J. L. *J. Am. Chem. Soc.* **2001**, *123*, 12724. (17) Krumper, J. R.; Gerisch, M.; Magistrato, A.; Rothlisberger, U.; Bergman, R. G.; Tilley, T. D. *J. Am. Chem. Soc.* **2004**, *126*, 12492. (18) Parkin, G. *Acc. Chem. Res.* **2009**, *42*, 315. (19) Bengali, A. A.; Schultz, R. H.; Moore, C. B.; Bergman, R. G. *J. Am. Chem. Soc.* **1994**, *116*, 9585. (20) Moravskiy and Stille studied the reductive elimination of dimethyl–Pd complexes. Different ethane- d_0 /ethane- d_6 ratios were obtained in different solvents demonstrating the necessity of a *cis*-disposition for the two Me groups: Moravskiy, A.; Stille, J. K. *J. Am. Chem. Soc.* **1981**, *103*, 4182. (21) Abis, L.; Sen, A.; Halpern, J. *J. Am. Chem. Soc.* **1978**, *100*, 2915. (22) (a) Michelin, R. A.; Faglia, S.; Uguagliati, P. *Inorg. Chem.* **1983**, *22*, 1831. (b) McCarthy, T. J.; Nuzzo, R. G.; Whitesides, G. M. *J. Am. Chem. Soc.* **1981**, *103*, 3396. (23) A similar explanation has been offered to account for even lower values of k_H/k_D in similar processes. (a) Bell, R. P. *Discuss. Faraday Soc.* **1965**, *39*, 16. (b) Westheimer, F. H. *Chem. Rev.* **1961**, *61*, 625. (c) Uguagliati, P.; Baddley, W. H. *J. Am. Chem. Soc.* **1968**, *90*, 5446. (24) (a) Buchanan, J. M.; Stryker, J. M.; Bergman, R. G. *J. Am. Chem. Soc.* **1986**, *108*, 1537. (b) Periana, R. A.; Bergman, R. G. *J. Am. Chem. Soc.* **1986**, *108*, 7332. (c) Bullock, R. M.; Headford, C. E. L.; Hennessy, K. M.; Kegley, S. E.; Norton, J. R. *J. Am. Chem. Soc.* **1989**, *111*, 3897. (d) Parkin, G.; Bercaw, J. E. *Organometallics* **1989**, *8*, 1172. (e) Gould, G. L.; Heinekey, D. M. *J. Am. Chem. Soc.* **1989**, *111*, 5502. (f) Wang, C.; Ziller, J. W.; Flood, T. C. *J. Am. Chem. Soc.* **1995**, *117*, 1647. (g) Howart, O. W.; McAteer, C. H.; Moore, P.; Morris, G. E. *J. Chem. Soc., Dalton Trans.* **1984**, 1171. (h) Jones, W. D.; Feher, F. J. *J. Am. Chem. Soc.* **1985**, *107*, 620. (i) Wick, D. D.; Reynolds, K. A.; Jones, W. D. *J. Am. Chem. Soc.* **1999**, *121*, 3974. (j) Jensen, M. P.; Wick, D. D.; Reinartz, S.; White, P. S.; Templeton, J. L.; Goldberg, K. I. *J. Am. Chem. Soc.* **2003**, *125*, 8614.

- (k) Bullock, R. M.; Headford, C. E. L.; Kegley, S. E.; Norton, J. R. *J. Am. Chem. Soc.* **1985**, *107*, 727. (l) Bengali, A. A.; Amdtsen, B. A.; Burger, P. M.; Schultz, R. H.; Weiller, B. H.; Kyle, K. R.; Moore, C. B.; Bergman, R. G. *Pure Appl. Chem.* **1995**, *67*, 281. (m) Jones, W. D.; Hessel, E. T. *J. Am. Chem. Soc.* **1992**, *114*, 6087.
- (25) Cheng, T.-Y.; Bullock, R. M. *J. Am. Chem. Soc.* **1999**, *121*, 3150.
- (26) Janak, K. E.; Churchill, D. G.; Parkin, G. *Chem. Commun.* **2003**, 22.
- (27) Northcutt, T. O.; Wick, D. D.; Vetter, A. J.; Jones, W. D. *J. Am. Chem. Soc.* **2001**, *123*, 7257.
- (28) Jones, W. D.; Feher, F. J. *J. Am. Chem. Soc.* **1984**, *106*, 1650.
- (29) Jones, W. D.; Feher, F. J. *Acc. Chem. Res.* **1989**, *22*, 91.
- (30) (a) Bender, B. R. *J. Am. Chem. Soc.* **1995**, *117*, 11239. (b) Abu-Hasanayn, F.; Krogh-Jespersen, K.; Goldman, A. S. *J. Am. Chem. Soc.* **1993**, *115*, 8019. (c) Slaughter, L.-G. M.; Wolczanski, P. T.; Klinckman, T. R.; Cundari, T. R. *J. Am. Chem. Soc.* **2000**, *122*, 7953.
- (31) Janak, K. E.; Parkin, G. *J. Am. Chem. Soc.* **2003**, *125*, 6889.
- (32) Janowicz, A. H.; Bergman, R. G. *J. Am. Chem. Soc.* **1982**, *104*, 352.
- (33) Bhalla, G.; Liu, X. Y.; Oxgaard, J.; Goddard, W. A., III; Periana, R. A. *J. Am. Chem. Soc.* **2005**, *127*, 11372.
- (34) Tenn, W. J., III; Young, K. J. H.; Oxgaard, J.; Nielsen, R. J.; Goddard, W. A., III; Periana, R. A. *Organometallics* **2006**, *25*, 5173.
- (35) Oxgaard, J.; Tenn, W. J., III; Nielsen, R. J.; Periana, R. A.; Goddard, W. A., III *Organometallics* **2007**, *26*, 1565.
- (36) (a) McGhee, W. D.; Bergman, R. G. *J. Am. Chem. Soc.* **1988**, *110*, 4246. For a related isomerization with an Os complex, see: (b) Esteruelas, M. A.; Lahoz, F. J.; Oñate, E.; Oro, L. A.; Sola, E. *J. Am. Chem. Soc.* **1996**, *118*, 89.
- (37) Peterson, T. H.; Golden, J. T.; Bergman, R. G. *J. Am. Chem. Soc.* **2001**, *123*, 455.
- (38) Stoutland, P. O.; Bergman, R. G. *J. Am. Chem. Soc.* **1988**, *110*, 5732.
- (39) Smith, K. M.; Poli, R.; Harvey, J. N. *Chem.—Eur. J.* **2001**, *7*, 1679.
- (40) Anstey, M. R.; Yung, C. M.; Du, J.; Bergman, R. G. *J. Am. Chem. Soc.* **2007**, *129*, 776.
- (41) Li, L.; Brennessel, W. W.; Jones, W. D. *Organometallics* **2009**, *28*, 3492.
- (42) Li, X.; Vogel, T.; Incarvito, C. D.; Crabtree, R. H. *Organometallics* **2005**, *24*, 62.
- (43) McGhee, W. D.; Hollander, F. J.; Bergman, R. G. *J. Am. Chem. Soc.* **1988**, *110*, 8428.
- (44) Esswein, A. J.; Veige, A. S.; Piccoli, P. M. B.; Schultz, A. J.; Nocera, D. G. *Organometallics* **2008**, *27*, 1073.
- (45) Choi, J.; Choliy, Y.; Zhang, X.; Emge, T. J.; Krogh-Jespersen, K.; Goldman, A. S. *J. Am. Chem. Soc.* **2009**, *131*, 15627.
- (46) The mechanisms of Pt C—H activation have been vigorously investigated using experimental and computational methods, and these studies have been extensively reviewed. (a) Rendina, L. M.; Puddephatt, R. J. *Chem. Rev.* **1997**, *97*, 1735. (b) Lersch, M.; Tilset, M. *Chem. Rev.* **2005**, *105*, 2471. (c) Fekl, U.; Goldberg, K. I. *Adv. Inorg. Chem.* **2003**, *54*, 259. For a review on computational studies of mechanistic Pt and Pd chemistry, see: (d) Dedieu, A. *Chem. Rev.* **2000**, *100*, 543.
- (47) (a) Romeo, R.; Minniti, D.; Lanza, S.; Uguagliati, P.; Belluco, U. *Inorg. Chem.* **1978**, *17*, 2813. (b) Belluco, U.; Michelin, R. A.; Uguagliati, P. *J. Organomet. Chem.* **1983**, *250*, 565. (c) Romeo, R.; Plutino, M. R.; Elding, L. I. *Inorg. Chem.* **1997**, *36*, 5909.
- (48) Kondo, Y.; Ishikawa, M.; Ishihara, K. *Inorg. Chim. Acta* **1996**, *241*, 81.
- (49) Romeo, R.; Minniti, D.; Lanza, S. *J. Organomet. Chem.* **1979**, *165*, C36.
- (50) (a) Stahl, S. S.; Labinger, J. A.; Bercaw, J. E. *J. Am. Chem. Soc.* **1996**, *118*, 5961. (b) Stahl, S. S.; Labinger, J. A.; Bercaw, J. E. *J. Am. Chem. Soc.* **1995**, *117*, 9371. (c) Holtcamp, M. W.; Labinger, J. A.; Bercaw, J. E. *Inorg. Chim. Acta* **1997**, *265*, 117.
- (51) Bercaw, J. E.; Chen, G. S.; Labinger, J. A. *J. Am. Chem. Soc.* **2008**, *130*, 17654.
- (52) Romeo, R.; D'Amico, G. *Organometallics* **2006**, *25*, 3435.
- (53) Bennett, B. L.; Hoerter, J. M.; Houliis, J. F.; Roddick, D. M. *Organometallics* **2000**, *19*, 615.
- (54) Butikofer, J. L.; Hoerter, J. M.; Peters, R. G.; Roddick, D. M. *Organometallics* **2004**, *23*, 400.
- (55) Fekl, U.; Zahl, A.; van Eldik, R. *Organometallics* **1999**, *18*, 4156 and references therein.
- (56) Crumpton-Bregel, D. M.; Goldberg, K. I. *J. Am. Chem. Soc.* **2003**, *125*, 9442.
- (57) (a) Gerdes, G.; Chen, P. *Organometallics* **2003**, *22*, 2217. (b) Heiberg, H.; Johansson, L.; Gropen, O.; Ryan, O. B.; Swang, O.; Tilset, M. *J. Am. Chem. Soc.* **2000**, *122*, 10831.
- (58) Stahl, S. S.; Labinger, J. A.; Bercaw, J. E.; Tilset, M. *Organometallics* **2006**, *25*, 805.
- (59) Zhong, H. A.; Labinger, J. A.; Bercaw, J. E. *J. Am. Chem. Soc.* **2002**, *124*, 1378.
- (60) Ackerman, L. J.; Sadighi, J. P.; Kurtz, D. M.; Labinger, J. A.; Bercaw, J. E. *Organometallics* **2003**, *22*, 3884.
- (61) Wik, B. J.; Lersch, M.; Krivokapic, A.; Tilset, M. *J. Am. Chem. Soc.* **2006**, *128*, 2682.
- (62) Chen, G. S.; Labinger, J. A.; Bercaw, J. E. *Proc. Natl. Acad. Sci. U. S. A.* **2007**, *104*, 6915.
- (63) Driver, T. G.; Day, M. W.; Labinger, J. A.; Bercaw, J. E. *Organometallics* **2005**, *24*, 3644.
- (64) Heyduk, A. F.; Driver, T. G.; Labinger, J. A.; Bercaw, J. E. *J. Am. Chem. Soc.* **2004**, *126*, 15034.
- (65) Williams, T. J.; Labinger, J. A.; Bercaw, J. E. *Organometallics* **2007**, *26*, 281.
- (66) Owen, J. S.; Labinger, J. A.; Bercaw, J. E. *J. Am. Chem. Soc.* **2006**, *128*, 2005.
- (67) Driver, T. G.; Williams, T.; Labinger, J. A.; Bercaw, J. E. *Organometallics* **2007**, *26*, 294.
- (68) Bercaw, J. E.; Hazari, N.; Labinger, J. A.; Oblad, P. F. *Angew. Chem., Int. Ed.* **2008**, *47*, 9941.
- (69) Lin, B.-L.; Bhattacharyya, K. X.; Labinger, J. A.; Bercaw, J. E. *Organometallics* **2009**, *28*, 4400.
- (70) Thomas, J. C.; Peters, J. C. *J. Am. Chem. Soc.* **2003**, *125*, 8870.
- (71) Lu, C. C.; Peters, J. C. *J. Am. Chem. Soc.* **2004**, *126*, 15818.
- (72) Peters, R. G.; White, S.; Roddick, D. M. *Organometallics* **1998**, *17*, 4493.
- (73) Griffiths, D. C.; Young, G. B. *Organometallics* **1989**, *8*, 875.
- (74) Norris, C.; Reinartz, S.; White, P. S.; Templeton, J. L. *Organometallics* **2002**, *21*, 5649.
- (75) Lo, H. C.; Haskel, A.; Kapon, M.; Keinan, E. *J. Am. Chem. Soc.* **2002**, *124*, 3226.
- (76) (a) Foley, P.; Whitesides, G. M. *J. Am. Chem. Soc.* **1979**, *101*, 2732. (b) Foley, P.; DiCosimo, R.; Whitesides, G. M. *J. Am. Chem. Soc.* **1980**, *102*, 6713. (c) Ibers, J. A.; DiCosimo, R.; Whitesides, G. M. *Organometallics* **1982**, *1*, 13. (d) DiCosimo, R.; Moore, S. S.; Sowinski, A. F.; Whitesides, G. M. *J. Am. Chem. Soc.* **1982**, *104*, 124. (e) Whitesides, G. M. *Pure Appl. Chem.* **1981**, *53*, 287.
- (77) Holcomb, H. L.; Nakanishi, S.; Flood, T. C. *Organometallics* **1996**, *15*, 4228.
- (78) Ruhland, K.; Eberhardt, H. *J. Organomet. Chem.* **2005**, *690*, 5215.
- (79) (a) Shul'pin, G. B.; Nizova, G. V.; Nikitaev, A. T. *J. Organomet. Chem.* **1984**, *216*, 115. For a review on the chemistry of stable Pt(IV) hydrides, see: (b) Puddephatt, R. J. *Coord. Chem. Rev.* **2001**, *219*–221, 157.
- (80) Li, J.-J.; Giri, R.; Yu, J.-Q. *Tetrahedron* **2008**, *64*, 6979.
- (81) van der Boom, M. E.; Kraatz, H.-B.; Hassner, L.; Ben-David, Y.; Milstein, D. *Organometallics* **1999**, *18*, 3873.
- (82) Asplund, M. C.; Snee, P. T.; Yeston, J. S.; Wilkens, M. J.; Payne, C. K.; Yang, H.; Kotz, K. T.; Frei, H.; Bergman, R. G.; Harris, C. B. *J. Am. Chem. Soc.* **2002**, *124*, 10605.
- (83) Vetter, A. J.; Flaschenriem, C.; Jones, W. D. *J. Am. Chem. Soc.* **2005**, *127*, 12315.

- (84) (a) Wei, C. S.; Jiménez-Hoyos, C. A.; Videa, M. F.; Hartwig, J. F.; Hall, M. B. *J. Am. Chem. Soc.* **2010**, *132*, 3078. (b) Chen, H. Y.; Schlecht, S.; Semple, T. C.; Hartwig, J. F. *Science* **2000**, *287*, 1995.
- (85) Selmeczy, A. D.; Jones, W. D.; Osman, R.; Perutz, R. N. *Organometallics* **1995**, *14*, S677.
- (86) Demonceau, A.; Noels, A. F.; Costa, J. L.; Hubert, A. J. *J. Mol. Catal.* **1990**, *58*, 21.
- (87) Wang, P.; Adams, J. J. *J. Am. Chem. Soc.* **1994**, *116*, 3296.
- (88) Nakamura, E.; Yoshikai, N.; Yamanaka, N. *J. Am. Chem. Soc.* **2002**, *124*, 7181.
- (89) Park, C. P.; Nagle, A.; Yoon, C. H.; Chen, C.; Jung, K. W. *J. Org. Chem.* **2009**, *74*, 6231.
- (90) (a) Wayland, B. B.; Ba, S.; Sherry, A. E. *J. Am. Chem. Soc.* **1991**, *113*, 5305. (b) Sherry, A. E.; Wayland, B. B. *J. Am. Chem. Soc.* **1990**, *112*, 1259.
- (91) (a) Cui, W.; Zhang, P.; Wayland, B. B. *J. Am. Chem. Soc.* **2003**, *125*, 4994. (b) Cui, W.; Wayland, B. B. *J. Am. Chem. Soc.* **2004**, *126*, 8266.
- (92) Ito, J.-I.; Nishiyama, H. *Eur. J. Inorg. Chem.* **2007**, 1114.
- (93) van der Boom, M. E.; Higgit, C. L.; Milstein, D. *Organometallics* **1999**, *18*, 2413.
- (94) Boese, W. T.; Goldman, A. S. *Organometallics* **1991**, *10*, 782.
- (95) Bercaw, J. E.; Hazari, N.; Labinger, J. A. *Organometallics* **2009**, *28*, 5489.
- (96) For a review on the direct functionalization of N-heterocycles, see: Lewis, J. C.; Bergman, R. G.; Ellman, J. A. *Acc. Chem. Res.* **2008**, *41*, 1013.
- (97) Wiedemann, S. H.; Lewis, J. C.; Ellman, J. A.; Bergman, R. G. *J. Am. Chem. Soc.* **2006**, *128*, 2452.
- (98) Rosini, G. P.; Soubra, S.; Vixamar, M.; Wang, S.; Goldman, A. S. *J. Organomet. Chem.* **1998**, *554*, 41.
- (99) Krug, C.; Hartwig, J. F. *J. Am. Chem. Soc.* **2002**, *124*, 1674.
- (100) Shen, Z.; Dornan, P. K.; Khan, H. A.; Woo, T. K.; Dong, V. M. *J. Am. Chem. Soc.* **2009**, *131*, 1077.
- (101) Hyatt, I. F. D.; Anderson, H. K.; Morehead, A. T.; Sargent, A. L. *Organometallics* **2008**, *27*, 135.
- (102) For a review, see: Foley, N. A.; Lee, J. P.; Ke, Z.; Gunnoe, T. B.; Cundari, T. R. *Acc. Chem. Res.* **2009**, *42*, 585.
- (103) Lail, M.; Bell, C. M.; Conner, D.; Cundari, T. R.; Gunnoe, T. B.; Petersen, J. E. *Organometallics* **2004**, *23*, 5007.
- (104) Foley, N. A.; Lail, M.; Lee, J. P.; Ke, Z.; Gunnoe, T. B.; Cundari, T. R.; Petersen, J. E. *J. Am. Chem. Soc.* **2007**, *129*, 6765.
- (105) Yi, C. S.; Yun, S. Y. *J. Am. Chem. Soc.* **2005**, *127*, 17000.
- (106) Hsu, G. C.; Kosar, W. P.; Jones, W. D. *Organometallics* **1994**, *13*, 385.
- (107) Kakiuchi, F.; Murai, S. *Acc. Chem. Res.* **2002**, *35*, 826.
- (108) Kakiuchi, F.; Ohtaki, S.; Sonoda, M.; Chatani, N.; Murai, S. *Chem. Lett.* **2001**, 918.
- (109) This method to measure ^{13}C -KIEs was developed by Singleton. See: (a) Singleton, D. A.; Thomas, A. A. *J. Am. Chem. Soc.* **1995**, *117*, 9357. (b) Frantz, D. E.; Singleton, D. A.; Snyder, J. P. *J. Am. Chem. Soc.* **1997**, *119*, 3383.
- (110) Yi, C. S.; Lee, D. W. *Organometallics* **2009**, *28*, 4266.
- (111) Similar studies to the reported in this section have been carried out using mainly lanthanide derived complexes. See: (a) Gribkov, D. V.; Hultsch, K. C.; Hampel, F. *J. Am. Chem. Soc.* **2006**, *128*, 3748. (b) Stubbert, B. D.; Marks, T. J. *J. Am. Chem. Soc.* **2007**, *129*, 6149. (c) Gagné, M. R.; Stern, C. L.; Marks, T. J. *J. Am. Chem. Soc.* **1992**, *114*, 275. (d) Giardello, M. A.; Conticello, V. P.; Brard, L.; Gagné, M. R.; Marks, T. J. *J. Am. Chem. Soc.* **1994**, *116*, 10241.
- (112) Reviews: (a) Müller, T. E.; Beller, M. *Chem. Rev.* **1998**, *98*, 675. (b) Taube, R. In *Applied Homogeneous Catalysis with Organometallic Compounds*; Cornils, B., Herrmann, W. A., Eds.; VCH: New York, 1996. (c) Brunet, J. J.; Neibecker, D. In *Catalytic Heterofunctionalization from Hydroamination to Hydrozirconation*; Togni, A., Grützmacher, H., Eds.; Wiley-VCH: New York, 2001.
- (113) Yi, C. S.; Yun, S. Y. *Org. Lett.* **2005**, *7*, 2181.
- (114) Yi, C. S.; Yun, S. Y. *Organometallics* **2004**, *23*, 5392.
- (115) Yi, C. S.; Zhang, J. *Chem. Commun.* **2008**, 2349.
- (116) Hesp, K. D.; Tobisch, S.; Stradiotto, M. *J. Am. Chem. Soc.* **2010**, *132*, 413.
- (117) For a related work using Pd complexes and ^{13}C -KIEs, see: Vo, L. K.; Singleton, D. A. *Org. Lett.* **2004**, *6*, 2469.
- (118) Seo, S.-Y.; Yu, X.; Marks, T. J. *J. Am. Chem. Soc.* **2009**, *131*, 263.
- (119) Yi, C. S.; Yun, S. Y.; He, Z. *Organometallics* **2003**, *22*, 3031.
- (120) Lail, M.; Gunnoe, T. B.; Barakat, K. A.; Cundari, T. R. *Organometallics* **2005**, *24*, 1301.
- (121) Takaoka, A.; Mendiratta, A.; Peters, J. C. *Organometallics* **2009**, *28*, 3744.
- (122) Waltz, K. M.; Hartwig, J. F. *J. Am. Chem. Soc.* **2000**, *122*, 11358.
- (123) Hartwig used KIEs as indirect evidences to discard a radical mechanism in the photochemical reaction of Fe, Mn, and Re complexes **177** with arenes and alkenes to form aryl- and vinylboronate esters in moderate to high yields. See: Waltz, K. M.; Muhoro, C. N.; Hartwig, J. F. *Organometallics* **1999**, *18*, 3383.
- (124) Schaller, C. P.; Bonanno, J. B.; Wolczanski, P. T. *J. Am. Chem. Soc.* **1994**, *116*, 4133.
- (125) Schaller, C. P.; Cummins, C. C.; Wolczanski, P. T. *J. Am. Chem. Soc.* **1996**, *118*, 591.
- (126) Cummins, C. C.; Baxter, S. M.; Wolczanski, P. T. *J. Am. Chem. Soc.* **1988**, *110*, 8731.
- (127) Bennett, J. L.; Wolczanski, P. T. *J. Am. Chem. Soc.* **1997**, *119*, 10696.
- (128) Cummins, C. C.; Schaller, C. P.; van Duyne, G. D.; Wolczanski, P. T.; Chan, A. W. E.; Hoffmann, R. *J. Am. Chem. Soc.* **1991**, *113*, 2985.
- (129) Schaller, C. P.; Wolczanski, P. T. *Inorg. Chem.* **1993**, *32*, 131.
- (130) Abbott, J. K. C.; Li, L.; Xue, Z.-L. *J. Am. Chem. Soc.* **2009**, *131*, 8246.
- (131) Hoyt, H. M.; Bergman, R. G. *Angew. Chem., Int. Ed.* **2007**, *46*, 5580.
- (132) Fryzuk, M. D.; Duval, P. B.; Mao, S. S. H.; Zaworotko, M. J.; MacGillivray, L. R. *J. Am. Chem. Soc.* **1999**, *121*, 2478.
- (133) Coles, N.; Harris, M. C. J.; Whitby, R. J.; Blaggt, J. *Organometallics* **1994**, *13*, 190.
- (134) Mayer, J. M.; Curtis, C. J.; Bercaw, J. E. *J. Am. Chem. Soc.* **1983**, *105*, 2651.
- (135) Chirik, P. J.; Bercaw, J. E. *Organometallics* **2005**, *24*, 5407.
- (136) Lin, Z.; Marks, T. J. *J. Am. Chem. Soc.* **1990**, *112*, 5515.
- (137) Piers, W. E.; Bercaw, J. E. *J. Am. Chem. Soc.* **1990**, *112*, 9406.
- (138) Burger, B. J.; Thompson, M. E.; Cotter, W. D.; Bercaw, J. E. *J. Am. Chem. Soc.* **1990**, *112*, 1566.
- (139) Veghini, D.; Henling, L. M.; Burkhardt, T. J.; Bercaw, J. E. *J. Am. Chem. Soc.* **1999**, *121*, 564.
- (140) Bradley, C. A.; Veiros, L. F.; Pun, D.; Lobkovsky, E.; Keresztes, I.; Chirik, P. J. *J. Am. Chem. Soc.* **2006**, *128*, 16600.
- (141) Buchwald, S. L.; Nielsen, R. B. *J. Am. Chem. Soc.* **1988**, *110*, 3171.
- (142) Schock, L. E.; Brock, C. P.; Marks, T. J. *Organometallics* **1987**, *6*, 232.
- (143) Deckers, P. J. W.; Hessen, B. *Organometallics* **2002**, *21*, 5564.
- (144) (a) Sadow, A. D.; Tilley, T. D. *J. Am. Chem. Soc.* **2003**, *125*, 9462. (b) Sadow, A. D.; Tilley, T. D. *J. Am. Chem. Soc.* **2002**, *124*, 6814.
- (145) Brown, S. N.; Myers, A. W.; Fulton, J. R.; Mayer, J. M. *Organometallics* **1998**, *17*, 3364.
- (146) Tahmassebi, S. K.; McNeil, W. S.; Mayer, J. M. *Organometallics* **1997**, *16*, 5342.
- (147) Watson, W. H.; Wu, G.; Richmond, M. G. *Organometallics* **2006**, *25*, 930.
- (148) Harper, T. G. P.; Shinomoto, R. S.; Deming, M. A.; Flood, T. C. *J. Am. Chem. Soc.* **1998**, *120*, 7915.
- (149) Balzarek, C.; Weakley, T. J. R.; Tyler, D. R. *J. Am. Chem. Soc.* **2000**, *122*, 9427.
- (150) Bruno, J. W.; Smith, G. M.; Marks, T. J.; Fair, C. K.; Schultz, A. J.; Williams, J. M. *J. Am. Chem. Soc.* **1986**, *108*, 40.

- (151) Additional studies in Th complexes have been reported: (a) Fendrick, C. M.; Marks, T. J. *J. Am. Chem. Soc.* **1984**, *106*, 2214. (b) Fendrick, C. M.; Marks, T. J. *J. Am. Chem. Soc.* **1986**, *108*, 425.
- (152) Thompson, M. E.; Baxter, S. M.; Bulls, A. R.; Burger, B. J.; Nolan, M. C.; Santarsiero, B. B.; Schaefer, W. P.; Bercaw, J. E. *J. Am. Chem. Soc.* **1987**, *109*, 203.
- (153) (a) Parkin, G.; Bunel, E.; Burger, B. J.; Trimmer, M. S.; van Asselt, A.; Bercaw, J. E. *J. Mol. Catal.* **1987**, *41*, 21. (b) van Asselt, A.; Burger, B. J.; Gibson, V. G.; Bercaw, J. E. *J. Am. Chem. Soc.* **1986**, *108*, 5347. (c) Nelson, J. E.; Parkin, G.; Bercaw, J. E. *Organometallics* **1992**, *11*, 2181.
- (154) Conroy, K. D.; Hayes, P. G.; Piers, W. E.; Parvez, M. *Organometallics* **2007**, *26*, 4464.
- (155) Zhang, S.; Piers, W. E.; Gao, X.; Parvez, M. *J. Am. Chem. Soc.* **2000**, *122*, 5499.
- (156) Castillo, I.; Tilley, T. D. *J. Am. Chem. Soc.* **2001**, *123*, 10526.
- (157) (a) McDonald, R. N.; Jones, M. T.; Chowdhury, A. K. *J. Am. Chem. Soc.* **1991**, *113*, 476. (b) McDonald, R. N.; Jones, M. T.; Chowdhury, A. K. *J. Am. Chem. Soc.* **1992**, *114*, 71. (c) Schalley, C. A.; Schröder, D.; Schwarz, H. *J. Am. Chem. Soc.* **1994**, *116*, 11089.
- (158) Woo, H.-G.; Heyn, R. H.; Tilley, T. D. *J. Am. Chem. Soc.* **1992**, *114*, 5698.
- (159) Woo, H.-G.; Tilley, T. D. *J. Am. Chem. Soc.* **1989**, *111*, 8043.
- (160) Woo, H.-G.; Walzer, J. F.; Tilley, T. D. *J. Am. Chem. Soc.* **1992**, *114*, 7047.
- (161) Sadow, A. D.; Tilley, T. D. *J. Am. Chem. Soc.* **2005**, *127*, 643.
- (162) Klei, S. R.; Tilley, T. D.; Bergman, R. G. *Organometallics* **2002**, *21*, 3376.
- (163) (a) Hart-Davis, A. J.; Graham, W. A. G. *J. Am. Chem. Soc.* **1971**, *93*, 4388. (b) Green, J. C.; Green, M. L. H.; Morley, C. P. *Organometallics* **1985**, *4*, 1302.
- (164) Ankianiec, B. C.; Christou, V.; Hardy, D. T.; Thomson, S. K.; Young, G. *J. Am. Chem. Soc.* **1994**, *116*, 9963.
- (165) Dakin, L. A.; Ong, P. C.; Panek, J. S.; Staples, R. J.; Stavropoulos, P. *Organometallics* **2000**, *19*, 2896.
- (166) Landais, Y.; Parra-Rapado, L.; Planchenaut, D.; Weber, V. *Tetrahedron Lett.* **1997**, *38*, 229.
- (167) (a) Hostetler, M. J.; Bergman, R. G. *J. Am. Chem. Soc.* **1992**, *114*, 787. (b) Hostetler, M. J.; Bergman, R. G. *J. Am. Chem. Soc.* **1992**, *114*, 7629. These studies were further extended to the alkene hydro-sylation/isomerization catalyzed by Ir complexes, see: (c) Hostetler, M. J.; Butts, M. D.; Bergman, R. G. *Organometallics* **1993**, *12*, 65.
- (168) Zheng, G. Z.; Chan, T. H. *Organometallics* **1995**, *14*, 70.
- (169) Ojima, I.; Kogure, T.; Kumagai, M.; Horiuchi, S.; Sato, T. *J. Organomet. Chem.* **1976**, *122*, 83.
- (170) Schneider, N.; Finger, M.; Haferkemper, C.; Bellemin-Laponnaz, S.; Hofmann, P.; Gade, L. H. *Angew. Chem., Int. Ed.* **2009**, *48*, 1609.
- (171) Schneider, N.; Finger, M.; Haferkemper, C.; Bellemin-Laponnaz, S.; Hofmann, P.; Gade, L. H. *Chem.—Eur. J.* **2009**, *15*, 11515.
- (172) Ison, E. A.; Trivedi, E. R.; Corbin, R. A.; Abu-Omar, M. M. *J. Am. Chem. Soc.* **2005**, *127*, 15374.
- (173) Nolin, K. A.; Krumper, J. R.; Pluth, M. D.; Bergman, R. G.; Toste, F. D. *J. Am. Chem. Soc.* **2007**, *129*, 14684.
- (174) Issenhuth, J.-T.; Notter, F.-P.; Dagorne, S.; Dedieu, A.; Bellemin-Laponnaz, S. *Eur. J. Inorg. Chem.* **2010**, 529.
- (175) Jiang, Y.; Blaque, O.; Fox, T.; Frech, C. M.; Berke, H. *Chem.—Eur. J.* **2009**, *15*, 2121.
- (176) Rendler, S.; Oestreich, M.; Butts, C. P.; Lloyd-Jones, G. C. *J. Am. Chem. Soc.* **2007**, *129*, 502.
- (177) Selected reviews on homogeneous hydrogenation: (a) *Handbook of Homogeneous Hydrogenation*; de Vries, J. G.; Elsevier, C. J., Eds.; Wiley-VCH, Weinheim, Germany, 2007. (b) Gladiali, S.; Alberico, E. *Chem. Soc. Rev.* **2006**, *35*, 226. (c) Samec, J. S. M.; Bäckvall, J.-E.; Andersson, P. G.; Brandt, P. *Chem. Soc. Rev.* **2006**, *35*, 237. (d) Clapham, S. E.; Hadzovic, A.; Morris, R. H. *Coord. Chem. Rev.* **2004**, *248*, 2201. (e) Noyori, R.; Hashiguchi, S. *Acc. Chem. Res.* **1997**, *30*, 97. (f) Zassinovich, G.; Mestroni, G.; Gladiali, S. *Chem. Rev.* **1992**, *92*, 1051. (g) Hauwert, P.; Maestri, G.; Sprengers, J. W.; Catellani, M.; Elsevier, C. J. *Angew. Chem., Int. Ed.* **2008**, *47*, 3223.
- (178) The active reducing agent in each of these catalytic systems contains electronically coupled acidic and hydridic hydrogens, which work in concert to efficiently hydrogenate polar unsaturated substrates. (a) Shvo, Y.; Czarkie, D.; Rahamim, Y.; Chodash, D. F. *J. Am. Chem. Soc.* **1986**, *108*, 7400. (b) Menashe, N.; Salant, E.; Shvo, Y. *J. Organomet. Chem.* **1996**, *514*, 97.
- (179) Menashe, N.; Shvo, Y. *Organometallics* **1991**, *10*, 3885.
- (180) (a) Casey, C. P.; Singer, S. W.; Powell, D. R.; Hayashi, R. K.; Kavana, M. *J. Am. Chem. Soc.* **2001**, *123*, 1090. Additional experiments and intermediate trapping: (b) Casey, C. P.; Bikzhanova, G. A.; Cui, Q.; Guzei, I. A. *J. Am. Chem. Soc.* **2005**, *127*, 14062. (c) Casey, C. P.; Clark, T. B.; Guzei, I. A. *J. Am. Chem. Soc.* **2007**, *129*, 11821. (d) Casey, C. P.; Beetner, S. E.; Johnson, J. B. *J. Am. Chem. Soc.* **2008**, *130*, 2285. (e) Casey, C. P.; Johnson, J. B.; Singer, S. W.; Cui, Q. *J. Am. Chem. Soc.* **2005**, *127*, 3100.
- (181) Samec, J. S. M.; Bäckvall, J.-E. *Chem.—Eur. J.* **2002**, *8*, 2955.
- (182) Thalén, K. L.; Zhao, D.; Sortais, J.-B.; Paetzold, J.; Hoben, C.; Bäckvall, J.-E. *Chem.—Eur. J.* **2009**, *15*, 3403.
- (183) (a) Casey, C. P.; Johnson, J. B. *J. Org. Chem.* **2003**, *68*, 1998. (b) Casey, C. P.; Johnson, J. B. *J. Am. Chem. Soc.* **2005**, *127*, 1883. (c) Casey, C. P.; Bikzhanova, G. A.; Guzei, I. A. *J. Am. Chem. Soc.* **2006**, *128*, 2286.
- (184) (a) Il, A. H.; Johnson, J. B.; Bäckvall, J. E. *Chem. Commun.* **2003**, 1652. (b) Samec, J. S. M.; Il, A. H.; Bäckvall, J. E. *Chem. Commun.* **2004**, 2748. (c) Samec, J. S. M.; Il, A. H.; Åberg, J. B.; Privalov, T.; Eriksson, L.; Bäckvall, J. E. *J. Am. Chem. Soc.* **2006**, *128*, 14293.
- (185) Comax-Vives, A.; Ujaque, G.; Lledós, A. *Organometallics* **2007**, *26*, 4136. (b) Comax-Vives, A.; Ujaque, G.; Lledós, A. *J. Mol. Struct.: THEOCHEM* **2009**, *903*, 123.
- (186) Casey and Johnson reported that the addition of water to THF led to a decrease of the RuD kinetic isotope effect with a concomitant increase of the OD kinetic isotope effect. The combined isotope effect also was found to increase. In dry THF (at 22 °C) the individual KIEs were 2.60 (0.09 for RuD and 1.30 ± 0.02 for OD), whereas the combined isotope effect was 3.38 ± 0.19. Conversely, addition of water (0.120 mol/L) led to values of 1.32 ± 0.11 for RuD and 2.99 ± 0.35 for OD, with a value of 4.25 ± 0.62 for the combined isotope effect. Casey, C. P.; Johnson, J. B. *Can. J. Chem.* **2005**, *83*, 1339.
- (187) Johnson, J. B.; Bäckvall, J. E. *J. Org. Chem.* **2003**, *68*, 7681.
- (188) Casey, C. P.; Guan, H. *J. Am. Chem. Soc.* **2009**, *131*, 2499.
- (189) (a) Casey, C. P.; Strotman, N. A.; Beetner, S. E.; Johnson, J. B.; Priebe, D. C.; Guzei, I. A. *Organometallics* **2006**, *25*, 1236. (b) Casey, C. P.; Strotman, N. A.; Beetner, S. E.; Johnson, J. B.; Priebe, D. C.; Vos, T. E.; Khodavandi, B.; Guzei, I. A. *Organometallics* **2006**, *25*, 1230.
- (190) Selected revisions on AHT: (a) Peris, E.; Crabtree, R. H. *Coord. Chem. Rev.* **2004**, *248*, 2239. (b) Ikariya, T.; Murata, K.; Noyori, R. *Org. Biomol. Chem.* **2006**, *4*, 393. (c) Mery, D.; Astruc, D. *Coord. Chem. Rev.* **2006**, *250*, 1965.
- (191) (a) Hashiguchi, S.; Fujii, A.; Takehara, J.; Ikariya, T.; Noyori, R. *J. Am. Chem. Soc.* **1995**, *117*, 7562. (b) Yamakawa, M.; Ito, H.; Noyori, R. *J. Am. Chem. Soc.* **2000**, *122*, 1466. (c) Noyori, R.; Yamakawa, M.; Hashiguchi, S. *J. Org. Chem.* **2001**, *66*, 7931.
- (192) Xiaofeng, W. X.; Liu, J.; Di Tommaso, D.; Iggo, J. A.; Catlow, C. R. A.; Bacsá, J.; Xiao, J. *Chem.—Eur. J.* **2008**, *14*, 7699.
- (193) Key references: (a) Noyori, R.; Ohkuma, T. *Pure Appl. Chem.* **1999**, *71*, 1493. (b) Noyori, R.; Ohkuma, T. *Angew. Chem., Int. Ed.* **2001**, *40*, 40.
- (194) Sandoval, C. A.; Ohkuma, T.; Muniz, K.; Noyori, R. *J. Am. Chem. Soc.* **2003**, *125*, 13490.
- (195) Zimmer-De Iulius, M.; Morris, R. H. *J. Am. Chem. Soc.* **2009**, *131*, 11263.
- (196) Kitamura, M.; Tsukamoto, M.; Bessho, Y.; Yoshimura, M.; Kobs, U.; Widhalm, M.; Noyori, R. *J. Am. Chem. Soc.* **2002**, *124*, 6649.
- (197) Yi, C. S.; He, Z.; Guzei, I. A. *Organometallics* **2001**, *20*, 3641.
- (198) Resales, M.; González, A.; Alvarado, Y.; Rubio, R.; Andriollo, A.; Sánchez-Delgado, R. A. *J. Mol. Catal.* **1992**, *75*, 1.

- (199) Yamaguchi, K.; Koike, T.; Kotani, M.; Matsushita, M.; Shinachi, S.; Mizuno, N. *Chem.—Eur. J.* **2005**, *11*, 6574.
- (200) Theoretical EIE studies: (a) Janak, K. E.; Parkin, G. *Organometallics* **2003**, *22*, 4378. (b) Janak, K. E.; Shin, J. H.; Parkin, G. *J. Am. Chem. Soc.* **2004**, *126*, 13054. (c) Hascall, T.; Rabinovich, D.; Murphy, V. J.; Beachy, M. D.; Friesner, R. A.; Parkin, G. *J. Am. Chem. Soc.* **1999**, *121*, 11402. (d) Bender, B. R.; Kubas, G. J.; Jones, L. H.; Swanson, B. I.; Eckert, J.; Capps, K. B.; Hoff, C. D. *J. Am. Chem. Soc.* **1997**, *119*, 9179. For a recent article about KIEs on reactivity and structure of transition metal dihydrogen complexes, see: (e) Heinekey, D. M. *J. Label Compd. Radiopharm.* **2007**, *50*, 1063.
- (201) Rabinovich, D.; Parkin, G. *J. Am. Chem. Soc.* **1993**, *115*, 353.
- (202) (a) Zhu, G.; Janak, K. E.; Parkin, G. *Chem. Commun.* **2006**, 2501. (b) Zhou, P.; Vitale, A.; San Filippo, J.; Saunders, W. *J. Am. Chem. Soc.* **1984**, *106*, 7482.
- (203) KIEs in the addition of H₂ to Vaska's complex **303** were among the earlier values determined for an organometallic transformation: (a) Chock, P. B.; Halpern, J. *J. Am. Chem. Soc.* **1966**, *88*, 3511. (b) Strohmeier, W.; Onoda, T. *Z. Naturforsch.* **1968**, *236*, 1377. (c) Strohmeier, W.; Onoda, T. *Z. Naturforsch.* **1968**, *236*, 1527. (d) Strohmeier, W.; Onoda, T. *Z. Naturforsch.* **1969**, *246*, 515. (e) Strohmeier, W.; Muller, F. J. *Z. Naturforsch.* **1969**, *246*, 770. (f) Strohmeier, W.; Muller, F. J. *Z. Naturforsch.* **1969**, *246*, 931. (g) Strohmeier, W.; Onoda, T. *Z. Naturforsch.* **1969**, *246*, 1185. (h) Vaska, L.; Werneke, M. F. *Trans. N. Y. Acad. Sci.* **1971**, *31*, 70. (i) Vaska, L. *Acc. Chem. Res.* **1968**, *1*, 335. (j) Paterniti, D. P.; Roman, P. J.; Atwood, J. D. *Organometallics* **1997**, *16*, 3371.
- (204) Janak, K. E.; Parkin, G. *J. Am. Chem. Soc.* **2003**, *125*, 13219.
- (205) Abu-Hasanayn, F.; Goldman, A. S.; Krogh-Jespersen, K. *J. Phys. Chem.* **1993**, *97*, 5890.
- (206) Parkin, G. *J. Label Compd. Radiopharm.* **2007**, *50*, 1088.
- (207) Hanna, T. A.; Lobkovsky, E.; Chirik, P. J. *Inorg. Chem.* **2007**, *46*, 2359.
- (208) Ma, K.; Piers, W. E.; Parvez, M. *J. Am. Chem. Soc.* **2006**, *128*, 3303.
- (209) Bradley, C. A.; Lobkovsky, E.; Keresztes, I.; Chirik, P. J. *J. Am. Chem. Soc.* **2006**, *128*, 6454.
- (210) Jones, W. D.; Kuykendall, V. L.; Selmecezy, A. D. *Organometallics* **1991**, *10*, 1577.
- (211) (a) Adams, R. D.; Captain, B.; Beddie, C.; Hall, M. B. *J. Am. Chem. Soc.* **2007**, *129*, 986. (b) Adams, R. D.; Captain, B.; Smith, M. D.; Beddie, C.; Hall, M. B. *J. Am. Chem. Soc.* **2007**, *129*, 5981.
- (212) (a) Dos Santos, P. C.; Igarashi, R. Y.; Lee, H. I.; Hoffman, B. M.; Seefeldt, L. C.; Dean, D. R. *Acc. Chem. Res.* **2005**, *38*, 208. (b) Eady, R. R. *Chem. Rev.* **1996**, *96*, 3013. (c) Burgess, B. K.; Lowe, D. J. *Chem. Rev.* **1996**, *96*, 2983.
- (213) Bernskoetter, W. H.; Lobkovsky, E.; Chirik, P. J. *J. Am. Chem. Soc.* **2005**, *127*, 14051.
- (214) Hanna, T. E.; Keresztes, I.; Lobkovsky, E.; Chirik, P. J. *Inorg. Chem.* **2007**, *46*, 1675.
- (215) Laplaza, C. E.; Johnson, M. J. A.; Peters, J. C.; Odom, A. H.; Kim, E.; Cummins, C. C.; George, G. N.; Pickering, I. J. *J. Am. Chem. Soc.* **1996**, *118*, 8623.
- (216) Heiden, Z. M.; Rauchfuss, T. B. *J. Am. Chem. Soc.* **2007**, *129*, 14303.
- (217) Denney, M. C.; Smythe, N. A.; Cetto, K. L.; Kemp, R. A.; Goldberg, K. I. *J. Am. Chem. Soc.* **2006**, *128*, 2508.
- (218) Hartwig, J. F.; Bhandari, S.; Rablen, P. R. *J. Am. Chem. Soc.* **1994**, *116*, 1839.
- (219) The photochemical H-transfer from R₃MH (M = Si, Ge, Sn) to the binuclear platinum(II) complex Pt₂(P₂O₅H₂)₄^{4−} has been studied. A KIE value of $k_{\text{H}}/k_{\text{D}} = 1.7$ was measured for the reaction of Bu₃SnH in accord with H atom transfer involving a linear Pt—H—Sn transition state with negligible charge transfer: Vlcek, A.; Gray, H. B. *J. Am. Chem. Soc.* **1987**, *109*, 286.
- (220) For a review about isotope effects in reactions of metal hydrides, see: Bullock, R. M. In *Transition Metal Hydrides*; Dedieu, A., Ed.; VCH: New York, 1992; Chapter 8, pp 263–307.
- (221) (a) Cordaro, J. C.; Bergman, R. G. *J. Am. Chem. Soc.* **2004**, *126*, 3432. (b) Cordaro, J. G.; Bergman, R. G. *J. Am. Chem. Soc.* **2004**, *126*, 16912.
- (222) Suenobu, T.; Guldi, D. M.; Ogo, S.; Fukuzumi, S. *Angew. Chem., Int. Ed.* **2003**, *42*, 5492.
- (223) Frost, B. J.; Mebi, C. A. *Organometallics* **2004**, *23*, 5317.
- (224) Rodkin, M. A.; Abramo, G. P.; Darula, K. E.; Ramage, D. L.; Santora, B. P.; Norton, J. R. *Organometallics* **1999**, *18*, 1106.
- (225) KIE data in radical hydride transfers are scarce. For example, the process of cobalt porphyrin catalyzed chain transfer in methacrylate free radical polymerizations shows a KIE > 3, indicating that hydrogen atom transfer occurs in the rds of the catalytic cycle. See: Gridnev, A. A.; Ittel, S. D.; Wayland, B. B.; Fryd, M. *Organometallics* **1996**, *15*, 5116.
- (226) (a) Basallote, M. G.; Durán, J.; Fernández-Trujillo, M. J.; Máñez, M. A.; Rodríguez de la Torre, J. J. *Chem. Soc., Dalton Trans.* **1993**, 3431. (b) Basallote, M. G.; Durán, J.; Fernández-Trujillo, M. J.; Máñez, M. A.; Rodríguez de la Torre, J. J. *Chem. Soc., Dalton Trans.* **1998**, 2205. (c) Basallote, M. G.; Durán, J.; Fernández-Trujillo, M. J.; Máñez, M. A. *J. Organomet. Chem.* **2000**, *69*, 29.
- (227) Henderson, R. A.; Oglieve, K. E. *J. Chem. Soc., Dalton Trans.* **1993**, 3431.
- (228) Cheng, T.-Y.; Bullock, R. M. *Organometallics* **2002**, *21*, 2325.
- (229) Cheng, T.-Y.; Brunschwig, B. S.; Bullock, R. M. *J. Am. Chem. Soc.* **1998**, *120*, 13121.
- (230) Abu-Hasanayn, F.; Coldman, M. E.; Goldman, A. S. *J. Am. Chem. Soc.* **1992**, *114*, 2520.
- (231) Fristrup, P.; Kreis, M.; Palmelund, A.; Norrby, P.-O.; Madsen, R. *J. Am. Chem. Soc.* **2008**, *130*, 5206.
- (232) Anslyn, E. V.; Green, M.; Nicola, G.; Rosenberg, E. *Organometallics* **1991**, *10*, 2600.
- (233) Pribich, D. C.; Rosenberg, E. *Organometallics* **1988**, *7*, 1741.
- (234) Evans, J.; Schwartz, J.; Urquhart, P. W. *J. Organomet. Chem.* **1974**, *87*, C37.
- (235) (a) Whitesides, T. H.; Nedan, J. P. *J. Am. Chem. Soc.* **1973**, *95*, 5811. (b) Chatt, J.; Coffey, R. B.; Gough, A.; Thompson, D. T. *J. Chem. Soc. A* **1968**, 190. (c) Whitesides, G.-M.; Gaasch, J. F.; Stedronsky, E. R. *J. Am. Chem. Soc.* **1972**, *94*, 5258.
- (236) Ozawa, F.; Ito, T.; Yamamoto, A. *J. Am. Chem. Soc.* **1980**, *102*, 6457.
- (237) Ikariya, T.; Yamamoto, A. *J. Organomet. Chem.* **1976**, *120*, 257.
- (238) This irreversible behavior of Pd complexes contrasts with the reversibility of the thermolysis of the platinum analogues, see: Komiya, S.; Yamamoto, T.; Yamamoto, A. *Chem. Lett.* **1978**, 1273.
- (239) McCarthy, T. J.; Nuzzo, R. G.; Whitesides, G. M. *J. Am. Chem. Soc.* **1981**, *103*, 3396.
- (240) A similar value of $k_{\text{H}}/k_{\text{D}} = 3.3$ was determined for elimination of CH₄/CD₄ from (Ph₃P)₂Pt(H,D)CH₃. See ref 21.
- (241) McCarthy, T. J.; Nuzzo, R. G.; Whitesides, G. M. *J. Am. Chem. Soc.* **1981**, *103*, 1676.
- (242) Komiya, S.; Morimoto, Y.; Yamamoto, A.; Yamamoto, T. *Organometallics* **1982**, *1*, 1528.
- (243) Blum, O.; Milstein, D. *J. Am. Chem. Soc.* **1995**, *117*, 4582.
- (244) An additional attractive at that time was that the mechanistic studies of β -hydride eliminations from octahedral alkyl complexes were rare and the use of KIEs was even more scarce.
- (245) For η^5 -CpFe(CO)(PPh₃)(alkyl) complexes, see: (a) Reger, D. L.; Culbenton, E. C. *J. Am. Chem. Soc.* **1976**, *98*, 2789. For η^5 -CpCo(PPh₃)₂Me₂, see: (b) Bryndra, H. E.; Evitt, E. R.; Bergman, R. G. *J. Am. Chem. Soc.* **1980**, *102*, 4948. In both studies no KIEs were observed.
- (246) These results contrast with the lack of KIEs obtained for the β -hydride elimination in (dppe)Pt(OCH₃)₂. See: Bryndza, H. E.; Calabrese, J. C.; Marsi, M.; Roe, D. C.; Tam, W.; Bercaw, J. E. *J. Am. Chem. Soc.* **1986**, *108*, 4805.
- (247) Zhao, Z.; Hesslink, H.; Hartwig, J. F. *J. Am. Chem. Soc.* **2001**, *123*, 7220.
- (248) Blum, O.; Milstein, D. *J. Organomet. Chem.* **2000**, 593–594, 479.
- (249) Ritter, J. C. M.; Bergman, R. G. *J. Am. Chem. Soc.* **1998**, *120*, 6826.

- (250) Saura-Llamas, I.; Gladysz, J. A. *J. Am. Chem. Soc.* **1992**, *114*, 2136.
- (251) Alexanian, E. J.; Hartwig, J. F. *J. Am. Chem. Soc.* **2008**, *130*, 15627.
- (252) The transition state for *syn*- β -H elimination has nonsymmetric vibrational modes involving H and thus an associated Δ ZPE. This limits predicted max $k_{\text{H}}/k_{\text{D}} \approx 1.7$ –2.3 at 25 °C. See: More O'Ferrall, R. A. *J. Chem. Soc. B* **1970**, 785. In the transition state for *anti*- β -H elimination where H in Pd–C–C–H is transferred to general base "B", the reaction coordinate involves what approximates as symmetric stretching, and the KIE is predicted to be limited to $k_{\text{H}}/k_{\text{D}} \approx 6.8$ at 25 °C.
- (253) Brainard, R. L.; Whitesides, G. M. *Organometallics* **1985**, *4*, 1550.
- (254) Romeo, R.; Alibrandi, G.; Scolaro, L. M. *Inorg. Chem.* **1993**, *32*, 4688.
- (255) Chrisope, D. R.; Beak, P.; Saunders, W. H. *J. Am. Chem. Soc.* **1988**, *110*, 230. This paper also contains an exhaustive kinetic and computational study applying the More O'Ferrall analysis.
- (256) Takacs, J. M.; Lawson, E. C.; Clement, F. *J. Am. Chem. Soc.* **1997**, *119*, 5956.
- (257) Lloyd-Jones, G. C.; Slatford, P. A. *J. Am. Chem. Soc.* **2004**, *126*, 2690.
- (258) Gonzalez, A. A.; Zhang, K.; Nolan, S. P.; Lopez de la Vega, S. L.; Mukerjee, S. L.; Hoff, C. D.; Kubas, G. J. *Organometallics* **1988**, *7*, 2429.
- (259) Foo, T.; Bergman, R. G. *Organometallics* **1992**, *11*, 1811.
- (260) Doherty, N. M.; Bercaw, J. E. *J. Am. Chem. Soc.* **1985**, *107*, 2670.
- (261) Burke, M. L.; Madix, R. J. *J. Am. Chem. Soc.* **1991**, *113*, 3675.
- (262) Martín-Matute, B.; Åberg, J. B.; Edin, M.; Bäckvall, J.-E. *Chem.—Eur. J.* **2007**, *13*, 6063.
- (263) A recent overview: (a) Fu, G. C. *Acc. Chem. Res.* **2008**, *41*, 1555. Selected revisions: Sonogashira coupling: (b) Chinchilla, R.; Nájera, C. *Chem. Rev.* **2007**, *107*, 874. (c) Plenio, H. *Angew. Chem., Int. Ed.* **2008**, *47*, 6954. (d) Doucet, H.; Hierso, J.-C. *Angew. Chem., Int. Ed.* **2007**, *46*, 834. (e) Brandsma, L. *Synthesis of Acetylenes, Allenes and Cumulenes: Methods and Techniques*; Elsevier: Oxford, U.K., 2004; p 293. (f) Sonogashira, K. In *Metal-Catalyzed Cross-Coupling Reactions*; Diederich, F., de Meijere, A., Eds.; Wiley-VCH: Weinheim, Germany, 2004; Vol. 1, p 319. (g) Tykewinski, R. R. *Angew. Chem., Int. Ed.* **2003**, *42*, 1566. (h) Sonogashira, K. In *Handbook of Organopalladium Chemistry for Organic Synthesis*; Negishi, E., de Meijere, A., Eds.; Wiley-Interscience: New York, 2002; p 493. (i) Sonogashira, K. In *Comprehensive Organic Synthesis*; Trost, B. M.; Fleming, I., Eds. Pergamon: Oxford, U. K., 1991; Vol. 3, p 521. Suzuki–Miyaura cross-coupling: (j) Martin, R.; Buchwald, S. L. *Acc. Chem. Res.* **2008**, *41*, 1461. (k) Miyaura, N.; Chemler, S. R.; Trauner, D.; Danishefsky, S. J. *Angew. Chem., Int. Ed.* **2001**, *40*, 4544. (l) Miyaura, N.; Suzuki, A. *Chem. Rev.* **1995**, *95*, 2457. (m) Suzuki, A. *J. Organomet. Chem.* **1999**, *576*, 147. (n) Phan, N. T. S.; Van Der Sluys, M.; Jones, C. W. *Adv. Synth. Catal.* **2006**, *348*, 609. (o) Felpin, F.-X.; Ayad, T.; Mitra, S. *Eur. J. Org. Chem.* **2006**, 2679. (p) Crociani, B.; Antonaroli, S.; Marini, A.; Matteoli, U.; Scrivanti, A. *Dalton Trans.* **2006**, 2698. Stille couplings: (q) Espinet, P.; Echavarren, A. M. *Angew. Chem., Int. Ed.* **2004**, *43*, 4704 and references therein. Negishi couplings: (r) Negishi, E.-i.; Hu, Q.; Huang, Z.; Wang, G.; Yin, N. In *The Chemistry of Organozinc Compounds*; Rappoport, Z.; Marek, I., Eds.; Wiley: New York, 2006; Chapter 11. (s) Negishi, E.-i.; Anastasia, L. *Chem. Rev.* **2003**, *103*, 1979. (t) Negishi, E.-i. *Acc. Chem. Res.* **1982**, *15*, 340.
- (264) Shi, Z.; Li, B.; Wan, X.; Cheng, J.; Fang, Z.; Cao, C.; Qin, C.; Wang, Y. *Angew. Chem., Int. Ed.* **2007**, *46*, 5554.
- (265) Ljungdahl, T.; Bennur, T.; Dallas, A.; Emtenäs, H.; Mårtensson, J. *Organometallics* **2008**, *27*, 2490.
- (266) Seregin, I. V.; Ryabova, V.; Gevorgyan, V. *J. Am. Chem. Soc.* **2007**, *129*, 7742.
- (267) (a) Park, C.-H.; Ryabova, V.; Seregin, I. V.; Sromek, A. W.; Gevorgyan, V. *Org. Lett.* **2004**, *6*, 1159. (b) Chiong, H. A.; Daugulis, O. *Org. Lett.* **2007**, *9*, 1449.
- (268) Tobisu, M.; Ano, Y.; Chatani, N. *Org. Lett.* **2009**, *11*, 3250.
- (269) Selected reviews: (a) Brase, S.; de Meijere, A. In *Metal-Catalyzed Cross-Coupling Reactions*; de Meijere, A., Diederich, F., Eds.; Wiley-VCH: New York, 2004; Chapter 5. (b) Brase, S.; de Meijere, A. In *Handbook of Organopalladium Chemistry for Organic Synthesis*; Negishi, E.-i., Ed.; Wiley Interscience: New York, 2002; Chapter IV.2. (c) Heck, R. F. *Acc. Chem. Res.* **1979**, *12*, 146. (d) de Meijere, A.; Meyer, F. E. *Angew. Chem., Int. Ed. Engl.* **1994**, *33*, 2379. (e) Amatore, C.; Jutand, A. *Acc. Chem. Res.* **2000**, *33*, 314. (f) Lindhardt, A. T.; Skrydstrup, T. *Chem.—Eur. J.* **2008**, *14*, 8756. (g) Shibasaki, M.; Vogl, E. M.; Ohshima, T. *Adv. Synth. Catal.* **2004**, *346*, 1533.
- (270) (a) Knowles, J. P.; Whiting, A. *Org. Biomol. Chem.* **2007**, *5*, 31. (b) Beletskaya, I. P.; Cheprakov, A. V. *Chem. Rev.* **2000**, *100*, 3009. (c) Dounay, A. B.; Overman, L. E. *Chem. Rev.* **2003**, *103*, 2945. (d) Rothenberg, G.; Cruz, S. C.; van Strijdonck, G. P. F.; Hoefsloot, H. C. J. *Adv. Synth. Catal.* **2004**, *346*, 467. (e) Crisp, G. T. *Chem. Soc. Rev.* **1998**, *27*, 427.
- (271) Böhm, V. P. W.; Herrmann, W. A. *Chem.—Eur. J.* **2001**, *7*, 4193.
- (272) Chuprakov, S.; Rubin, M.; Gevorgyan, V. *J. Am. Chem. Soc.* **2005**, *127*, 3714.
- (273) Mandal, A. B.; Lee, G.-H.; Liu, Y.-H.; Peng, S.-M.; Leung, M. J. *Org. Chem.* **2000**, *65*, 332.
- (274) Shue, R. S. *J. Am. Chem. Soc.* **1971**, *93*, 7116.
- (275) Danno, S.; Moritani, I.; Fujiwara, I. *Tetrahedron* **1969**, *25*, 4819.
- (276) Weissman, H.; Song, X.; Milstein, D. *J. Am. Chem. Soc.* **2001**, *123*, 337.
- (277) Boele, M. D. K.; van Strijdonck, G. P. F.; de Vries, A. H. M.; Kamer, P. C. J.; de Vries, J. G.; van Leeuwen, P. W. N. M. *J. Am. Chem. Soc.* **2002**, *124*, 1586.
- (278) (a) Jia, C.; Piao, D.; Oyamada, J.; Lu, W.; Kitamura, T.; Fujiwara, Y. *Science* **2000**, *287*, 1992. (b) Jia, C.; Lu, W.; Oyamada, J.; Kitamura, T.; Matsuda, K.; Irie, M.; Fujiwara, Y. *J. Am. Chem. Soc.* **2000**, *122*, 7252. (c) Jia, C.; Kitamura, T.; Fujiwara, Y. *Acc. Chem. Res.* **2001**, *34*, 633.
- (279) Tunge, J. A.; Foresee, L. N. *Organometallics* **2005**, *24*, 6440.
- (280) For examples of palladation of arenes by Pd(OAc)₂ through a C–H activation mechanism, see: (a) [$k_{\text{H}}/k_{\text{D}} = 5.0(5)$] Gretz, E.; Oliver, T. F.; Sen, A. *J. Am. Chem. Soc.* **1987**, *109*, 8109. (b) [$k_{\text{H}}/k_{\text{D}} = 3$] ref 277. (c) [$k_{\text{H}}/k_{\text{D}} = 5.0(4)$], ref 274. (d) [$k_{\text{H}}/k_{\text{D}} = 3.5$] Stock, L. M.; Tse, K.; Vorvick, L. J.; Walstrum, S. A. *J. Org. Chem.* **1981**, *46*, 1757.
- (281) Pinto, A.; Neuville, L.; Retaillieu, P.; Zhu, J. *Org. Lett.* **2006**, *8*, 4927.
- (282) (a) Reactions proceeding by electrophilic aromatic substitution mechanisms typically have $k_{\text{H}}/k_{\text{D}} \approx 1$. See: Zollinger, H. *Adv. Phys. Org. Chem.* **1964**, *2*, 163. (b) Experimentally, a small deuterium KIE and the increased rate of cyclometalation with electron-donating arene substituents have been used as evidence of a conventional electrophilic aromatic substitution mechanism, see: Davies, D. L.; Donald, S. M. A.; Macgregor, S. A. *J. Am. Chem. Soc.* **2005**, *127*, 13754.
- (283) Martín-Matute, B.; Mateo, C.; Cárdenas, D. J.; Echavarren, A. M. *Chem.—Eur. J.* **2001**, *7*, 2341.
- (284) (a) García-Cuadrado, D.; Braga, A. A. C.; Maseras, F.; Echavarren, A. M. *J. Am. Chem. Soc.* **2006**, *128*, 1066. (b) García-Cuadrado, D.; de Mendoza, P.; Braga, A. A. C.; Maseras, F.; Echavarren, A. M. *J. Am. Chem. Soc.* **2007**, *129*, 6880. (c) Pascual, S.; García-Cuadrado, D.; de Mendoza, P.; Braga, A. A. C.; Maseras, F.; Echavarren, A. M. *Tetrahedron* **2008**, *64*, 6021.
- (285) (a) Campeau, L. C.; Parisien, M.; Jean, A.; Fagnou, K. *J. Am. Chem. Soc.* **2006**, *128*, 581. (b) Campeau, L. C.; Parisien, M.; Leblanc, M.; Fagnou, K. *J. Am. Chem. Soc.* **2004**, *126*, 9186. (c) Lafrance, M.; Lapointe, D.; Fagnou, K. *Tetrahedron* **2008**, *64*, 6015.
- (286) A KIE study of the nature of the Pd(0) active species in the Heck reaction based on the presence of phosphine ligands, see: Schmidt, A. F.; Smirnov, V. V. *Kinet. Catal.* **2005**, *46*, 495. Translated from *Kinet. Katal.* **2005**, *46*, 529.
- (287) Chiong, H. A.; Pham, Q.-N.; Daugulis, O. *J. Am. Chem. Soc.* **2007**, *129*, 9879.

- (288) Lafrance, M.; Rowley, C. N.; Woo, T. K.; Fagnou, K. *J. Am. Chem. Soc.* **2006**, *128*, 8754.
- (289) Lafrance, M.; Fagnou, K. *J. Am. Chem. Soc.* **2006**, *128*, 16496.
- (290) Gorelsky, S. I.; Lapointe, D.; Fagnou, K. *J. Am. Chem. Soc.* **2008**, *130*, 10848.
- (291) Pivsa-Art, S.; Satoh, T.; Kawamura, Y.; Miura, M.; Nomura, M. *Bull. Chem. Soc. Jpn.* **1998**, *71*, 467.
- (292) Wang, J.-X.; McCubbin, J. A.; Jim, M.; Laufer, R. S.; Mao, Y.; Crew, A. P.; Mulvihill, M. J.; Snieckus, V. *Org. Lett.* **2008**, *10*, 2923.
- (293) Lane, B. S.; Brown, M. A.; Sames, D. *J. Am. Chem. Soc.* **2005**, *127*, 8050.
- (294) Liégault, B.; Fagnou, K. *Organometallics* **2008**, *27*, 4841.
- (295) Chaumontet, M.; Piccardi, R.; Audic, N.; Hitce, J.; Peglion, J.-L.; Clot, E.; Baudoin, O. *J. Am. Chem. Soc.* **2008**, *130*, 15157.
- (296) Lafrance, M.; Gorelsky, S. I.; Fagnou, K. *J. Am. Chem. Soc.* **2007**, *129*, 14570.
- (297) Álvarez-Bercedo, P.; Flores-Gaspar, A.; Correa, A.; Martin, R. *J. Am. Chem. Soc.* **2010**, *132*, 466.
- (298) Hennessy, E. J.; Buchwald, S. L. *J. Am. Chem. Soc.* **2003**, *125*, 12084.
- (299) (a) Lloyd-Jones, G. C. *Org. Biomol. Chem.* **2003**, *1*, 215. (b) Trost, B. M.; Krische, M. J. *Synlett* **1998**, 1.
- (300) Grigg, R.; Malone, J. F.; Mitchell, T. R. B.; Ramasubbu, A.; Scott, R. M. *J. Chem. Soc., Perkin Trans. 1* **1984**, *1*, 1745.
- (301) Bray, K. L.; Lloyd-Jones, G. C.; Muñoz, M. P.; Slatford, P. A.; Tan, E. H. T.; Tyler-Mahon, A. R.; Worthington, P. A. *Chem.—Eur. J.* **2006**, *12*, 8650.
- (302) Widenhoefer, R. A. *Acc. Chem. Res.* **2002**, *35*, 905.
- (303) Goj, L. A.; Widenhoefer, R. A. *J. Am. Chem. Soc.* **2001**, *123*, 11133.
- (304) Alibrandi, G.; Scolaro, L. M.; Minniti, D.; Romeo, R. *Inorg. Chem.* **1990**, *29*, 3467.
- (305) Alibrandi, G.; Cusumano, M.; Minniti, D.; Scolaro, L. M.; Romeo, R. *Inorg. Chem.* **1989**, *28*, 342.
- (306) Takacs, J. M.; Clement, F.; Zhu, J.; Chandramouli, S. V.; Gong, X. *J. Am. Chem. Soc.* **1997**, *119*, 5804.
- (307) Selected revisions: (a) Zhang, L.; Sun, J.; Kozmina, S. A. *Adv. Synth. Catal.* **2006**, *348*, 2271. (b) Cristina Nieto-Oberhuber, C.; López, S.; Jiménez, E.; Echavarren, A. M. *Chem.—Eur. J.* **2006**, *12*, 5916. (c) Steven T. Diver, S. T.; Giessert, A. J. *Chem. Rev.* **2004**, *104*, 1317. (d) Aubert, C.; Buisine, O.; Malacria, M. *Chem. Rev.* **2002**, *102*, 813. (e) Trost, B. M. *Acc. Chem. Res.* **1990**, *23*, 34. (f) Ojima, I.; Tzaniarioudaki, M.; Li, Z.; Donovan, R. J. *Chem. Rev.* **1996**, *96*, 635. (g) Bruneau, C. *Angew. Chem., Int. Ed.* **2005**, *44*, 2328. (h) Ma, S.; Yu, S.; Gu, Z. *Angew. Chem., Int. Ed.* **2006**, *45*, 200. (i) Añorbe, L.; Domínguez, G.; Pérez-Castells, J. *Chem.—Eur. J.* **2004**, *10*, 4938. (j) Echavarren, A. M.; Nevado, C. *Chem. Soc. Rev.* **2004**, *33*, 431. (k) Shen, H. C. *Tetrahedron* **2008**, *64*, 7847. (l) Shen, H. C. *Tetrahedron* **2008**, *64*, 3885.
- (308) Cheong, P. H.-Y.; Morganelli, P.; Luzung, M. R.; Houk, K. N.; Toste, F. D. *J. Am. Chem. Soc.* **2008**, *130*, 4517.
- (309) Horino, Y.; Yamamoto, T.; Ueda, K.; Kuroda, S.; Toste, F. D. *J. Am. Chem. Soc.* **2009**, *131*, 2809.
- (310) See, for example: (a) Sulikowski, G. A.; Lee, S. *Tetrahedron Lett.* **1999**, *40*, 8035. (b) Mbuvi, H. M.; Woo, L. K. *Organometallics* **2008**, *27*, 637. (c) Davies, H. M. L.; Hansen, T.; Churchill, M. R. *J. Am. Chem. Soc.* **2000**, *122*, 3063. (d) Ishii, S.; Zhao, S.; Helquist, P. *J. Am. Chem. Soc.* **2000**, *122*, 5897.
- (311) Bekele, T.; Christian, C. F.; Lipton, M. A.; Singleton, D. A. *J. Am. Chem. Soc.* **2005**, *127*, 9216.
- (312) Tobisu, M.; Nakai, H.; Chatani, N. *J. Org. Chem.* **2009**, *74*, 5471.
- (313) Li, L.; Jones, W. D. *J. Am. Chem. Soc.* **2007**, *129*, 10707.
- (314) An early review on Transition Metal Catalyzed Rearrangements of Small Ring Organic Molecules, collects the work of Paquette in the studies of bicyclobutane rearrangements mediated by Ag(I) and in the Rh(I) and Ag(I) mediated metal-catalyzed rearrangements of cubanes to tricyclooctadienes. See: Bishop, K. C. *Chem. Rev.* **1976**, *76*, 461.
- (315) For a review about the transition metal chemistry involving cyclopropenes and cyclopropanes, see: Rubin, M.; Rubina, M.; Gevorgyan, V. *Chem. Rev.* **2007**, *107*, 3117.
- (316) Rasmussen, T.; Jensen, J. F.; stergaard, N.; Tanner, D.; Ziegler, T.; Norrby, P.-O. *Chem.—Eur. J.* **2002**, *8*, 177.
- (317) Nowlan, D. T., III; Gregg, T. M.; Davies, H. M. L.; Singleton, D. A. *J. Am. Chem. Soc.* **2003**, *125*, 15902.
- (318) Nowlan, D. T.; Singleton, D. A. *J. Am. Chem. Soc.* **2005**, *127*, 6190.
- (319) Wolf, J. R.; Hamaker, C. G.; Djukic, J.-P.; Kodadek, T.; Woo, L. K. *J. Am. Chem. Soc.* **1995**, *117*, 9194.
- (320) Brown, K. C.; Kodadek, T. *J. Am. Chem. Soc.* **1992**, *114*, 8336.
- (321) Lai, T.-S.; Chan, F.-Y.; So, P.-K.; Ma, D.-L.; Wong, K.-Y.; Che, C.-M. *Dalton Trans.* **2006**, 4845.
- (322) Polse, J. L.; Andemen, R. A.; Bergman, R. G. *J. Am. Chem. Soc.* **1995**, *117*, 5393.
- (323) Singleton, D. A.; Schulmeier, B. E. *J. Am. Chem. Soc.* **1999**, *121*, 9313.
- (324) Ragaini, F.; Rapetti, A.; Visentin, E.; Monzani, M.; Caselli, A.; Cenini, S. *J. Org. Chem.* **2006**, *71*, 3748.
- (325) DelMonte, A. J.; Haller, J.; Houk, K. N.; Sharpless, K. B.; Singleton, D. A.; Strassner, T.; Thomas, A. A. *J. Am. Chem. Soc.* **1997**, *119*, 9907.
- (326) Dehestani, A.; Lam, W. H.; Hrovat, D. A.; Davidson, E. R.; Borden, W. T.; Mayer, J. M. *J. Am. Chem. Soc.* **2005**, *127*, 3423.
- (327) Yip, W.-P.; Yu, W.-Y.; Zhu, N.; Che, C.-M. *J. Am. Chem. Soc.* **2005**, *127*, 14239.
- (328) (a) Gable, K. P.; Phan, T. N. *J. Am. Chem. Soc.* **1994**, *116*, 833. (b) Gable, K. P.; Juliette, J. J. *J. Am. Chem. Soc.* **1996**, *118*, 2625.
- (329) Gable, K. P.; Zhuravlev, F. A. *J. Am. Chem. Soc.* **2002**, *124*, 3970.
- (330) Lalic, G.; Krinsky, J. L.; Bergman, R. G. *J. Am. Chem. Soc.* **2008**, *130*, 4459.
- (331) Fox, R. J.; Lalic, G.; Bergman, R. G. *J. Am. Chem. Soc.* **2007**, *129*, 14144.
- (332) Hours, A. E.; Snyder, J. K. *Organometallics* **2008**, *27*, 410.
- (333) Paquette, L. A.; Micheli, R. P.; Photis, J. M. *J. Am. Chem. Soc.* **1977**, *99*, 7911.
- (334) Revisions: (a) Bernasconi, C. F. *Chem. Soc. Rev.* **1997**, *26*, 299. (b) Bernasconi, C. F. *Adv. Phys. Org. Chem.* **2002**, *37*, 137.
- (335) Bernasconi, C. F.; Flores, F. X.; Sun, W. *J. Am. Chem. Soc.* **1995**, *117*, 4875.
- (336) Bernasconi, C. F.; Sun, W. *Organometallics* **1995**, *14*, S615.
- (337) (a) Bernasconi, C. F.; Leyes, A. E. *J. Am. Chem. Soc.* **1997**, *119*, 5169. (b) Bernasconi, C. F.; Leyes, A. E. *J. Chem. Soc., Perkin Trans. 2* **1997**, 1641.
- (338) Bernasconi, C. F.; Leyes, A. E.; García-Rio, L. *Organometallics* **1998**, *17*, 4940.
- (339) Bernasconi, C. F.; Flores, F. X.; Kittredge, K. W. *J. Am. Chem. Soc.* **1997**, *119*, 2103.
- (340) Bernasconi, C. F.; Sun, W. *J. Am. Chem. Soc.* **1993**, *115*, 12526.
- (341) Pipoh, R.; van Eldik, R.; Henkell, G. *Organometallics* **1993**, *12*, 2236.
- (342) Pipoh, R.; van Eldik, R. *Inorg. Chim. Acta* **1994**, *222*, 207.
- (343) Pipoh, R.; van Eldik, R.; Henkell, G. *Organometallics* **1993**, *12*, 2668.
- (344) The chemistry of vinylidene complexes has been profusely reviewed. For selected reviews, see: (a) Selegue, J. P. *Coord. Chem. Rev.* **2004**, *248*, 1543. (b) Bruce, M. I. *Chem. Rev.* **1991**, *91*, 197.
- (345) Grotjahn, D. B.; Zeng, X.; Cooksy, A. L.; Kassel, W. S.; DiPasquale, A. G.; Zakharov, L. N.; Rheingold, A. L. *Organometallics* **2007**, *26*, 3385.
- (346) Katayama, H.; Ozawa, F. *Coord. Chem. Rev.* **2004**, *248*, 1703.
- (347) Katayama, H.; Wada, C.; Taniguchi, K.; Ozawa, F. *Organometallics* **2002**, *21*, 3285.

- (348) Ipaktschi, J.; Mohsseni-Ala, J.; Uhlig, S. *Eur. J. Inorg. Chem.* **2003**, 4313.
- (349) Bassetti, M.; Cadierno, V.; Gimeno, J.; Pasquini, C. *Organometallics* **2008**, 27, 5009 and the pertinent references therein.
- (350) Carvalho, M. F. N. N.; Almeida, S. S. P. R.; Pombeiro, A. J. L.; Henderson, R. A. *Organometallics* **1997**, 16, 5441.
- (351) Fischer, H.; Jungklaus, H. *J. Organomet. Chem.* **1999**, 572, 105.
- (352) Roger, C.; Bodner, G. S.; Hatton, W. G.; Gladysz, J. A. *Organometallics* **1991**, 10, 3266.
- (353) Caulton, K. G.; Chisholm, M. H.; Streib, W. E.; Xue, Z. *J. Am. Chem. Soc.* **1991**, 113, 6082.
- (354) McDade, C.; Green, J. C.; Bercaw, J. E. *Organometallics* **1982**, 1, 1629.
- (355) Qian, B.; Scanlon, W. J., IV; Smith, M. R., III; Motry, D. H. *Organometallics* **1999**, 18, 1693.
- (356) Bulls, A. R.; Schaefer, W. P.; Serfas, M.; Bercaw, J. E. *Organometallics* **1987**, 6, 1219.
- (357) Agapie, T.; Day, M. W.; Bercaw, J. E. *Organometallics* **2008**, 27, 6123.
- (358) Cheon, J.; Rogers, D. M.; Girolami, G. S. *J. Am. Chem. Soc.* **1997**, 119, 6804.
- (359) (a) Schrock, R. R.; Fellmann, J. D. *J. Am. Chem. Soc.* **1978**, 100, 3359. (b) Malatesta, V.; Ingold, K. U.; Schrock, R. *J. Organomet. Chem.* **1978**, 152, C53. (c) Wood, C. D.; McLain, S. J.; Schrock, R. R. *J. Am. Chem. Soc.* **1979**, 101, 3210.
- (360) Carney, M. J.; Walsh, P. J.; Hollander, F. J.; Bergman, R. G. *Organometallics* **1992**, 11, 761.
- (361) Carney, M. J.; Walsh, P. J.; Hollander, F. J.; Bergman, R. G. *J. Am. Chem. Soc.* **1989**, 111, 8751.
- (362) Petasis, N. A.; Fu, D.-K. *Organometallics* **1993**, 12, 3776.
- (363) Michael, F. E.; Duncan, A. P.; Sweeney, Z. K.; Bergman, R. G. *J. Am. Chem. Soc.* **2003**, 125, 7184.
- (364) Sweeney, Z. K.; Polse, J. L.; Bergman, R. G.; Andersen, R. A. *Organometallics* **1999**, 18, 5502.
- (365) Gountchev, T. I.; Tilley, T. D. *J. Am. Chem. Soc.* **1997**, 119, 12831.
- (366) Hayes, P. G.; Beddie, C.; Hall, M. B.; Waterman, R.; Tilley, T. D. *J. Am. Chem. Soc.* **2006**, 128, 428.
- (367) Blau, R. J.; Chisholm, M. H.; Eichhorn, B. W.; Huffman, J. C.; Kramer, K. S.; Lobkovsky, E. B.; Streib, W. E. *Organometallics* **1995**, 14, 1855.
- (368) Budzichowski, T. A.; Chisholm, M. H.; Folting, K.; Huffman, J. C.; Streib, W. E. *J. Am. Chem. Soc.* **1995**, 117, 7428.
- (369) Chisholm, M. H.; Eichhorn, B. W.; Huffman, J. C. *Organometallics* **1989**, 8, 67.
- (370) Riley, P. N.; Thorn, M. G.; Vilaro, J. S.; Lockwood, M. A.; Fanwick, P. E.; Rothwell, I. P. *Organometallics* **1999**, 18, 3016.
- (371) Idmoumaz, H.; Lin, C.-H.; Hersch, W. H. *Organometallics* **1995**, 14, 4051.
- (372) Doherty, S.; Hogarth, G.; Waugh, M.; Scanlan, T. H.; Clegg, W.; Elsegood, M. R. *J. Organometallics* **1999**, 18, 3178.